UNIVERSITY OF SOUTHAMPTON

Faculty of Science

Geology

submitted for the degree of Doctor of Philosophy

THE FALKLAND ISLANDS AND THEIR POSITION WITHIN GONDWANA

Daniel Mark Hyam

October 1997

For my Father in Heaven.

UNIVERSITY OF SOUTHAMPTON

ABSTRACT

FACULTY OF SCIENCE

GEOLOGY

Doctor of Philosophy

THE FALKLAND ISLANDS AND THEIR POSITION WITHIN GONDWANA

by Daniel Mark Hyam

Detailed mapping, at scales of 1:25000 and less, has been undertaken at key points across the Falkland Islands to understand the structural history of this displaced part of Gondwana. This mapping has revealed, previously undiscovered, downwardly injected diamictite dykes of Early Carboniferous age formed during the main phase of the Gondwana glaciation. Interference fold patterns on West Falkland have shown a relative chronology for the sub-orthogonal E-W (D_1) and NE-SW (D_2) structural trends on the Falkland Islands. D_1 structures, related to Early Permian to Early Triassic N-S compression, form an E-W striking, southerly verging fold-belt across East Falkland, which changes strike to WNW-ESE on West Falkland, coincident with a marked decrease in strain. D_2 structures include N-S and NE-SW folds, however these are dominated by the NE-SW Hornby Monocline, which is underlain by an oblique (reverse-dextral) basement fault causing West Falkland to be uplifted relative to East Falkland by 6 - 8 km. Seismic and gravity data reveal the offshore continuation of this basement fault to the SW for at least 60 km along strike. Comparison of vitrinite reflectance data, sedimentary facies and formation thicknesses between East and West Falkland has shown that this fault was active from at least Early Carboniferous times and throughout D_1, and that it was reactivated during the Late Triassic-Early Jurassic E-W D_2 compression.

The geology of the Falkland Islands, including the stratigraphy (palaeocurrents, facies and lithologies), structure (fold vergence, thrust directions and cleavage orientations) and thermal history of the Lafonian foreland basin derived from vitrinite reflectance data is almost identical to that of the Eastern Cape of South Africa. This confirms that in Gondwana reconstructions, the Falkland Islands should be rotated by 180° and placed to the east of South Africa as an eastward extension and lateral termination of the South African Cape Fold Belt.

Table of Contents:

Table List

Figure List

(Figures appear, in order, after the Tables at the end of each chapter)

Chapter 1

Chapter 2

Chapter 5

Additional Material:

Maps (in back pocket).

Map 1: Eastern Wickham Heights: Port Stanley-Bluff Cove, East Falkland, 1:25,000 scale map.

Map 2: Greenpatch, East Falkland, 1:25,000 scale map.

Map 3: San Carlos, East Falkland, 1:25,000 scale map.

Map 4: Port Howard, West Falkland, 1:25,000 scale map.

Map 5: Carcass Bay, West Falkland, 1:25,000 scale map.

Appendix (journal offprint in back pocket).

Curtis, M.L. & Hyam, D.M. 1998. Late Palaeozoic to Mesozoic structural evolution of the Falkland Islands: a displaced segment of the Cape Fold Belt. *Journal of the Geological Society of London* **155**, 115-130.

Acknowledgements

It is hard at the end of three years of research to remember all the people to whom I am indebted for their help, support and encouragement. However, first and foremost, and above all others, I must thank and praise my Lord Jesus, for being there at all times, wherever I have been, and without whom, none of what I have done in the last three years would have been possible.

Thanks also must be given to Dr. John Marshall and Prof. David Sanderson for their patience and guidance in getting me through this Ph.D., as well as to all the other staff, technicians and students at the University of Southampton Geology Department for their help, patience and friendship.

Others who should be thanked include; Dr.'s Bryan Storey and Mike Curtis at the British Antarctic Survey, Dr. David Macdonald at the Cambridge Arctic Shelf Programme, Dr. Don Aldiss of the British Geological Survey, Marc Goedhart and Dr. Bob Thomas of the South African Geological Survey, Geoffrey Grant at Geco-Prakla U.K. Ltd., RAF Squadron 216 and the Falkland Island Government.

It now only leaves me to thank Su for being who you are; my parents, for their support and encouragement; my family in the Central Southampton Vineyard for their love, hugs and prayers; and innumerable Falkland Islanders for their care, help, hospitality, Land Rovers and for making my stays on the islands memorable.

Chapter 1: Introduction

Chapter 1: Introduction

1.1 Location

The Falkland Islands are an archipelago of several hundred islands lying in the South Atlantic Ocean between 51° and 52°30'S and 57°30' and 61°30'W. They lie 600 km east of Patagonia and form the only emergent part of the Falkland Plateau which extends eastwards from Tierra del Fuego for 1500 km (Fig 1.1). The archipelago is dominated by the two main islands of East and West Falkland which together cover an area of around 8500 km^2 separated by the NE-SW trending Falkland Sound.

1.2 Previous and ongoing research

Previous work on the geology of the Falkland Islands is sparse and spread over a time span of 150 years since Darwin's (1846) first report from his observations during a brief visit of the H.M.S. 'Beagle'. Since Darwin there have been long gaps in research into the islands punctuated by occasional papers and reports. The first substantial geological survey of the Falkland Islands was carried out and published in the early part of this century by a group of Swedish researchers (Halle 1912) who produced one of the first attempts at a geological map of the islands. Further to this, in the 1920's, the Falkland Islands Government recruited Howard Baker for two years to map and assess the economic potential of the islands. His report (Baker 1924) remained one of the most complete geological works on the islands for 50 years. It was at this time, in both Halle's (1912) and Baker's (1924) reports, that correlations to other parts of Gondwana started to be made, especially the sequences in South Africa. This was also supported by the early work of du Toit (1927, 1937) when first suggesting the correlation of South America and Africa. Little interest was then paid to the Falkland Islands until the 1950's when Raymond Adie of the Falkland Islands Dependency Survey produced a series of papers (Adie 1952a, b, 1958). In one of these (Adie 1952b) he correlated the geology of the Falkland Islands to the geology of the Eastern Cape of South Africa invoking a 180° rotation of the islands to fit them into a Gondwana reconstruction. This theory was not supported as no mechanism for

rotation was known and the discussion was largely forgotten until the mid 1980's. The most substantial works since Adie were the publication of the first complete geological map of the Falkland Islands produced from aerial photograph interpretation (Greenway 1972) and the first studies offshore of the islands on the Maurice Ewing Bank (Barker *et al.* 1976a). Other research focused primarily on the stratigraphy of the Falkland Islands (Borello 1963, Dawson 1967, Frakes and Crowell 1967, Cingolani & Varella 1976, Turner 1980, Rex & Tanner 1982, Scasso & Mendia 1985). In the mid to late eighties the discussion of 180° rotation was once again raised as new research, based on the palaeomagnetism of the dolerite dykes on the Falkland Islands, indicated that the islands had indeed undergone a 180° rotation (Mitchell *et al.* 1986, Taylor & Shaw 1989) as suggested by Adie (1952b). This lead to the proposition that the Falkland Islands were in fact a microcontinent and had been able to move independently during the break-up of Gondwana (Mitchell *et al.* 1986). Research in the early 1990's, before this PhD commenced, was limited. Publications included Marshall (1994a, b), who undertook the first detailed study of the Devonian sequence and onshore hydrocarbon potential, Mussett & Taylor (1994), who re-dated the dyke swarms of the islands and Richards & Fannin (1994) who published some initial findings on the offshore potential of the Falkland Islands. The British Antarctic Survey (BAS) began a programme in 1993 studying palaeomagnetism and structural geology on the Falkland Islands.

Since the start of this study geological research in the Falkland Islands has increased, mainly due to the growing interest of the hydrocarbon industry in the potential of the offshore basins. Most of the current work onshore is still unpublished, however, detailed studies have been published looking at the structural geology (Curtis & Hyam 1998) and the Cape Meredith Complex (Thomas *et al.* 1995, Thistlewood *et al.* 1997). Other current research includes an in depth assessment of the stratigraphy of the Lafonian Basin (Cambridge Arctic Shelf Programme (CASP)), a remapping of the islands (British Geological Survey), studies into the dyke swarms (Aberdeen University/CASP) and studies into the Devonian stratigraphy (Southampton University, Aberdeen University/CASP, BAS). Along side this there has been an increase in published work concerning the offshore basins around the islands (Platt & Philip 1995, Richards *et al.* 1996). This has especially focused on the

North Falkland Basin (Richards & Fannin 1997) where, following the initial licensing round in 1996, drilling will commence in mid 1998.

1.3 Rationale

The Falkland Islands are unequivocally an isolated piece of the Gondwanian supercontinent which broke away from South Africa during its early fragmentation. The geology of the islands, which is dominated by two Palaeozoic sedimentary clastic successions and by two almost orthogonal structural trends, shows distinct affinities to the eastern end of the South African Cape.

Despite previous research there is still discussion regarding whether the islands have rotated by 180° or 60° and, although there is evidence from the stratigraphy for a rotation of 180°, very little work has been carried out to understand the structure of the islands and how this is related within Gondwana.

The aim of this research has been to bridge this gap in the knowledge of the Falkland Islands by undertaking structural field mapping in selected areas of the islands, to compare this to eastern South Africa and to understand the overall history of the islands and relate this within the context of Gondwana.

The main part of this research has been based around 4 months of fieldwork on the Falkland Islands mapping at 1:25,000 scale in five main areas on East and West Falkland covering a total of over 700 km^2. Wide use of aerial photographs for mapping, although initially suggested, was not undertaken as a policy change at the Ordinance Survey where they were held, meant restricted availability. Purchasing was considered but proved to be too costly. Other areas on the Falkland Islands were visited to follow up questions raised from previous research. A short field-trip was taken to South Africa to view the eastern Cape Fold Belt and southern Natal, areas where correlatives of the geology of East and West Falkland would be expected to be found.

1.4 Outline

From the data collected during fieldwork several aspects of Falkland Islands geology have been addressed as chapters in this thesis, these are summarised below:

Chapter 2: The stratigraphy of the Falkland Islands is reviewed using data collected during this study and published literature. The evidence for the correlation of this stratigraphy with that of the Eastern Cape of South Africa is then discussed. This includes new data which have been derived from this study such as new exposures of the Port Stephens Formation and analysis of the kerogen in the Port Sussex Formation.

Chapter 3: The question of the presence of a correlative to the South African Parkhuis Tillite around South Harbour, raised by Baker (1924), has been resolved with the discovery and description of several diamictite dykes. These are described and their palaeogeographic significance is also considered. This chapter has been accepted for publication in The Journal of African Earth Sciences (Hyam *et al.* 1997).

Chapters 4 & 5: From structural mapping in key places across the main structures on both East and West Falkland it has been possible to describe in detail, and propose models for the E-W structures seen on East Falkland and the NE-SW structure on West Falkland. A paper describing the overall structural evolution of the Falkland Islands, given the present state of knowledge, has been accepted for publication in The Journal of the Geological Society of London (Curtis & Hyam 1998).

Chapter 6: A large vertical displacement in the basement has been imaged and modelled in an area to the SW of the Falkland Islands using seismic and gravity data made available by Geco-Prakla. The structure appears to be an along-strike continuation of the NE-SW striking structure seen between East and West Falkland.

Chapter 7: Vitrinite reflectance data, taken from shale samples collected during mapping, have increased the existing data for the Falkland Islands and allow comparisons to be made between East and West Falkland for given horizons. The data also gives further insight into the tectonic evolution of the Falkland Islands.

Chapter 8: In the light of the previous chapters the evolution of the Falkland Islands is discussed. Given the structural and stratigraphic evidence for the position of

the Falkland Islands against the Eastern Cape of South Africa within Gondwana reconstructions, a review and discussion is made of the various break-up models for Gondwana and how the Falkland Islands managed to rotate by 180° during this event.

In summary, this work is the first field-based, regional overview of the structural history of the Falkland Islands since 1912. By looking at a number of different aspects of the geology; structure, stratigraphy, geophysics and vitrinite reflectance, this study provides new evidence for their evolution within the context of Gondwana.

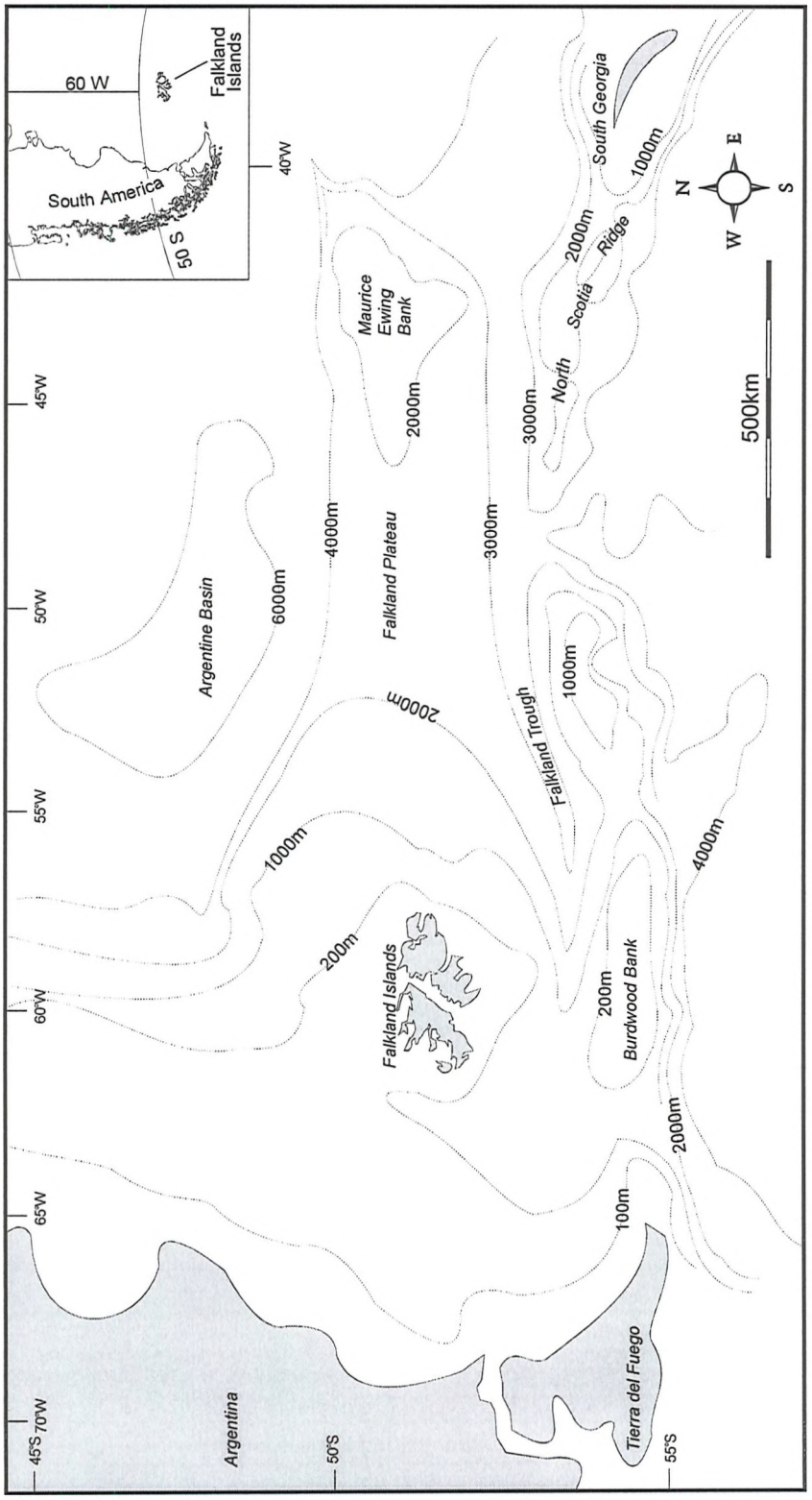

Figure 1.1: Summary bathymetric map and inset showing the location of the Falkland Islands on the Falkland Plateau to the East of Argentina. (Bathymetry after Ludwig *et al.* 1979).

Chapter 2: The Stratigraphy of the Falkland Islands and its context within Gondwana

Chapter 2: Stratigraphy of the Falkland Islands and its context within western Gondwana

2.1 Introduction

It has long been noted that the stratigraphy of the Falkland Islands shows a poor affinity to the stratigraphy of the Paraná and Sauce Grande Basins of South America (Clarke 1913, du Toit 1927) to which they are geographically close. In contrast the Falkland Islands show a far greater correlation to the stratigraphy of the Cape and Karoo Basins of South Africa (Clarke 1913, Baker 1924, du Toit 1927), especially that of the Eastern Cape (Adie 1952b, Marshall 1994a). This includes the correlation of: a) the South African Cape Supergroup with the Falkland Islands Gran Malvina Group; b) the E-W striking Cape Fold Belt in South Africa with the E-W striking Wickham Heights on the Falkland Islands; and c) the Permo-Triassic Karoo Basin of South Africa with the Permian Lafonian Basin of the Falkland Islands. This correlation requires that the Falkland Islands be rotated by 180° and be placed against the Eastern Cape in Gondwana palaeo-reconstructions (e.g. Adie 1952b). The position of the Falkland Islands in such reconstructions is now an area of dispute and discussion, mostly forgotten for 30 years, which arose when Adie (1952b) first suggested that the islands be rotated by 180° based on the correlation of the stratigraphy and structure of the Falkland Islands and the Eastern Cape of South Africa. The discussion is mainly based on whether or not the Falkland Islands are considered to be a microplate and able to move independently of the South American plate. The two opposing models (Fig. 2.1) as to where the Falkland Islands should be are:

(1) that the Falkland Islands are a microplate and that they lay off the eastern coast of South Africa and have been rotated by 180°, 120° of which occurred before the main opening of the South Atlantic (Adie 1952b, Mitchell *et al.* 1986, Taylor & Shaw 1989, Ben-Avraham *et al.* 1993, Marshall 1994a,b).

(2) that the Falkland Islands have always been rigidly attached to South America and that in Gondwana reconstructions they lay some 500 km south of Cape Town. In this model the islands simply rotated passively by 60° with the opening of the

Atlantic Ocean during Gondwana break-up (de Wit *et al.* 1988, Richards *et al.* 1996).

This chapter outlines the stratigraphy of the Falkland Islands based on field observations and published data. This includes new data regarding outcrop extent and palaeogeography based on field mapping and experimental results. Further to this is a discussion of the correlation within Gondwana of this stratigraphy and recent evidence amplifying the original hypothesis of Adie (1952b) that the islands should be rotated by 180° to a palaeogeographic position against eastern South Africa.

2.2 Falkland Island Stratigraphy

Overviews of the stratigraphy of the Falkland Islands have been given by Halle (1912), Baker (1924), Adie (1958) and Turner (1980), further studies have dealt with individual aspects of the sequence. The geology of the Falkland Islands, (Fig. 2.2) shows the basal Precambrian Cape Meredith Complex overlain by two major clastic sedimentary sequences, the tri-part, mainly Devonian, Gran Malvina Group and the Permo-Carboniferous Lafonian Supergroup. Each of these shall be looked at, in turn, in the following sections.

2.2.1 Cape Meredith Complex

The Cape Meredith Complex is exposed as a thin strip at the southern extremity of West Falkland at Cape Meredith (Fig. 2.2). The area has been studied by several authors namely Baker (1924) who looked at the geology, and Cingolani & Varella (1976) and Rex & Tanner (1982) who assessed the age of the sequence. The sequence has been restudied in depth by Thomas *et al.* (1995) who mapped the area in detail and Thistlewood *et al.* (1997) who have undertaken further age analysis on the dyke swarms. These studies have shown the oldest rocks to be biotite-hornblende and amphibolite gneisses which have been intruded by granodiorite dykes, granitic gneiss, leucocratic granites, pegmatites and a further three types of dykes, mafic, lamprophyre and dolerite in ascending relative age (Thomas *et al.* 1995). Age analysis of these dyke sets shows that possibly 3 ages of lamprophyres exist with K-Ar dates of c. 500 -

550 Ma (Cingolani & Varella 1976, Thistlewood *et al.* 1997), 473±12 Ma and 306±8 Ma (Thistlewood *et al.* 1997). The dolerite dykes also show three ages with K-Ar dates of c. 480 Ma, 422±39 Ma (Thistlewood *et al.* 1997) and 192±10 Ma (Cingolani & Varella 1976). Further K-Ar dating of this basement sequence reveals ages of 1110±55 Ma and 1124±50 Ma (Cingolani & Varella 1976) and 977±40 Ma and 953±30 Ma (Rex & Tanner 1982). The Cape Meredith Complex is overlain unconformably by the Port Stephens Formation of the Gran Malvina Group.

2.2.2 Gran Malvina Group

The Gran Malvina Group, so named by Borrello (1963), is made up of a clastic sedimentary sequence consisting of three formations: the Port Stephens, Fox Bay and Port Stanley formations. These shall be dealt with individually below.

i) Port Stephens Formation: The Port Stephens Formation, estimated at 1600 m (Baker 1924) to 1250 m (Port Howard) in thickness, was, until recently, thought to outcrop solely on West Falkland (Baker 1924, Greenway 1972). Recent mapping by the author has shown that an extensive area in the centre of East Falkland, the Onion Range, including the Malo Hills, is also composed of the same formation (see Fig. 2.3). It can also be inferred that the hilly region between Johnson Harbour and the north coast of East Falkland is also composed of the Port Stephens Formation. This is based on the occurrences of Fox Bay Formation at Johnson Harbour dipping south (D.I.M. Macdonald *pers. comm.* 1995).

The Port Stephens Formation lies unconformably on the Precambrian Cape Meredith Complex in southern West Falkland. Although not seen during mapping, the basal sequence consists of red micaceous shales and quartz rich sandstones grading up into white quartzites with minor conglomeratic pebbles (Baker 1924, Cingolani & Varella 1976, Scasso & Mendia 1985). The main part of the sequence, observed at Port Howard, Rat Castle and South Harbour on West Falkland and in the Malo Hills on East Falkland, is dominated by well bedded, white to grey arkosic arenites (Fig. 2.4). The arenites are poorly to reasonably sorted showing sub-angular to sub-rounded, sub-spherical grains varying in size from medium (2-3 mm) to very

coarse (5-6 mm) sand. Across West Falkland, the arenites show an increase in maturity northwards seen as an increase in the quartz content from Cape Meredith and South Harbour to Port Howard and Shag Cove (see Table 2.1). The level of induration and cementation also increases northwards with exposures around South Harbour being relatively weak and friable compared to the hard indurated rocks in the north of West Falkland at Port Howard and West Lagoons.

At Port Howard, sedimentary structures include graded bedding and cross bedding, which is common throughout, with foresets varying from 100 - 400 mm to 1-2 m. At South Harbour, lenticular bedding, shale rip-up clasts and cross-bedding are common. Cross-bed sets, corrected for local dip[1], from across the mapped sections (Fig. 2.3) show N-NW directed palaeocurrents in the south of West Falkland and NE-SSE directed palaeocurrents in the north of West Falkland. None were measured in the East Falkland section.

This difference in the sedimentary structures and maturity of the rocks implies a change in facies within the upper part of the Port Stephens Formation from north to south. In the south of West Falkland the main sequence consists of a shallow marine facies consisting of quartzites with skolithos burrows (D.T. Aldiss *pers. comm.* 1997) however, the upper part of the sequence at South Harbour is a fluvial facies. This fluvial facies shows northward palaeocurrents, low maturity and lenticular bedding and shale rip-up clasts. In the north of West Falkland the upper part of the Port Stephens Formation is a shallow marine tidal facies showing increased maturity and almost bipolar palaeocurrents. This change in facies represented in the upper part of the Port Stephens Formation indicates: (1) that the southern part of West Falkland was relatively elevated, possibly a basement high; (2) movement of sediment down a gentle northward palaeoslope from this basement high in the south into a shallow sea in the north.

The age of the formation is still poorly constrained. The trace fossil *Arthrophycus* has been recorded near Cape Meredith (Scasso & Mendia 1985) and implies an age of Ordovician to Silurian for the base of the formation based on correlation to its occurrence in Argentina. This fossil however is not conclusive proof

[1] In this case, and all further reference to palaeocurrents being corrected for local dip, the correction was calculated using the method outlined by Mustard (1989).

of age as *Arthrophycus* is found in Lower Cambrian (Alpert 1977, Crimes *et al.* 1977) to Silurian (Seilacher 1970) age rocks as well as Cretaceous (Frey & Howard 1970) to Tertiary age rocks (Roniewicz & Pienkowski 1977). Thistlewood *et al.* (1997), using K-Ar methods, have dated a set of dykes in the Cape Meredith Complex at 422±39 Ma which do not cut the Port Stephens Formation. This 422 Ma age is Silurian but the 2σ error bar covers the late Ordovician to early Devonian interval. This would imply that, in support of the presence of *Arthrophycus*, the base may be as old as late Ordovician but as young as early Devonian. However, given that the top of the formation is constrained by the Emsian age for the base of the overlying Fox Bay Formation (Marshall 1994a), an early Devonian age is unlikely for the base of the Port Stephens Formation as it leaves only a short time span in which to deposit 1250 m of quartz arenites. The South African lithostratigraphic correlative, the Table Mountain Group, shows a similar thickness of arenites which accumulated on a slowly subsiding stable shelf over a long period of time (Visser 1974). These show a distinct Hirnantian fauna of latest Ordovician age in the Cedarberg Formation (Cocks & Fortey 1986) (c.f. Fig. 2.14). If this is used as an analogy, then an Ordovician, or possibly early Silurian age for the base of the Port Stephens Formation is not unreasonable, so allowing time for deposition of the thickness of strata seen.

ii) Fox Bay Formation: The Fox Bay Formation, logged between Port North and Dunbar by Marshall (1994a) and mapped at Port Howard by the author, forms a 1250 m thick succession of alternating sandstones and shales. It is exposed across the middle of West Falkland from Fox Bay in the south to Port Howard in the north and Port North in the west, and in the north of East Falkland from Greenpatch in the east to San Carlos in the west (Fig. 2.5). Detailed stratigraphic logging at Port North (Fig. 2.6) by Marshall (1994a) and mapping at Port Howard has revealed five shale horizons on West Falkland. At Greenpatch on East Falkland, there are six shale horizons of greater thickness than on West Falkland (M.L. Curtis *pers. comm.* 1995, J.E.A. Marshall *pers. comm.* 1996). It was suggested by Baker (1924), following the discovery by Halle (1912) of poorly preserved plant fragments at Halfway Cove in Port Philomel, to further subdivide the Fox Bay Formation and isolate the upper part of it as the Port Philomel Formation based on this occurrence of fossil plants. This

division has not been followed in this study as Greenway (1972) found that it was not definable on aerial photographs and because the occurrence, or not, of plant fossils is not a valid definition for a mappable unit.

The sandstone units are composed generally of thinly bedded, fine grained (0.5 - 1 mm) dirty grey-brown, immature, micaceous sandstones (Table 2.1) with occasional shale rip-up clasts. The sandstones become coarser grained and quartz rich towards the top of the sequence as they grade into the overlying Port Stanley Formation. Sorting varies from poor to relatively good and grains range from sub-angular to sub-rounded and from sub- to non- spherical. The shale units are composed of fine-grained, dark grey, micaceous shales and siltstones showing thin light and dark laminations and often slightly undulatory bedding. Both the sandstone and shale units show sedimentary structures such as cross bedding, hummocky cross stratification and lode casts and these have been logged by Marshall (1994a) and are detailed in Figure 2.6. Observed cross-bedding directions in the sandstones, when corrected for dip, show varied orientations but with a consistent bipolar distribution. This is mainly NW-SE at Port North (Marshall 1994a), Port Howard and Greenpatch but swings to N-S around Rat Castle and Shag Cove (Fig. 2.5).

The basal shale in the formation shows a locally abundant invertebrate fauna of brachiopods, trilobites and crinoids which have been well documented by Morris & Sharpe (1846), Clarke (1913) and Edgecombe (1994). Their studies show that this fauna is part of the Malvinokaffric fauna found across Gondwana, and indicates that the base of the Fox Bay Formation is Lower Devonian (Emsian) in age. This age is further supported by palynological dating by Marshall (1994a).

The Fox Bay Formation, representing a tectonically more active period than the Port Stephens Formation, displays several cycles of deltaic deposition (c.f. Fig. 2.6), seen as deep water shales and shallower water slope and tidal facies sandstones, deposited on a generally northward palaeoslope. This cyclicity in sedimentation followed an initial flooding event, seen as the first and thickest shale horizon, which drowned the high energy shallow marine and fluvial environments of the Port Stephens Formation. The deltaic nature, and development of lobes in the Fox Bay Formation may have bearing on the varied distribution of palaeocurrent data across the islands (Fig. 2.5). There is an overall shallowing through out the sequence as the

shales become thinner and the sandstones more coarse grained up section until the base of the Port Stanley Formation.

iii) Port Stanley Formation: The Port Stanley Formation, 450 m - 700 m in thickness, is exposed across the northern parts of both East and West Falkland. It is defined by the first occurrence of well lithified grey-white quartzites which comprise the majority of the formation (Fig. 2.7) with a prominent orthoquartzite ridge towards the centre of the formation (Figs. 2.6, 2.7). The orthoquartzite ridge is the most commonly exposed part of the whole formation. Shales are rare but have been recorded as discrete horizons from the Port North section on West Falkland (Marshall 1994a) and as lenses in the Port Stanley section. The quartzites are dominated by medium to coarse-grained (1 - 2 mm) quartz grains which are sub-rounded to sub-angular showing low sphericity and sorting which varies from good to poor up the section. Towards the top of the formation, at both Port Howard and Port Stanley, the quartzites become greyer owing to an increase in fine-grained organic matter from 0 - 8% (Table 2.1). Cross-bedding appears throughout the sequence and, after correction for tectonic dip, can be seen to show a consistent northward palaeocurrent direction across both islands with a subsidiary E-W component (Fig. 2.8).

From palynological work in the shales at the top of the sequence at Port North (Marshall 1994a) no evidence was found for an age younger than Upper Devonian (Famennian) for the top of the Port Stanley Formation.

The Port Stanley Formation represents a period of high energy shallow marine sedimentation on a stable shelf where sediment, derived from the south, was extensively worked by wave action giving rise to the deposition of clean, mature quartzites.

2.2.3 Lafonian Supergroup

The Lafonian Supergroup (Greenway 1972) or Lafonia Group (D.T. Aldiss *pers. comm.* 1997), lying unconformably upon the Gran Malvina Group, occurs across the whole of southern East Falkland, Lafonia (from which the name of the Supergroup is derived). It is also present as a thin strip along the northern and eastern coasts of West

Falkland. The Supergroup is divided into Lower and Upper groups which in turn are divided into a number of formations. The subdivision into individual formations is still an area of confusion as various authors since Baker (1924) have suggested different nomenclature and boundaries for formations within the Supergroup.

i) Lower Lafonian Group: The Lower Lafonian Group, which outcrops across East Falkland and as a thin band along the north and eastern coasts of West Falkland (Fig. 2.2), is divided into the Bluff Cove, Lafonian Diamictite and Port Sussex formations which are detailed below.

Bluff Cove Formation. This formation, up to 200 m thick (Dawson 1967), is only found on East Falkland where it rests unconformably on the Port Stanley Formation (Baker 1924, Dawson 1967). The formation has been logged by Dawson (1967) and informally divided into a lower sandstone facies (150-180 m) and an upper shale facies (up to 45 m). The sandstone facies consists of well bedded, brown and greenish interbedded sandstones showing cross-stratification and bioturbation with minor interbeds of dark grey shale and light brown siltstone (Dawson 1967). The sandstones in this facies are immature showing good to poor sorting and angular to sub-rounded medium (0.3 mm) to fine (0.1 mm) sand-sized grains which are mostly quartz, but with a significant mica content. Palaeocurrents, derived from cross-bedding and alignment of occasional clasts, show a prominent W-E current direction (Dawson 1967). The shale facies is conformable with the underlying sandstones and consists of finely laminated dark grey-black siltstones and shales. At the top of this facies an increase in glacial dropstones has been recorded (Adie 1952a, Dawson 1967) and there is a conformable gradation into the overlying Lafonian Diamictite Formation.

The age of this formation can only be guessed at as there is no macrofauna and the preserved microfauna have all been affected by deformation so as to be unidentifiable. However, it has been attributed to the Late Carboniferous (Frakes & Crowell 1967).

The formation represents a period of glaciomarine sedimentation (Dawson 1967, Frakes & Crowell 1967), probably as turbiditic outwash deposits from glaciers

to the west, before the start of deposition of the main diamictite by grounded and floating glaciers (Frakes & Crowell 1967).

Lafonian Diamictite Formation. This formation, 350 - 850 m in thickness (Frakes & Crowell 1967), is found across East Falkland and as thin or isolated outcrops across the east and north coasts respectively of West Falkland (Fig. 2.2). The main body of the formation is a massive blue-black, weathering to a grey-brown, diamictite (Fig. 2.9) with visible clasts from 1 - 2 mm up to 7 m in size (Frakes & Crowell 1967). These are mainly granitic or metamorphic with minor sandstone, quartzite and silt/shale clasts (Fig. 2.10). The matrix is a gradation from sand-sized grains through silt to mud-sized material; the grains and clasts are sub-rounded to sub-angular, sphericity is variable and sorting is poor. The dominant component of the matrix is quartz (77 -88%) with minor feldspars (3.5 - 8%) and clay sized particles (micas and small quartz grains) (9 - 16%). The formation is not composed entirely of massive diamictite as Frakes & Crowell (1967) recorded linear sand bodies at Hill Cove and bedded diamictites towards the top of the sequence at Port Fitzroy. The basal sequences at Port Howard (2 m thick) and Carcass Bay (10 m thick) show bedded shales, sandstones and, at Carcass Bay only, a prominent boulder conglomerate. A narrow (5 m thick) bedded sequence is also seen at Shag Cove (Scasso & Mendia 1985) towards the centre of the formation.

The age of the formation is uncertain as there is no preserved fauna in the sequence. However, it has been assigned a Late Carboniferous to Early Permian age (Adie 1952a, Frakes & Crowell 1967). A further control on the age of this formation comes from the Dwyka Group, the South African lithostratigraphic correlative of the Lafonian Diamictite Formation, which has been dated as Late Carboniferous (Visser 1990). A more secure upper age constraint is provided in the Falkland Islands by the overlying Black Rock Member which has been dated, from bisaccate pollen, to be Early Permian in age (J.E.A. Marshall *pers. comm.* 1995).

The deposition of the Lafonian Diamictite Formation occurred in three main facies across East and West Falkland (Frakes & Crowell 1967). In the west, at Hill Cove, linear sand bodies are interpreted as eskers and imply grounded ice. Around Port Purvis contorted slabs of sandstone are found within the diamictite and imply a

slope facies and floating ice. In the east at Port Fitzroy, debris, mud and turbiditic flows with dropstones from floating ice rafts allow a more basinal facies to be inferred (Fig. 2.11) (Frakes & Crowell 1967). This facies change, coupled with a decrease eastwards of both mean and maximum clast sizes, implies an eastward palaeoslope from a relative high on West Falkland to a basin on East Falkland.

Port Sussex Formation. This formation, divided into the Black Rock and Shepherds Brook Members (Frakes & Crowell 1967), conformably overlies the Lafonian Diamictite Formation and is found across East Falkland and as isolated outcrops along the east coast and at West Lagoons on West Falkland. A laminated sandstone with dropstones has been identified as the basal unit on East Falkland (D.I.M. Macdonald *pers. comm.* 1996), however, this has not been identified in exposures on West Falkland. The Black Rock Member, which grades up from the diamictites below, varies from 20 m (West Lagoons) to 100 m (Carcass Bay) to 125 m (Frakes & Crowell 1967) in thickness and consists of interbedded dark grey to black shales and cherts with subsidiary sandstones and siltstones towards the top of the formation (Fig. 2.12). The sequence changes up-section with the shales becoming more grey and silty and the amount of chert beds decreasing upwards only to return again towards the top of the sequence at West Lagoons or be replaced by thin sandstone beds in the Carcass Bay section (Fig. 2.12). It is likely that the top of the Black Rock Member is missing at West Lagoons, as the sequence matches well with the basal 20 m of the Carcass Bay section where a further 80 m, not seen at West Lagoons, is exposed. However, it is also possible that West Lagoons represents a condensed sequence relative to Carcass Bay and that there never was 100 m of the Black Rock Member at West Lagoons.

An analysis of the organic carbon and kerogen contents show that on East Falkland (Port Sussex) the shales yield Total Organic Carbon (TOC) contents of up to 40% (mean 15.5%) and show a dominance of amorphous organic matter (AOM) (Marshall 1994b). In contrast, at West Lagoons and Carcass Bay on West Falkland, the shales yield TOC contents of 0 - 2.3% (mean 0.35%) (Table 2.2) and are dominated by phytoclast material rather than AOM. The West Lagoons exposure has

also yielded bisaccate pollen and trilete spores allowing it to be dated as Lower Permian (J.E.A. Marshall *pers. comm.* 1995).

. The Black Rock Member, which represents a marine transgression following a period of glaciation, shows a major facies change from West to East Falkland (c.f. Marshall 1994b). West Falkland is preserving a relatively proximal marine (probably outer shelf) facies, where coarse terrigenous clastics did not reach and which was supplied with terrestrial phytoclast and palynomorphs by distal turbidites. The resulting cherts in the Black Rock Member may have formed either from siliceous turbidites or from background hemipelagic sedimentation (Iijima *et al.* 1985). On East Falkland a more deeper/distal marine, basinal facies is preserved where the terrestrial input of phytoclasts did not reach and fully marine anaerobic conditions existed giving rise to AOM and high TOC values. These data indicate that the W-E palaeoslope seen in the Bluff Cove (Dawson 1967) and Lafonian Diamictite Formations (Frakes & Crowell 1967) continues throughout the formation of the Black Rock Member. The age of this member is Permian (Adie 1952a) confirmed as Lower Permian from bisaccate pollen preserved at West Lagoons (J.E.A. Marshall *pers. comm.* 1995).

A sequence, up to 100m in thickness (Frakes & Crowell 1967), of immature, fine grained, friable brown sandstones (cf. Table 2.1) interbedded with thin light grey shales containing numerous plant fragments rests conformably over the Black Rock Member. This unit, mapped by the author at Port Howard, Shag Cove and Carcass Bay, closely resembles descriptions by Adie (1952a) of a unit which has been defined as the Shepherds Brook Member by Frakes & Crowell (1967). Sedimentary structures, seen at Port Howard, include cross lamination, ripple sets, lode casts, nodules and channels, up to 50 cm deep, which lens out laterally into shales. Similar features have been seen by Scasso & Mendia (1985) at Shag Cove who interpreted the sequence as being predominantly quiet water deposition with occasional inputs of higher energy deposition.

The gradation into sandstones from the dark shales of the Black Rock Member indicates the input of terrigenous material, probably as turbidites, into the previously sediment starved, anaerobic basin.

ii) Upper Lafonian Group: The Upper Lafonian Group is believed to be up to 3000m in thickness (Baker 1924) and covers Lafonia in the southern half of East Falkland and a number of small islands such as the Tyssen and Swan Islands in the Falkland Sound (Fig. 2.2). Starting at the base, the group, consists of massive sandstones overlain by interbedded siltstones and soft sandstones which coarsen upwards. This is succeeded by a thick sequence of laminated sediments interbedded with thick massive sandstone beds commonly showing dewatering and lode cast structures. The laminites die out up-section and thick channelled, cross bedded sandstones dominate with interbedded laminated silty mudstones with abundant plant debris (see Fig. 2.13). The sequence (unpublished CASP report, D.I.M. Macdonald 1996) represents the progression from a basinal environment with turbidites through a shallowing upwards slope facies with mass flows grading into wave influenced sedimentation moving finally into a mostly emergent lower delta plain environment.

The sub-division of this group has been, and continues to be, a matter of dispute. Baker (1924) divided up the sequence into the Choiseul Sound, Brenton Loch, Bay of Harbours and West Lafonia Beds based on lithological criteria, Adie (1952a) identified the Lafonian Sandstone at the base of this sequence, named the Terra Motas Sandstone by Frakes & Crowell (1967). Work by CASP (D.I.M. Macdonald *pers. comm.* 1996) has endorsed similar divisions to that of Baker (1924). However, Macdonald (*pers. comm.* 1997) implies that no distinct boundaries can be seen and that Baker's (1924) and Adie's (1952a) Lafonian Sandstone, Choiseul Sound and Brenton Loch Beds are facies changes within one unit. The most recently revised lithostratigraphy of Lafonia (D.T. Aldiss *pers. comm.* 1997) takes a similar division to that of Baker (1924) with the inclusion of still further sub-divisions. As little work was undertaken in Lafonia by the author, this thesis presents no new data regarding the Upper Lafonian Group. So, until further research is carried out, the sub-division of this group shall remain unclear and throughout this thesis it shall be referred to simply as the Upper Lafonian Group.

The age of this group has been determined mainly on the identification of the abundant plant material mentioned above. Halle (1912), Baker (1924) and Adie (1952a) have identified these plants as belonging to the Gondwanian *Glossopteris* fauna and a Triassic age has been ascribed to the uppermost strata (Baker's West

Lafonia Beds) exposed around Cygnet Harbour and Egg Harbour (Seward & Walton 1923). This age has since been refined due to palynological samples collected at Egg Harbour yielding a microflora which has been dated as Late Permian (J.E.A. Marshall *pers. comm.* 1996) in age.

2.2.4 Dolerite Intrusions

On the islands there are three sets of dolerite dykes trending N-S, E-W and NE-SW (Fig 2.2, Greenway 1972, Taylor & Shaw 1989) which are thought to have formed contemporaneously (Mussett & Taylor 1994). Until recently they were mostly known from West Falkland where they cut through the Cape Meredith Complex (Cingolani & Varella 1976) and the Gran Malvina Group, decreasing in number northwards across the island (Greenway 1972). Recent research (M.J. Hole *pers. comm.* 1995) has shown there to be several NE-SW striking dykes on East Falkland which, although less abundant, are up to 30m wide and laterally extensive. The dykes, which consist of a groundmass of plagioclase feldspar and pyroxenes with phenocrysts of olivine and plagioclase feldspar and pyroxene, have been described variously as coarse grained dolerite (Greenway 1972) or microgabbro (Mussett & Taylor 1994).

The dykes have been dated as 192±10 Ma using K-Ar methods (Cingolani & Varella 1976) and 188±2, 189±3 and 190±4 Ma using ^{40}Ar-^{39}Ar stepwise degassing methods (Mussett & Taylor 1994). More recent K-Ar dating by Thistlewood *et al.* (1997) has revealed ages of 173±7 and 162±6 Ma. All these results indicate that they are early Jurassic in age.

2.3 Gondwanian comparisons

It has for a long time been noted that the stratigraphy and palaeontology of the Falkland Islands is part of the Gondwanian succession exposed in South America (Sauce Grande & Paraná basins) and South Africa (Cape & Karoo basins) (du Toit 1927, 1937). Researchers on the Falkland Islands have continually noted the close to identical similarity of the Falkland Island stratigraphy to that exposed in the South African Cape and Karoo Basins (e.g. Halle 1912, Clarke 1913, Baker 1924, du Toit

1927, 1937, Adie 1952a, Marshall 1994a), and especially to the Eastern Cape province (Adie 1952b). A correlation of the stratigraphy of the Paraná, Sauce Grande, western and eastern Cape & Karoo, Falkland Island and Ellsworth-Whitmore successions (Fig. 2.14) confirms these conclusions by previous workers. The strong similarities between the age and lithologies of these successions, initially noted by du Toit (1937), have since been refined as knowledge has increased over the last 60 years so that more precise correlation of specific horizons is now possible (cf. Fig. 2.14). The strong similarities between the successions can are summarised below:

(1) The overall dominance of quartz arenites in the Devonian sequences, save for the upper Ventana Group of the Sauce Grande Basin which is composed of greywackes (Lopez Gamundi *et al.* 1994).

(2) The prominent early Devonian (Emsian) flooding event with its distinct Malvinokaffric fauna.

(3) The Permo-Carboniferous glacial sediments.

(4) The overlying Permo-Triassic succession, of varying thickness in the basins, which shows an overall regressive sequence from starved basinal facies through flysch and prograding delta to fluvial and, in the Ellsworth, East Cape and Paraná successions, aeolian environments (see Fig. 2.14).

The correlation of the Falkland Islands stratigraphy to the South American, and Antarctic basins is good. However, this is weakened by the presence of Cambrian strata and poor correlatives to the Port Stanley Formation in both the Sauce Grande and Ellsworth Mountain successions. In contrast, the South African succession, although thicker, is almost identical to that on the Falkland Islands.

The remainder of this chapter will be devoted to looking at the correlation to South Africa and to recent evidence that supports Adie's (1952b) original correlation to the Eastern Cape province.

2.4 South African correlation

The correlation between the individual groups and formations of the Cape/ Karoo Supergroups of South Africa and the Gran Malvina Group/ Lafonian Supergroup of the Falkland Islands has long been established (eg. Baker 1924, Adie 1952a) (see Fig.

2.14). Existing data from the stratigraphy of the Falkland Islands only makes sense to South African correlations if the islands are rotated by 180°. This data includes:

(1) the position of the Lafonian and Karoo basins relative to the deformation front (Adie 1952a).

(2) the ice flow directions from the Lafonian Diamictite Formation and Dwyka Group (Visser 1987).

(3) the palaeocurrent directions in the Fox Bay Formation (Marshall 1994a) and Bokkeveld Group (Tankard & Barwis 1982).

(4) correlation of the Precambrian Cape Meredith Complex to basement in southern Natal (Thomas *et al.* 1995).

(5) palaeomagnetic data from the Jurassic dolerite dykes from the Falkland Islands and South Africa (Mitchell *et al.* 1986, Taylor & Shaw 1989).

What follows is a series of points raised from new evidence on the Falkland Islands that add further weight to this correlation.

2.4.1 Palaeocurrents

The palaeocurrent data from the Port Stephens, Fox Bay and Port Stanley Formations of the Gran Malvina Group on the Falkland Islands show a general northward palaeocurrent direction, especially in the Port Stanley Formation (see Figs. 2.3, 2.5 & 2.8). Data from the Lafonian Supergroup gives a general W-E palaeoflow for the Lower Lafonian Group (Dawson 1967) and a SW palaeoflow for the Upper Lafonian Group (Curtis & Hyam *in press*). Palaeocurrent data from South Africa shows a dominant southward palaeoflow direction for the Table Mountain (Rust 1973, Johnson 1991), Bokkeveld (Rust 1973, Theron 1970, Tankard & Barwis 1982) and Witteberg Groups (Hiller & Taylor 1992, Johnson 1991) of the Cape Supergroup. The Karoo Supergroup shows a dominantly E-W palaeoslope for the Dwyka Group in the Eastern Cape (Visser 1992) and a northward palaeoflow for the Ecca, Beaufort and Stormberg Groups (Johnson 1991). These palaeocurrents have opposite senses and only align if the Falkland Islands are rotated by 180° (Fig. 2.17).

2.4.2 The Black Rock Member

There is a distinct correlation of facies between the Black Rock Member (BRM) on the Falkland Islands and its correlative the Prince Albert, Whitehill, Collingham and Vryheid Formations of South Africa (Adie 1952a). On the Falkland Islands there are two clear facies on East and West Falkland. On East Falkland the black shales of the BRM are characterised by high TOC values (mean 15.5%) and abundant AOM and represent a basinal facies. In contrast, on West Falkland the BRM shows a high phytoclast content and low TOC values (mean 0.35%) and represents a more proximal shallower marine facies. The two are separated by a W-E palaeoslope across the Falkland Sound. There has been no occurrence of the *Mesosaurus* fauna on either East (Adie 1952a) or West Falkland. In the main Karoo basin the Whitehill Formation, which is a deep water anoxic facies, shows a progressive shallowing and thinning eastwards (Oelofsen 1987, Cole & McLachan 1991, Visser 1991b) and a decrease in organic carbon and AOM content to the north and north-east towards the basin centre (Rowsell & de Swardt 1976). The occurrence of the *Mesosaurus* fauna, characteristic of both the Karoo and Paraná basins also peters out eastwards (Oelofsen 1987). In the north and north-east of the Karoo basin, the Whitehill Formation disappears and is replaced by the Vryheid Formation which is characterised by coals formed from south-easterly prograding deltas (Cairncross 1989, Smith 1990).

There is thus a clear correlation between the basinal facies of the BRM on East Falkland and the basinal anoxic Whitehill Formation in the southern Karoo (Cole & McLachan 1991) which both show high TOC and AOM values and a lack of the *Mesosaurus* fauna (Marshall 1994b). The more proximal shallower marine facies of the BRM on West Falkland correlates to neither the southern Karoo basinal facies nor the deltaic coal and sandstone facies of northern Natal, instead it has close similarities to shales of the Ecca Group in southern Natal which show both low TOC values (mean 0.5%) (Rowsell & de Swardt 1976) and high phytoclast content, indicative of a distal prodelta facies (Visser 1993) (see Fig. 2.15).

Only when the Falkland Islands are rotated by 180° and placed against the Eastern Cape is: (1) the transition from basinal to shallow marine facies, not exposed along the east coast of South Africa, completed; (2) the easterly palaeoflow, indicated

by Visser (1992), consistent with the easterly palaeoslope (after rotation) from West to East Falkland indicated by the facies changes across the islands; and (3) the open end to the Karoo Basin closed, as first suggested by Adie (1952a).

2.4.3 The Bluff Cove Formation

Studies of the Bluff Cove Formation (Dawson 1967) on East Falkland have shown the interbedded sandstones, siltstones and shales to be glaciomarine in origin. These show W-E palaeocurrents and grade upwards into the overlying Lafonian Diamictite Formation (Dawson 1967). In South Africa the Kommadagga Subgroup, which is the uppermost part of the Witteberg Group and only found in the Eastern Cape, lies below the glacial Dwyka Group and has a similar stratigraphic position to that of the Bluff Cove Formation on the Falkland Islands (Fig. 2.14). The correlation of the Bluff Cove Formation to the Lower Dwyka Shales (Kommadagga Subgroup) was initially observed by Adie (1952a). Further work on the Kommadagga Subgroup (Loock 1967) reveals that it consists of sandstone, shale, siltstone and a diamictite (Fig. 2.16) which show overall E-W palaeocurrents and have an upper gradational boundary into the overlying glacial Dwyka Group. The environment of deposition for the Subgroup has been interpreted as pro-glacial (Loock 1967, Johnson 1976) however Swart (1982) considers them part of a deltaic sequence. Although the stratigraphy of the Kommadagga Subgroup is similar but not identical to the Bluff Cove Formation, based on: (1) the environment of deposition implied from the evidence of Loock (1976) and Johnson (1976); (2) their stratigraphic position as transitional beds between the quartzites of the Witpoort Formation and Lake Mentz Subgroup below and the glacial Dwyka Group above; and (3) their geographic distribution, being found only in the Eastern Cape, the Kommadagga Subgroup are correlated as being a direct correlative of the Bluff Cove Formation on East Falkland. The lithostratigraphic and palaeocurrent correlation of these two units only aligns when the Falkland Islands are restored to a palaeo-position east of the Eastern Cape having been rotated by 180° (Fig 2.17).

2.4.4 The Port Stephens Formation

The discovery of exposures of the Port Stephens Formation in the northern half of East Falkland provides a further link in positioning the Falkland Islands against the Eastern Cape in Gondwana reconstructions. With the islands placed east of Port Alfred, as in the original reconstruction by Adie (1952b), the newly found exposures of the Port Stephens Formation in the north of East Falkland lie directly along strike of known exposures of the Table Mountain Group at Port Elizabeth (Fig. 2.17) so completing the match of the Cape Supergroup/Gran Malvina Group stratigraphy.

2.4.5 The Parkhuis and Cedarberg Formations

The Uppermost Ordovician Parkhuis Tillite and Cedarberg Shale Formations of South Africa occur as a distinct horizon in the Table Mountain Group in the Western Cape (Fig. 2.14). These thin eastwards across the Cape with the Parkhuis Formation being completely absent in the Eastern Cape (Cocks & Fortey 1986). No presence of a Cedarberg or Parkhuis Formation correlative has been found in the Port Stephens Formation, the equivalent of the Table Mountain Group on the Falkland Islands. This could indicate, if the base of the Port Stephens Formation is old enough, that the Falkland Islands must have lain to the east of the Eastern Cape, beyond the eastern extent of this prominent horizon.

2.4.6 The Fox Bay Formation

Research in progress into the stratigraphy of the Fox Bay Formation on East Falkland shows up to 6 distinct shale horizons which correlate closely to those which are seen in the classic cycles of the Bokkeveld Group of South Africa (Tankard & Barvis 1982).

2.4.7 Summary

All of these new lines of evidence from the stratigraphy; (1) the palaeocurrents; (2) the correlation Black Rock Member to the Whitehill/ Collingham/Vryheid Formations; (3) the correlation of the Bluff Cove Formation with the Kommadagga Subgroup; (4) the matching of outcrops of the Port Stephens and Fox Bay Formations to stratigraphic equivalents in South Africa and; (5) the lack of the Parkhuis Formation, only found in the Western Cape, all go to increase the evidence that the Falkland Islands originally lay to the east of Port Alfred, Eastern Cape Province, in reconstructions of Gondwana and that they have since undergone a 180° rotation to lie offshore of Tierra del Fuego in the present day.

Formation	*Location*	*Quartz*	*Feldspar*	*Micas*	*Accessory*	*Organic*
Shepherds Brook	Carcass Bay	40	2	46	3	9
Member	Shag Cove	55	3	33	2	7
	AVERAGE	**47.5**	**2.5**	**39.5**	**2.5**	**8**
Bluff Cove	Bluff Cove-1	53	6	35	3	3
Formation	Bluff Cove-2	81	1	16	2	0
	AVERAGE	**67**	**3.5**	**25.5**	**2.5**	**1.5**
Port Stanley	Port Howard-1	88	1	11	0	0
Formation	Port Howard-2	87	1	12	0	0
	Port Stanley-1	85	0	13	2	0
	Port Stanley-2	73	2	14	3	8
	Chata Hill	92	0	6	2	0
	Shag Cove-1†	94	2	2	2	0
	Shag Cove-1†	85	8	3	0	6
	Mt. William†	95	0	2	3	0
	Tumbledown†	96	0	3	1	0
	AVERAGE	**88**	**1.5**	**7**	**2**	**1.5**
Fox Bay	Port Howard	68	7	16	2	7
Formation	Rat Castle	54	11	16	3	16
	Carcass Bay-1	46	2	41	1	10
	Carcass Bay-2	58	6	31	1	4
	Carcass Bay-3	49	8	34	4	5
	Carcass Bay-4	57	6	21	2	14
	San Carlos	53	9	30	0	8
	Shag Cove-1†	50	29	13	2	4
	Shag Cove-2†	60	30	11	2	5
	AVERAGE	**55**	**12**	**23**	**2**	**8**
Port Stephens	Port Howard-1	84	10	6	0	0
Formation	Port Howard-2	80	12	8	0	0
	South Harbour	70	11	17	2	0
	Malo Hills -1	78	5	16	1	0
	Malo Hills-2	67	9	24	0	0
	Shag Cove-1†	82	9	6	3	0
	Shag Cove-2†	80	12	6	2	0
	Shag Cove-3†	80	12	6	2	0
	Shag Cove-4†	95	0	3	2	0
	Cape Meredith†	73	22	4	1	0
	AVERAGE	**78.9**	**10.2**	**9.6**	**1.3**	**0**

Table 2.1: Composition, derived from point counting, of the lithologies from the main formations in the Gran Malvina and Lower Lafonian Groups. († data from Scasso & Mendia (1985))

Sample location	*Total Organic Carbon (TOC) (%)*
Hill Cove -A	0.2
Hill Cove -B	0.03
Hill Cove -C	0.1
Hill Cove -D	0
Hill Cove -E	0.07
Carcass Bay -20-1	0.21
Carcass Bay -20-2	2.3
Carcass Bay -20-3	0.17
Carcass Bay -20-4	0.24
Carcass Bay -20-5	0.21

Table 2.2. TOC contents from the Black Rock Member at Hill Cove/ West Lagoons and Carcass Bay, West Falkland (c.f. Fig. 2.12).

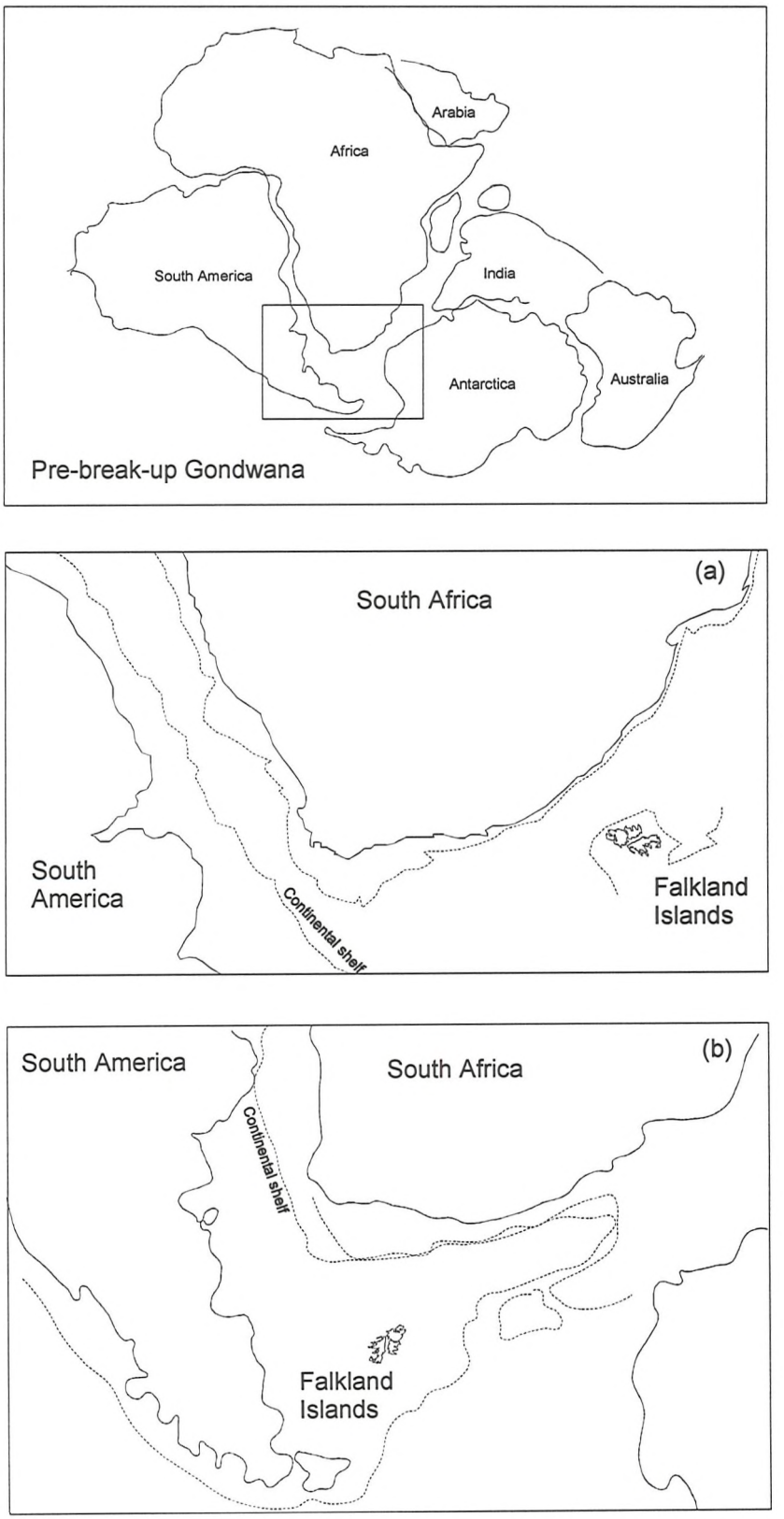

Figure 2.1: The two suggested positions of the Falkland Islands in a pre-break-up reconstruction of western Gondwana (map). (a) after Adie (1952b), (b) after de Wit *et al.* (1988).

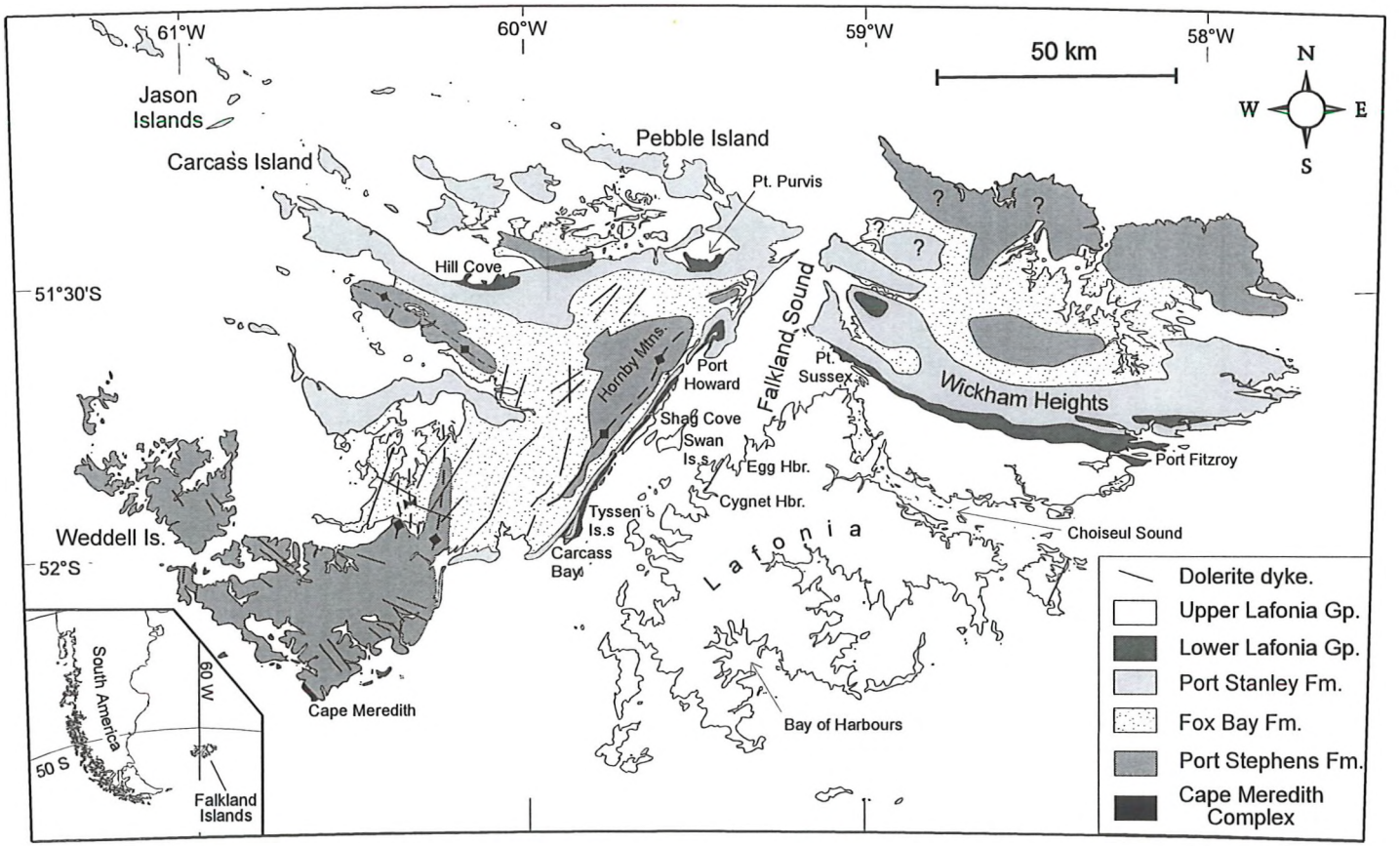

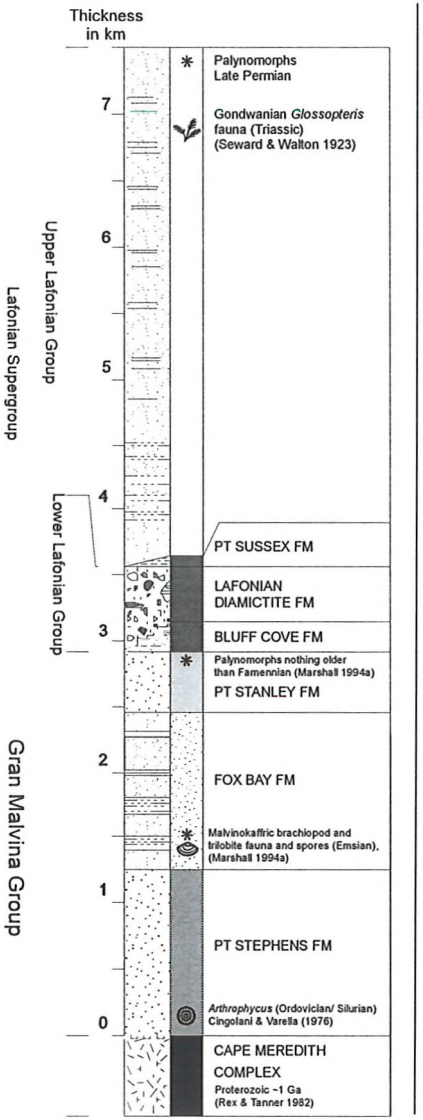

Figure 2.2: Geological map (modified from Greenway 1972) and stratigraphic column for the Falkland Islands(compiled from field observations, Lafonian Supergroup thickness after Baker 1924) .

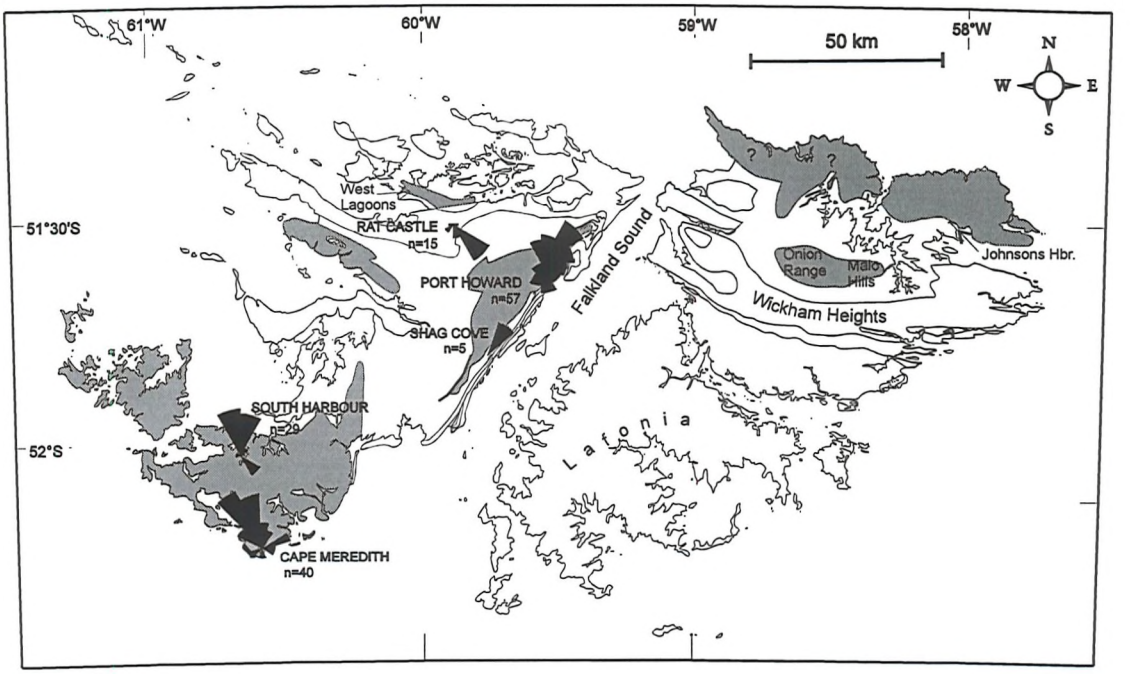

Figure 2.3: Map showing the outcrop extent ((shaded area) including newly discovered exposures in East Falkland) and palaeocurrent directions for the Port Stephens Formation on the Falkland Islands. Cape Meredith data from Cingolani & Varella (1976); Shag Cove data from Scasso & Mendia (1985).

Figure 2.4: Photograph, facing east, of quartz arenites of the Port Stephens Formation, Freezer Rocks, Port Howard, West Falkland. (UTM 21FUC225794).

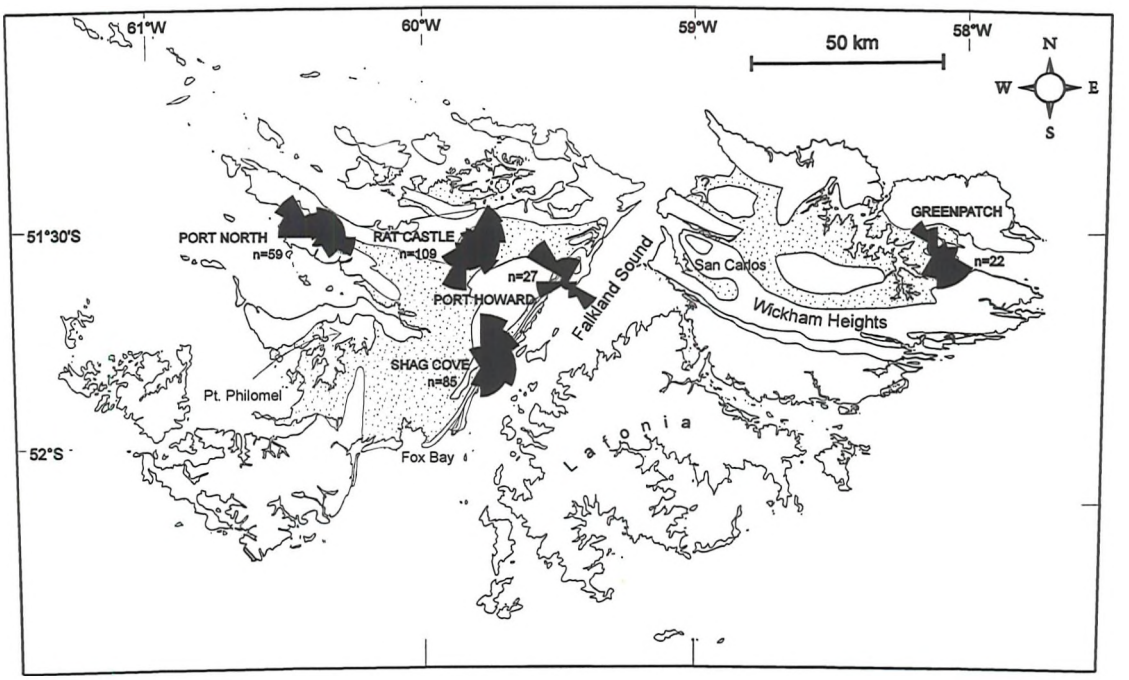

Figure 2.5: Map showing outcrop extent (shaded area) and palaeocurrent data for the Fox Bay Formation on the Falkland Islands. Port North data from J.E.A. Marshall *pers.comm.* (1995).

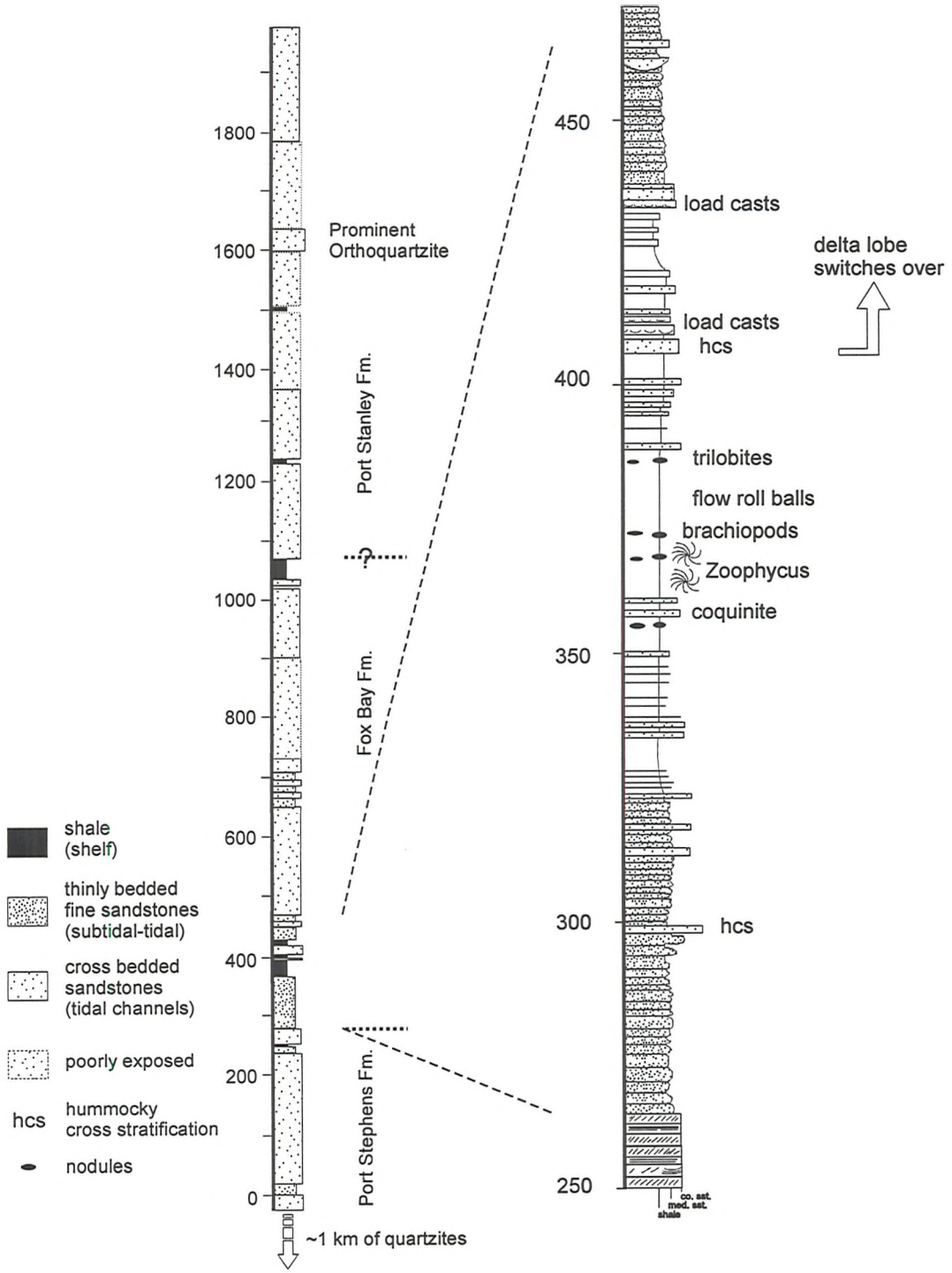

Figure 2.6: Stratigraphic log from the Port Stephens Formation to the Port Stanley Formation from western West Falkland, detail of sequence in the Fox Bay Formation shown on the right. (After Marshall 1994a).

Figure 2.7: Photograph, facing north, of quartzites of the Port Stanley Formation, Shag Cove, West Falkland. The prominent outcrop at the top of the cliff is the orthoquartzite ridge most commonly exposed across the Falkland Islands. (UTM 21FUC183646).

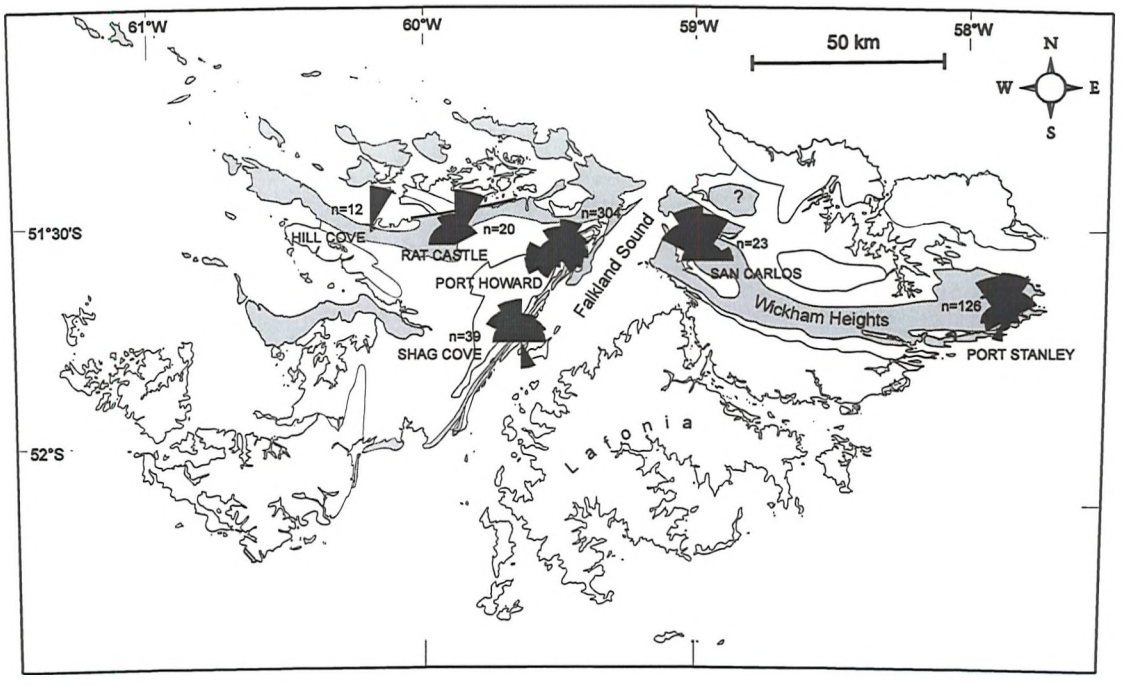

Figure 2.8: Map showing the outcrop extent (shaded area) and palaeo-current directions for the Port Stanley Formation on the Falkland Islands.

Figure 2.9: Photograph, facing west, of diamictite from the Lafonian Diamictite Formation, Bluff Cove, East Falkland. (Sub-vertical fabric are cleavage planes) Notebook shows a 5 cm scale bar (UTM 21FVC205678).

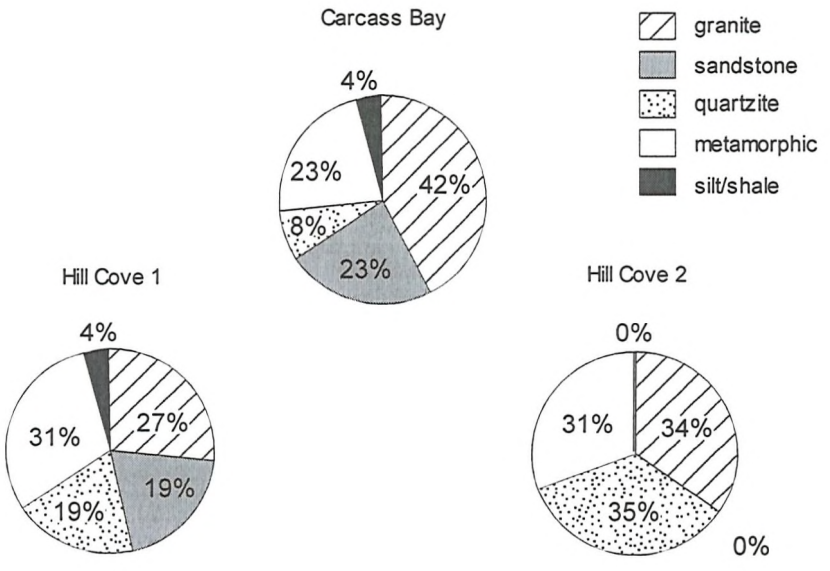

Figure 2.10: Pie Charts of clast counts from the Lafonian Diamictite Formation at Hill Cove and Carcass Bay, West Falkland.

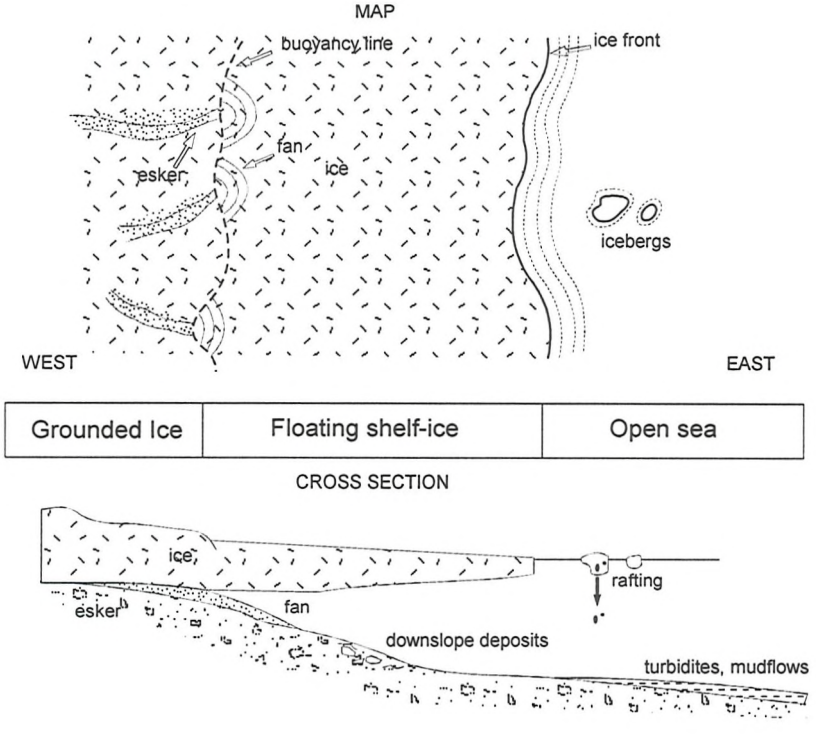

Figure 2.11: Diagramatic representation of paleaogeography across the Falkland Islands during deposition of the Lafonian Diamictite Formation. From Frakes & Crowell (1967).

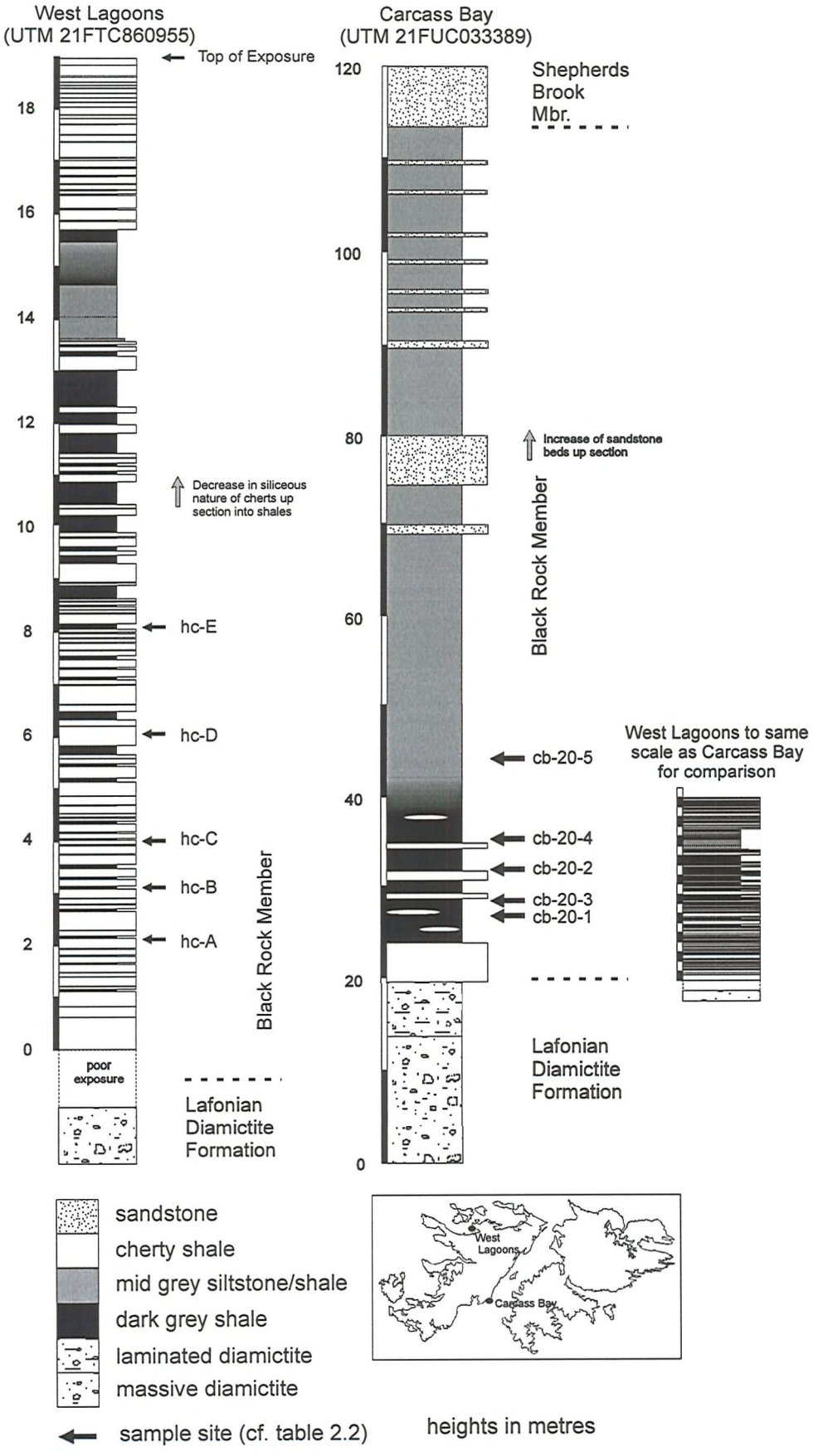

Figure 2.12: Stratigraphic log sections of the Black Rock Member from West Lagoons and Carcass Bay, West Falkland.

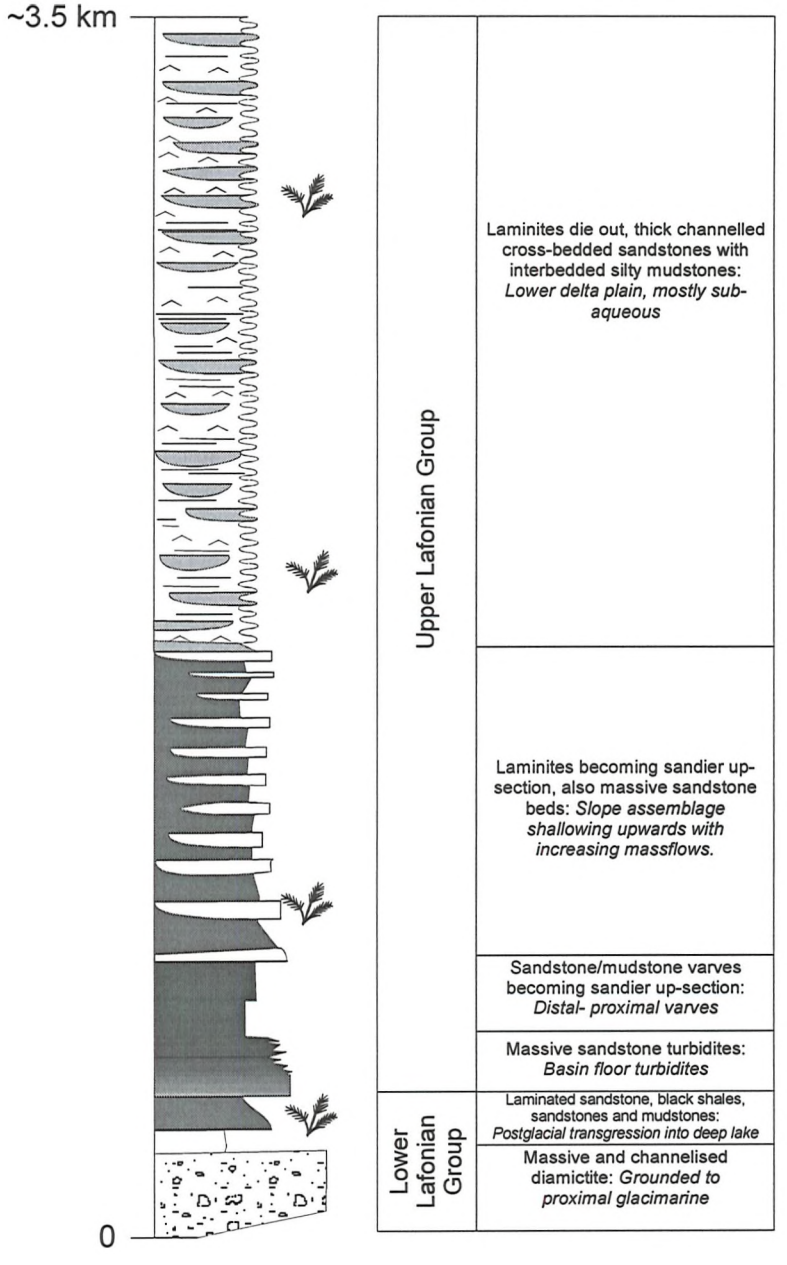

Figure 2.13: Schematic lithostratigraphy with interpretation of depositional environments for the Lafonian Supergroup. After Macdonald (*pers. comm.* 1996). Scale is approximate as the exact definitions of units is still a matter of dispute (see text). Leaf symbol denotes the presence of plant fossils.

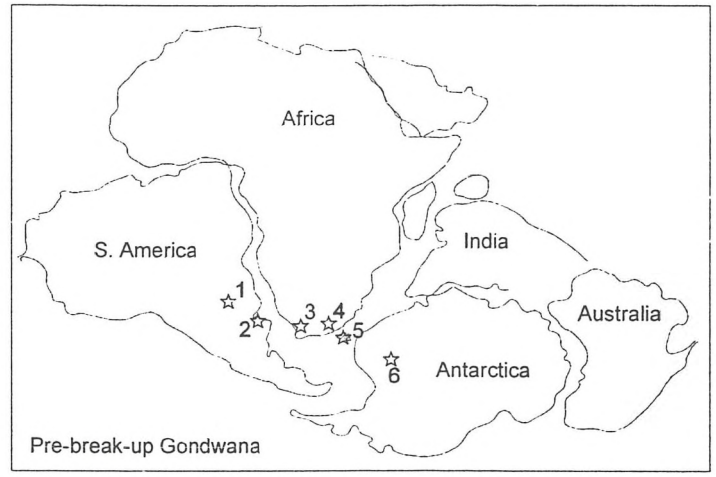

Figure 2.14: Correlation chart across western Gondwana showing lithological and chronological correlation. Ages of formations are shown as Є (Cambrian), O(Ordovician), S (Silurian), D (Devonian),C (Carboniferous), P (Permian), Tr (Triassic), J (Jurassic), K (Cretaceous). Ellsworth Mountains after Webers *et al.* (1992), Eastern and Western Cape after Cloetingh *et al.* (1992), Sierra de la Ventana after Selles-Martinez (1989), Parana after Sanford & Lange (1960) and Zalan *et al.* (1991).

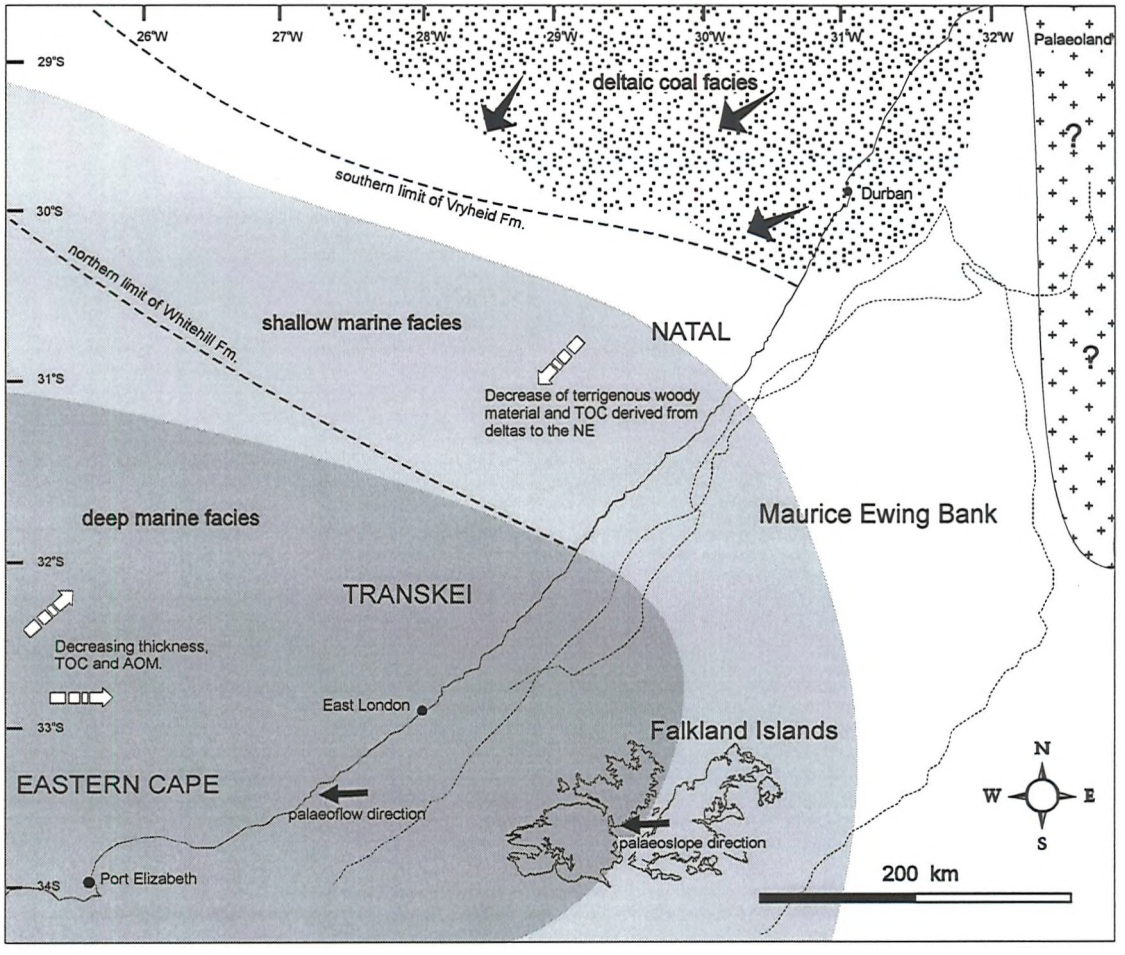

Figure 2.15: Schematic palaeogeography of the South African Whitehill Sea with an extension over the Falkland Islands. The deeper water organic shales of East Falkland correlate to the Whitehill Formation of the southern Karoo whilst the more shallow water, terrestrially influenced facies of West Falkland correlate to prodelta and shelf facies of southern Natal, influenced by the coal deltas of the Vryheid Formation in the north of Natal. After Cole & McLachan (1991), Cole (1992), Visser (1992, 1995), Marshall (1994b).

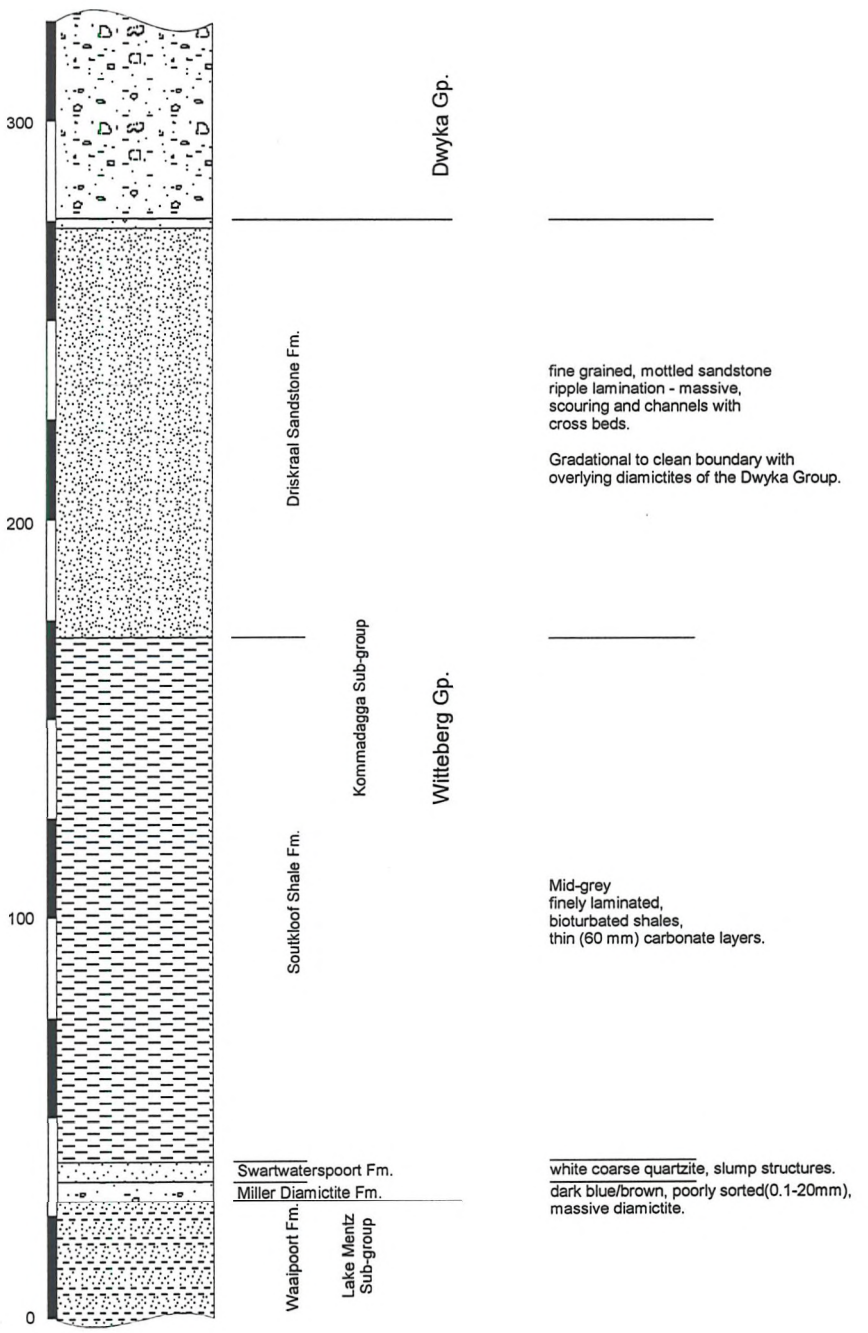

Figure 2.16: Composite stratigraphic log of the Kommadagga Subgroup. Scale in metres. (After Loock 1967, SACS 1980, Swart 1982).

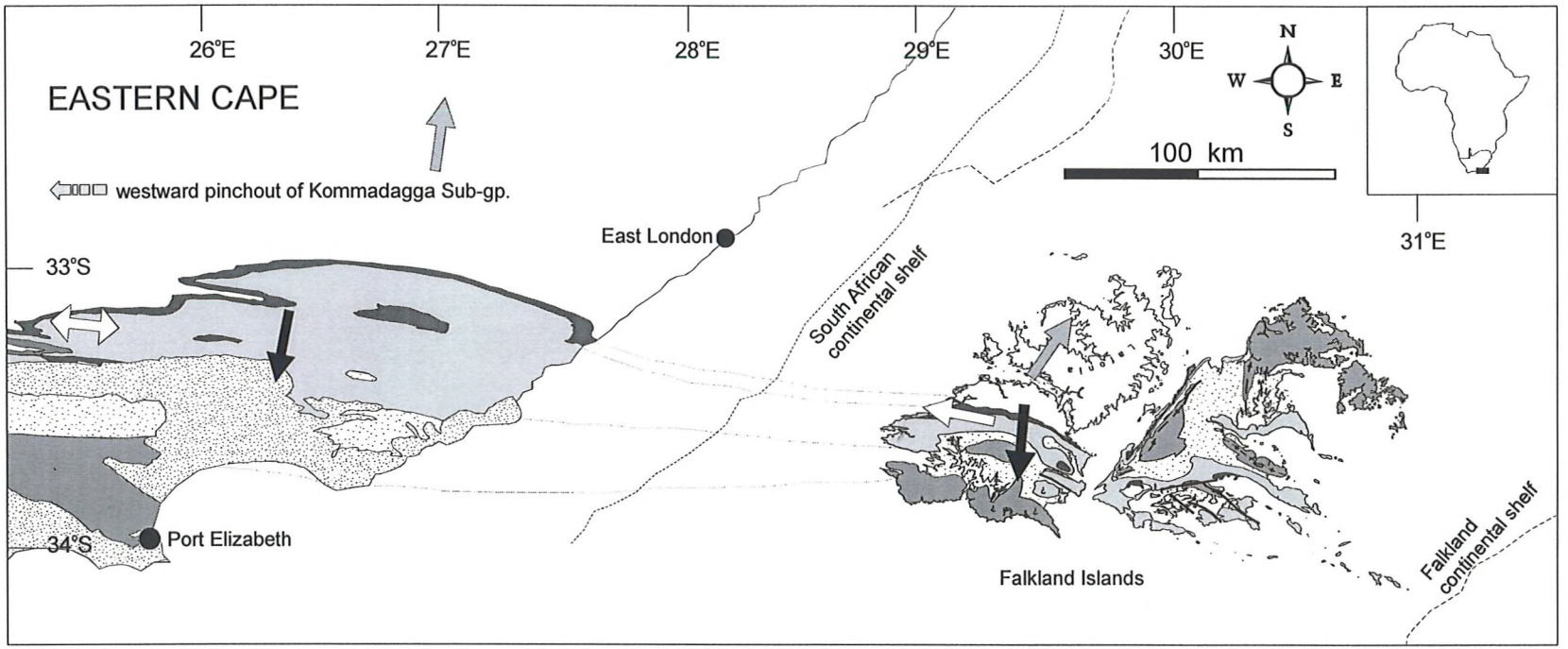

Figure 2.17: Restoration of the Falkland Islands against the Eastern Cape of South Africa showing recent stratigraphic correlations. These include palaeocurrent data from the Gran Malvina Group/ Cape Supergroup, Bluff Cove Fm./Kommadagga Sub-group and Lafonian/Karoo Supergroups and matching of the complete Gran Malvina Group stratigraphy to that exposed in the Eastern Cape.

Chapter 3: Carboniferous diamictite dykes on the Falkland Islands

The following chapter, Chapter 3: *Carboniferous diamictite dykes on the Falkland Islands*, has been published as a paper with the Journal of African Earth Sciences (Vol. 26, no. 4, p505-517) under the joint authorship of D.M. Hyam, J.E.A. Marshall and D.J. Sanderson. The content of the chapter is unchanged from the published manuscript save for the abstract which has not been included here.

The manuscript was written by D.M. Hyam, except for the first three paragraphs of section 3.5 which were written by J.E.A. Marshall. Processing and identification of spore taxa, as well as vitrinite analysis were also undertaken by J.E.A. Marshall. Discussion with J.E.A. Marshall and D.J. Sanderson, reviews by M.J. Hambrey, J.N.J. Visser and D.I.M. Macdonald and editorial comments by B.C. Storey have all contibuted to the final manuscript.

Chapter 3: Carboniferous diamictite dykes in the Falkland Islands

3.1 Introduction

The Falkland Islands are an archipelago comprising two main islands, East and West Falkland, and several hundred smaller islands. The islands are found in the South Atlantic Ocean, lying 600 km east of Patagonia between 51° and 52°30'S and 57°30' and 61°30'W. They form the only emergent part of the Falkland Plateau which is a spur at the southern end of the South American continental shelf extending eastwards for 1500 km (Fig. 3.1).

This chapter describes previously undiscovered sedimentary dykes, filled with diamictite, which have been found on both East and West Falkland during an investigation for a possible Ordovician bedded tillite mentioned by Baker (1924). The dykes have been intruded downwards and are found in three separate formations, two of Devonian and one of Carboniferous age. Absolute and relative dating of the dykes shows there to be two groups, an Early Carboniferous group, formed during the main period of ice coverage of the Gondwana glaciation and an Early Permian group, formed during the early stages of diamictite deposition towards the end of the glaciation. The presence and depth of burial, determined by vitrinite reflectance, of the Early Carboniferous group of dykes, found only on West Falkland, has new implications for the palaeogeography of the Falkland Islands during the Gondwana glaciation.

3.2 Geology of the Falkland Islands

A simplified geological map of the Falkland Islands is shown in Fig. 3.1 and a detailed stratigraphy in Fig. 3.2d. Precambrian crystalline basement is exposed only at Cape Meredith on West Falkland. Unconformably overlying this crystalline basement is a clastic, sandstone- dominated, sequence, referred to as the Gran Malvina Group (Borrello 1963), which covers the north of East Falkland and most of West Falkland. It has been divided into three units: the Silurian/Ordovician? (Scasso & Mendia 1985) Port Stephens Formation, the Devonian (Marshall 1994a) Fox Bay

Formation and the Port Stanley Formation, the top of which is not likely to be older than Famennian (Late Devonian) in age (Marshall 1994a). Lying disconformably above the Gran Malvina Group is the Lafonian Supergroup (Greenway 1972), a sequence of Permian age clastic sediments, divided into Lower and Upper Lafonian Groups, present in the southern half of East Falkland (Lafonia), and along the east coast of West Falkland. The basal unit to the Lower Lafonian Group is the Lafonian Diamictite Formation, which, on East Falkland, is underlain by the Bluff Cove Formation (Adie 1952a). This formation disconformably overlies the Port Stanley Formation (Dawson 1967) and is conformable with the overlying Lafonian Diamictite Formation. The Lafonian Diamictite Formation is conformably overlain by the Port Sussex Formation (Frakes & Crowell 1967), which comprises a conspicuous organic-rich black mudstone, a clear lithostratigraphic correlative of the Whitehill Formation in South Africa (du Toit 1927). Above this is a thick clastic sequence of the Upper Lafonian Group, covering most of the southern half of East Falkland, the top of which is of late Permian age. Dolerite dykes of Jurassic age (Mussett & Taylor 1994) are found on both East and West Falkland intruded throughout the stratigraphic sequence, although they are much more common in the Devonian strata.

Despite the close proximity of the Falkland Islands to South America, both the structure and stratigraphy correlate more closely with those of southern Africa. This includes correlation of Precambrian basement in Natal to the Cape Meredith Complex (Thomas *et al.* 1995), the Cape Supergroup to the Gran Malvina Group using palaeontology (Clarke 1913, Edgecombe 1994) and stratigraphy (Baker 1924, Marshall 1994a), and Karoo Supergroup to the Lafonia Supergroup (du Toit 1927, Adie 1952a, Frakes & Crowell 1967). This close correlation to the Cape Fold Belt and Karoo Basin has lead to widespread acceptance of reconstructions of Gondwana in which the Falkland Islands are rotated by 180° and emplaced against the eastern coast of South Africa (Adie 1952b, Visser 1987, Marshall 1994a). These reconstructions are consistent with palaeomagnetic evidence (Mitchell *et al.* 1986). However Richards *et al.* (1996) present contrary ideas that the Falkland Islands have only passively rotated by 60° during opening of the South Atlantic and were not attached to eastern South Africa, instead lying some 500 km south of Cape Town in the Western Cape.

3.3 Sedimentary Dykes

3.3.1 South Harbour (60°44'W 52°00'S)

Baker (1924) first noted that a tillite was present in the South Harbour area (Fig. 3.2a) when studying a collection of hand specimens that were made available to him. His impression was that they were possibly related to the Ordovician-aged Pakhuis Tillite of South Africa. Subsequent study (Frakes & Crowell 1967)has failed to locate this tillite. However, this study at South Harbour in the SW of West Falkland, has revealed 11 sedimentary dykes in the Port Stephens Formation, which is here developed as fluvial arkosic sandstones (Fig. 3.2a). These dykes mark conspicuous depressions in the low cliffs which can be easily traced across the wave-cut platform (Fig. 3.3). The dykes take the form of sub-vertical, straight, parallel-sided sheets of diamictite which are discordant to the surrounding flat-lying sandstones. The Port Stephens Formation shows no evidence of displacement across the sedimentary dykes nor are there any signs of brecciation as a result of the dyke emplacement. The width of the dykes ranges from 0.2 - 3.4 m with individual dykes showing no appreciable vertical changes in width. One dyke can be traced laterally across tidal flats for up to 600 m (Fig. 3.3). The exposed vertical extent of the dykes is 1 - 10 m. However, the true extent is unknown as outcrop is limited to low cliffs, tidal flats and rare inland exposures. A total of only 30 m of stratigraphy has been observed to contain the dykes. The dykes are dominantly oriented N-S, although three show an approximately E-W direction (Fig. 3.2e). These orientations correspond to local jointing patterns in the Port Stephens Formation.

The lithology of the dykes consists of a grey-brown, weakly cemented, fine to coarse grained, quartz-rich arenaceous matrix with poorly sorted clasts up to 50 mm in size consisting mainly of quartzite with minor igneous, metamorphic and clastic sedimentary fragments (Fig. 3.4). In thin section, the majority of the rock consists of poorly sorted, rounded to sub-angular, elongate to spherical quartz grains of varying sizes from coarse sand to silt. The clasts are mostly grain-supported with interstitial spaces filled by clay sized particles (Fig. 3.5). Vertical, side-parallel lamination is common towards the margins of many of the dykes, the centres of the wider dykes

being massive in character. In the field, these laminations appear as lighter and darker grey coloured bands within the arenaceous matrix. In thin section, the laminae appear as finer and coarser grained bands with a preferred orientation of elongate grains parallel to the lamination (Fig. 3.6). There is a general fining of grain-size towards the edges of the dykes and in four dykes a mudstone bed 20 - 50 mm thick is developed at both margins of the dyke (Fig. 3.7). Microfossil plant fragments and spores have been found in two of these dykes, enabling the dykes to be dated palynologically.

3.3.2 Bluff Cove (50°10'W 51°45'S)

A single sedimentary dyke, oriented N-S (Fig. 3.2e), was located by Dawson (1967) in the Bluff Cove Formation at Bluff Cove, East Falkland (see Fig. 3.2a). It is a sub-vertical, parallel-sided, slightly sinuous sheet which shows smooth, unbrecciated walls and varies laterally in width from 0.7 - 0.9 m. The orientation of the dyke is the same as that of the dominant joint set in the area. It consists of a light grey, brown-weathering, sand-rich, diamictite (cf. Dawson 1967) which consists mostly of poorly sorted fine to coarse sand sized grains surrounded by a more silt and clay rich matrix. The rock also contains clasts up to 10 - 20 mm. Faint side-parallel vertical laminations can be picked out from grain alignments but no mudstones are developed at the margins. Small reverse shears cutting the dyke are produced by a later N-S compressional event.

3.3.3 Monty Dean's Creek (58°08'W 51°30'S)

A single dyke within the Fox Bay Formation was found in Monty Dean's Creek to the south of Port Louis Harbour on East Falkland (see Fig. 3.2c). It strikes NE-SW, and dips steeply to the NW (Fig. 3.2e). The dyke is filled with a pale grey-brown, poorly sorted diamictite which is composed mostly of fine to coarse grained, sand-sized quartz grains with minor feldspar ranging from 5 - 20 mm in size. In thin section, interstitial spaces can be seen to be filled with a clay and silt-sized matrix. The

overall lithology of this dyke is almost identical to that seen in both the South Harbour and Bluff Cove dykes.

3.4 Comparison to the Lafonian Diamictite Formation.

As noted earlier, Baker (1924) described a loose hand specimen from South Harbour as a tillite, similar to the Lafonian Diamictite on East Falkland. A similar interpretation as a glacial diamictite was made by Dawson (1967) when first describing the dyke material at Bluff Cove. Flint *et al.* (1960a, b) defined a diamictite as "any non-sorted or poorly sorted terrigenous sediment that consists of sand and/or larger particles in a muddy matrix." (Flint *et al.* 1960a, p509). In the case of the Lafonian Diamictite Formation on the Falkland Islands, Frakes & Crowell (1967) have clearly interpreted it as a glacial diamictite with clasts up to 7 m across in a fine grained "clay-sized" matrix. In order to compare the dyke material with the diamictite within the Lafonian Diamictite Formation, a petrographic comparison including modal analysis and clast counting has been undertaken, the results of which are presented below.

3.4.1 Petrographic Comparisons

The Lafonian Diamictite Formation is essentially consistent across the Falkland Islands. When fresh it is blue-grey, weathering to a grey-brown, with visible clasts up to several metres in size. The matrix is a poorly sorted mixture of sand, silt and mud-sized material; grains and clasts are sub-rounded to sub-angular, sphericity is variable and sorting is poor (Fig. 3.8). A modal analysis (Fig. 3.9a) on thin sections from samples of known diamictite from Port Howard, Carcass Bay, Hill Cove and Bluff Cove shows that the rock is dominated by mono- and polycrystalline quartz grains with lesser amounts of feldspar and mud sized matrix. A count of *in situ* clasts at Hill Cove and Carcass Bay (Fig. 3.9b) shows that granite and metamorphic clasts are generally dominant with sandstone, silt/shale and quartzite clasts in varying proportions.

The dyke material is grey when fresh, weathering to a grey-brown colour. The matrix appears to be more sandy than that of the Lafonian Diamictite Formation, possibly a reflection of the source of the material (Hambrey 1994) or of the nature of formation of the diamicton, the more sandy matrix being terrestrial in nature, the more clay-rich being glaciomarine. However, the same poorly sorted gradation from sand through silt to mud-sized material is seen in the dykes. A modal analysis of thin sections from dykes at Bluff Cove, Monty Dean's Creek and four from South Harbour show an almost identical distribution of quartz, feldspar and clay-sized matrix to that obtained from the Lafonian Diamictite Formation at Port Howard, Carcass Bay, Hill Cove and Bluff Cove (Fig. 3.9a) and the values obtained fall within the boundaries of a similar analysis by Frakes & Crowell (1967) at Hill Cove. Clast counting from South Harbour shows a quartzite and sandstone dominated distribution with subsidiary granite, metamorphic and sedimentary clasts. As noted earlier this is probably due to differences in the source of the material (Hambrey 1994).

From these analyses, it is clear that the dykes share common characteristics such as modal distributions, overall appearance and texture with known diamictites of glacial origin from the Falkland Islands. The dykes also meet the criteria of Flint *et al.* (1960a ,b) for a diamictite, being poorly sorted with grain-sizes varying smoothly from pebble to clay-sized material. This supports the original observations by Baker (1924) and Dawson (1967) that dykes are filled by glacigenic diamictite.

3.5 Age

Palynological dating was attempted on several of the dykes which showed the development of mudstone at the margins. Of those analysed, positive results were obtained from only two dykes at South Harbour (Fig. 3.2a, localities *1 and *2) on West Falkland. At locality *1, the palynomorphs were recovered from within vertically laminated mudstone containing plant fragments at the margins of the dyke. At locality *2 the palynomorphs were retrieved from a dark grey, argillaceous diamictite in the central part of the dyke. The palynomorphs from both dykes are well preserved and are generally diverse although not particularly abundant. Both dykes have a comparable palynological assemblage; Table 3.1 lists significant taxa which

could be identified. The dominant elements are trilete spores with saccate pollen forms being very rare.

Within the assemblage from the diamictite dykes conspicuous taxa include *Indotriletes kuttungensis*, *Reticulatisporites magnidictyus*, *Acetospora carnosa* and *Grandispora* cf. *maculosa* (Fig. 3.10). In addition there are a number of unidentified and probably as yet undescribed taxa. The presence of the identified forms is significant in that they are characteristic of the interval which pre-dates the incoming of conspicuous saccate pollen in Namurian times (Powis 1984, Jones & Truswell 1992).

The palynological assemblage is distinctively different from, and older than that which characterises Dwyka and younger rocks from South Africa (Anderson 1977, McRae 1988). This immediately highlights a problem in finding comparative microfloras, since no palynomorphs of this age have been reported within South Africa. In South America, the situation is little better, with very few documented and independently dated microfloras of this age (e.g. Azcuy 1981). The best described microfloras which are comparable are from the Carboniferous of Australia (Playford & Helby 1968, Powis 1984; Jones & Truswell 1992).

Within eastern Australia, comparable spore assemblages have now been correlated (using brachiopods) to the European sequence and can be regarded as late Visean to early Namurian in age (Roberts *et al.* 1993). Therefore it is likely that these Falkland Island sedimentary dykes formed at some time within the late Visean to early Namurian interval. The palynomorphs were probably derived locally from spore-bearing plants growing close to the edge of the glaciers, a feature recognised in similar glaciogenic sedimentary rocks in both South Africa (McRae 1988) and western Australia (Backhouse 1991). The possibility that this spore assemblage has been reworked from strata eroded before the main onset of glacial sedimentation, and therefore not preserved anywhere else in the stratigraphy is dismissed because the sampled dykes have assemblages which are too similar and internally consistent to have been randomly derived from reworking.

The age of the two diamictite dykes on East Falkland at Bluff Cove and Monty Dean's Creek cannot be determined palynologically as no mudstone fraction was present in the dykes, however relative age dating can be achieved. The Bluff Cove

dyke has a sinuous outcrop which Dawson (1967) supposed was caused by post-injection deformation of the dyke. A similar situation is recorded in the Eastern Cape of South Africa (Whittingham 1980) where a tillite dyke is found in strata of the Kommadagga Formation which is of a similar stratigraphic position to the Bluff Cove Formation beneath the glacial sediments. The dyke was interpreted as having formed after the induration of the host rock and during the early stages of glacial deposition as the tillite in the dyke correlates closely to local basal Dwyka sediments. It could therefore be implied that the Bluff Cove sedimentary dyke formed similarly in the early stages of glaciation in the Late Carboniferous, but before the onset of deformation in the Early Permian (Hälbich *et al.* 1983). Evidence is less conclusive for the dyke at Monty Dean's Creek as exposure is poor, although it would not be unreasonable to assume a similar age to that of the dyke at Bluff Cove.

3.6 Vitrinite Reflectance

Vitrinite reflectivity values of 0.79% and 1.1% have been determined from the organic matter isolated from the South Harbour dykes. The higher reflectivity value can be discounted as it is from a diamictite dyke close to Jurassic igneous dykes and has probably been affected by contact metamorphism. The value of 0.79% contrasts with vitrinite reflectivities of 1.8 - 2.2% from the Permian Port Sussex Formation in eastern West Falkland and around 4% in East Falkland (Marshall 1994b). It would be expected that Visean - Namurian aged rocks, found lower down the stratigraphy, should yield higher reflectivities. Instead the dyke-infills yield a markedly lower reflectivity. This value shows that since mid-Carboniferous times the SW area of the Falkland Islands has only ever undergone shallow burial in the order of 2 - 3 km (calculated using the methodology of Creaney 1989). It is possible that this value has been increased due to the close proximity of the Cape Fold Belt deformation to the north. If so, then it would be expected that the vitrinite reflectance derived purely from burial without this added effect would be lower and would therefore imply that burial was less than the 2 - 3 km given here. This burial history suggests that the Lafonian Supergroup was not deposited in its entirety in the SW of the Falkland Islands.

3.7 Dyke Formation

Clastic dykes are commonly produced by one of two processes: either injection of material from below (e.g. Hayashi 1966, Hiscott 1979, Taylor 1982, Dixon *et al.* 1995) or from above (e.g. Vitanage 1954, Hayashi 1966, Young 1972, Eyal 1988, Chown & Gobiel 1990). In the case of the clastic dykes seen on the Falkland Islands, the palynological date is younger than the host rock and demonstrates unequivocally that the dykes were sourced from above. This is supported by the fact that Precambrian crystalline basement occurs beneath the Port Stephens Formation with no intervening shales which could act as a source for the fossiliferous mudstone bands in the dykes.

Clastic dykes fed from above may form from either downward injection of a liquefied sediment due to overlying pressure (Hayashi 1966, Young 1972, Chown & Gobiel 1990) or passive infilling of fractures (Eyal 1988). Downward injection may result in features such as brittle deformation of host and dyke material (Young 1972), uneroded walls (Vitanage 1954) and lamination parallel to the side walls (Young 1972, Chown & Gobiel 1990), probably due to viscous fluid flow. Commonly, the downward injection of the sediment is initiated by the pressure of overlying sediments, or possibly ice (Chown & Gobiel 1990).

Passive infilling of open fissures results in sediments which are brecciated, contain large fallen blocks of the overlying sediment and which show no side-parallel lamination (Eyal 1988). Such features, associated with passive infilling, are not found in the Falkland Islands sedimentary dykes.

The sedimentary dykes seen on the Falkland Islands would appear to have been formed by the downward injection of a semi-fluidized sediment rather than the passive infill of open fissures. This is supported by the presence of parallel uneroded walls, side-parallel laminations and the grading of clasts from coarse to fine towards the edges indicating fluid flow (Bagnold 1954) and also by the lack of brecciation or fallen blocks from the surrounding host rock.

3.8 Discussion

The material of the dykes is a diamictite and is of similar modal composition to more arenaceous parts of the Lafonian Diamictite Formation found across the Falkland Islands, especially on West Falkland. This formation is the direct litho- and chrono-stratigraphic correlative of the Dwyka Formation of South Africa (Adie 1952b), and is considered to be Late Carboniferous (Stephanian) to Permian (Visser 1990, Loock & Visser 1992). This is clearly significantly younger than the late Visean to early Namurian age determined palynologically from the dykes at South Harbour. The age of the dykes falls within a time period that was a major sedimentary hiatus and period of erosion (Veevers & Powell 1987, Visser 1987) or non-deposition (Loock & Visser 1992) throughout central Gondwana (Africa, Falkland Islands, India, West Antarctica). Only at the edges of Gondwana, in western South America (González-Bonorino 1992) and Australia (Veevers & Powell 1987), was sedimentation occurring throughout the Carboniferous period. The Carboniferous age of the dykes on the Falkland Islands suggests that they represent a rare record of sedimentation during a time when, throughout central Gondwana, polar and subpolar ice sheets were advancing across the continent (Veevers & Powell 1987, Visser 1987, 1991a, González-Bonorino & Eyles 1995).

To preserve evidence of the glacial episode would mean that, following a period of erosion, debris from the basal ice zone was injected downwards as a viscous sediment, exploiting a pre-existing joint system. This could have taken place either (1) during advance of an ice sheet where the weight of overlying ice causes liquefaction and downward injection of the diamicton, or (2) during retreat of an ice sheet where the retreat of ice, frozen to the substrate, creates stresses which may open fractures into which semi-fluidized sediment can be later injected when conditions become more temperate (Pusch *et al.* 1990). This would imply a grounded rather than floating glacier to provide the downward pressure or stresses during ice movement. This is similar to the conclusions of Frakes & Crowell (1967) who envisaged grounded glaciers over western West Falkland during the main deposition of the Lafonian Diamictite Formation. Although there is a significant age difference between the dykes and the main Lafonian Diamictite Formation, evidence from

vitrinite reflectance indicates that West Falkland was a positive block through this time implying that ice was probably grounded on West Falkland throughout the Permo-Carboniferous period.

It is implausible that sediments preserved in the dykes were injected down through the 2.5 km of the Gran Malvina Group to be emplaced in the basal Port Stephens Formation, this sequence then being removed during the rest of the glaciation to reveal the dykes as they are now. It is also unlikely that 2.5 km of the Gran Malvina Group was removed through glacial erosion by the end of the Visean. What is most probable is that the SW of the Falkland Islands was a relatively uplifted area and that the Gran Malvina Group was thinned in that region due to erosion during the earliest Carboniferous, so allowing the glacial sediment to be injected down into the Port Stephens Formation during late Visean - Namurian times. The implication of a reduced sedimentary succession in the SW of the Falkland Islands is consistent with (1) the facies in the Port Stephens Formation across West Falkland which, towards the top of the 1200 m succession, is fluvial at South Harbour and marine to the north; (2) with the low induration of the arkosic Port Stephens Formation and; (3) with the vitrinite reflectance data which implies that the SW of the Falkland Islands was a relatively uplifted area from Late Carboniferous times.

In summary, diamictite dykes of Early Carboniferous and Late Carboniferous/ Early Permian age are seen on West Falkland and East Falkland respectively. The Early Carboniferous aged dykes formed during a period of glaciation seen as a hiatus in the sedimentary record of central Gondwana and are therefore preserving a rare fragment of the stratigraphy from that time. The dykes were emplaced by downward injection of sediment in a state of liquefaction, probably triggered by the weight of the ice sheet above. Low vitrinite reflectance values and the stratigraphic relationship of the dykes on West Falkland indicate that neither the Gran Malvina Group nor Lafonian Supergroup were deposited in their entirety and that the SW area of the Falkland Islands was an uplifted block since the middle of the Palaeozoic Era.

	Dyke *1	Dyke *2
Acetosporites carnosus Playford, 1983	+	+
Endosporites sp.	+	
Foveosporites pellucidus Playford & Helby, 1968	+	
Grandispora cf *maculosa* Playford & Helby ,1968		+
Indotriletes kuttungensis Playford & Helby, 1968; Playford, 1990	+	+
Raistrickia accinta Playford & Helby, 1968	+	
Reticulatisporites magnidictyus Playford & Helby, 1968	+	+
Verrucosisporites aspratilis Playford & Helby, 1968	+	+
Verrucosisporites quasigobbettii Jones & Truswell, 1992	+	+
Botryococcus sp.	+	+

Table 3.1. Significant identifiable palynological taxa from sedimentary dykes, South Harbour.

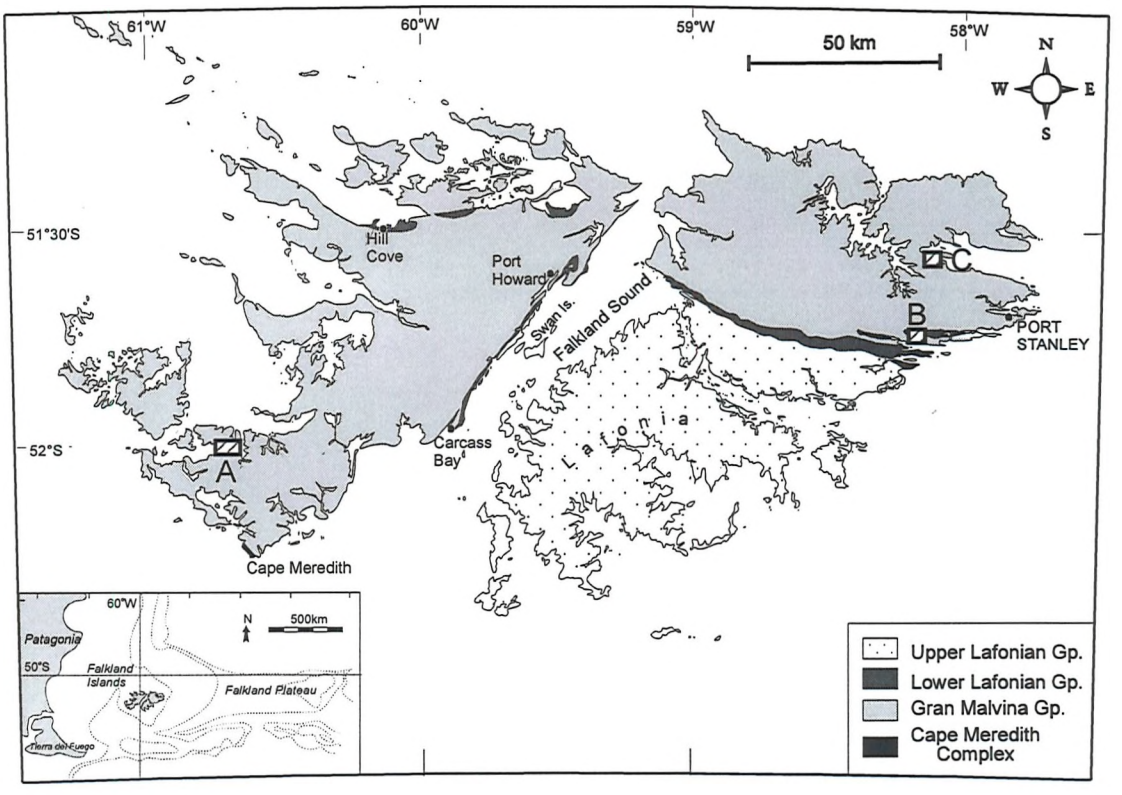

Figure 3.1: A simplified geology of the Falkland Islands, after Greenway (1972), location of maps for Figures 3.2a-c shown.

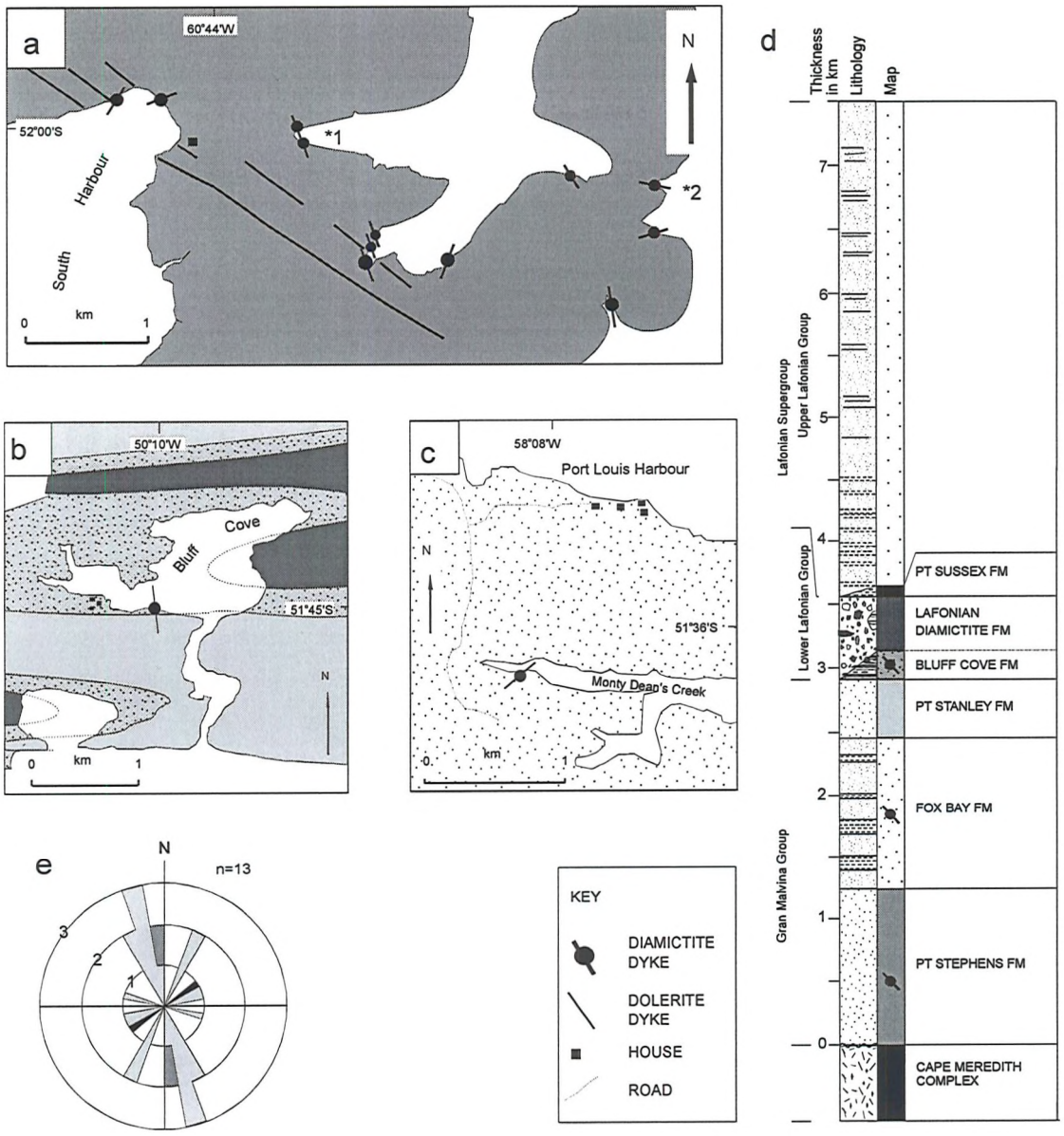

Figure 3.2: (a) geology of the South Harbour area, showing location of 11 diamictite dykes within the Port Stephens Formation; *1 and *2 refer to dykes sampled for palynological dating; (b) geology of the Bluff Cove area showing the location of a single diamictite dyke lying just below the Lafonian Diamictite Formation within the Bluff Cove Formation; (c) geology of Monty Dean's Creek showing the location of a single diamictite dyke within the Fox Bay Formation; (d) simplified stratigraphy of the Falkland Islands; thicknesses are maximum known. Shows map key for (a)-(c); (e) Rose diagram showing the frequency of different orientations of dykes at South Harbour (light grey), Bluff Cove (mid grey) and Monty Dean's Creek (black).

Figure 3.3: Field photograph, facing north, of surface expression of a diamictite dyke, South Harbour. This dyke, some 600 m in length, can be seen running across the bay through the centre of the picture to the low cliff and cleft on the horizon beyond. The dyke is 3.4 m wide in the foreground. (UTM location from maps 21FTC443320)

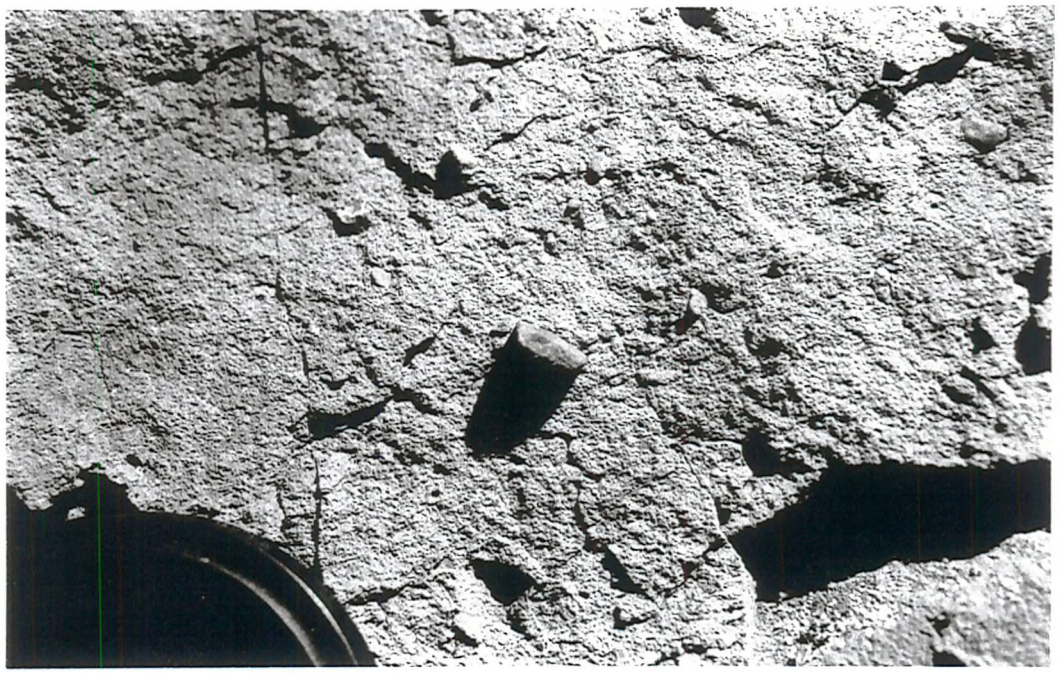

Figure 3.4: Photograph of arenaceous diamictite dyke lithology showing clasts up to 15 mm in an arenaceous matrix, South Harbour. Edge of camera lens for scale. (UTM location 21FTC443320).

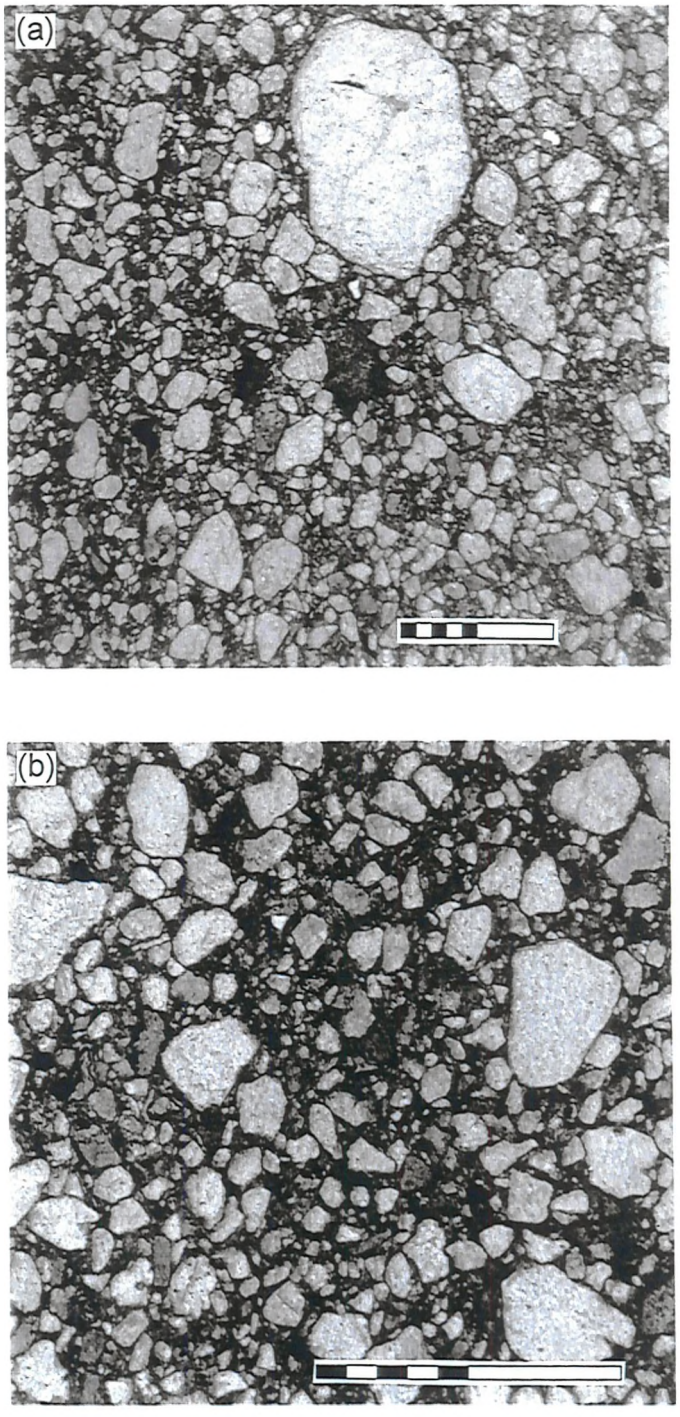

Figure 3.5a & b: Photomicrographs (plane polarised light) of a diamictite dyke from South Harbour (UTM location 21FTC443320). Most grains are quartz, sub-rounded to sub-angular in shape. The dykes show an unsorted gradation from sand-sized grains through silt to clay-sized material filling interstitial spaces. Scale bar is 1 mm in both (a) and (b).

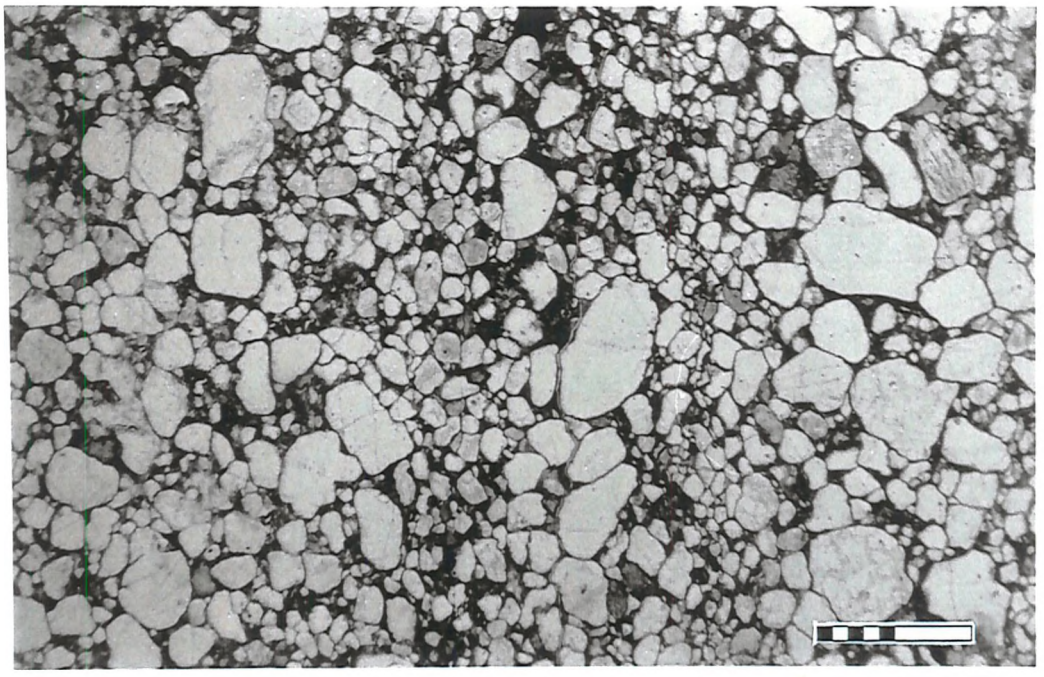

Figure 3.6: Photomicrograph (plane polarised light) of the edge of a diamictite dyke, South Harbour (UTM location 21FTC448311). The dyke is composed mostly of quartz grains in a clay matrix, showing differentiation of grains into fine and coarse bands. Note the alignment of elongate grains parallel to this lamination. Scale bar is 1 mm.

Figure 3.7: Photograph of the margin of dyke *1 from South Harbour (Fig. 3.2a). The diamictite shows vertical laminations (V) and the development of mudstone (M) towards the margin of the dyke (denoted by dashed line). The Port Stephens Formation (PS) shows a clean, sharp, uneroded boundary with the dyke. Notebook is 13 cm across and shows a 10 cm scale bar.

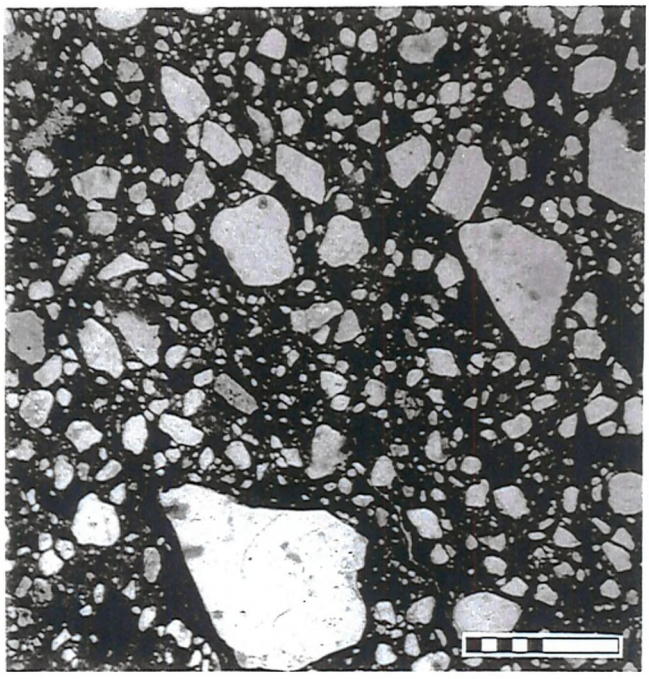

Figure 3.8: Photomicrograph (plane polarised light) of a diamictite from the Lafonian Diamictite Formation at Hill Cove, West Falkland (UTM location 21FTC835900). There is a clear gradation from sand-sized, mostly quartz, grains through silt to clay-sized material. Scale bar is 1 mm.

(a)

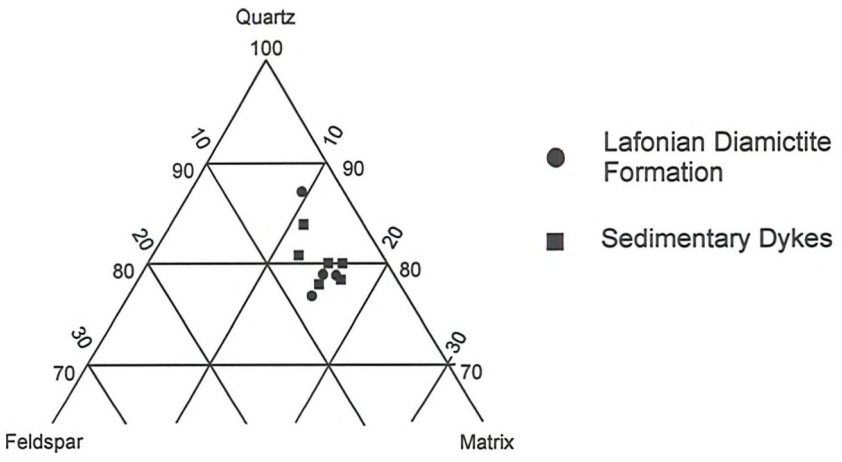

(b)

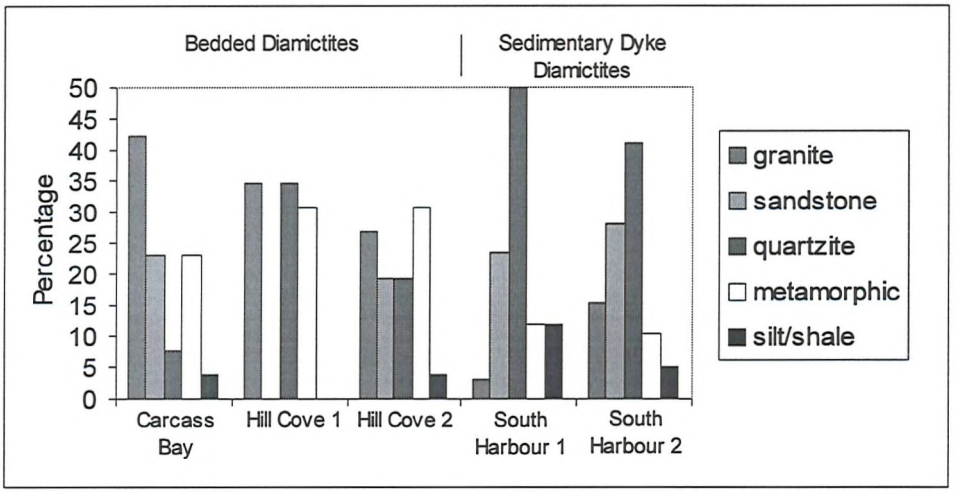

Figure 3.9: (a) Triangular Quartz/Feldspar/Matrix plot for diamictite samples from: the Lafonian Diamictite Formation at Hill Cove, Port Howard, Carcass Bay and Bluff Cove; and sedimentary dykes from South Harbour, Bluff Cove and Monty Dean's Creek. (b) Frequency bar chart of clast counts from diamictite from Carcass Bay, Hill Cove and South Harbour.

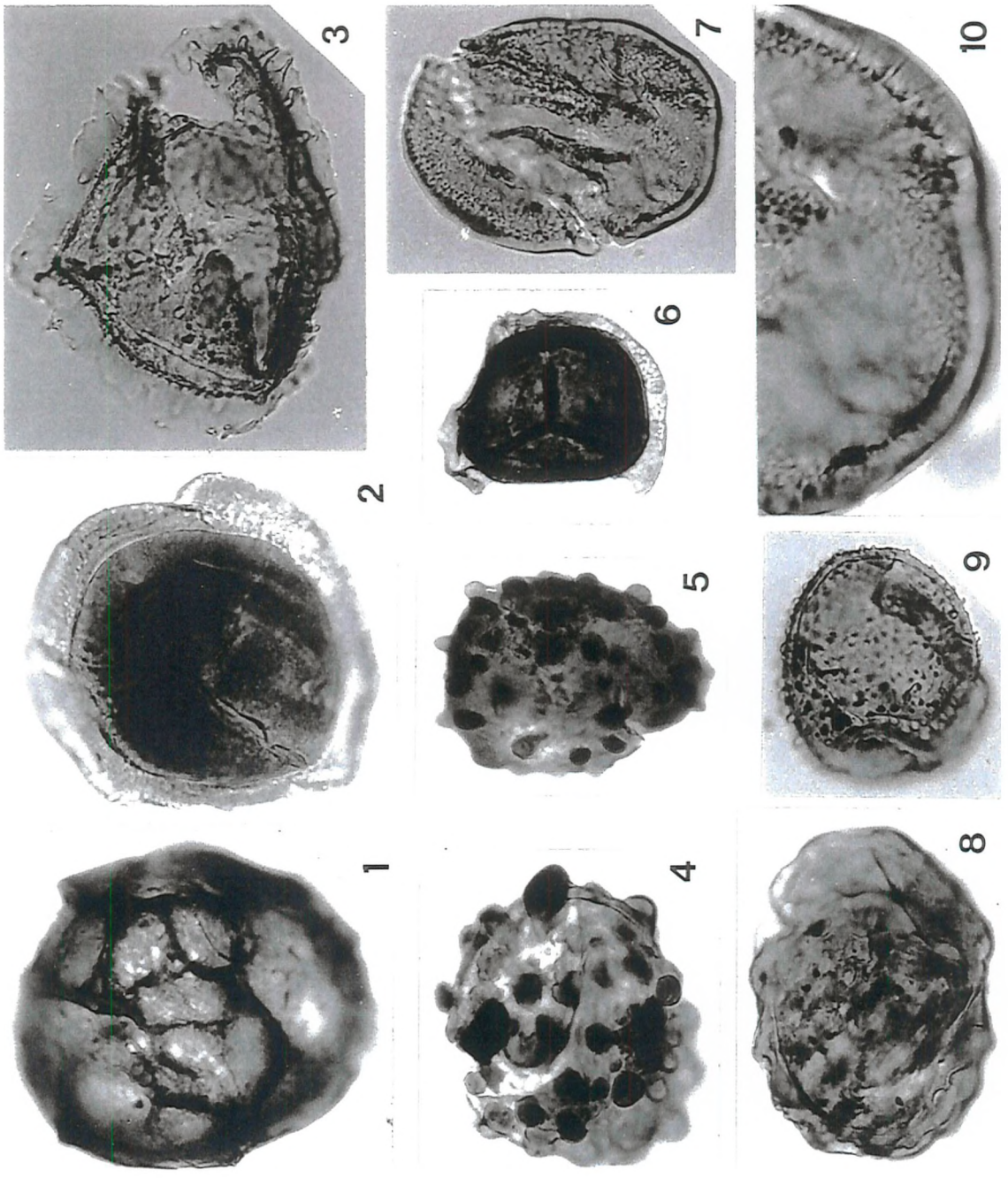

Figure 3.10. Significant spore taxa from the South Harbour sedimentary dykes. (*1 and *2 refer to dykes in Fig. 3.2a). **1.** *Reticulatosporites magnidictyus* x650 *1 ox (114, 11.2) **2.** *Grandispora* cf. *maculosa* x650 *2 (114.4, 13.8) **3.** *Indotriletes kuttungensis* x650 *1 ox (127.6, 14.1) **4.** *Verrucosisporites quasigobbettii* x650 *2 (133.7, 20) **5.** *Verrucosisporites quasigobbettii* x650 *1 (137, 18.2) **6.** *Endosporites* sp x650 *1 ox (137.2, 5.7) **7.** *Acetospora carnosa* x650 *2 (134.6, 7) **8.** *Foveosporites pellucidus* x650 *2 (122, 22) **9.** *Verrucosisporites aspratilis* x650 *2 (131.6, 19.7) **10.** *Acetospora carnosa* x2300 *2 (134.6, 7) Detail of internal sculpture of Fig. 3.10.7.
All co-ordinate references refer to an Olympus BHS-313 microscope (No. 210685).

Chapter 4: The Structural Geology of East Falkland

Chapter 4: Structural Geology of East Falkland

4.1 Introduction

East Falkland shows two distinct provinces, a northern part which is dominated by the Gran Malvina Group and has been deformed into an E-W fold-belt and a southern part which is relatively undeformed and equates to a foreland basin of the fold-belt to the north. A marked deformation front, running approximately E-W just to the south of the Wickham Heights, divides the two (Fig. 4.1).

Four areas have been studied across East Falkland (see Fig. 4.1), two at the eastern end of the fold-belt, Port Stanley - Bluff Cove and Greenpatch, one at the western end of the fold-belt, San Carlos and one to the south of the deformation front at Egg Harbour.

4.2 Port Stanley, Bluff Cove - Eastern East Falkland

This large area in the east of the island has been mapped to show the deformation in the succession from the Port Stanley Formation to the Lafonian Diamictite Formation (see Fig. 4.2, Map 1). The area is dominated by quartzites of the Port Stanley Formation, which have been deformed along an E-W axis. In the south of the area the Bluff Cove and Lafonian Diamictite Formations are also incorporated into the folding.

4.2.1 Folding

The region is dominated by intense folding (Fig. 4.2) with fold axes striking consistently E-W (see Fig. 4.3a). The folds have interlimb angles of 0 - 160° which show that the folds are mostly open to close with rare tight to isoclinal and gentle folds. The folds generally verge southwards (Fig. 4.4) and, commonly, have steeply dipping southern limbs (around 80° plus some overturned) and more shallowly dipping northern limbs, dipping around 30 - 50° (Fig. 4.3b). This dominance of steeper southern limbs is not seen everywhere and occasional more steeply dipping northern limbs are seen (Fig. 4.5). However, in these cases the steeper limb is never

as steep as in the folds with steeper southern limbs. Cross-sections across the area (Fig. 4.2) show this southerly vergence as the shorter, steeper limbs are most commonly on the south side of the folds. The fold axes, where seen, plunge gently at between 5 - 10° to either the east or west (see Fig. 4.3a) indicating that they are sub-horizontal. From cross-sections (Fig. 4.2), the folds have axial planes which dip between vertical and 54° to the north, showing that they are moderately to steeply inclined. It is possible that some folds are underlain by thrusts as some anticlines show a steepening of the southerly limb in the central core of the fold. Larger folds can be traced laterally for up to 10 - 20 km along strike and have wavelengths of 2 - 3 km whilst the smaller folds have wavelengths from 0.2 - 1 km down to metre scale and are more localised and less laterally continuous.

The fold style has been mainly controlled by both lithology and bed thickness. Lithological effects are that folds in the more competent Port Stanley Formation show much steeper dips and interlimb angles from 0 - 130° forming open to isoclinal folds (see Fig. 4.2). In contrast folds in the less competent Bluff Cove Formation and Lafonian Diamictite Formation, exposed around Bluff Cove, show much lower bedding angles and interlimb angles of 100 - 160° giving only gentle to open folds (see Fig. 4.2). Bed-thickness affects fold style in that thicker bedded units form parallel (1B type) folds, whilst the thinner bedded units form similar (2 type) folds (Ramsay 1967, p365) (Fig. 4.6). All the folds are harmonic and no disharmonic folding was recorded.

In the Port Stanley region, the steeper southerly limbs of folds within the Port Stanley Formation show commonly low to moderately-dipping semi-ductile shear planes (Fig 4.7), generally with reverse top-to-the-south displacements with occasional conjugate reverse top-to-the-north shears (Fig. 4.8). These features commonly take the form of zones of semi-ductile rotation and thinning of the bedding planes often accompanied by en echelon, sigmoidal veining, showing a movement of up to 10 cm (Fig. 4.7). Less commonly the shearing causes brittle failure and a defined fracture appears (Fig. 4.8). The net effect of these features is vertical extension of the steep to vertical limbs. Comparison to structures seen by Hancock *et al.* (1983) in the Variscan deformation of Pembrokeshire shows that these structures

are commonly found on the steeper limbs of asymmetric folds and that they are contemporaneous with the fold formation.

There is abundant evidence for flexural slip on the limbs of the folds exposed in the Port Stanley Formation with the development of quartz slickensides on the movement horizons. These movement horizons occur on many bedding and even some cross-bedding planes. The slickensides on these horizons demonstrate reverse, dip-slip movement, which on southerly dipping limbs is top-to-the-north and on northerly dipping limbs is top-to-the-south (Fig. 4.9). The use of a P/T dihedra plot, as outlined by Angelier (1984), gives an indication of the principal stresses which formed these flexural-slip planes and presumably the folds to which they are related. The plot (Fig. 4.10) shows that σ_1 is approximately N-S and σ_3 approximately vertical whilst σ_2, calculated from σ_1 and σ_3, is horizontal in the E-W plane. These results would imply a N-S compression to form these features. As the slip directions are generally dip-slip on these flexural slip planes the variation in slip directions that is seen may be due to variations in the bedding directions across the area although anomalous movement directions may in fact be bed parallel thrusts, however, this is unclear from field observations.

4.2.2 Cleavage

A well defined, steep, mainly northerly dipping, axial planar cleavage (Fig. 4.11) is clearly seen in the argillaceous and less competent arenaceous units of the Bluff Cove, Lafonian Diamictite and Black Rock Formations (seen at Port Fitzroy to the south of the Port Stanley-Bluff Cove section). In these units, cleavage is well developed as a slaty cleavage in shaly units and as a spaced cleavage in sandstones. Cleavage in the more competent formations is limited to a weak, steep northerly-dipping cleavage (Fig. 4.12) developed locally in the Port Stephens Formation (seen in the Malo Hills to the west of Port Salvador) and a pressure solution cleavage in the cores of a few tight third order folds in the Port Stanley Formation. Southerly-dipping cleavage is also seen and is due to either variations around the vertical of a steep cleavage or to fanning around first order fold axes.

4.2.3 Faulting

No macroscale faults were observed, however, two have been postulated by previous workers to the south of Sapper's Hill (Ashley 1961, Greenway 1972). Mesoscale faulting, both reverse and normal, is seen in the area and is relatively common. Reverse faults show generally north-south slip directions (Fig. 4.13) and measurable displacements of up to 10 m (Fig. 4.15). These observed reverse faults are commonly found in the shallower northerly dipping limbs of folds. However, near Surf Bay is an example of reverse faults cutting through the crests of southward verging anticlines (Fig. 4.16) and near Stanley Airport there is an example of apparently early-formed top-to-the-south thrusts which have since been folded around an E-W axis (Fig. 4.17). A P/T dihedra plot of the thrusts exposed in the area (Fig. 4.14) shows that σ_1 and σ_2 are sub-horizontal trending approximately N-S and E-W respectively and that $\sigma 3$ is almost vertical. This is identical to that seen from flexural slip planes related to the folding, indicating that they both formed from a similar N-S compressional event.

It could be suggested that a mesoscale, top-to-the-south, reverse fault exists to the south of Bluff Cove. This is because of the intensity of the folding seen at The Bluff itself. As mentioned earlier this fold is the only isoclinal fold mapped in the area (Fig. 4.18) and is very anomalous. The fold plunges westwards and the intensity of the deformation dies out similarly. An explanation for this intensity of folding could be an underlying top-to-the-south thrust with the Bluff Cove fold being a hanging wall anticline that has been tightened by further top-to-the-south movement (Fig. 4.19). As mentioned earlier in section 4.2.1, it has been suggested that some of the folds may have thrusts in the cores of the folds causing local steepening of the limbs. If these, and the Bluff Cove fold, are indeed underlain by thrusts then it implies that thrusting may be far more common across the area than the data from the present exposure implies. A more detailed study across the scattered exposures may reveal more thrusts however, at present, they remain undetected.

Occasional small-scale shears with a N-S strike displaying predominantly sinistral, and occasional dextral strike slip displacements of less than 10 cm were also recorded from across the Port Stanley area (Fig. 4.20)

4.2.4 Veining

Quartz veining is very common in the Port Stanley Formation. The veins are often parallel-sided however some are sigmoidal and either type may show an en echelon pattern. Quartz crystals commonly show fibres growing at 90° to the vein-walls but oblique growth with fibres up to 60° to the walls are also seen. Vein orientations are highly varied (Figs. 4.21, 4.22a), however the majority dip in a southerly direction.

The veins vary in length from 10 - 2550 mm and in width from 1 - 25 mm however, most veins are 100 - 600 mm long (Figs. 4.22b, d) and 1 - 6 mm wide (Figs. 4.22c, e). Length values are minimum estimates as some veins extend beyond the exposure. The distribution of these is reminiscent of a fractal pattern where there are lots of small veins and fewer and fewer larger veins. Plots of log (width) and log (length) against strike (Figs. 4.22d, e) show that the main bulk of the veins fall within the ranges noted above. Anomalies within this data are indistinct, however, a cluster of veins which are notably longer and wider can be seen striking at around 100° (Figs. 4.22d, e). A plot of log (length) against log (width) (Fig. 4.22f) shows a scattered distribution with length:width ratios varying from 3 - 1100, clustering mainly between 20 and 400, showing no strong correlation to any one length:width ratio. One general trend observable in the data is that the longer veins are also the widest.

Despite the variability of the dataset as a whole, in terms of strike, width and length, three rough groupings can be seen on from the strike of the veins (Fig. 4.23):

Group 1: striking N-S and dipping at 80 - 90° to east or west.

Group 2: striking NE-SW and dipping, on average, SE showing sigmoidal S and en echelon patterns indicating sinistral strike-slip motion.

Group 3: striking E-W to NW-SE dipping, on average S-SW.

All three groups are seen in two independent datasets; the first (Fig. 4.23a) collected from five traverse lines, the second (Fig. 4.23b) collected more randomly from locations visited during mapping in the area.

Having defined these three groups it has been possible to give relative ages based on cross-cutting relationships recorded from the first dataset. This is demonstrated in Figure 4.24 where, for each pair of cross-cutting veins, the strike of

the early vein (x-axis) has been plotted against the strike of the late cross-cutting vein (y-axis). As the bar graphs for each axis show, there are three distinct groups of veins.

Group 1: striking at 000 - 020° and 160 - 180°, generally N-S, only appearing as late veins.

Group 2: striking 040 - 080°, generally NE-SW, appearing as late and early veins.

Group 3: striking from 080 - 120°, approximately E-W, only appearing as early veins.

These groups picked out from cross-cutting relationships correspond to the three groups picked out in Fig. 4.23. By analysing the relationship of these three groups the relative ages become clear.

Looking first at Group 1, it is clear that late veins of this group cross-cut earlier veins of both Groups 2 and 3 (A & C, Fig. 4.24), however only rarely do any veins from this group appear as early veins cut by Groups 2 or 3 (A' & C', Fig. 4.24). This implies that Group 1 is later than both Groups 2 and 3.

With Group 2, late veins of this group can be seen to cross-cut early veins of Group 3 (B, Fig. 4.24) and only rarely are any veins of this group cut by later veins of Group 3 (B', Fig. 4.24). This implies that although veins of Group 2 are older than Group 1, they are younger than Group 3.

From this it is clear that a relative chronology of veining from oldest to youngest would be that Group 3, striking ± E-W, formed first, then Group 2, striking ± NE-SW, formed next and finally Group 1, striking ± N-S, formed last. The time scale of veins is unclear from the data.

Relating the formation of the veins to the known structures is somewhat enigmatic. It is possible that Group 3 formed initially as extensional features parallel to the fold axial planes. Group 2, with its NE-SW strike and significant number of veins showing sigmoidal and en echelon patterns, appear to be related to sinistral shear in an E-W direction across the area. Finally Group 1, and the N-S striking set of joints, the only joints in the area, formed as extensional structures across the folds (e.g. Hancock *et al.* 1983).

It should be noted that, owing to the exposures available, the data used in this analysis were all collected from northward dipping beds, leaving a gap in the data set for the southward dipping beds. However, the second data set which was collected

from a wide variety of locations across the area shows an identical distribution to that for the solely northward dipping limbs (Fig. 4.23) which would imply that Groups 1 - 3 recorded from the northerly dipping limbs are seen also on the southerly dipping limbs. However, a more thorough study of veins on the southerly dipping limbs would be required to assess this distribution.

4.3 Greenpatch - Eastern East Falkland

The area of Greenpatch, lying on the south side of Port Louis Harbour, and to the north-west of Port Stanley (Fig 4.1), was mapped to assess the amount of deformation at the eastern end of the Wickham Heights in the interbedded sandstones and shales of the Fox Bay Formation. Folding around an approximately E-W axis has produced a major anticline through Port Louis Harbour (Fig. 4.25 & Map 2) with the development of an axial planar cleavage. Deformation resulting from faulting is minor.

4.3.1 Folding

The dominant structure in the area is a first order anticline the hinge of which strikes approximately E-W through Port Louis Harbour (Fig. 4.25, Map 2). This 'Port Louis Anticline' shows an interlimb angle of approximately 120°, a vertical fold axis (Fig. 4.25) and a plunge of 0 - 5° E and W indicating that it is an open to gentle, upright, sub-horizontal fold. Smaller, second order folds are developed on the southern limb of the anticline, little is known about folding on the northern limb as this was not mapped. These second order folds are upright, gentle to open and sub-horizontal with sub-vertical axes, interlimb angles of 90 - 140° and plunges of 0 - 7° (Figs. 4.25, 4.26). The folds show dips of 30 - 53° on the southerly dipping limbs and 20 - 38° on northerly dipping limbs (Fig. 4.26). Note that the bias in these data towards southerly dipping strata is due to mapping primarily on the southern limb of the fold. The intensity of folding dies out southwards into southward dipping strata with little signs of deformation.

Flexural-slip related to the folding is only seen occasionally on bedding planes as quartz veining with slickensides showing a reverse sense of movement.

4.3.2 Cleavage

There is a strongly developed, steep, mainly northerly dipping axial planar cleavage (Fig. 4.27) throughout the area in both the shales, as a slaty cleavage, and the sandstones as a spaced cleavage. In the core of the Port Louis Anticline, the intensity of cleavage development is such that bedding is almost obscured. This intensity of cleavage decreases away from the core of the fold into the less folded strata. There appears to be no fanning of the cleavage around the first order fold with northerly dipping cleavage developed on both the northerly and southerly dipping limbs.

4.3.3 Faulting

Faulting is uncommon across the area although both reverse and normal faults are developed (Fig. 4.28). Of the faults observed, both reverse and extensional faults dip N-S, with the extensional faults dipping more steeply (Fig. 4.28). The few reverse faults that there are, show shallow dips and the development of quartz slickensides indicating dip-slip with top-to-the-north or top-to-the-south movement. These would appear to be related to the N-S compression indicated by the folding and cleavage development. On the northern coast of Port Louis Harbour, the steeply northward dipping cleavage is clearly cut by later extensional faults (Fig. 4.29), indicating a late stage of extension after the main fold and cleavage development.

4.3.4 Veining

Quartz veining is not abundant in the area and is confined primarily to the sandstone units of the sequence. Of the veins recorded (Fig. 4.30) two clear groups can be distinguished, group 1 dipping steeply west and group 2 dipping moderately north. No cross-cutting relationships were observed and so a direct chronology is not available here. Comparison to the dataset from the Port Stanley area shows that these

two groups correlate closely to the N-S striking group 1 and the E-W striking group 3, respectively. Cross-cutting relationships from Port Stanley show that group 1 is younger than group 3 and it is possible that this relationship is the same at Greenpatch (i.e. group 1 is younger than group 2).

4.4 San Carlos - Western East Falkland

Study in this area concentrated primarily on the Port Stanley Formation to allow a comparison to the deformation seen at Port Stanley, less attention was paid to the Fox Bay Formation as less work had been accomplished at the eastern end of the fold-belt. The data collected has been supplemented by communications with Dr. M.L. Curtis from the British Antarctic Survey who mapped more extensively in the Fox Bay Formation at the centre of the fold.

San Carlos lies at the western end of the Wickham Heights (Fig. 4.1) in a region with an overall strike of NW-SE, a marked swing from the E-W strike in the east and central parts of the island. The overall structure of the area is a first order gentle to open anticline with a sub-horizontal axis. The Fox Bay Formation outcrops in the core of the fold and is flanked to the NE and SW by ridges of the Port Stanley Formation, farther to the east it is possible that the Lafonian Diamictite Formation outcrops (Fig. 4.31, Map 3).

4.4.1 Folding

As already noted the overall structure of the area is a first order, open to gentle anticline, slightly asymmetrical to the SW, with interlimb angles of 100 - 135° (Fig. 4.31). The major fold is upright to gently inclined towards the SW and sub-horizontal, plunging at about 10° to the NW (Fig. 4.32). The axial trace of this fold is seen to swing in strike from NW-SE in the NW and SE of the area to almost N-S in the centre. The first order fold is mainly picked out in the competent Port Stanley Formation which forms the flanks of the exposed fold. The less competent Fox Bay Formation, which is exposed in the centre of the fold, shows several second and third order folds, only one second order fold pair was mapped in the Port Stanley

Formation on the western limb at Wreck Point. In the Fox Bay Formation the lower order folding, mapped around White Rincon, Little Rincon and Doctors Head, occurs as tight to open, upright to moderately inclined, sub-horizontal to gently plunging folds (plunges of 0 - 25°), with interlimb angles of 35 - 110° striking NW-SE (Fig. 4.32). The SW limbs of the anticlines are commonly steep to overturned and shorter relative to the NE limbs indicating a vergence towards the SW. Folding is seen to intensify and shorten in wavelength locally, for example in the footwall of the thrust exposed at White Rincon (Fig. 4.33) where several third order folds have developed. There is no evidence for flexural slip on the limbs of the folds. The overall structure of this area could imply relatively disharmonic folding between the well-bedded competent Port Stanley Formation and the less competent, more intensely folded, Fox Bay Formation. Any disharmony in the folding is unclear because the Port Stanley Formation has been eroded from the centre of the fold, however if deformation in the exposed sections is used as an indicator then the Port Stanley Formation has undergone little in the way of internal deformation.

4.4.2 Cleavage

There is only a weak, steep, north-easterly dipping cleavage developed in shales of the Fox Bay Formation in the core of the main anticline in the Head of the Bay Creek (Fig. 4.32). Farther to the NW, away from the core of the fold and in the more competent sandstones and quartzites of the Fox Bay and Port Stanley Formations, cleavage is not developed at all.

4.4.3 Faulting

Faulting is not common and appears to be confined to the Fox Bay Formation. The largest fault seen is a top-to-the-SW thrust cutting through the zone of folding on the south side of White Rincon and possibly extending SE to the far side of Little Rincon (Fig. 4.34). The throw on the fault is unclear as beds are difficult to correlate in outcrop and on the cross section (Fig. 4.31, Map 3). This is due to the presence of at least six shale horizons in the Fox Bay Formation (Marshall *pers. comm.* 1996) which

have not been fully mapped out in the San Carlos area. Other reverse and extensional faults are small and uncommon with observed throws of the order of 50 - 100 mm. The orientations of reverse faults show a scattered distribution but predominantly dip N or NE with N-S and SW slip directions (Fig. 4.34). At Wreck Point, close to the Falkland Sound, the Port Stanley Formation shows shearing with a wide variety of planar orientations however lineations show a consistent SW direction, perpendicular to the fold axis (Fig. 4.35). These shears combined with the exposed thrusts are consistent with the SW vergence for the whole structure seen in the fold pattern.

4.4.4 Veining

Quartz veining, although common along the minor fault planes in the Fox Bay Formation, is rarely seen across the main structure. As a quantitative comparison to veining seen at the eastern end of East Falkland, a study of the veins within the Port Stanley Formation has been undertaken. In this formation veining is rare to absent in the studied exposures with only two exposures found on the western limb and none on the eastern limb giving any vein data. The few veins (n=30) that were measured are steep to vertical, 1 - 4 m long and 2 - 3 mm wide showing one dominant orientation striking 065/245° (Fig. 4.36a), perpendicular to the fold hinge. These veins, similar in orientation to that of a major joint set (Fig. 4.36b) exposed around Rocky Mountain on the eastern limb, are orthogonal to the regional strike and are probably extensional structures related to the formation of the anticline.

Veining in the Fox Bay Formation occurs in isolated zones, often related to faulting, rather than as a pervasive feature and shows a diverse range of orientations. Two dominant orientations are seen in the data recorded; one striking ESE/WNW, the second and more common set dipping steeply and striking NNE/SSW (Fig. 4.37). Of the two sets, the first is sub-parallel to bedding, whilst the second is sub-perpendicular to bedding. No cross-cutting relationships were observed in the veins seen in either of the formations studied.

4.5 Egg Harbour - South of the deformation front

Deformation dies out rapidly to the south of the Wickham Heights away from the main folding in the north of East Falkland so that there is very little in the way of tectonic structures in Lafonia, the southern half of the East Falkland. The area has been mapped as horizontal (Greenway 1972) to gently folded (D.I.M. Macdonald *pers. comm.* 1996).

Egg Harbour, lying on the western coast of Lafonia, was visited briefly as a reconnaissance survey to assess future work in the area. It was decided not to continue this research as CASP were intending to work in the same area.

Egg Harbour shows brown, cross-bedded sandstones and grey/brown shales and siltstones, of late Permian age, dipping at 11 - 20° NW (Fig. 4.38). Deformation is very minor with only occasional northward dipping thrusts showing only a small throw, probably less than 1 m, and slickensides showing a distinct top-to-the-south-west trend (see Figs. 4.39, 4.40). A second deformation feature at Egg Harbour is a set of laterally extensive, closely spaced joints (20 - 100 mm apart) which show a strike of circa. 40°, parallel to the Falkland Sound. Cross-cutting these joints is a second set of joints striking at around 90° which show a sigmoidal Z shape with angles relative to the main joint set of ~30° at the tips rotating to about 40 - 50° in the centre of the sigmoidal joints. This relationship of cross-cutting joints implies a dextral sense of strike-slip movement along the main joints parallel to the Falkland Sound (Fig. 4.41). This main NE-SW striking joint set, which increases in intensity north-westward, is probably related to a NE-SW structure within the Falkland Sound as are the locally developed large dolerite intrusions in the area, one of which is located to the NW at Long Point (M. Hole *pers. comm.* 1995).

4.6 Strain measurements across East Falkland

Estimates of strain across the fold-belt on East Falkland have been made using bed length measurements from cross-sections. In these calculations the original length (l_0) is measured by tracing the length of a given horizon on the cross-section, the present length (l_1) is also measured from the section.

The relationship of:

$$(l_0 - l_1) / l_0$$

where l_0 is original length and l_1 the current length has been used to determine the percentage of shortening, or strain, along the section. Five sections were used in these estimates, three from the Port Stanley area, one from Greenpatch and one from San Carlos. Strain estimates from these cross-sections are, not accounting for unknown faults or flexural slip, 29%, 19% and 16% for Port Stanley, 13% for Greenpatch and 5 - 12% for San Carlos. These show a clear decrease in strain from Port Stanley and Greenpatch at the eastern end and San Carlos at the western end of the fold-belt.

Strain estimates have also been made from quartz veins using the methods outlined by Peacock & Sanderson (1993). This method was originally developed for measuring strain from faulting but, as the authors noted, it can be applied also to veins or stylolites. The method involves recording the orientation and displacement of all known veins along a sample line. This data is then weighted to compensate for structures which strike sub-parallel to the sample line. Strain is then calculated from the magnitude of two vectors, parallel to displacement and normal to the plane of the vein. The resulting strain estimate is the total strain, summed from all the deformation events that have occurred in the area. Accuracy increases with increasing length of the sample line and increasing numbers of veins recorded. This method has been applied to the data from Port Stanley and San Carlos acquired along transects 1m wide rather than from a single line.

4.6.1 Port Stanley

Vein orientations were recorded along five strike-parallel, E-W traverses 1 m wide and up to 60 m long (Fig. 4.42). As the calculations show (Fig. 4.42), strain values are very low.

The relationship of the three principal strains can be expressed as the k value:

$$k = \ln A / \ln B$$

where $A= [(1+e_1)/(1+e_2)]$ and $B= [(1+e_2)/(1+e_3)]$. For the five traverses, k varies from 2.2 to 15.9 averaging around 7 indicating prolate strain (Price & Cosgrove 1992). These low strains have produced volume changes due to veining, varying from +0.6 to +4.3%, and dilation, or increase in surface area across the traverse, from +0.2% to +1.0% (Fig. 4.42). The orientations of the principal strain directions for the five traverses (Figs. 4.43a-e) vary widely according to the distribution of veins on any given traverse (Figs. 4.43a-e). However, if all the data are plotted together as a traverse totalling 162.5 m in length, striking at 270° (only feasible owing to the close similarity of strike in the five traverses) an bulk strain showing e_1 dipping steeply north, e_2 in an E-W horizontal plane and e_3 dipping shallowly south (Fig. 4.43f) is obtained. It should be noted that as the data was collected solely from northward dipping strata there may be a bias in the calcuated strains.

4.6.2 Greenpatch

No systematic measurements of strain from veins were recorded from this area. However, strained fossils on some of the bedding planes indicate small shear strains showing that there have been low strains across the area.

4.6.3 San Carlos

The strains estimated from two traverses on the western limb of the fold (Fig. 4.42) are very low and give k values of 1.4 and 31, indicating prolate strain and a constriction of the strain ellipse. These low strains have produced dilations of +0.03% and 0.01%, and 0.3% and 0.1% volume increases (Fig. 4.42). The principal strain directions in both cases show e_1 oriented NNW-SSE in a sub-horizontal plane, e_2 dipping SW and e_3 dipping ENE (Fig. 4.44).

4.6.4 Discussion

These data shows the principal strains calculated from the veins at San Carlos are an order of magnitude lower that those from the Port Stanley region. Also of note, is the change in orientation of the principal strain directions from Port Stanley where e_1 is orthogonal to the fold axis and dips steeply north whereas at San Carlos e_1 is parallel to the fold axis and sub-horizontal (Fig. 4.45). In the Port Stanley region the relationship of the principal strains to the calculated principal stresses is also unclear. The stresses calculated from flexural-slip and thrust faults show σ_1 and σ_3 to be horizontal and vertical respectively, however, strain measurements from veins show e_1 dipping 55°N and e_3 dipping 30°S. These strains could be related to movement across a top-to-the-south, shallowly northward dipping plane creating a similar geometry to that seen in transpression (Sanderson & Marchini 1984). This would therefore be related to the thrusting seen in the area. However, there are some constraints in considering the relationship of these calculated stresses and strains. First, the strain is the overall strain from all the deformation events and, in the case of the veins, at least three phases of vein formation are distinguishable. Second, the bias of data collection from northerly dipping limbs may have biased the strain calculations. So, although there is a model where the strains and stresses could be related to thrusting, it is unlikely that such a simple model can account for what is seen and that further study of the strain in this area is required.

4.7 Discussion

4.7.1 Summary of Deformation on East Falkland

A summary of the deformation across East Falkland can be found in Table 4.1. The deformation on East Falkland appears to show one main phase of N-S compression with a late minor relaxation and the development of extensional structures seen around Greenpatch. The main phase of N-S compression seen in the east as southward verging, E-W striking folds, top-to-the-south and top-to-the-north reverse faults and the development of a single, mainly northward dipping, axial planar

cleavage is supported from estimates of the principal stress and strain orientations from flexural slip, reverse fault and vein data.

Overall there is a clear decrease in the deformation westwards across the fold-belt which is seen in several ways. A marked decrease of quartz vein intensity westwards, with a corresponding decrease in the estimated strains, such that strains at San Carlos are 0.7 and 3.7% of the magnitude of the strains obtained from vein analysis around Port Stanley. There is also a decrease in the strain obtained from bed length estimates. The amount of cleavage development changes from being a strong, northerly dipping cleavage in both shales and sandstones in the east at Port Stanley and Greenpatch to, in the west, a weak, locally developed cleavage found only in shales in the core of the main fold at San Carlos.

The nature of the folding across East Falkland is characterised by the development of a continuous train of folds, changing from upright in the north to inclined in the south, which show lateral shortening of 13 - 29%. Calculated principal stresses show σ_1 (from reverse faults and flexural slip planes) oriented N-S in the horizontal plane indicating horizontal compression to form the fold train. Thrusting plays a minor role and no major thrust horizons have been identified in the area. The fold-front is abrupt from the deformed Wickham Heights in the north to the Lafonian Basin in the south. This is characterised by continuous and decreasing deformation with no evidence for overthrusting or any discontinuity that would suggest an emergent frontal thrust sheet.

4.7.2 Thick or thin skinned deformation

The deformation seen could be the result of either thin or thick skinned deformation depending on the involvement of basement in the deformation. Thin skinned deformation is characterised by décollement horizons, thrusting and nappe development (Moores & Twiss 1995, p267-276) as well as repeated stratigraphy owing to thrust duplication, complex folds and polyphase evolution. Such structures are seen in the European Alps (e.g. Debelmas *et al.* 1983), the Appalachians in eastern America (e.g. Neathery & Thomas 1983) the Canadian Rockies (e.g. Price 1981, Thompson 1981) and the central Variscan of Europe exposed in Spain, France and

southern Britain (e.g. Matte 1983, Hobson & Sanderson 1983). The external parts of the Variscan Orogeny, in Wales (Hancock *et al.* 1983) and southern Ireland (Naylor *et al.* 1983), are more characterised by fold trains with only subsidiary thrusting and cleavage development, décollements and sole thrusts are not present. Abrupt terminations of the deformation in these mountain fronts are often seen (e.g. Alps, Pyrennes & northern Rockies) and may be formed by a number of mechanisms: (1) foreland propagation of the thrust front; (2) backthrusting at the mountain front; (3) thrust propagation over the palaeo-land surface or; (4) rapid termination of thrusting without emergence (Vann *et al.* 1986). All four of these form frontal anticlines and an apparent rapid termination of deformation.

Thick skinned deformation has been described from the Cape Fold Belt of South Africa where there is significant basement involvement (e.g. Hälbich 1983). The fold belt is characterised by intense asymmetric folds, occasional overfolds and forelimb thrusts and strong cleavage development. Thrusting is developed at the fold front in the central zone (Coetzee 1983, Newton 1993), however further east deformation decreases and is mainly seen as folds with only minor thrusting (Haughton 1928, Mountain 1962) although more may be presently undetected (Johnson & Le Roux 1994). There is a gradation from the gentle flexing in the foreland Karoo Basin to the folding within the Cape Supergroup (Mountain 1945) with no major frontal thrusts or basal décollements.

The characteristics of the deformation on East Falkland of a continuous fold train, cleavage development, minor thrusting and a continuous deformation front with no emergent frontal thrust is closely comparable to the Cape Fold Belt of South Africa or the external parts of the Variscan deformation in Wales and southern Ireland. The solution to whether the deformation on East Falkland has resulted from thin or thick skinned tectonism would be resolved by the recognition of a décollement horizon and therefore a sole thrust. If such a large scale thrust is present on East Falkland it is not emergent in the main fold-belt or at the deformation front. The only place in the stratigraphy from the Precambrian metamorphic Cape Meredith Complex through the quartzites, sandstones and shales of the Gran Malvina Group where a such a horizon could be is within the shales of the Fox Bay Formation. A continuous section of this Formation has been logged by Marshall (*pers. comm.* 1995) at, and further to the

south of, Greenpatch. In the uppermost shale a near vertical fault was mapped in the gently southward dipping strata (J.E.A. Marshall *pers. comm.* 1997). However, if the strata are restored to horizontal, the fault dips southward which is the wrong way for a ramp in a southward propagating thrust system which will cut up the stratigraphy, i.e. dip northwards in this case. As no décollement horizon can presently be identified in the exposed stratigraphy it can be implied that the deformation across East Falkland is thick skinned, that there is no major sole or frontal thrust and that the deformation is similar to that in South Africa (Hälbich 1983). This model can be supported by the shortening estimates from cross-sections across East Falkland of up to 29% which is within the maximum shortening of 36.3% expected from buckling (Kneller & Bell 1993). However, although the present level of understanding of the fold-belt implies a model of thick-skinned deformation further research may produce evidence for thin skinned tectonism, such as a décollement horizon lower in the stratigraphy, perhaps at the contact with the underlying crystalline basement.

4.7.3 Strike swing at the western end of the fold-belt

A further question arises when looking at the evolution of East Falkland as to the marked changes in strike at the western end of the island around Port Sussex and San Carlos. Two models could be presented to explain this (Fig. 4.46): (1) an arcuate nature to the fold-belt produced as deformation dies out westward (Fig. 4.46a); or (2) differential movement along shear zones between thrust sheets (Coward & Kim 1981, Rattey & Sanderson 1982, Coward & Potts 1983, Erikson 1991) or between fold fronts (Cook 1978) producing folds which are oblique to the regional strike (Figs. 4.46b, c).

The first model implies the 'bow and arrow' style of deformation suggested by Elliott (1976) for thrust faults (Fig 4.46a) where deformation tails off laterally from a central point to a lateral tip. If this is applied to East Falkland it would explain the arcuate nature of the fold-belt and the overall change in strike from E-W to ESE-WNW. This lateral tip model is supported by the strain data at Port Stanley and San Carlos. At Port Stanley (centre of deformation front) e_1 dips steeply northwards, orthogonal to the fold axis, and indicates N-S compression, possibly thrusting,

whereas at San Carlos (lateral tip of deformation front) e_1 strikes NW-SE, parallel to the fold axis, implying strike parallel extension (Fig. 4.45). This is similar to what has been seen by Coward & Potts (1983) and Hyett (1990) at lateral tips of propagating thrusts. However, although this lateral tip model fits the overall strike swing across East Falkland it is not sufficient to explain the localised changes in strike at San Carlos and Port Sussex which can clearly be seen on satellite imagery for the area (Fig. 4.47).

The second model, of differential movement between thrust sheets or fold fronts resulting in oblique folds, has been well documented for thrust zones in the Moine of Scotland (Coward & Kim 1981, Coward & Potts 1983), in the Appalachians of Alabama (Erikson 1991) and especially around the Lizard Complex of Cornwall (Rattey & Sanderson 1982). Such a model requires movement along shear zones orthogonal to the regional fold axis creating a stepped geometry of folds parallel and oblique to the regional trend as seen by Rattey & Sanderson (1982) (Fig. 4.46c). On East Falkland, faults sub-orthogonal to the regional fold axis are seen defining the Goose Green Isthmus and a stepped geometry in the strike of the fold-belt is clear to the south and east of San Carlos (Fig. 4.47). It has been demonstrated (D.T. Aldiss *pers. comm.* 1997) that the faults defining the Goose Green Isthmus represent a significant break in the fold-front with deformation dying out some 10 - 12 km farther south on the east side of the Isthmus relative to the west side (see Fig. 4.47). This differential deformation appears to be defining a dextral lateral ramp in the deformation front. Given the presence of a postulated dextral lateral ramp it is also possible that the dextral displacements seen in the strike of the fold-belt around Port Sussex and San Carlos have also been formed by faults, similar to those on the Goose Green Isthmus but at depth in the basement, acting as lateral ramps across the deformation front.

It would seem then that the geometry of the deformation at the western end of the fold-belt on East Falkland represents the tail end of the fold-belt and that it can be attributed to elements of both the lateral tip and lateral ramp/differential shear models.

In summary, the deformation on East Falkland appears to have been formed by N-S compression with the development of a fold train and not of thrust sheets, and that elements of both lateral tip and lateral ramp models are responsible for the dextral

kinks and 45° swing in strike at the western end of the fold-belt.

Area	*Port Stanley*	*Greenpatch*	*San Carlos*	*Egg Harbour*
Folding-hinges	E-W	E-W	NW-SE	none
vergence	S	S	SW	none
tightness	Open-close, (rare gentle, tight and isoclinal folds)	Open - gentle	Tight - open	none
Bed-length strain	16-29%	13%	5-12%	<1%
Thrusting	Common, top-to-the-south and north, throw up to 10 m	Rare, top-to-the-south	One, significant top-to-the-SW	Minor top-to-the-SW, throw < 1 m.
Cleavage	Strong cleavage	Strong cleavage	Weak cleavage	no cleavage
Veining	Intense quartz veining	Quartz veining common	Occasional quartz veins	Veins developed in thrust plane only.
Vein strain	e_1 strains ~1.9×10^{-2} oriented N-S	Unknown	e_1 strains ~5.4×10^{-4} oriented NE-SW	Unknown

Table 4.1: Summary of deformation features for the four areas studied across East Falkland.

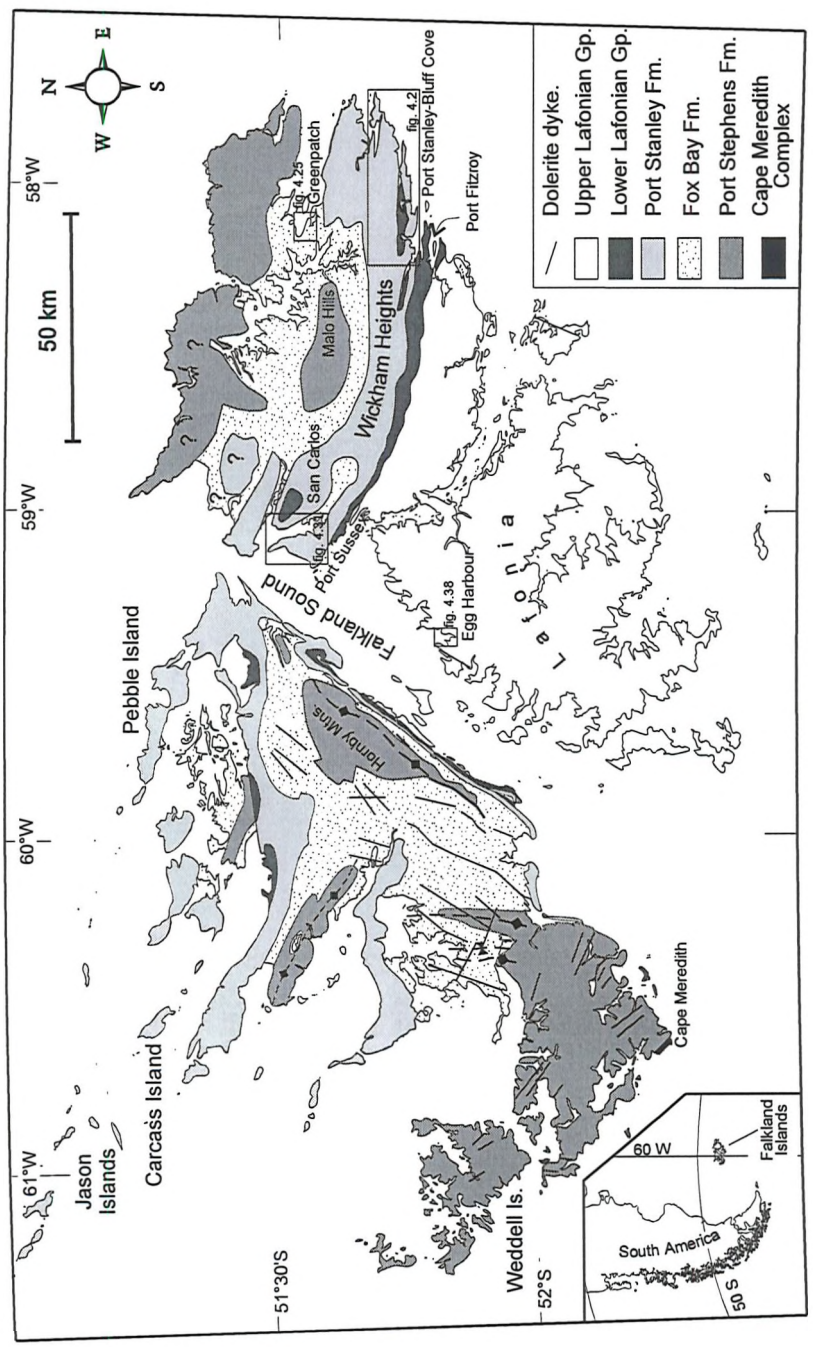

Figure 4.1: Simplified geological map (modified from Greenway (1972)) showing relevant place names and areas mapped on East Falkland.

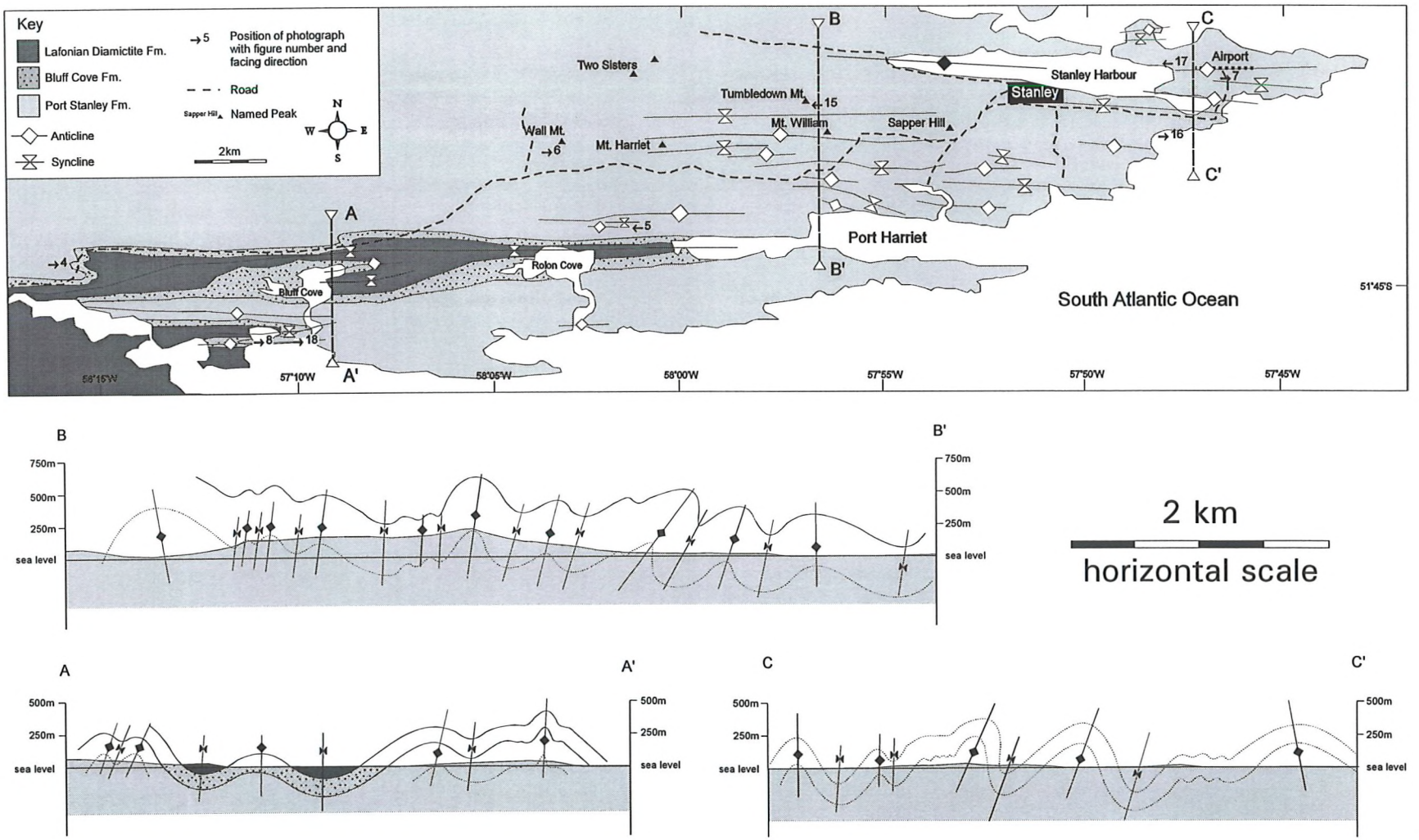

Figure 4.2: Summary geological map and cross-sections from the Port Stanley-Bluff Cove section (see figure 4.1 for location)

(a)

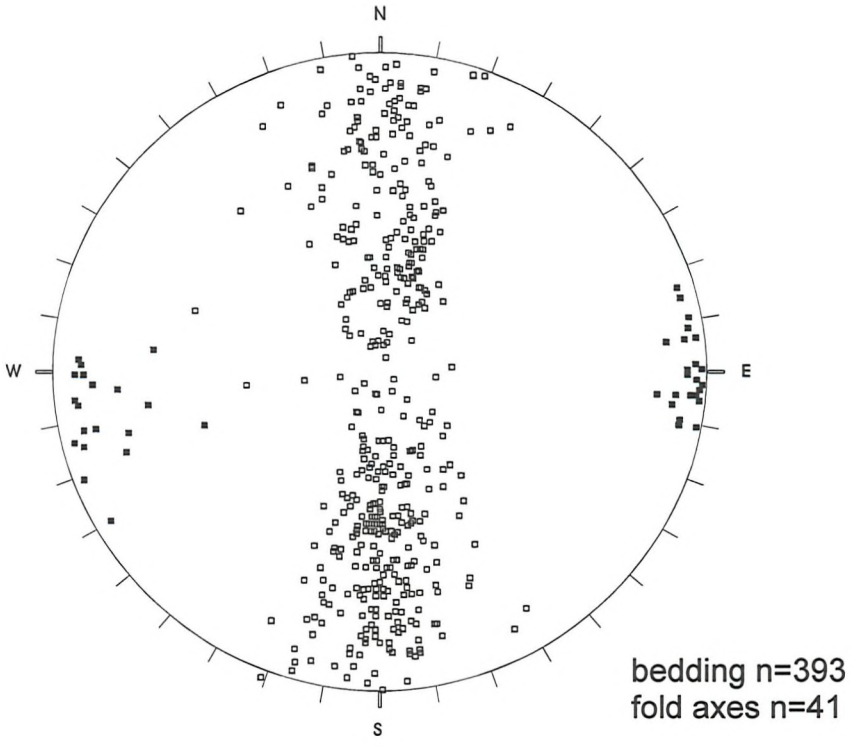

(b)

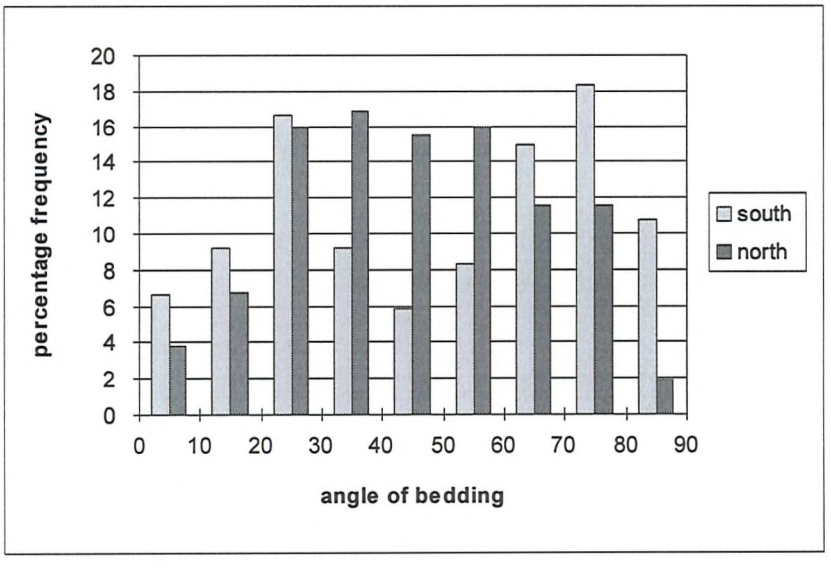

Figure 4.3: (a) Equal-area lower hemisphere projection showing combined data of poles to bedding (open squares) and fold axes (black squares) for the Port Stanley- Bluff Cove area. (b) Percentage frequency distribution of angles of dip for northward (dark) and southward (light) dipping strata.

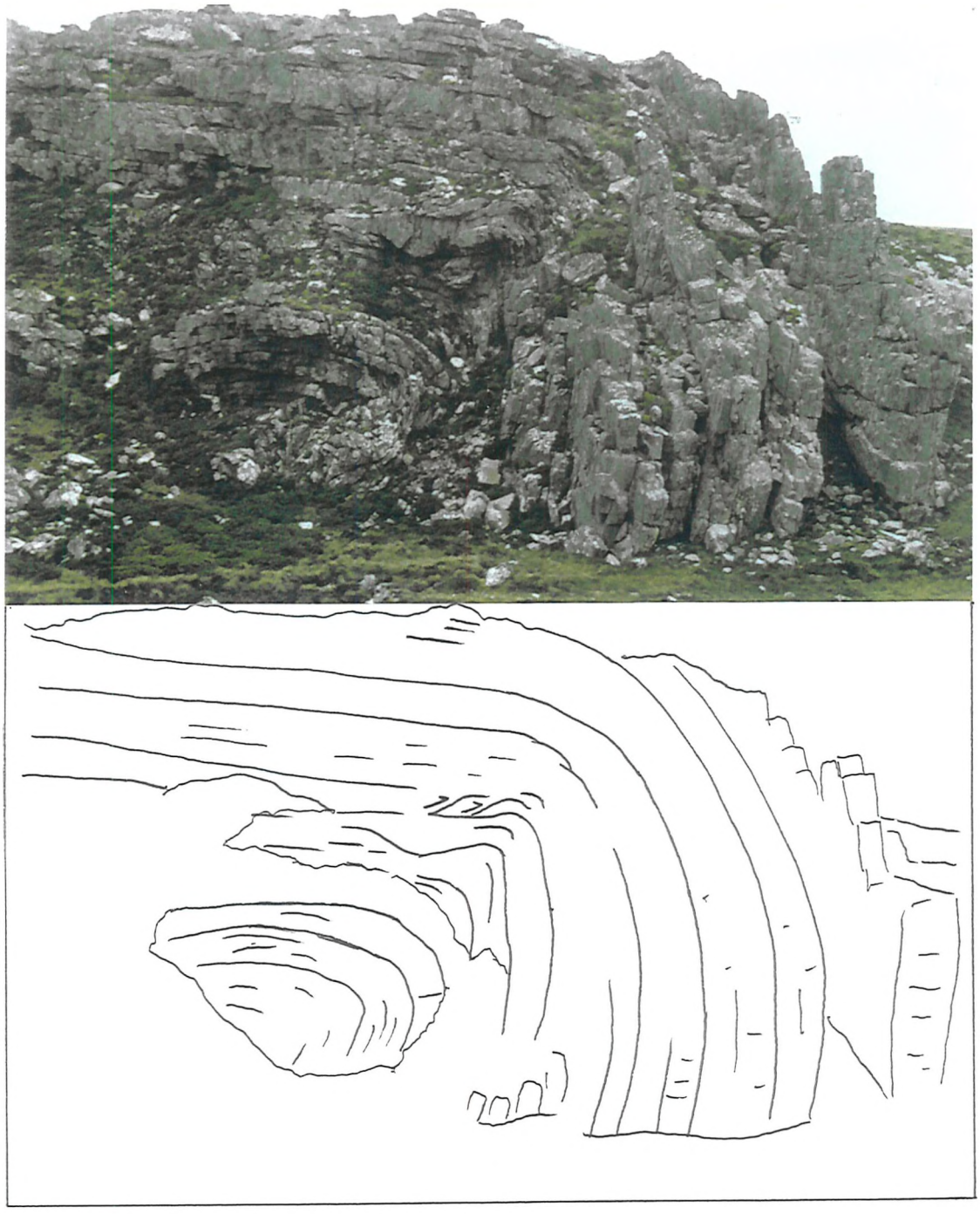

Figure 4.4: Photograph and line drawing, looking east, of a southward verging anticline in quartzites of the Port Stanley Formation. Note small thrusts appearing in the core of the folding. Outcrop is approx. 20 m high. (UTM grid location, taken from maps, 21FVC122672).

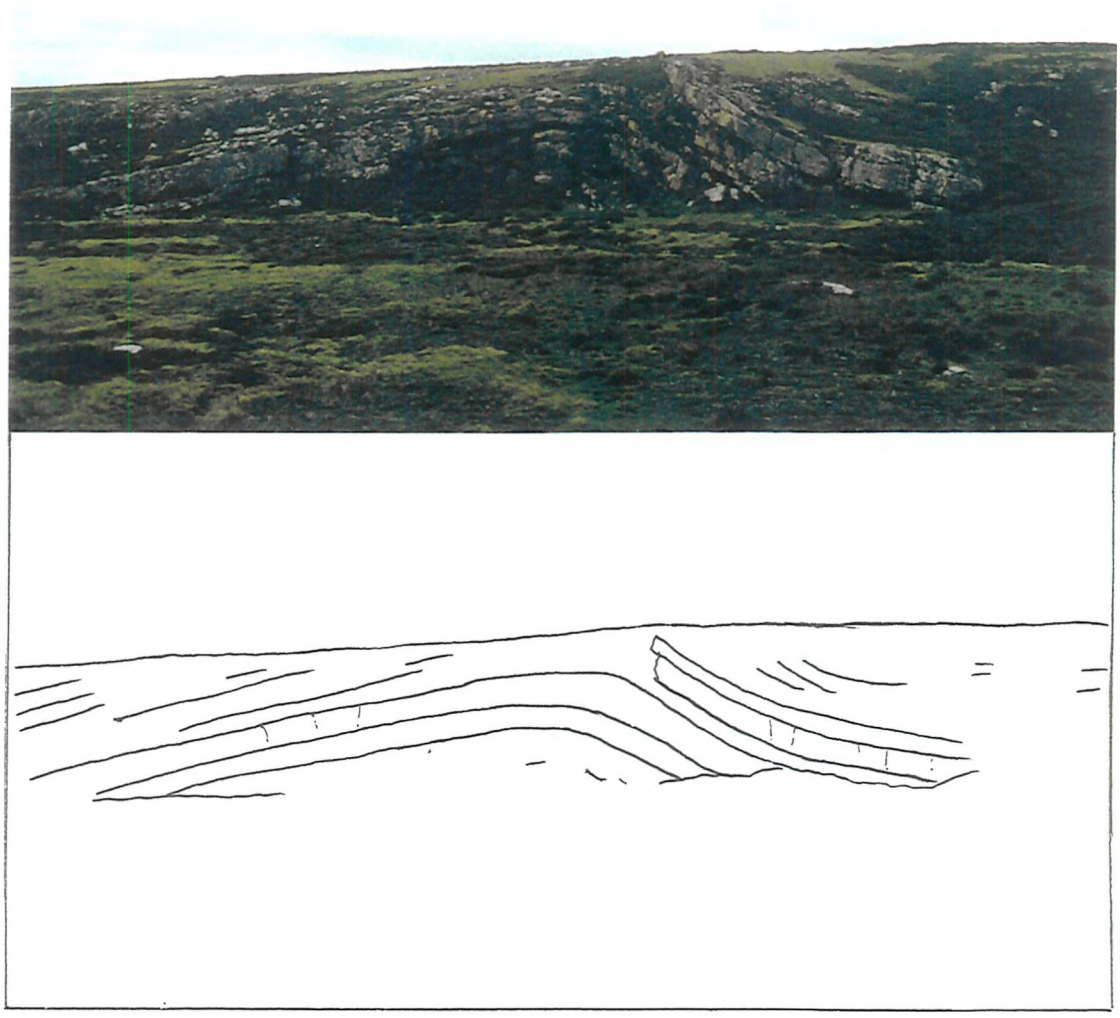

Figure 4.5: Photograph and line drawing, looking west, of a northward verging anticline in quartzites of the Port Stanley Formation, note that dips are far less and interlimb angle far higher than in the southward verging anticline in Figure 4.4. Outcrop is approx. 50 m across. (UTM location 21FVC285685).

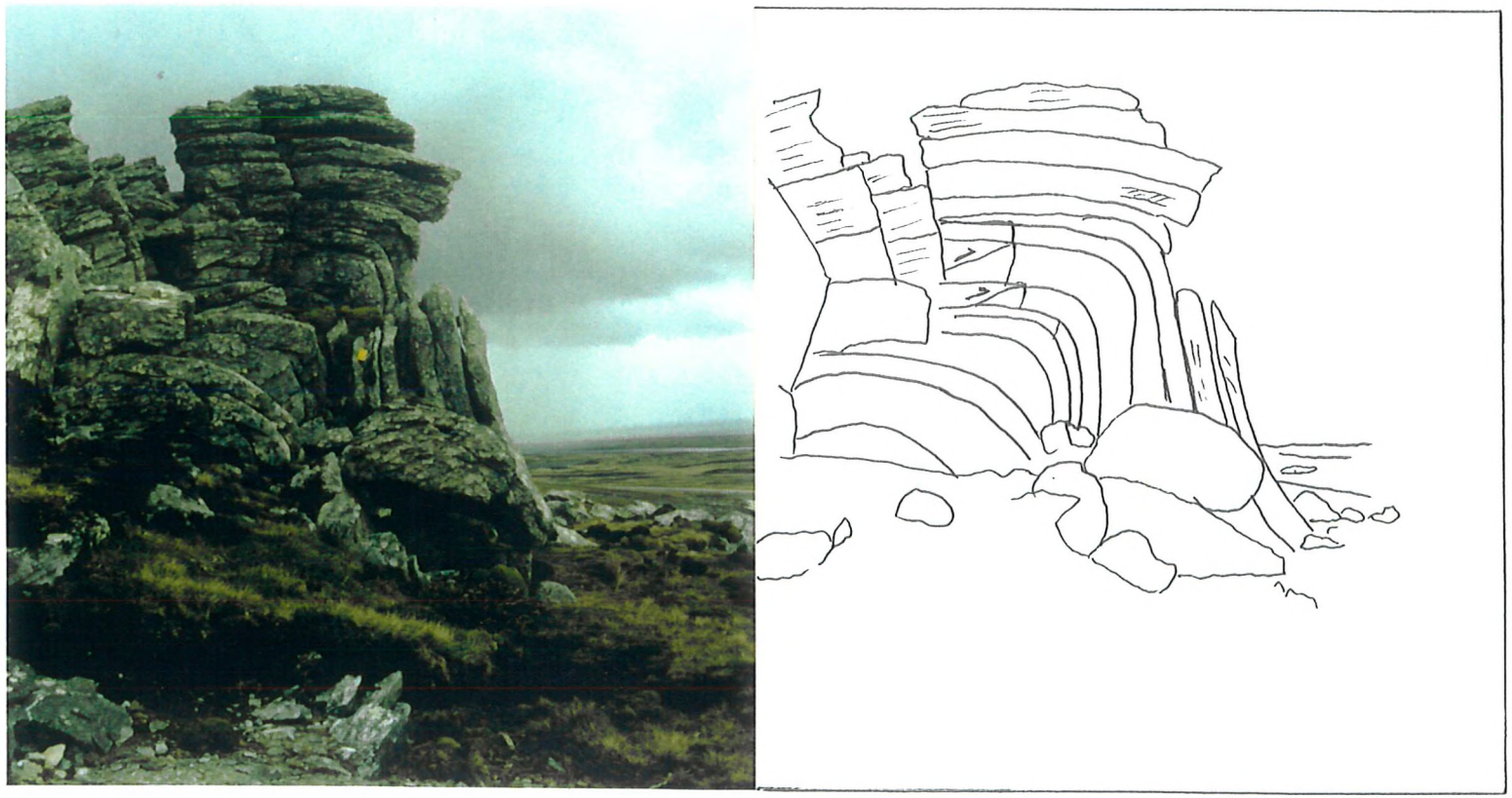

Figure 4.6: Photograph and line drawing, looking east, of southerly verging anticline in the Port Stanley Formation showing differing fold styles between the thicker units, showing class 1B folding, at the base and the thinner units, showing class 2 folding, at the top of the outcrop. Notebook is 13 cm in width. (UTM location 21FVC266707).

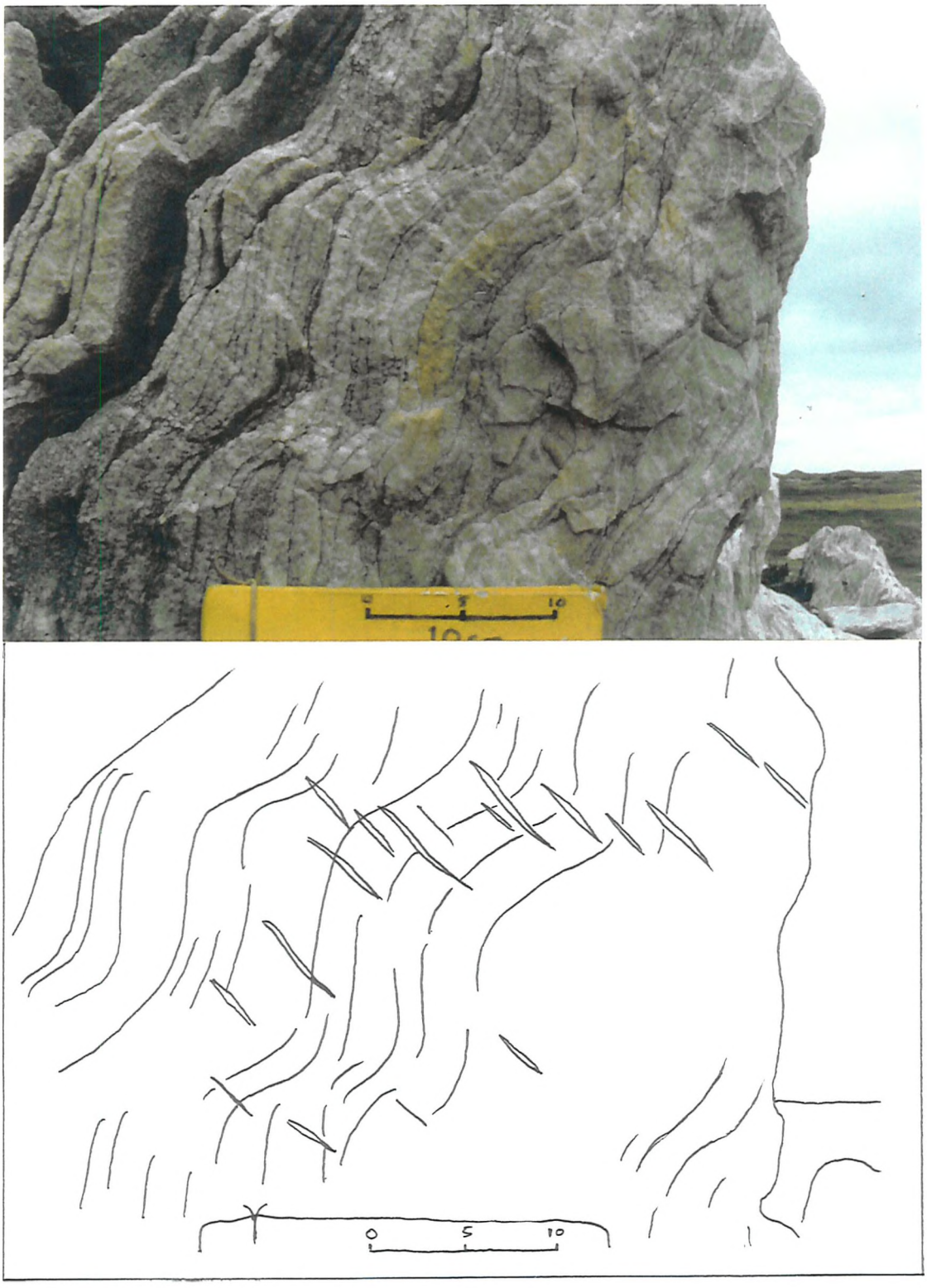

Figure 4.7: Photograph and line drawing, looking east, of top-to-the-south semi-ductile shearing in thinly bedded quartzites of the Port Stanley Formation. Displacements are around 10 cm and quartz veins can be seen to have developed as a result of the shearing. Notebook shows 10 cm scale bar. (UTM location 21FVC475734)

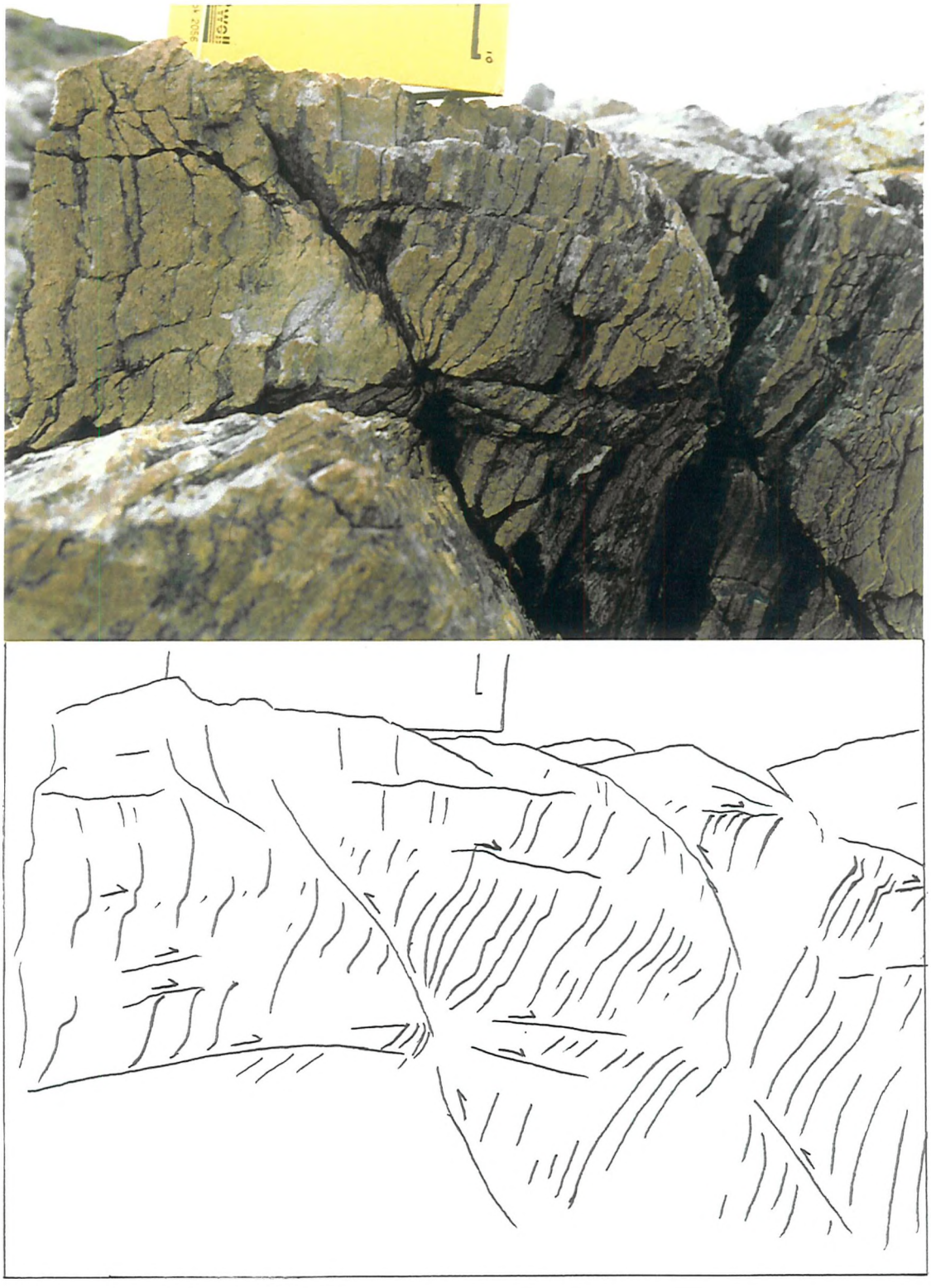

Figure 4.8. Photograph and line drawing, looking east, of conjugate shears in thinly bedded, steeply dipping quartzites of the Port Stanley Formation showing curvature of the beds into the shear planes and the development of brittle fractures rather than ductile shearing. Notebook is 20 cm long. (UTM location 21FVC191649).

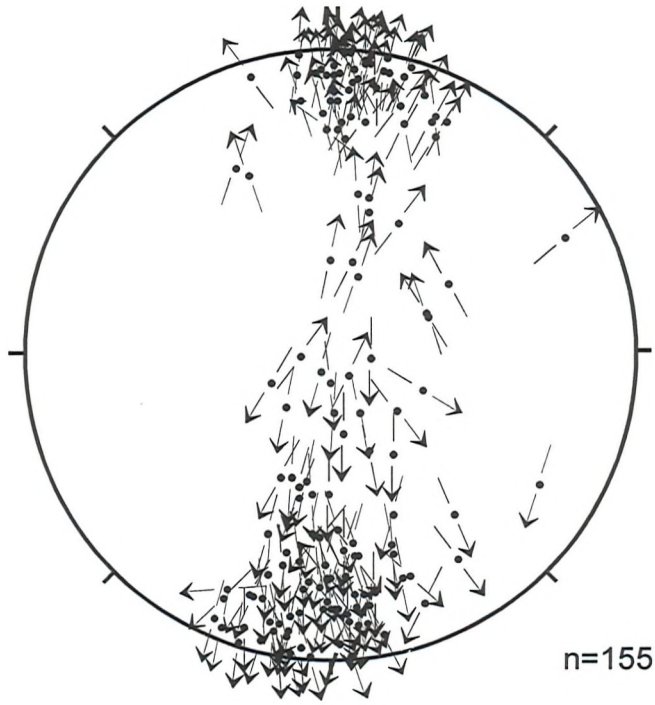

Figure 4.9: Hoeppenor plot of flexural slip planes and slip directions, Port Stanley Formation, Port Stanley-Bluff Cove area.

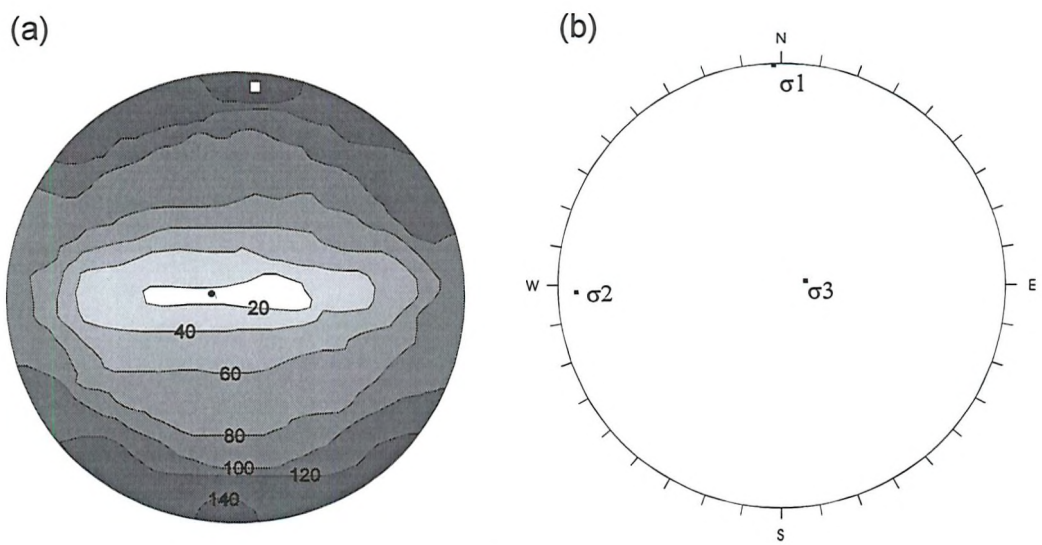

n=155
contours denote density of data closest to σ_1.

Figure 4.10: (a) P/T dihedra plot for flexural slip planes in the Port Stanley Formation, Port Stanley-Bluff Cove area. Square denotes most likely position of σ_1, circle denotes most likely position of σ_3. (b) principal stress directions calculated from P/T dihedra plot.

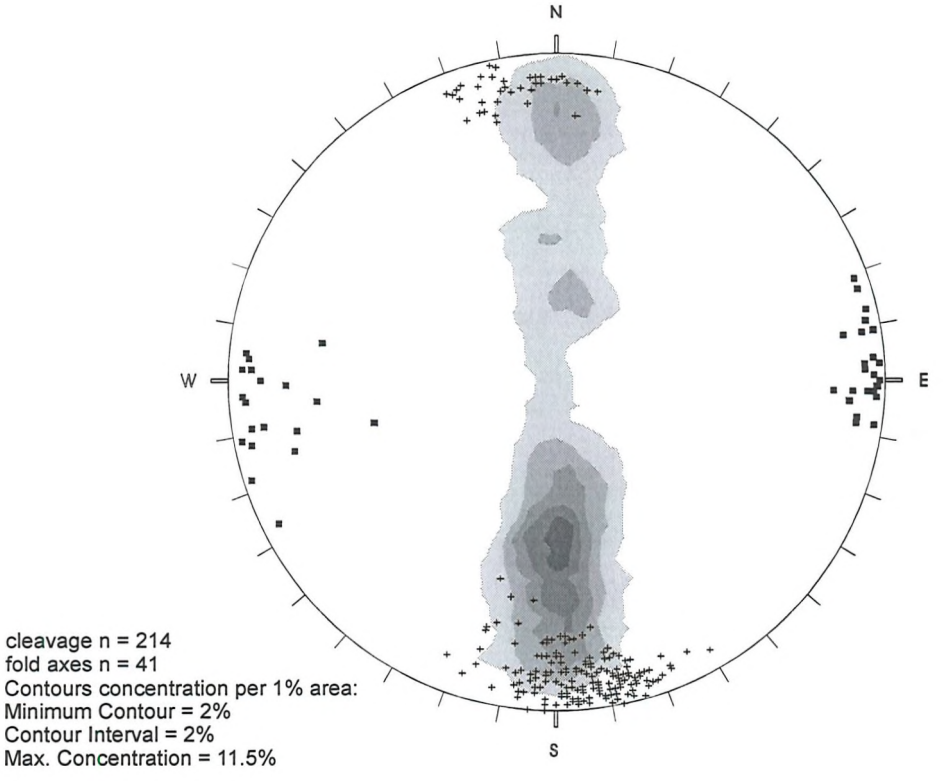

Figure 4.11: Equal-area lower hemisphere projection showing poles to cleavage (crosses) in the Bluff Cove and Lafonian Diamictite Formations from the Port Stanley-Bluff Cove area; fold axes (black squares) and contours of poles to bedding display the axial planar nature of the cleavage in this area.

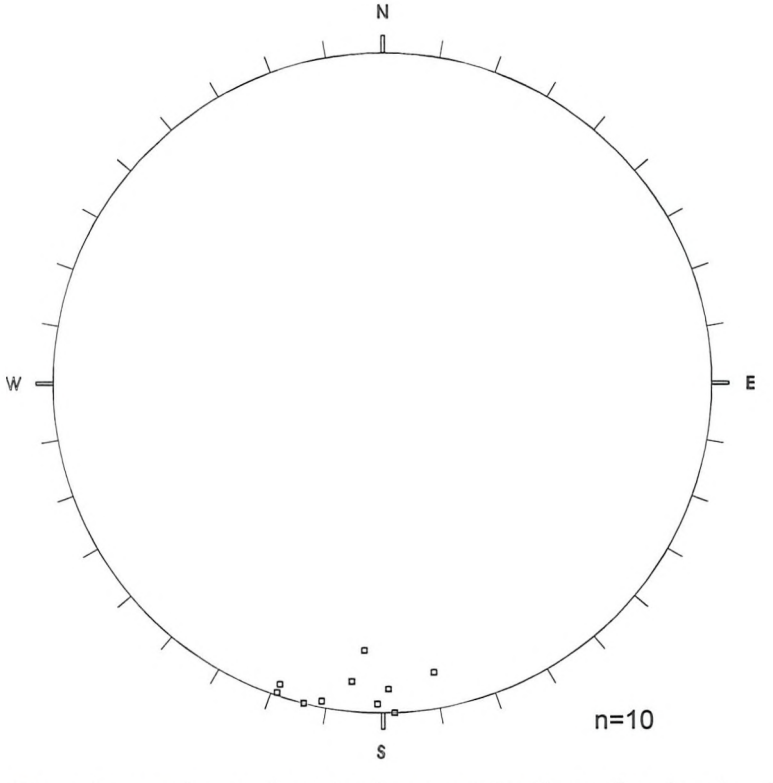

Figure 4.12: Equal-area lower hemisphere projection of poles to cleavage from the Port Stephens Formation, Malo Hills.

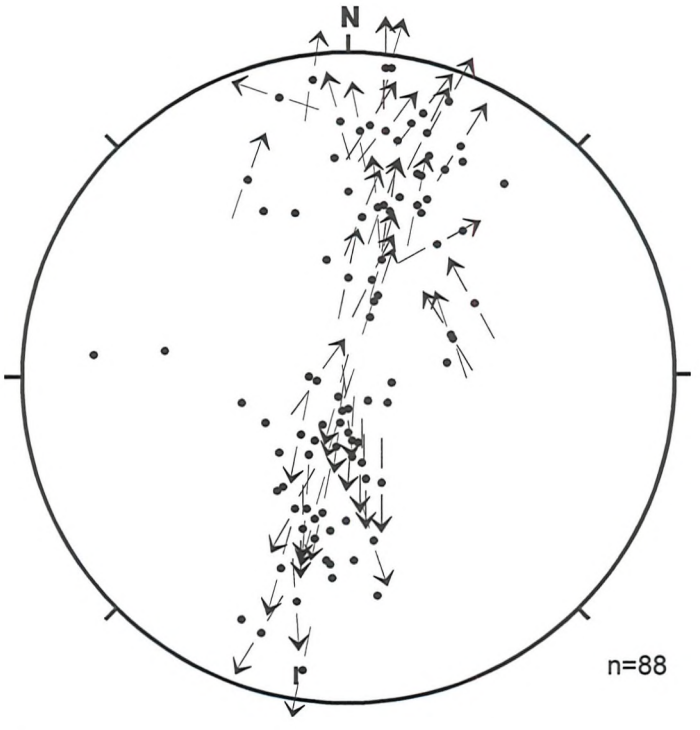

Figure 4.13: Hoeppenor plot of reverse faults within the Port Stanley Formation, Port Stanley-Bluff Cove area.

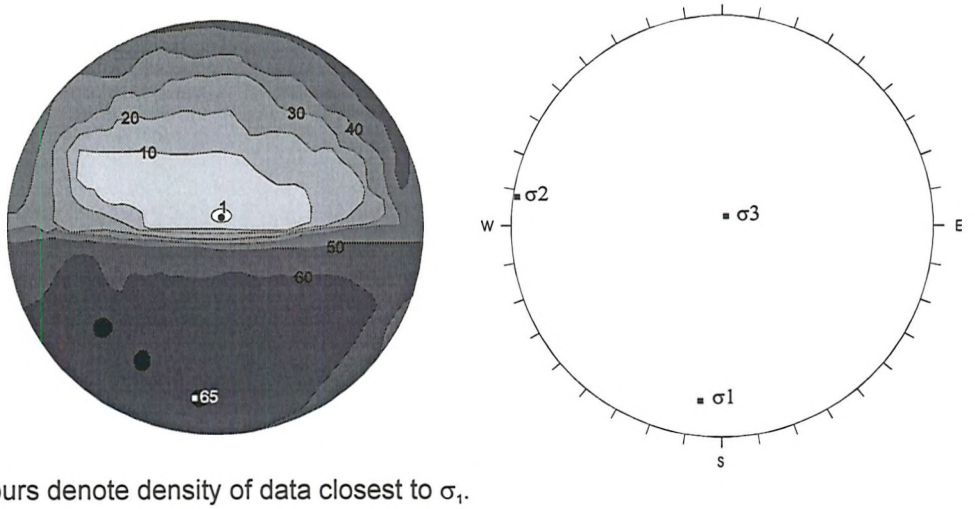

n=88
contours denote density of data closest to σ_1.

Figure 4.14: (a) P/T dihedra plot of reverse faults in the Port Stanley Formation in the Port Stanley-Bluff Cove area. Square denotes most likely position of σ_1, circle denotes most likely position of σ_3. (b) principal stress directions calculated from P/T dihedra plot.

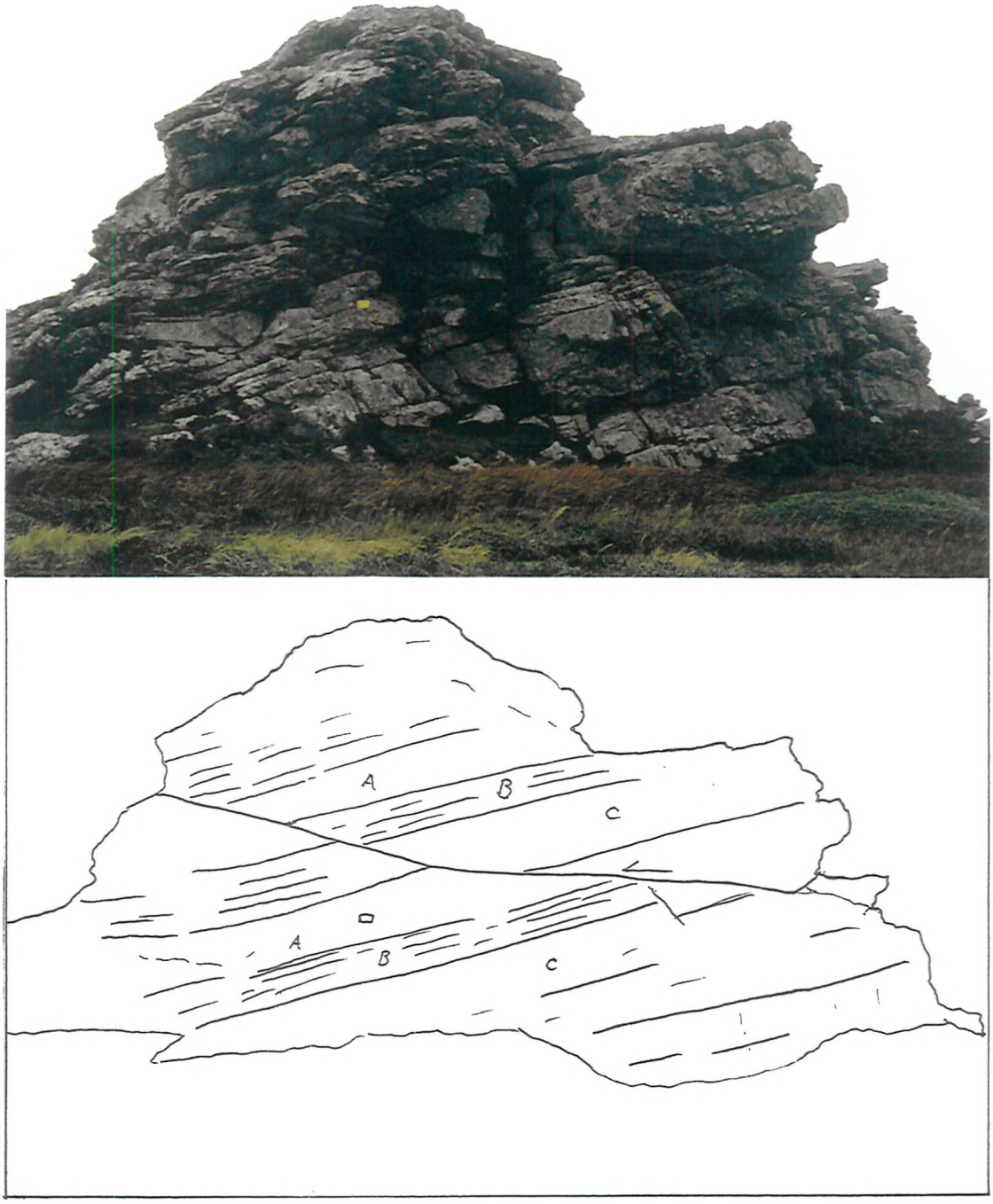

Figure 4.15: Photograph and line drawing, looking west, of a low angle reverse fault in quartzites of the Port Stanley Formation on Tumbledown Mountain. The fault dips gently to the north, bedding dips gently south. Displacement, which is top-to-the-south, is of the order of 10 m. Notebook is 13 cm in width. (UTM location 21FVC342742).

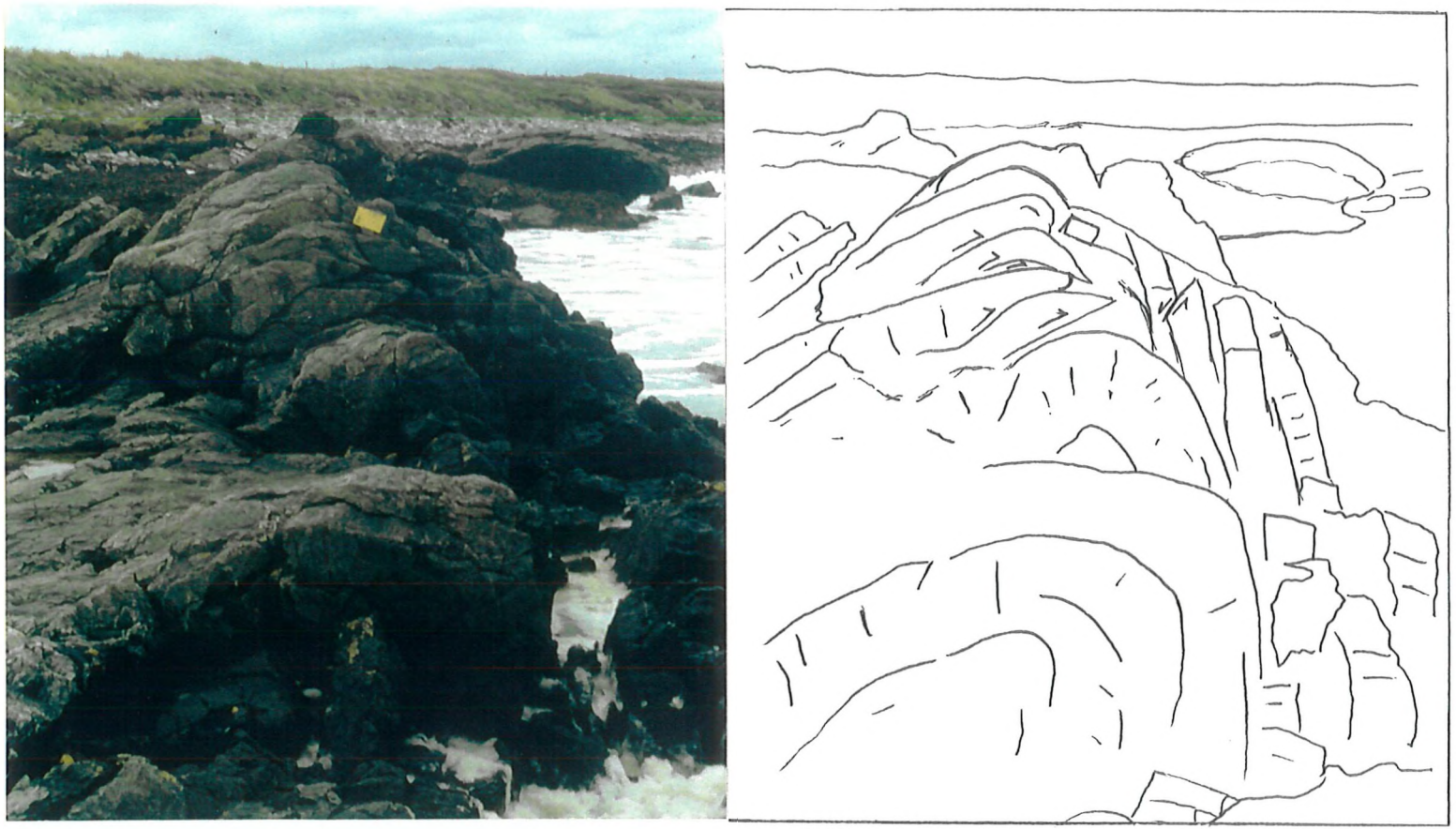

Figure 4.16: Photograph, looking east, of an anticline in quartzites of the Port Stanley Formation south of Surf Bay, showing top-to-the-south reverse faulting through the crest of the anticline. Notebook is 13 cm in width. (UTM location 21FVC435718).

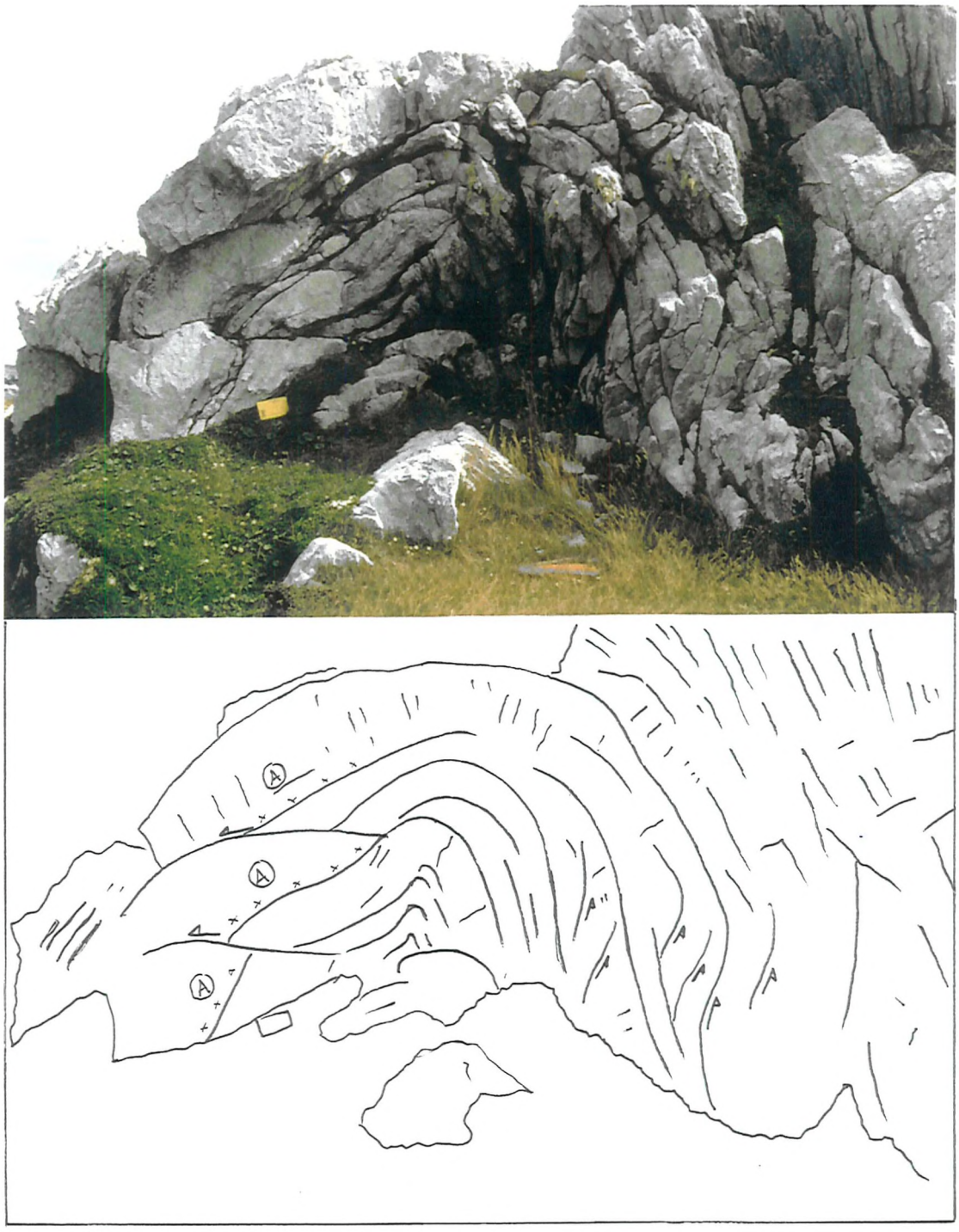

Figure 4.17: Photograph and line drawing, looking west, of an anticline in quartzites of the Port Stanley Formation located west of Stanley Airport, showing early thrust faults which have been refolded around the hinge of an E-W striking anticline. Notebook is 13 cm in width. (UTM location 21FVC449737).

Figure 4.18: Photograph, looking east, of the tight to isoclinal folding in quartzites of the Port Stanley Formation at Bluff Cove. Cliff is approx. 20m high. (UTM location 21FVC198649).

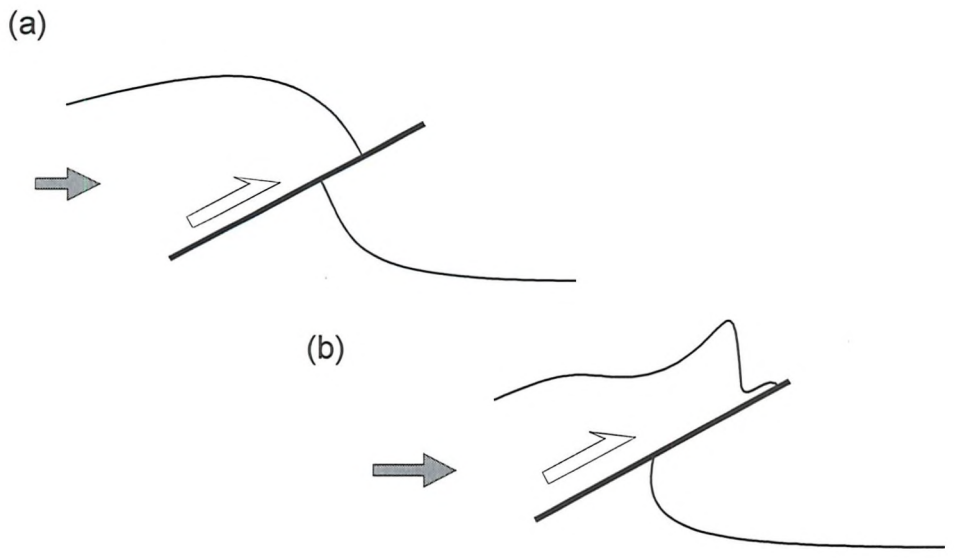

Figure 4.19: Sketch to show possible development of the Bluff Cove Fold above a thrust fault. (a) initial hanging-wall anticline above a thrust fault. (b) Further movement on the fault tightens the initial fold and causes smaller, lower amplitude folds to develop.

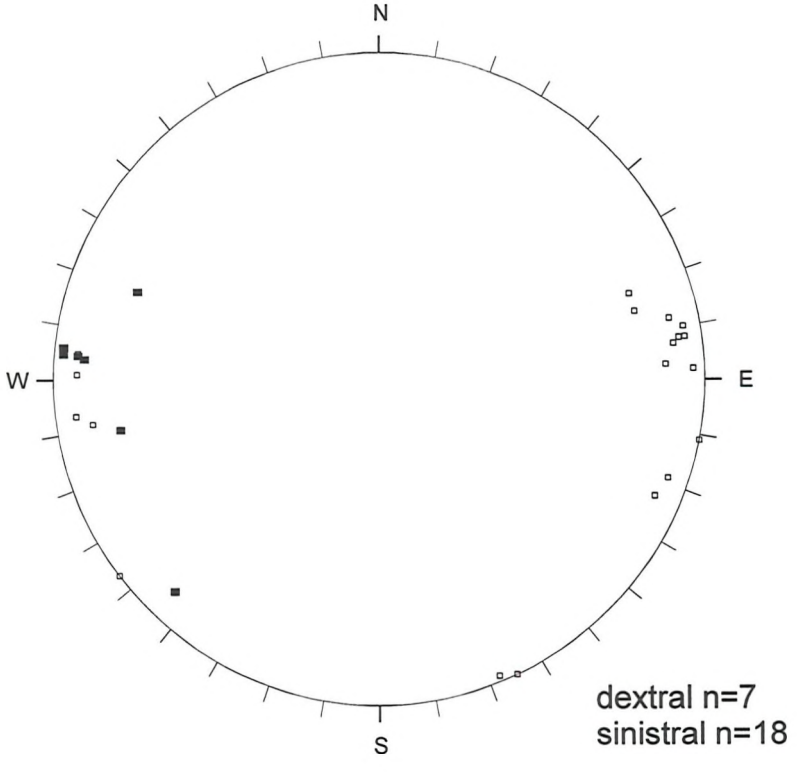

Figure 4.20: Equal-area lower hemisphere projection of poles to shears showing dextral (black squares) or sinistral (open squares) displacements. Data from the Port Stanley Formation, Port Stanley-Bluff Cove.

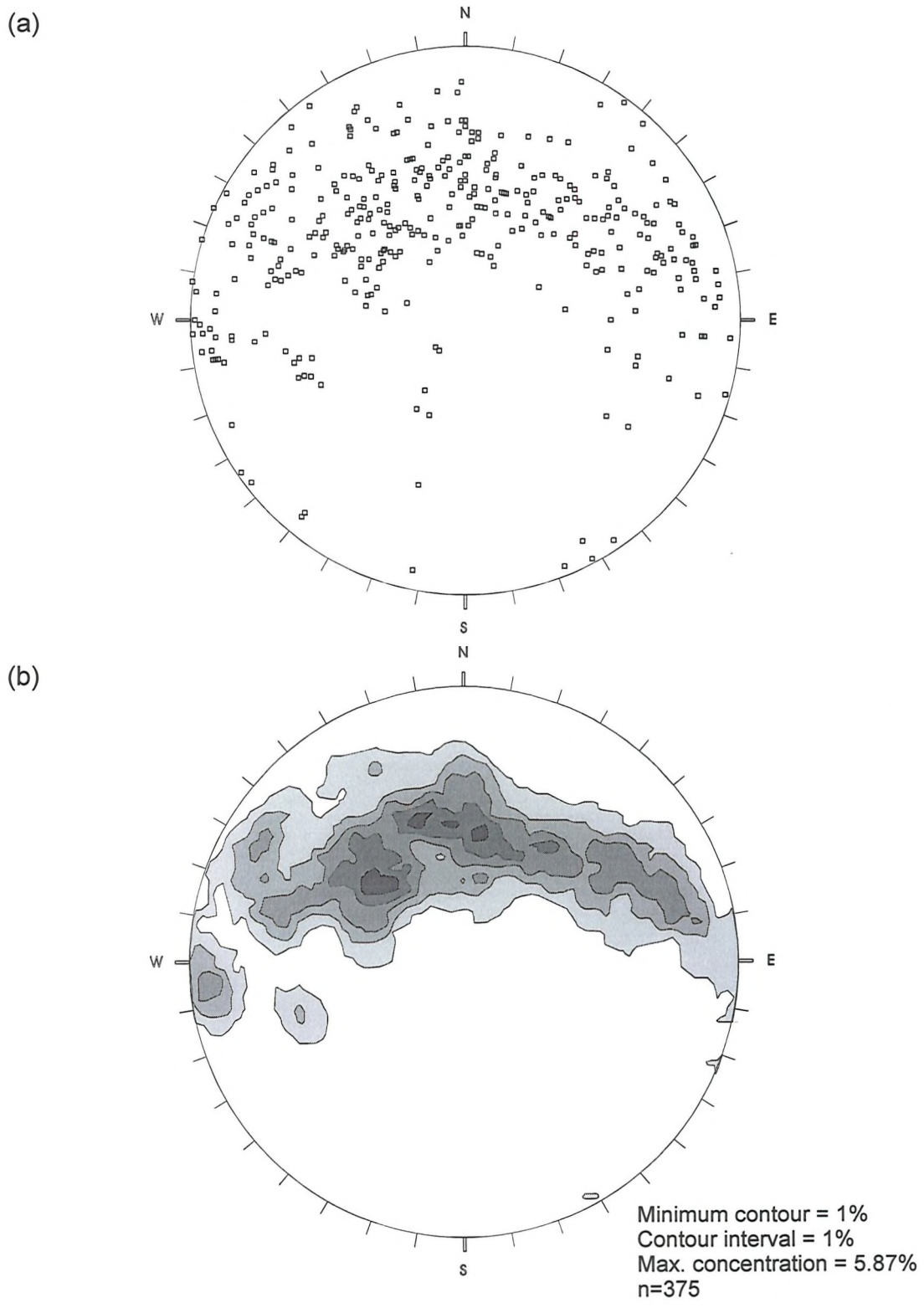

Figure 4.21: Equal-area lower hemisphere projections for quartz veins from the Port Stanley Formation in the Port Stanley-Bluff Cove area: (a) poles to veins; (b) contoured plot of poles to veins.

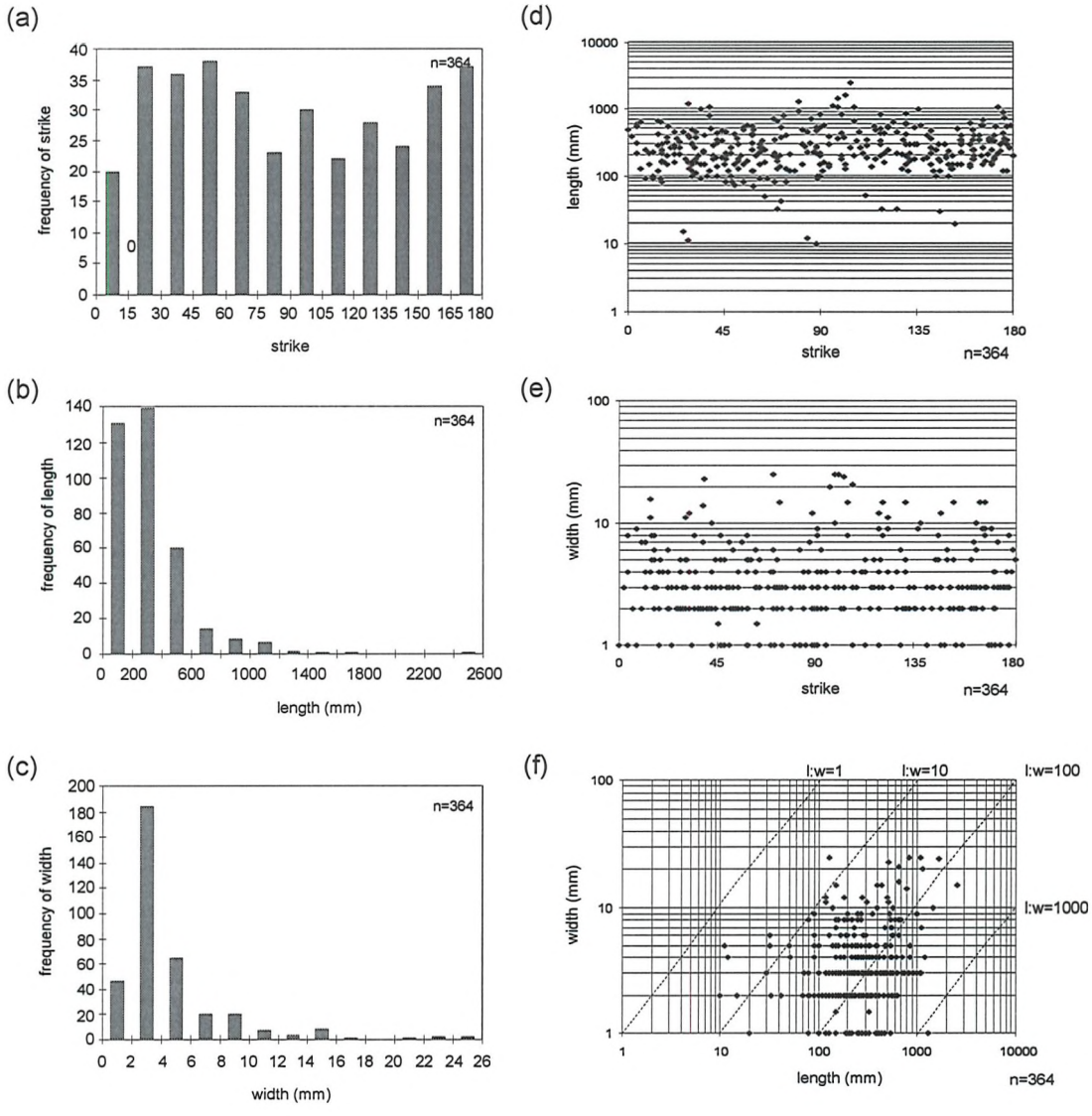

Figure 4.22: Data from quartz veins in the Port Stanley Formation; (a) strike frequency; (b) length frequency; (c) width frequency; (d) plot of log (length) against strike; (e) plot of log (width) against strike; (f) log/log plot of length against width.

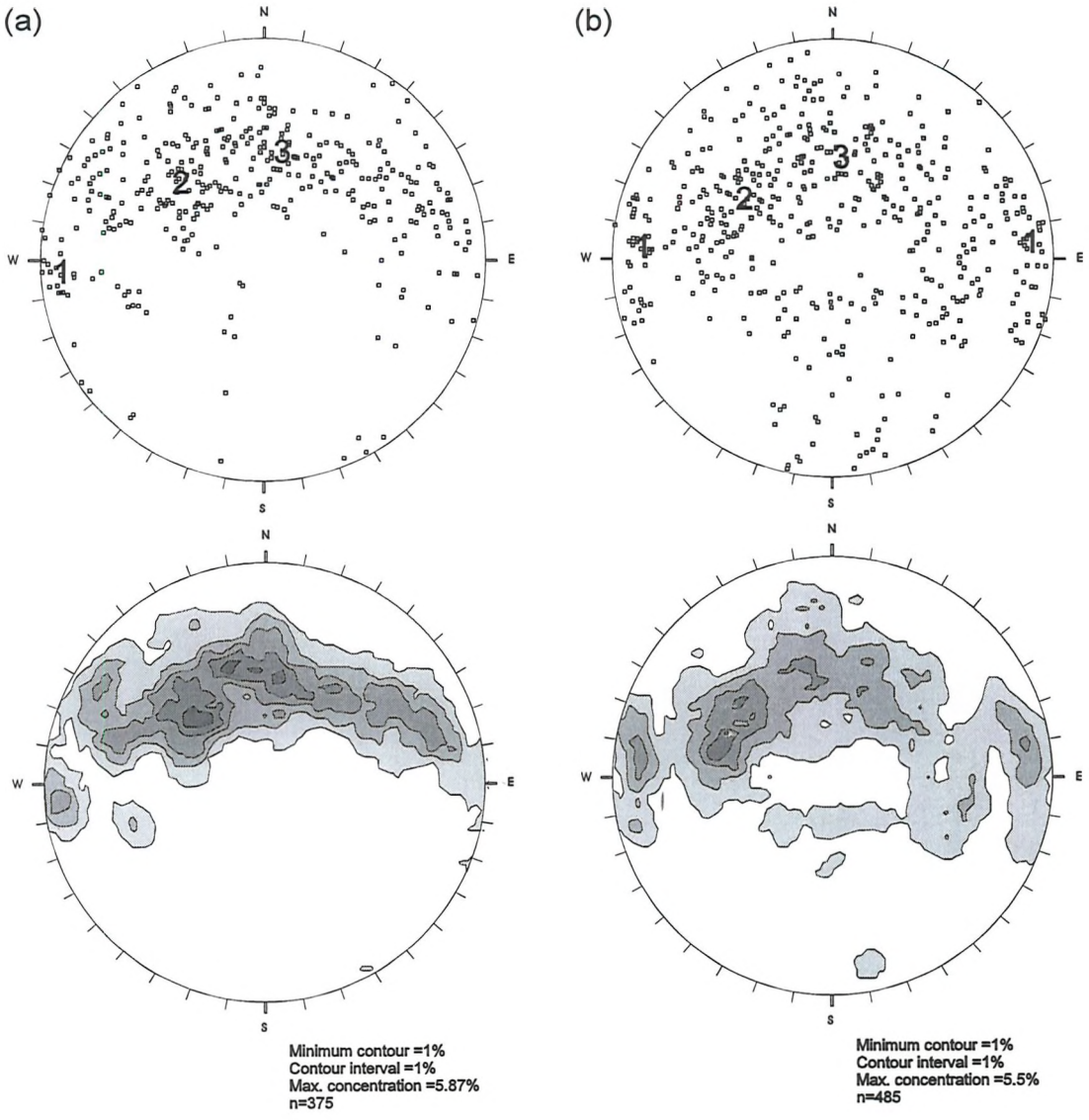

Figure 4.23: Equal-area lower hemisphere projections comparing poles to veins and contoured plots of (a) dataset from specific transects used for strain estimations and cross-cutting relationships and (b) a second dataset collected from exposures of the Port Stanley Formation mapped across the Port Stanley-Bluff Cove area. Numbers 1, 2 & 3 on contour plots indicate vein groups 1, 2 & 3 referred to in the text and highlight the close similarity of the two datasets.

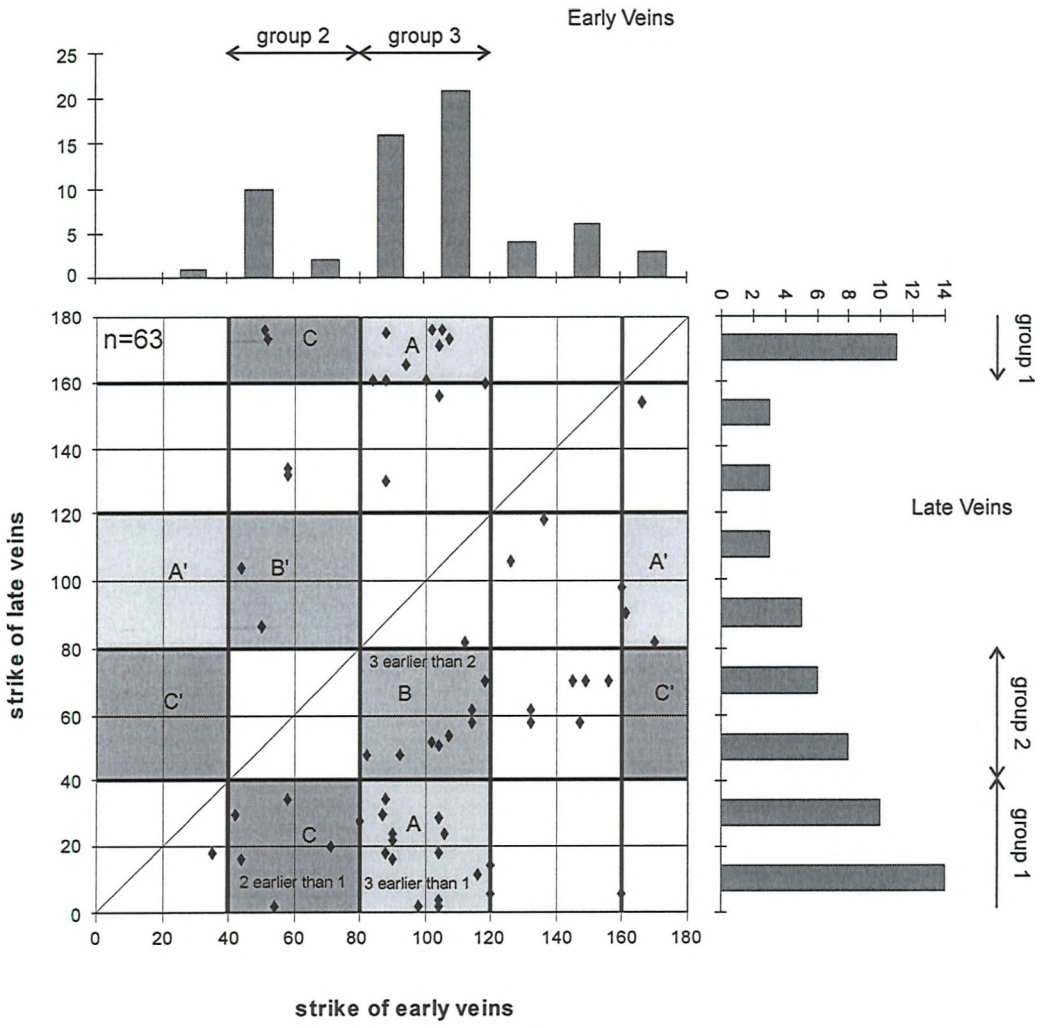

Figure 4.24: Graph showing the cross-cutting relationship of the three groups of veins in the Port Stanley Formation located along 5 transects around Stanley. Each point represents one pair of veins, the strike of the earlier vein plotted on the x-axis, the strike of the later vein plotted on the y-axis. The two bar charts show the strike frequency of early and late formed veins and highlight three distinct groups of veins. Blocks A, A', B, B', C & C' represent clusters of cross-cutting veins, e.g. veins in block A=> group 3 older than group 1, however, veins in A'=> group 1 older than group 3.

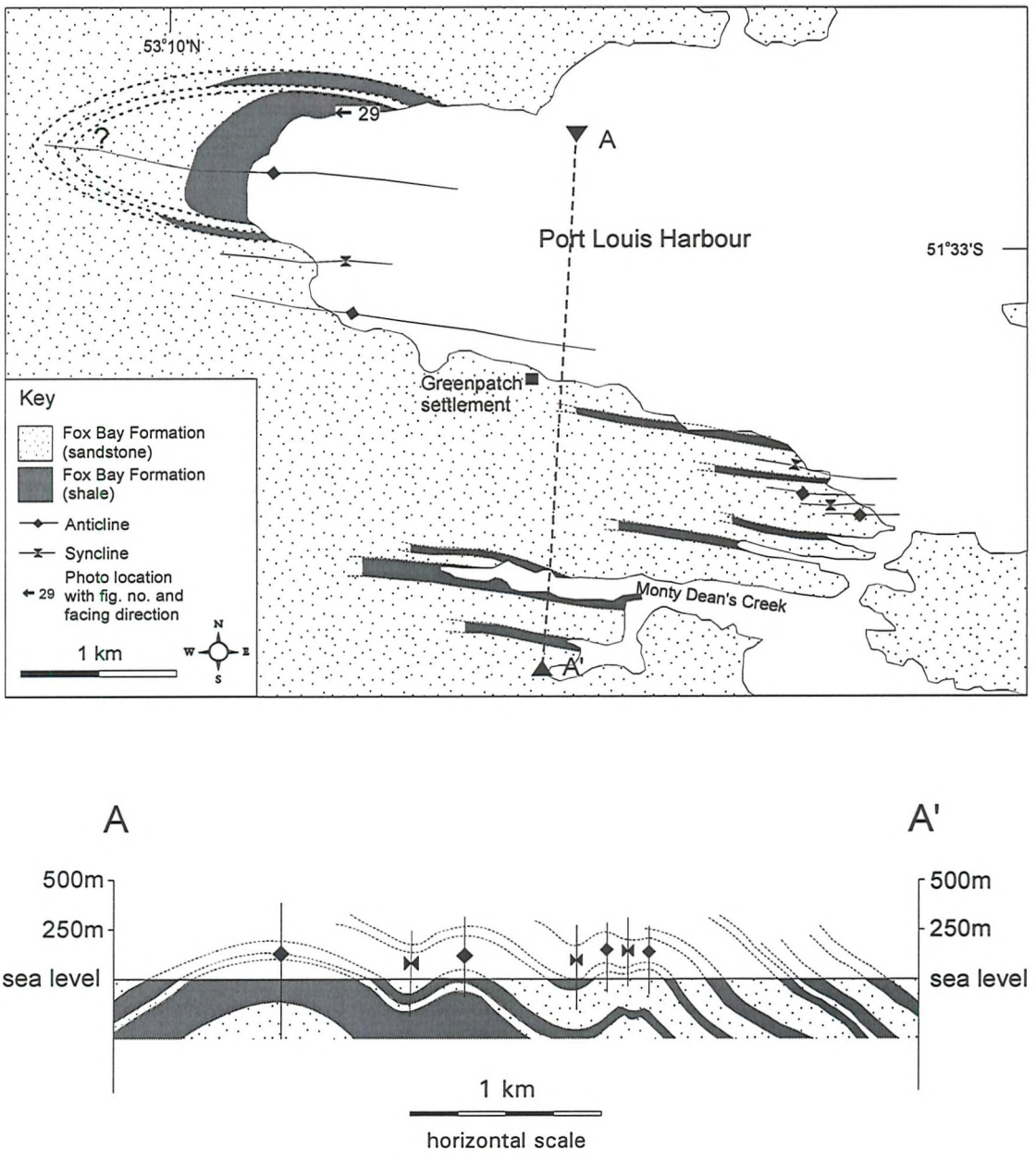

Figure 4.25: Summary geological map and cross-section of the Greenpatch area.

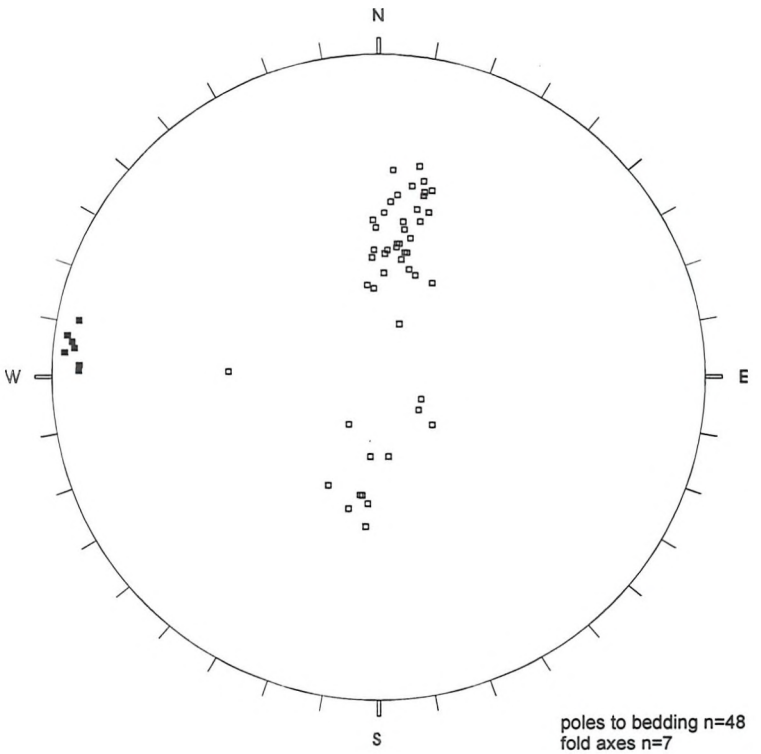

Figure 4.26 : Equal-area lower hemisphere projection of poles to bedding (open squares) and fold axes (black squares) from the Greenpatch area.

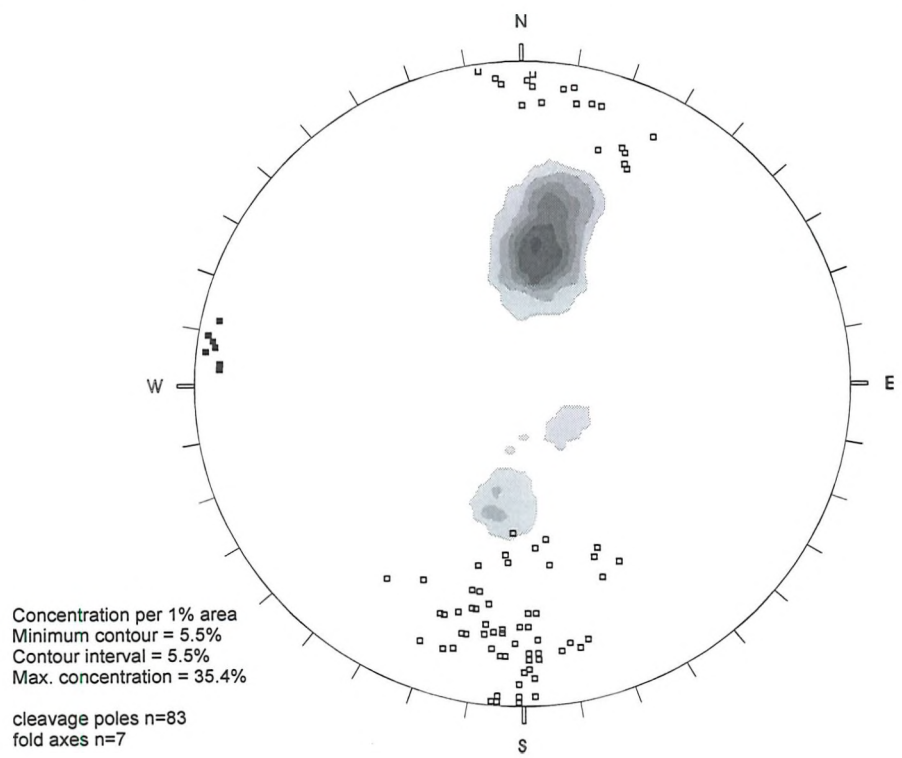

Figure 4.27: Equal-area lower hemisphere projection showing poles to cleavage (open squares), fold axes (black squares) and contours of bedding, Greenpatch.

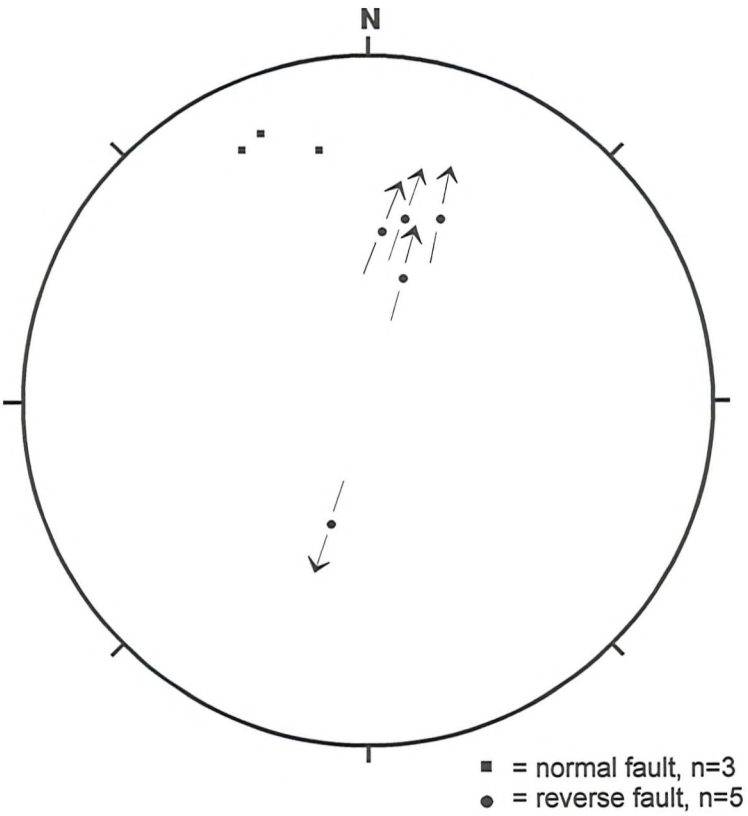

Figure 4.28: Hoeppenor plot of poles to normal and reverse faults from the Fox Bay Formation, Greenpatch.

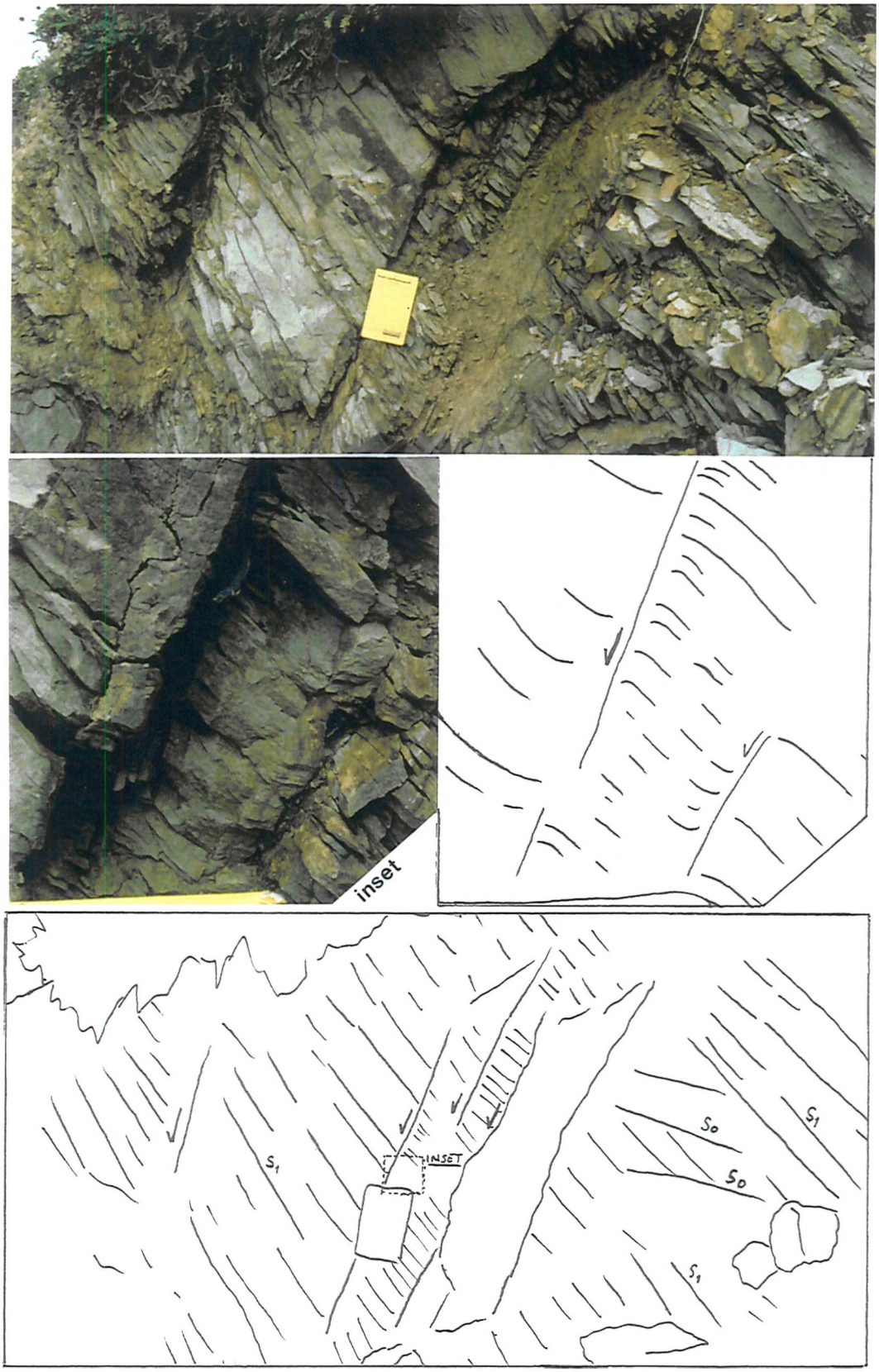

Figure 4.29: Photograph and line drawing, looking west, of normal faults, downthrowing to the south, in sandstones of the Fox Bay Formation on the north side of Port Louis Harbour. Inset shows detail of cleavage planes being curved by the faulting. Notebook is 13 cm in width. (UTM location 21FVC292803).

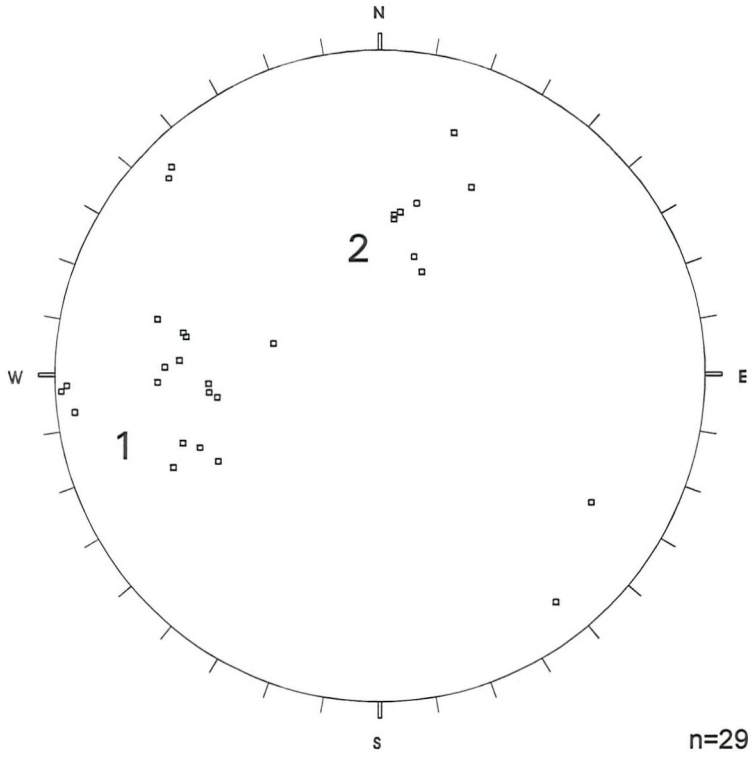

Figure 4.30: Equal-area lower hemisphere projection of poles to quartz veins from the Fox Bay Formation at Greenpatch.

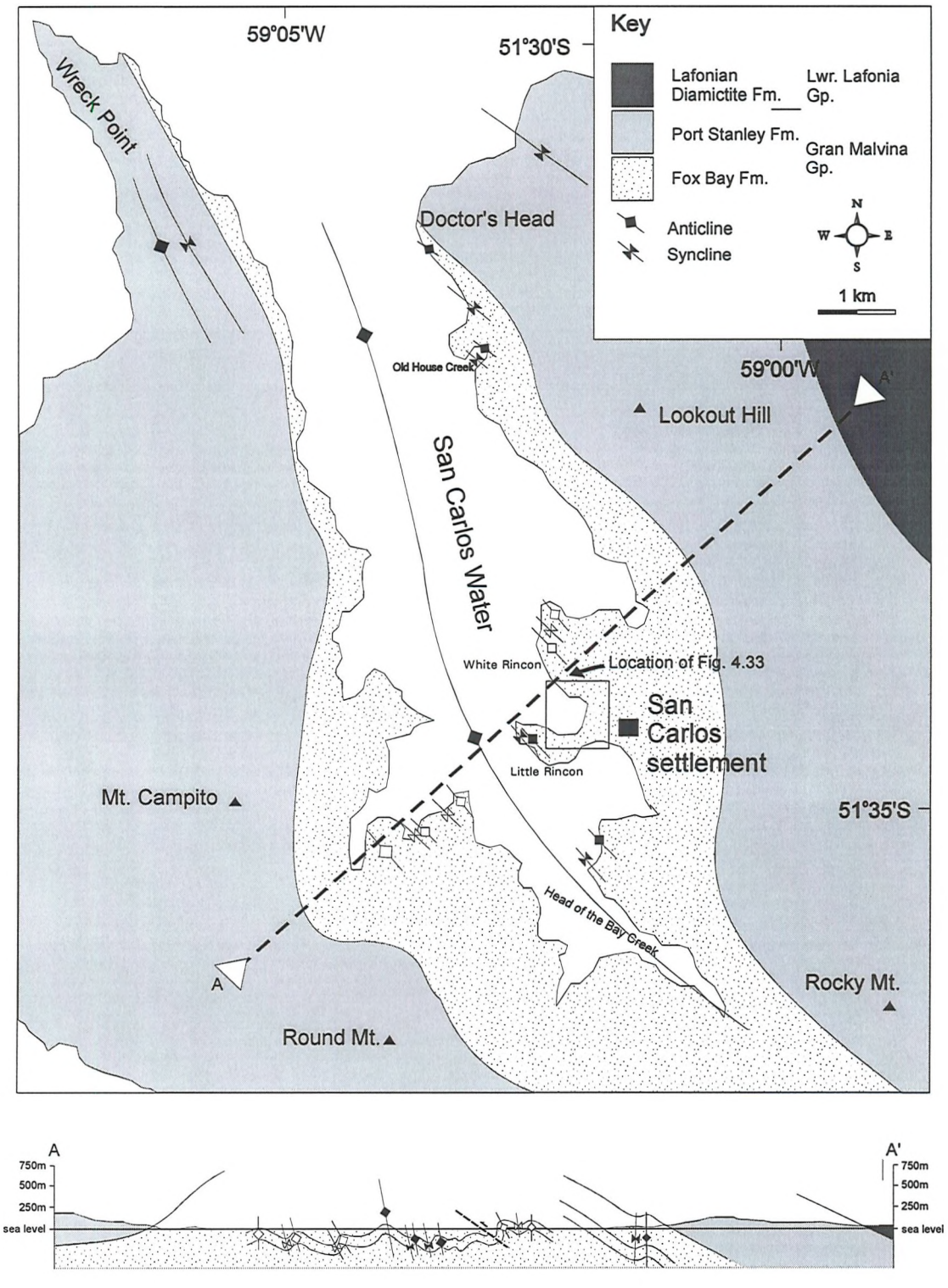

Figure 4.31: Summary geology map and cross-section for San Carlos area. Additional data from Curtis & Hyam (*in press*). For cross-section A-A' horizontal=vertical=map scale

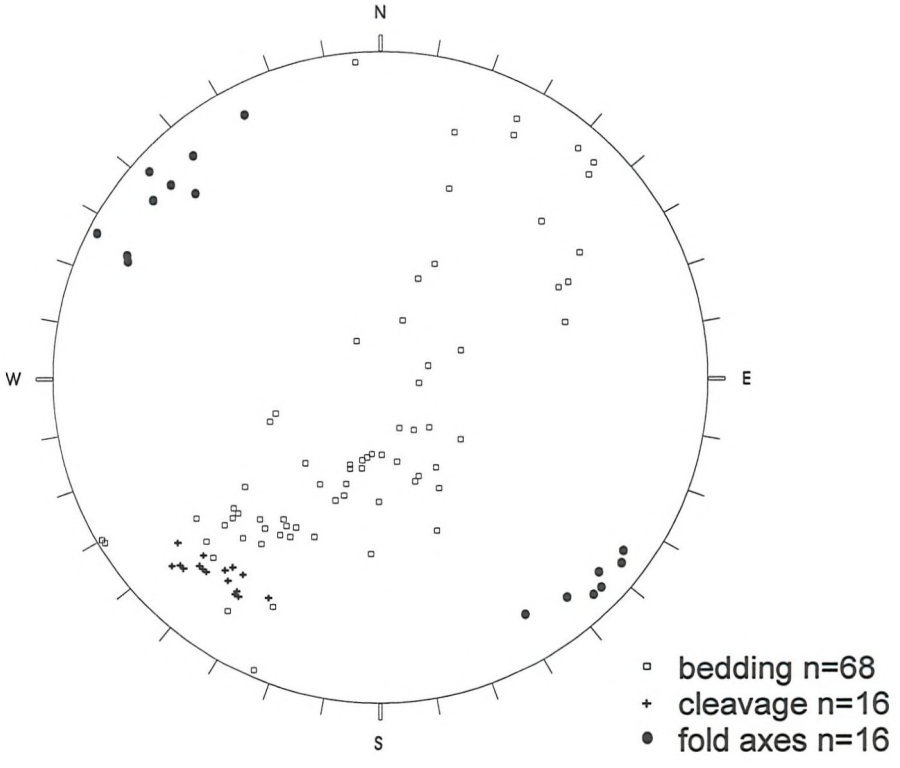

Figure 4.32: Equal-area lower hemisphere projection of poles to bedding (squares), cleavage (crosses) and fold axes (black circles) for the San Carlos area.

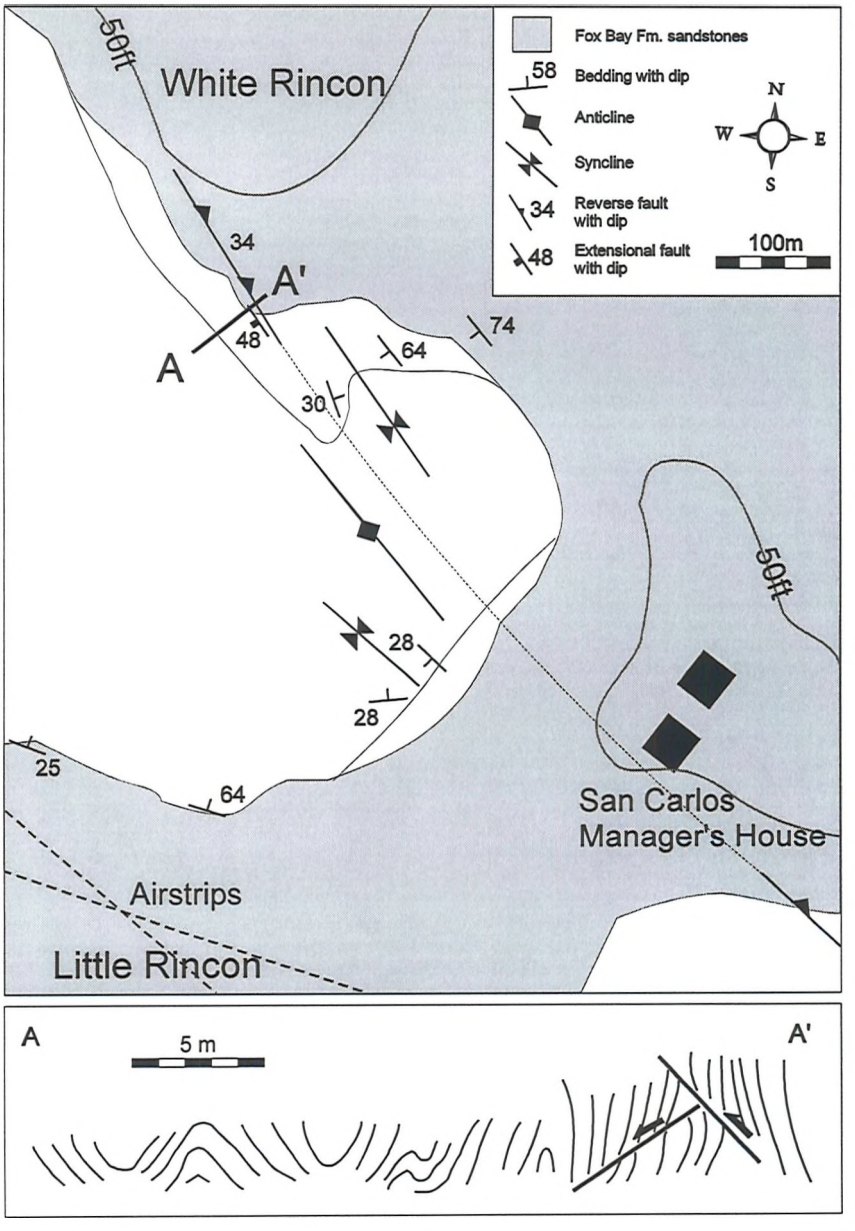

Figure 4.33: Detail of footwall deformation related to thrusting in the Fox Bay Formation around San Carlos. map shows location of section A-A' and detail of larger folds; the section A-A' is taken from field sketches.

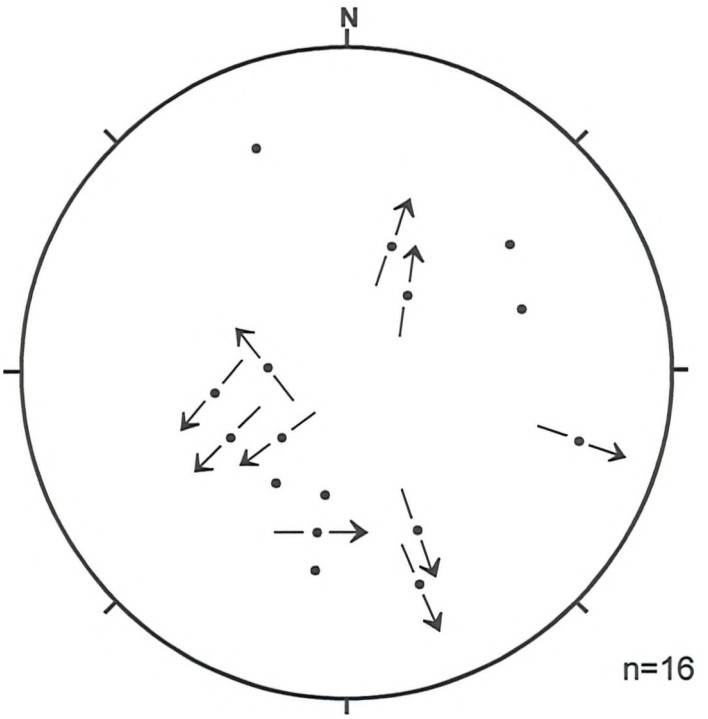

Figure 4.34: Hoeppenor plot of reverse faults within the Fox Bay Formation, San Carlos.

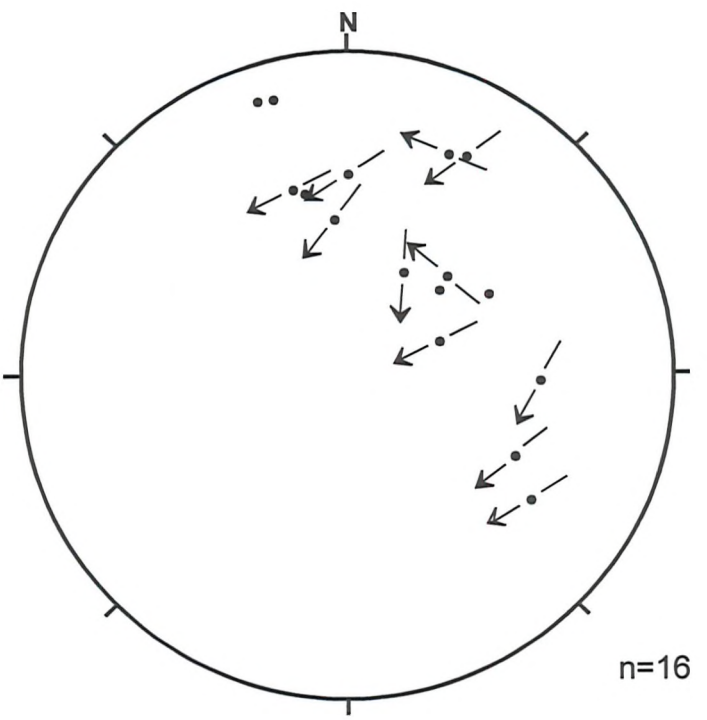

Figure 4.35: Hoeppenor plot of shears within the Port Stanley Formation at Wreck Point, San Carlos.

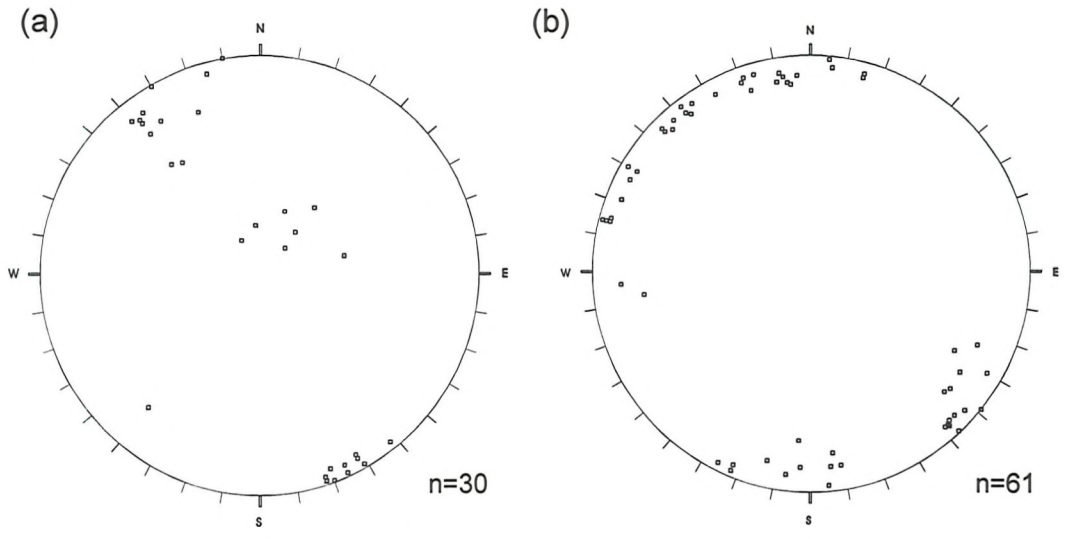

Figure 4.36: Equal-area lower hemisphere projections showing poles to planes of; (a) quartz veins and (b) joints in the Port Stanley Formation, San Carlos.

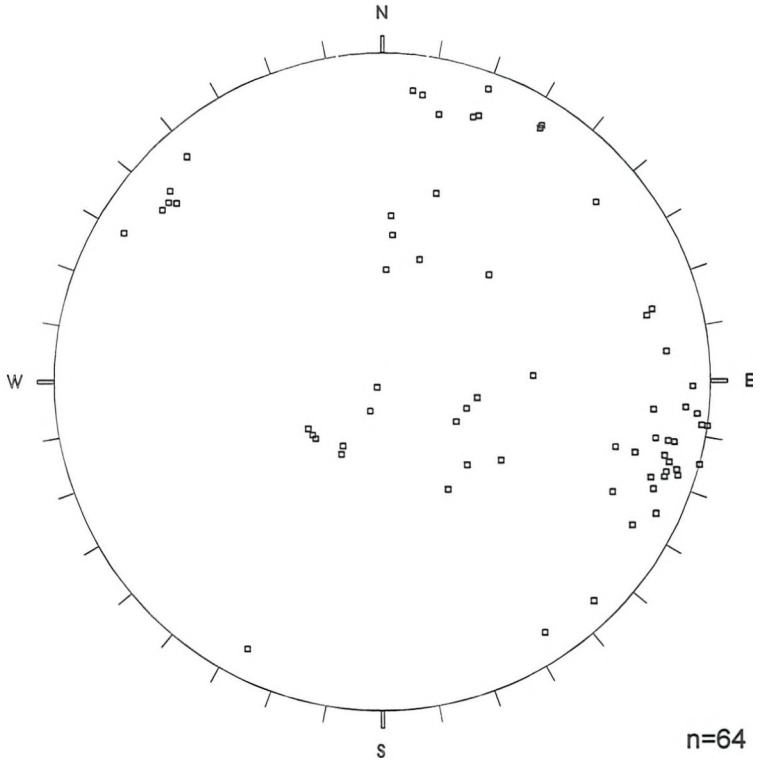

Figure 4.37: Equal-area lower hemisphere projection of poles to planes of quartz veins in the Fox Bay Formation, San Carlos.

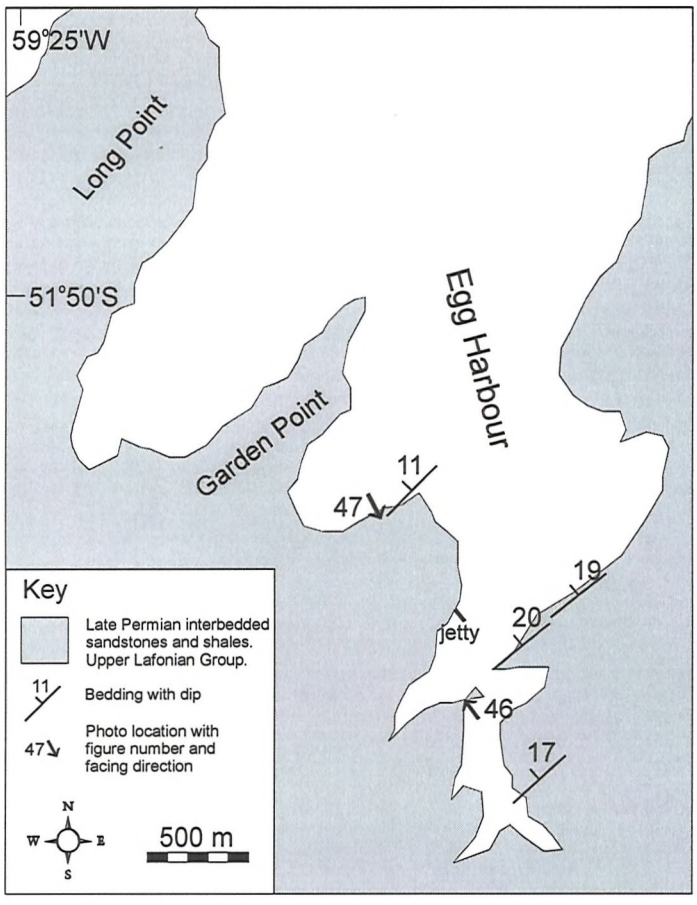

Figure 4.38: Summary map of Egg Harbour.

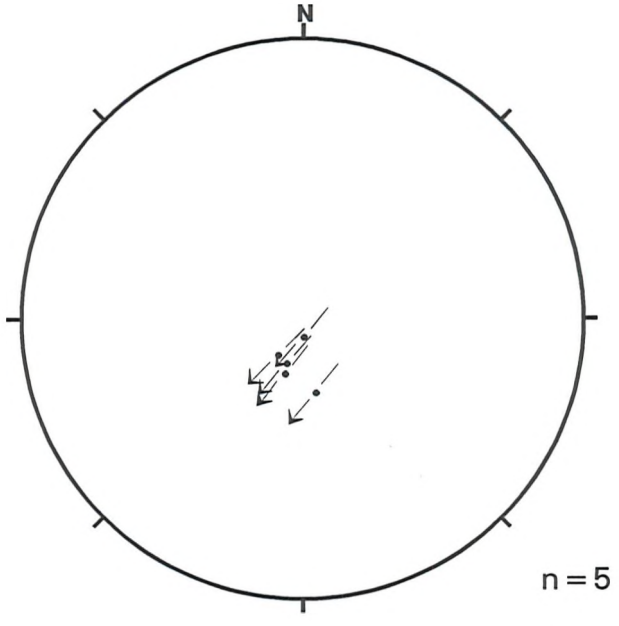

Figure 4.39: Hoeppenor plot of thrusts at Egg Harbour.

Figure 4.40: Photograph and line drawing, looking north-west, of a small top-to-the-south-west reverse fault in thinly bedded, Late Permian aged sandstones at Egg Harbour. Notebook shows 10 cm scale. (UTM location 21FUC357525).

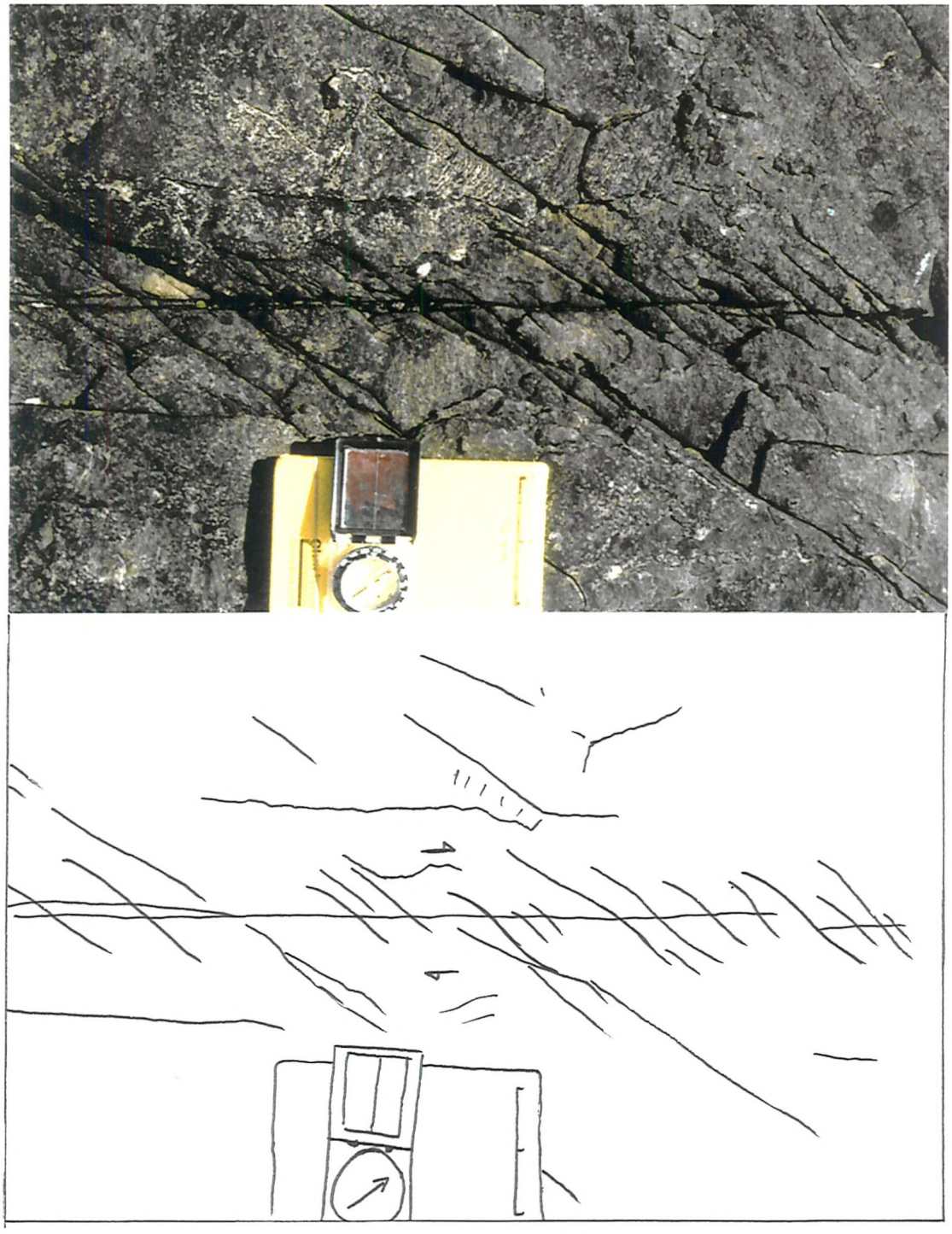

Figure 4.41: Photograph and line drawing of joint system in Late Permian sandstones at Egg Harbour. Note long NE-SW joints cut by sigmoidal lazy-Z joints which indicate dextral strike-slip movement along the joints. Compass clinometer for scale showing the direction of north. (UTM location 21FUC355534).

Location	strike	length (m)	e_1	plunge	azimuth	e_2	plunge	azimuth	e_3	plunge	azimuth	dilation	k	volume Δ.
2pst1-2	267	6	1.9×10^{-2}	21	49	5.5×10^{-3}	22	311	1.6×10^{-3}	59	178	+0.6%	3.5	+2.6%
2pst1-3	276	5.5	3.2×10^{-2}	30	344	8.2×10^{-3}	18	85	2.3×10^{-3}	54	201	+0.7%	4.0	+4.3%
2pst-3	264	60	5.0×10^{-3}	47	53	8.5×10^{-4}	25	173	5.9×10^{-4}	32	280	+0.9%	15.9	+0.6%
2pst-4	270	46	3.2×10^{-2}	58	354	4.6×10^{-3}	6	254	1.8×10^{-3}	31	160	+1.0%	9.5	+3.8%
2pst-5	273	45	7.1×10^{-3}	53	319	2.7×10^{-3}	21	79	6.3×10^{-4}	29	181	+0.2%	2.2	+1.1%
2pstall	270	162.5	1.4×10^{-2}	56	359	3.7×10^{-3}	2	266	1.5×10^{-3}	34	175	+0.7%	4.4	+1.8%
scr-8	321	14	7.5×10^{-4}	13	339	3.2×10^{-4}	32	240	2.0×10^{-5}	55	88	+0.01%	1.4	+0.1%
scr-10	205	150	3.2×10^{-4}	3	333	1.0×10^{-5}	66	236	4.0×10^{-6}	24	64	+0.03%	31	+0.03%

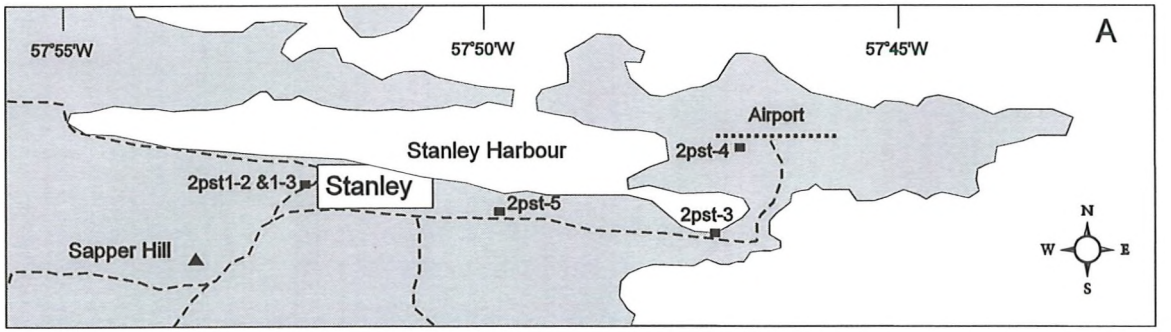

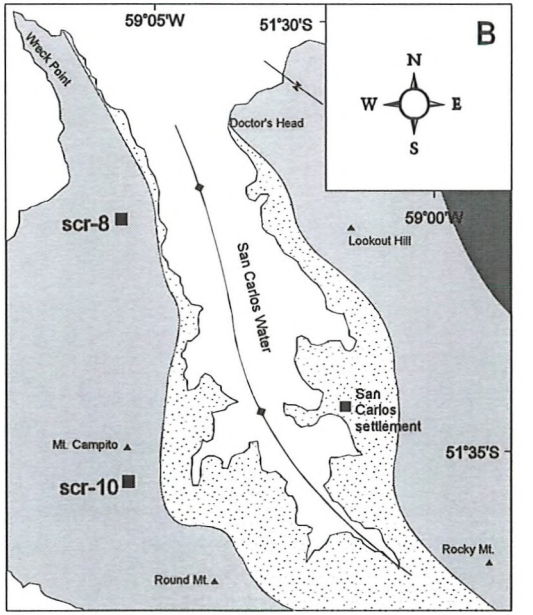

Figure 4.42: Table showing principal strains, k values, dilation and volume change estimated from quartz veins measured along 7 traverses, 5 at Stanley (location map A) and 2 at San Carlos (location map B).

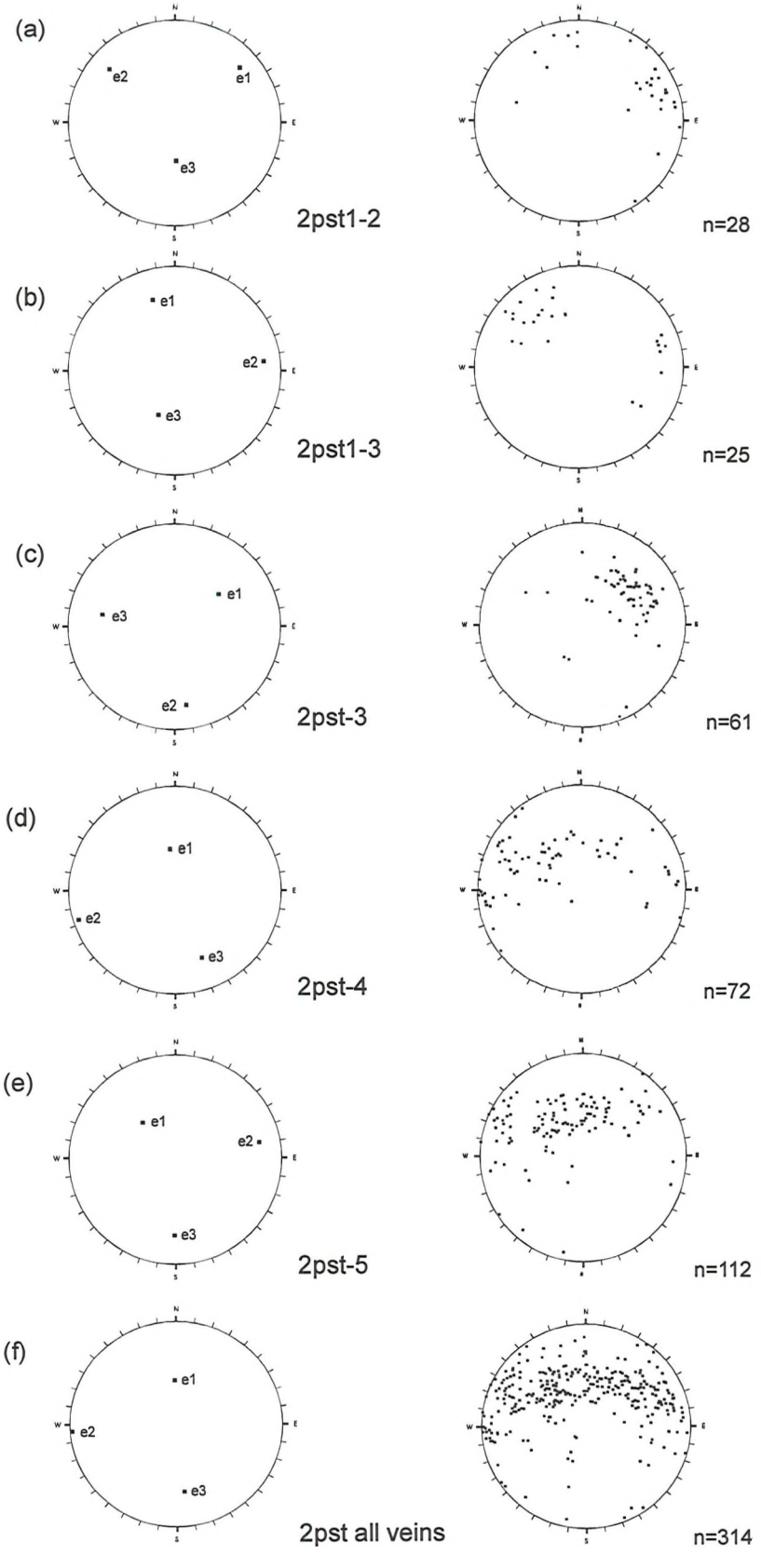

Figure 4.43: Principal strain directions (on the left) calculated from quartz vein sets (on the right)in the Port Stanley Formation near Stanley: (a) 2pst1-2, (b) 2pst1-3, (c) 2pst-3, (d) 2pst-4, (e) 2pst-5, (f) combined data from (a)-(e).

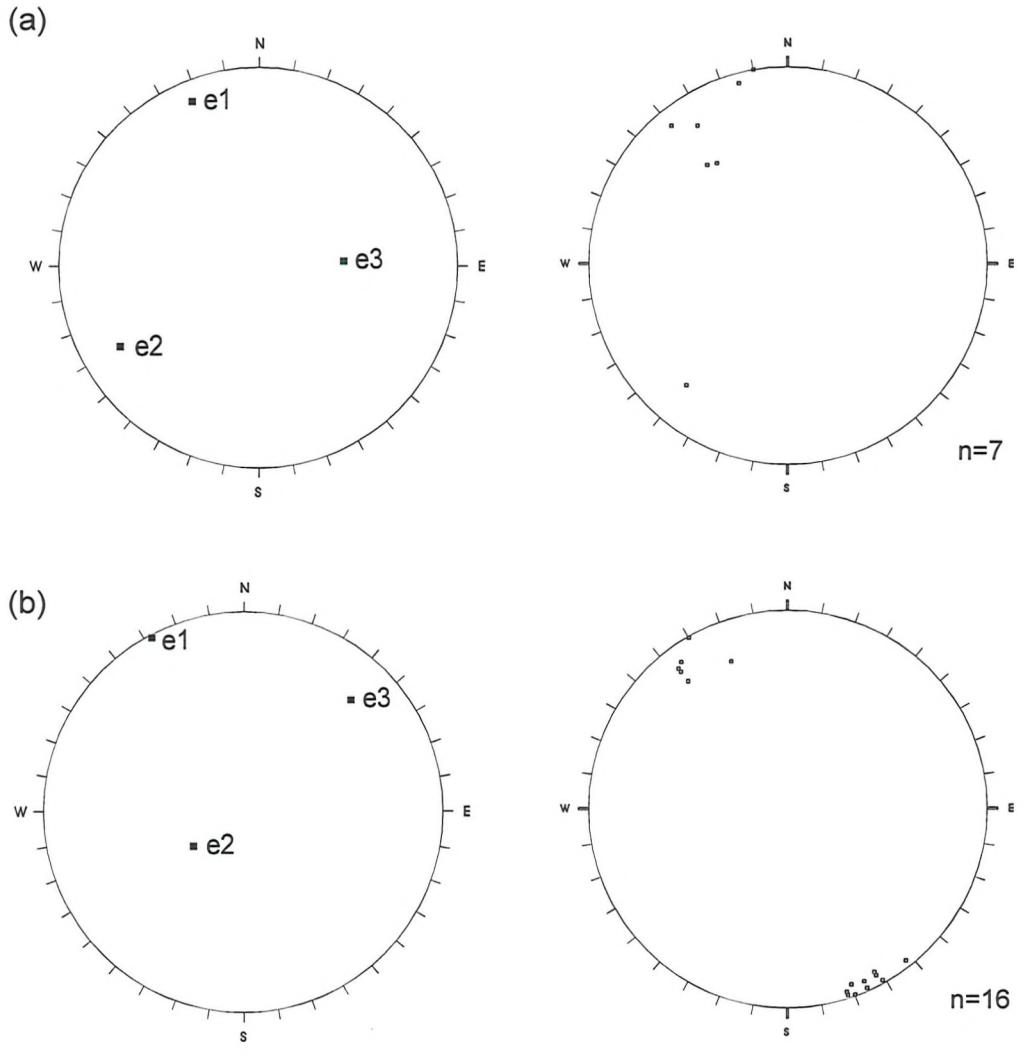

Figure 4.44: Strain data for quartz veins from San Carlos: Principal strain directions (right) and vein sets used (left) for: (a) scr-8 and (b) scr-10.

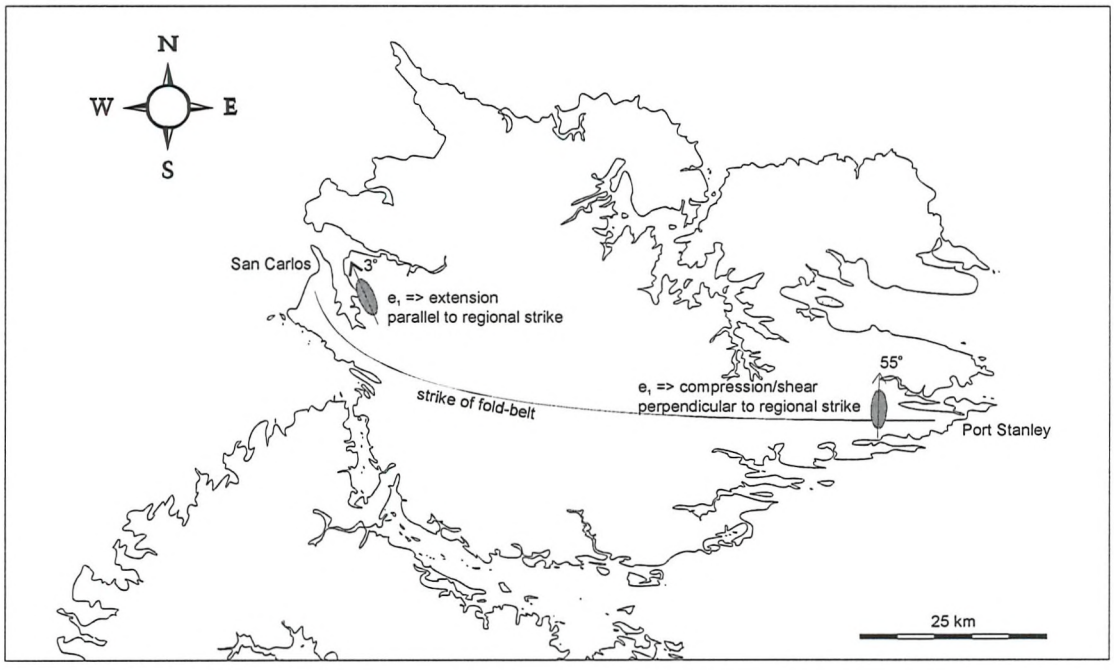

Figure 4.45: Map of East Falkland showing the relationship of strain measured from veins in the Port Stanley Formation at Port Stanley and San Carlos. Note the change in orientation and dip of e_1 between east and west. In both cases e_2 is sub-horizontal.

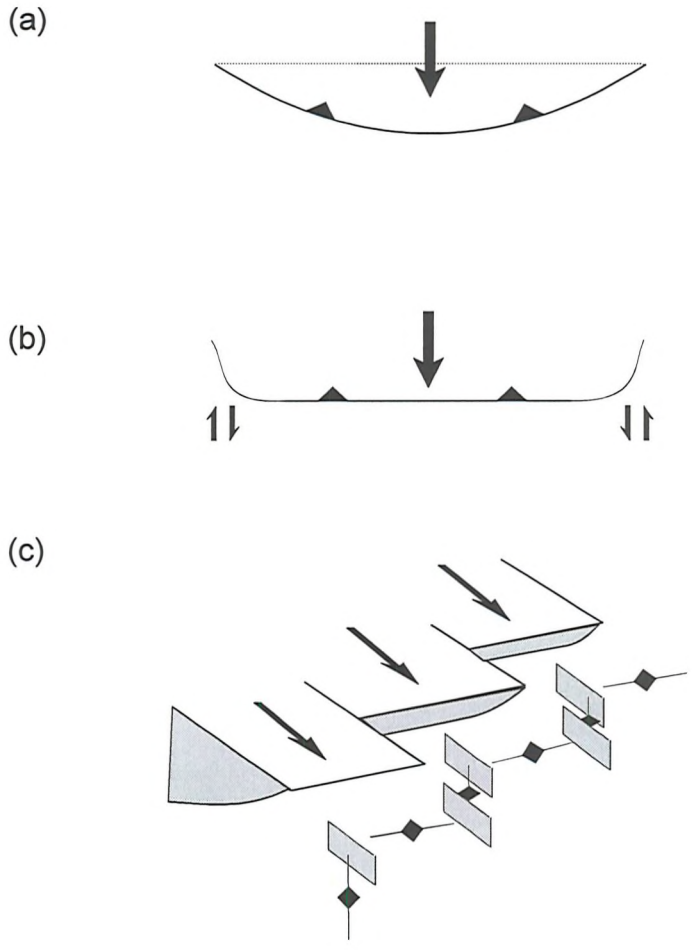

Figure 4.46: Models suggested for comparison to explain the orientation of the San Carlos folding: (a) 'Bow and Arrow' model of Elliott (1976); (b) lateral-tip shear zone model of Coward & Potts (1983); (c) differential movement across deformation zone model of Rattey & Sanderson (1982).

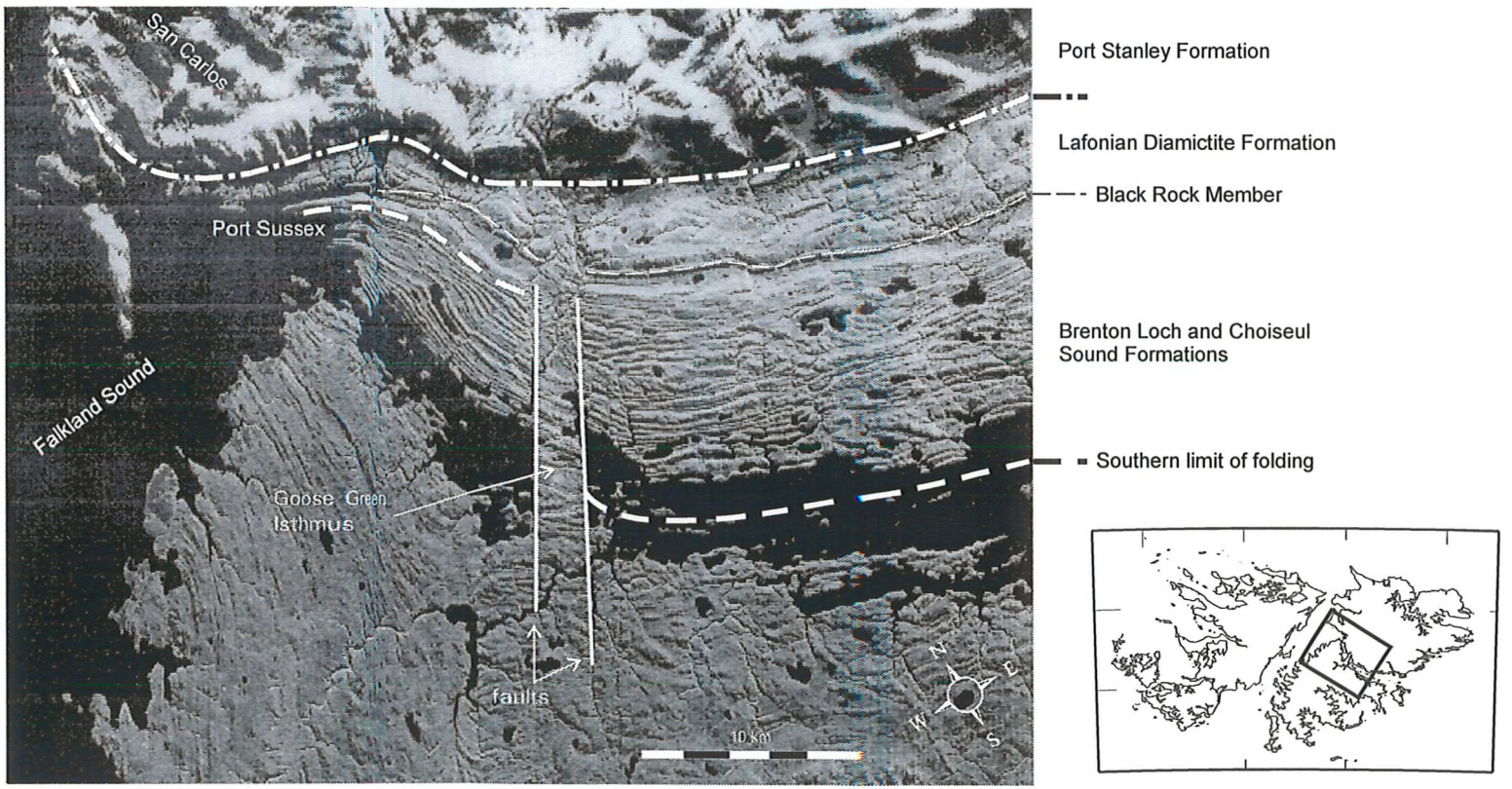

Figure 4.47: Satellite image of part of western central East Falkland with interpretation shown in white. Note the changes in strike in the outcrop pattern of the Port Stanley Formation in the north and the 10 - 12 km northward displacement, from east to west, of the southern limit of folding across the Goose Green Isthmus.

Chapter 5: The Structural Geology of West Falkland

Chapter 5: Structural Geology of West Falkland.

5.1 Introduction

The stratigraphy of West Falkland is dominated by the Gran Malvina Group which is exposed across the majority of the island, younging generally northward away from an unconformable contact with the Precambrian Cape Meredith Complex in the south (Fig. 5.1). The Lafonian Supergroup is poorly exposed with only scattered outcrops of the Lower Lafonian Group across the north and along the east coast of the island. Only thin exposures of the Upper Lafonian Group occur along the east coast.

The structural trend across the north of West Falkland (see Fig. 5.1) is the same WNW-ESE striking trend as seen on the west of East Falkland and is developed as gentle folds, which tighten northwards as seen on Pebble Island and Carcass Island. The WNW-ESE structures die out towards the south of West Falkland so that around Port Stephens and Weddell Island, there is no observable folding. Cross-cutting this trend, and almost orthogonal to it, is the major NE-SW striking asymmetrical Hornby Anticline along the east coast of the island, parallel to the Falkland Sound. A third structural trend of gentle N-S striking folds is seen around Port Edgar and Symonds Harbour in the mid-west of West Falkland.

Several areas have been studied on West Falkland related to the NE-SW striking Hornby Anticline (Fig. 5.1). These are at the northern end of the fold at Port Howard, in the centre at Shag Cove, to the west at Rat Castle and in the south at Carcass Bay (Fig. 5.1). The two main areas at Port Howard and Carcass Bay were chosen for study because they show departures from the simple geometry of the large anticline defined by the strata at Shag Cove and Rat Castle (Fig. 5.2). At Port Howard there is a series of folds developed around Bold Cove and Many Branch Harbour which appear to show an interaction of the E-W and NE-SW structures. Carcass Bay is an area of anomalously intense deformation in an otherwise undeformed region. These areas, have been studied in an attempt to unravel the history of deformation on West Falkland.

5.2 Port Howard

Around the Port Howard area, from Mount Maria in the west to the Falkland Sound in the east, a complete sequence from the middle of the Port Stephens Formation right through to the uppermost Lower Lafonian Group is exposed. This sequence has been deformed into a number of folds, to the north-east of Port Howard these strike E-W (Greenway 1972, M.L. Curtis *pers. comm.* 1996) and around Port Howard and Bold Cove the folds strike NE-SW. The largest of these folds is the Hornby Anticline which forms half of the Hornby Monocline, the syncline of which is beneath the waters of the Falkland Sound.

5.2.1 Folding

The area is dominated by the Hornby Anticline which parallels the Falkland Sound and by a series of folds around Bold Cove (see Figs. 5.2, 5.3, Map 4).

i) Hornby Anticline: This large, open anticline has been studied at Shag Cove and Rat Castle, where it has been possible to see the central part of the fold and at Port Howard, which reveals the closure of the fold. Across the central part of the fold the shallow limb, around Rat Castle, on the western side of Mt. Maria (Fig. 5.2), dips at 5 - 10° towards the NW and the steeper limb, at Shag Cove, dips steeply to the SE at around 75° (Fig 5.4). The fold axial plane dips NW and the axis plunges a 2 - 3° to the NE (Fig. 5.4). In contrast, at Port Howard, at the fold closure, the shallow limb dips N to NNE at 15 - 30° and the steep limb is vertical or overturned by up to 75° towards the NW (Fig. 5.5). Here, the fold is overturned slightly towards the SE, and has a gently inclined axis plunging gently at 20° to the NE (Figs. 5.3, 5.5, Map 4). The fold dies out north-eastwards towards Many Branch Harbour only to be picked out again further to the NE around White Rock Bay. The deformation on this steeper limb varies between the lithologies, being more intense in the shales of the Fox Bay Formation and in the quartzites of the Port Stephens Formation in the core of the fold with little deformation in the sandstones and quartzites of the Fox Bay and Port Stanley formations.

The transition from the shallow to the steep limb of the fold is marked by a series of folds, confined to the Fox Bay Formation, around Cemetery Creek. These can be seen as zones of low dip, alternating across strike with steeply dipping zones, creating a series of folds which have a stepped or terraced appearance (Fig. 5.6). The zone is characterised by numerous small reverse faults in the shales, and by the development of a weak spaced cleavage in the sandstones. These secondary folds appear to have formed by buckling of the less competent and more thinly bedded shales and sandstones in the transition zone between the steep and shallow limbs. This would be consistent with the conclusions of Ramsay (1967, p376) who noted that thinner layers (e.g. Fox Bay shales and sandstones) will form folds with a smaller wavelength and amplitude to thicker layers (e.g. Port Stephens and Port Stanley quartzites). This zone appears to demonstrate accommodation structures caused by the transition across the fold from the shallow to the steep limb.

ii) Bold Cove Folds: The area around Bold Cove to the NE of Port Howard is dominated by a ridge of the Port Stanley Formation which picks out the Bold Cove syncline and anticline pair, and, to the south of Bold Cove, the Bold Point syncline and anticline (Fig. 5.7). The Bold Cove folds plunge SW at 20° and 16° whilst the Bold Point folds plunge at 20° and 24° northwards. It would seem that the axial traces of the folds curve and merge, with the Bold Point and Bold Cove anticlines merging southwards, and the Bold Point and Bold Cove synclines merging northwards. The axial trace of the Bold Point anticline passes westwards into a fault with apparent dextral strike-slip movement on the quartzite ridge. Very little is seen in the way of internal deformation around the folds and an axial cleavage is only developed in the Lafonian Diamictite Formation in the core of the Bold Point syncline (Fig. 5.8).

Mapping around Many Branch Harbour (M.L. Curtis *pers. comm.* 1996) has shown a hook shaped outcrop pattern which could be a type II or III interference fold pattern between the E-W striking Many Branch Harbour Anticline and the northward continuation of the Bold Cove folds (Fig. 5.7). The pattern is developed where the E-W striking Many Branch Harbour Anticline (F_1) has been refolded across the NE-SW axis (F_2), and continues southwards as the NNE-SSW striking Bold Cove anticline

(Fig. 5.7). The style of folding changes around the F_2 axis, with the F_1 fold tightening from being an E-W striking open fold (interlimb angle of ~105°) at Many Branch Harbour to a NNE-SSW striking tight fold (interlimb angle of ~65°) at Bold Cove (Fig. 5.9a) where the refolded F_1 fold axis becomes almost parallel with the regional F_2 axis (Figs. 5.7, 5.9b, c).

5.2.2 Faulting

Of the reverse, extensional and strike-slip faults seen in the area, small-scale reverse faults are by far the most common and nearly all are found on the limbs of the Hornby Anticline. The intensity of faulting varies across the Hornby Anticline. On the shallow limb of the fold, top-to-the-south thrusts, with displacements in the order of 1 - 3 m, are exposed in the shales of the Fox Bay Formation around Purvis Pond and in the Port Stephens Formation between Freezer Rocks and the summit of Mount Maria (Fig. 5.10). Thrusts, exposed in the Fox Bay Formation near Purvis Pond, show a northward-dipping cleavage developed in the planes of thrusts, indicating a transport direction to the SSW (Fig. 5.11). Subordinate top-to-the-north-west backthrusts exposed around Freezer Rocks often create pop-up structures in the Port Stephens Formation (Fig. 5.12).

On the steeper limb of the Hornby Anticline reverse faults are far more numerous and show a much wider distribution of strike and dip, especially in the Fox Bay Formation. The faults, confined solely to the shale horizons of the Fox Bay Formation, show two main groups, one striking E-W, the other striking NE-SW (Fig. 5.13), the two appearing as a conjugate set (Fig 5.14) causing a general bed-parallel extension in the steep limb of the fold. A further cluster of faults exposed in the transition zone from shallow to steep limbs, shows a NW-SE strike and a shallow dip to the NE, parallel to bedding.

Extensional faults are late, brittle features and can be seen to cross-cut the more numerous reverse faults on Mount Maria. These faults generally strike N-S and show E-W extension directions (Fig. 5.15). Where seen, throws are from 1- 3 m. On the steeper limb extensional faults are rarely seen.

Strike-slip faulting is demonstrated by two N-S striking lateral offsets in the coastal ridge south of Port Howard and to the west of Bold Cove, both of which show dextral displacement (Fig. 5.3). The offset of the coastal ridge south of Port Howard does not appear onshore to the west at Port Howard, and the Bold Cove displacement does not appear to the east at Bold Point. This could indicate that, in both cases, the faults curve and become parallel to the regional NE-SW trend. Other small strike-slip faults, seen in the Port Stephens Formation on the steep limb of the Hornby Anticline south of Mount Maria, although limited in number, show a consistent dextral displacement (Fig. 5.16).

5.2.3 Cleavage

Cleavage is only developed locally in the core of the Bold Point syncline, in the planes of top-to-the-south thrusts in the Fox Bay Formation and as a weak fracture cleavage in sandstones around Cemetery Creek. A weak cleavage is also developed locally in the shales of the Fox Bay Formation at Port Howard where mesoscale thrusts and folds have caused, in places, the cleavage to become folded (Fig. 5.17).

5.2.4 Veining and fracturing

Quartz veins were observed across the Hornby Anticline in the Port Stephens and Fox Bay formations. The veins, as with the reverse faults, show an increase in intensity and spread of orientations from the shallow to the steep limb of the Hornby Anticline (Fig. 5.18). Despite the varied orientations there is a prominent set of steeply dipping veins with a strike of around 150° which are developed across the entire structure (Figs. 5.18a-d) and appear to be extensional structures equivalent to cross joints (e.g. Hancock *et al.* 1983) related to the formation of the Hornby Anticline. In the Port Stephens Formation, veining is only developed in the steep limb where a conjugate set of SE (set 1 (cf. Fig. 5.19)) and NW (set 2 (cf. Fig. 5.19)) dipping veins is developed in addition to the NW- SE set (Fig. 5.18c). One example of a cross-cutting relationship (Fig. 5.19) shows that set 1 are bed-parallel and are cut by the later veins of set 2 which are almost perpendicular to bedding. In the Fox Bay Formation,

veining is developed on both limbs of the Hornby Anticline and in the zone of terraced folding around Cemetery Creek (Fig. 5.18a,b,d). All these areas show the steeply dipping set of NW-SE striking veins. However, other groups of veins include a steeply dipping N-S striking set on the shallow limb; a weakly developed, steeply dipping E-W striking set in the area of the terraced folds; and the development of two sets of shallowly dipping veins dipping SW and SE in the steeper limb of the fold. No cross-cutting relationships were observed in the Fox Bay Formation.

A prominent feature towards the core of the Hornby Anticline is an increase in the intensity of fracturing or jointing within the quartzites of the Port Stephens Formation, developed mostly on the steeper limb to the south of Freezer Rocks, and SW along strike at least as far as Shag Cove. Several sets of joints are seen across the observed outcrops (Fig. 5.20) which include a NW-SE striking set, developed to varying extents in all the outcrops studied from Freezer Rocks to Shag Cove; a N-S striking set; and an E-W striking set. Displacement on these joints is seen as slickensides on some of the planar surfaces, those observed generally show WNW-ESE dip-slip movement. A plot of the P/T dihedra for these limited data shows that σ_1 was approximately horizontal and oriented NW-SE (Fig. 5.21). Quartz veining is weakly developed in this zone showing dominantly WNW/NW dipping veins which tend to be located along the joint planes.

5.2.5 Discussion

There are two main points to be discussed regarding the Port Howard area, the development of the Bold Cove and Many Branch Harbour fold structures, and the development of the Hornby Anticline.

i) Bold Cove / Many Branch Harbour: The hook-shaped outcrop of the Fox Bay and Port Stanley formations, caused by the interaction of the Bold Cove and Many Branch Harbour folds, clearly shows a pattern of refolding. In this case an originally E-W fold axis (F_1) has been refolded and tightened around a NE-SW axis (F_2). The southern part of the refolded F_1 axis becomes parallel to the NE-SW F_2 fold axes around Bold Point (Fig. 5.9b & c) and appears to have been overprinted by the trend

of the Hornby Anticline, which is increasingly dominant southwards from Bold Cove. Two models are suggested for this apparent rotation of 100°; firstly, refolding around a NE-SW, F_2 fold axis; secondly, clockwise rotation about a vertical axis.

In the first model, the type II interference pattern formed when the steeply dipping NE-SW (F_2) Bold Cove fold axis was superposed over the early (F_1) Many Branch Harbour fold axis. This model can be supported by features of these folds such as the change in the F_2 axis from an anticline to a syncline across the F_1 axis (see Fig. 5.7) and the variation in plunge of the F_2 axis at the cross over point with the F_1 axis (see Fig. 5.9a). Such features have been shown by Ghosh & Ramberg (1968) and Grujic (1993) to be characteristic of type II interference folds caused by the superposition of two fold generations. The Bold Cove structure is not unique, as Clifford *et al.* (1957, fig. 11) have mapped an identical structure of a hook-shaped, type II interference pattern, formed where older E-W (F_1) fold axes are rotated by 90° to N-S due to the superposition of a larger NE-SW (F_2) fold axis.

In this first model, the folds at Bold Point could be either: (1) refolded F_1 folds where the development of the F_2 axis has destroyed the F_1 axis in the region of Bold Cove. However, the F_1 axis may continue to the west as the gentle E-W striking syncline picked out around Purvis Pond (Fig. 5.7) or; (2) accommodation structures related to the refolding of the F_1 fold.

In the second model, it is proposed that the hook-shaped outcrop pattern formed by a 100° clockwise rotation of the eastern end of the E-W fold around a vertical axis (Fig. 5.22). This model would imply a NE-SW strike-slip fault or shear zone with significant dextral movement along it (c. 10 - 12 km) to cause such a rotation. However, although Curtis & Hyam (1998) imply such a zone with 3.3 km dextral displacement, little internal deformation is seen around the Bold Cove area which does not support such a model involving substantial shearing. In this second model, the Bold Point folds would have developed as accommodation structures due to the tightening and rotation of the F_1 fold axis.

A test of these models can be made using the abundant palaeocurrent data (n=304) collected from the Port Stanley Formation around the Bold Cove folds. It has been demonstrated (Chapter 2, Fig. 2.8) that the quartzites of the Port Stanley Formation show a dominant northward palaeocurrent direction with a minor E-W

component also developed. If the data from the three limbs of the Bold Cove folds are rotated to correct simply for the effect of bedding tilt (therefore assuming only one tectonic event) then two directions are seen: an E-W direction and a NNE/NE direction (Fig. 5.23). The two models, both involving a second tectonic event, can now be applied to this dataset.

In the first model, originally N and E-W palaeocurrent directions have been refolded about a NE-SW F_2 fold axis (Fig. 5.24). If the data on the rotated limbs of the Bold Cove fold are corrected simply for bedding-tilt, as outlined above, without any effects of refolding being taken into consideration, then the originally northward palaeocurrent direction would appear to be NNE on the now easterly dipping limbs and NE on the now westerly dipping limb whilst the E-W component would appear to be WNW-ESE (Fig. 5.24). This is exactly what is seen in the data from the three limbs (Fig. 5.23).

The second model assumes that the Bold Cove anticline has been bodily rotated clockwise by 100° around a vertical axis from an originally E-W strike. If this is the case then the data derived from a simple correction for bedding tilt should show a northward palaeocurrent direction if it is rotated anticlockwise by 100° around a vertical axis, restoring it to its original E-W strike. However when this is applied to the data the dominant palaeocurrents are directed W, NW and S with only a minor component directed N (Fig. 5.25).

So, from the comparison of the fit of the palaeocurrent data and geometry of the folds it appears the formation of the Bold Cove and Many Branch Harbour interference folds are due to refolding about a shallowly plunging NE-SW F_2 fold axis rather than rotation around a vertical axis.

ii) Hornby Anticline: The Hornby Anticline is an asymmetric fold with a steep to overturned SE limb and a shallow NW limb, both of which show minor structures such as faulting, veining and joint development. The interpretation of these minor features becomes a lot clearer in the light of the recognition of an early (D_1) E-W striking deformation (the F_1 Many Branch Harbour Anticline) and a later (D_2) NE-SW striking deformation (the F_2 Hornby Anticline and Bold Cove syncline). The

interpretation of the minor structures and their relation to D_1 and D_2 is summarised in Table 5.1.

On the shallow limb of the fold, early D_1 structures are easily recognised as little D_2 deformation has occurred on this limb. The D_1 structures on this limb are a series of northward dipping, top-to-the-south thrusts developed in the Port Stephens and Fox Bay formations at Freezer Rocks and near Purvis Pond; and a set of contemporaneous top-to-the-north-west backthrusts, also developed at Freezer Rocks, giving rise to pop-up structures.

On the steeper limb of the fold, many of the minor structures can be easily related to the D_2 deformation and no structures were observed that could be related to the D_1 deformation event. The two sets of reverse faults in the steep limb, which dip north and south-east, have formed as a conjugate set (Figs. 5.13, 5.14) causing an overall extension of the steep limb in a similar way to the semi-ductile shears in the steeper limbs of folds in the Port Stanley Formation on eastern East Falkland (see Figs. 4.7, 4.8, Chapter 4.2.1).

In both the Fox Bay and Port Stephens formations, there are sets of veins which are perpendicular to bedding and which generally extend the steep limb of the fold (Figs. 5.18, 5.19). The NW-SE striking set of veins seen across both limbs of the fold and the similarly oriented set of joints seen in the core of the fold, south of Freezer Rocks, appear to be equivalent to cross-joints. Hancock *et al.* (1983) have described similar features from the Variscan of South Wales and their work supports the interpretation that the veins and fractures can be ascribed to the formation of the SE verging Hornby Anticline. The model of a SE verging anticline is also supported by the evidence from the shears in the core of the fold which show σ_1 oriented NW-SE. Not all the veins can be easily related to this model, however, and cross-cutting relationships between two sets of veins in the Port Stephens Formation show that a set of bed-perpendicular veins cut and displace a set of bed-parallel veins (Fig. 5.19). These bed-parallel veins are obviously earlier structures and are likely to be D_1 structures related to the stress system which formed the top-to-the-south thrusts. These have since been tilted and cross-cut during the formation of the D_2 structures.

The few normal faults exposed on both limbs of the fold show an approximately N-S strike and cross-cut the reverse faults seen on the shallow limb

with generally E-W extension directions. These late features probably post-date the main D_2 deformation and may imply a late E-W extensional event.

The presence of small dextral strike-slip faults on the steep limb of the fold is an indication that there has been an element of dextral shearing across the Hornby Anticline although its effects are quite small.

In summary, the structures at Port Howard show an initial N-S compression (D_1) giving rise to E-W striking folds and thrust faults which have been overprinted and refolded by later NE-SW striking folds (D_2). An E-W extension is probably the last event to occur in the area.

5.3 Carcass Bay

Carcass Bay, a small promontory at the south-western end of the coastal ridge of West Falkland, is a structurally complex area, especially when compared to the surrounding areas (Fig. 5.26, Map 5). Fieldwork in the area has been supplemented by aerial photograph interpretation owing to the poor exposure of structures, such as faults, and the scattered nature of the outcrop. Major reverse faults and minor normal faults have been recognised across the area, striking between NNE/SSW and E/W, based on stratigraphic juxtapositions and aerial photograph interpretation.

Traversing from SE to NW, the youngest rocks exposed along the eastern coast are the upper beds of the Shepherds Brook Member overlying the Black Rock Member, both of which are overturned to the SE. To the NW, the Lafonian Diamictite Formation outcrops as low cliffs behind which the Port Stanley Formation is exposed along a broken ridge on Vulture Headland, Caracara Hill and northwards to the coastal ridge. The Fox Bay Formation outcrops on Vulture Headland in the hanging- wall of a south-easterly dipping reverse fault and in the main valley. The overall structure of the area is a simple anticline/syncline pair. However, this has been complicated by reverse faulting and areas of intense lower order folding.

5.3.1 Folding

The folding is quite complex with three main orientations of fold axes which are: NE-SW in the main valley and on Vulture Headland; ~N-S to the NE of Caracara Hill; and ~E-W around Caracara Hill (Fig. 5.26). The folds in the area are tight to open (interlimb angles of 1-105°), gently to moderately inclined and gently plunging to sub-horizontal showing an overall fold axis plunging at 22° to 218° (Figs. 5.26, 5.27). Despite this complexity, cross-sections of the area (Fig. 5.26, Map 5) show the overall structure to be quite simple consisting of a first order anticline/syncline pair with NE-SW fold axes and a wavelength of approximately 500 m. The hinges of the first order anticline/syncline pair can be seen respectively in the Fox Bay Formation just to the south-east of the coastal ridge, in the main valley; and in the Port Stanley Formation between the Main Carcass Bay and Bay Faults. The two SSE dipping limbs are the coastal ridge in the west and the eastern coastline in the east whilst the NNW dipping limb is poorly exposed around Caracara Hill, being complicated by faulting and intense lower order folding of wavelengths down to 10 m. The lower order folds are exposed around Caracara Hill, where they trend ~E-W, and on Vulture Headland, in both the Fox Bay and Port Stanley formations (Fig. 5.28), where they trend NE-SW. The overlying, younger strata of the Lafonian Diamictite and Port Sussex formations, although tilted to approximately vertical and incorporated into the broader first order folding on the SE side of the area, show none of the lower order folds seen in the underlying units.

5.3.2 Faulting

Owing to outcrop extent, vegetation coverage and recent alluvium, exposures of the faults interpreted across the area are limited to the southern end of the Headland Thrust and the western end of the Headland Fault. Despite this lack of exposure, stratigraphic juxtapositions and geomorphological features seen on aerial photographs have been used to interpret a further six reverse and three normal faults in the area.

i) Reverse faults: The major NE-SW striking Main Carcass Bay Fault (MCBF) has been interpreted from aerial photographs to account for the juxtaposition of the Lafonian Diamictite and Fox Bay formations in the main valley. Structure contours across this fault reveal it to dip shallowly (approx. 30°) ESE and cross-sections imply an up-dip movement, in the centre of the area, of up to 550 - 560 m towards the WNW (Fig. 5.26, Map 5). At its northern end, where the line of the fault meets the coast, the fault shows virtually no displacement in the Lafonian Diamictite Formation. Although the majority of the displacement on the fault is interpreted as reverse there are, however, some small-scale, dextral, strike-slip faults sub-parallel to the strike of the MCBF (Fig. 5.29) which indicate that there has also been some minor dextral strike-slip movement.

The Bay Fault (BF), again interpreted from aerial photographs and field relationships, strikes parallel to the MCBF and appears to dip ESE at approximately 30° linking north-eastwards into the MCBF (Fig. 5.26, Map 5). Cross-sections across the fault show it to have a similar sense of movement to the MCBF showing up-dip movement of approximately 240 m towards the WNW. The linkage of this fault north-eastwards into the MCBF is responsible for the north-eastern truncation of the first order syncline exposed between the two faults.

The Caracara Fault shows a curved outcrop from the eastern coast, where it displaces the ridge of the Port Stanley Formation, to the central valley, where it merges with the MCBF. It has been interpreted as a reverse fault showing intense footwall deformation with overturned folds and small top-to-the-south-east thrusts exposed in the Port Stanley Formation on its south-eastern side and, in the hanging-wall, a deflection and steepening of the Fox Bay Formation into the fault on the north-western side, similar to a hanging-wall anticline (Fig. 5.26, Map 5). Cross-sections show it to have top-to-the-south-east movement of up to 200 m and that it probably links down-dip with the MCBF. Minor top-to-the-north, south and south-south-east thrust faults (Fig. 5.29) occur on Caracara Hill, in the footwall of the Caracara Fault, reflecting the larger scale movement on this structure.

The Headland Thrust is located around the western side of Vulture Headland. Where it is exposed, at the SW end of the peninsula, it dips shallowly south-east and shows apparent top-to-the-north-west displacement juxtaposing overturned and folded

quartzites of the Port Stanley Formation north-westwards directly on top of overturned, folded sandstones and shales of the Fox Bay Formation (Fig. 5.28).

ii) Normal faults: The E-W striking Headland Fault, which dips steeply north truncating the deformation on Vulture Headland, is exposed at its western end at the coast. In this exposure, diamictites of the Lafonian Diamictite Formation on the north side are juxtaposed against shales of the Fox Bay Formation on the south side. Cross-sections show this to be a normal fault which is down-throwing approximately 250 m to the north, truncating the Headland Thrust at its northern end. The only normal fault measured in outcrop shows a N-S extension direction, parallel to the Headland Fault (Fig. 5.29).

The marked lateral steps in the outcrop pattern of the steeply dipping Port Stanley Formation along the eastern ridge have been interpreted as resulting from normal faulting. The strike of the faults is approximately N-S with throws to either east or west. It appears that these are unrelated to the Headland Fault as the southern most fault, on the east side of Vulture Headland, is truncated against it.

iii) Strike-slip faults: In the Fox Bay Formation to the north-east of the coastal ridge there is a conjugate set of faults, one striking approximately N-S and the second NW-SE. The first of these sets shows apparent sinistral displacements whilst the second set shows apparent dextral displacements. These relationships infer that these are strike-slip faults.

The few outcrop-scale strike-slip faults observed are mostly in the central valley and strike ENE-WSW showing dextral displacements in the order of 10 - 100 mm.

5.3.3 Cleavage

There is no cleavage development in any of the lithologies despite the intensity of the deformation.

5.3.4 Veining and fracturing

Quartz veins, measured mostly from the Port Stanley Formation with some from the Fox Bay Formation, show two clear groupings (Fig. 5.30), a NNW-SSE striking set and a E-W striking set. No cross-cutting relationships were observed. Joints developed in the Port Stanley Formation show two sets, a ENE-WSW striking set and a NE-SW striking set (Fig. 5.31). No cross-cutting relationships were seen.

It is unclear how most of the veining and fracturing is related to the map-scale structures interpreted in the area. However, it is possible that the southward dipping veins are related to the southward dipping, top-to-the-north thrusts developed in the Port Stanley Formation to the south of the Caracara Fault and that the NE-SW joints are related to the main NE-SW faults and fold-axes which dominate the area.

5.3.5 Discussion

It should be clear from the above descriptions that the area of Carcass Bay has undergone a far from simple deformation history. The oldest deformation is a NW-SE compression seen in the main folds and major thrust faults, younger extension is evidenced from the N-S and E-W extensional faults which cut the NE-SW structures, NE-SW compression is inferred from the apparent strike-slip offsets in the Fox Bay Formation and minor ENE-WSW dextral strike-slip is seen from small-scale faults. There is no evidence for original E-W structures, as at Port Howard, and it appears that the overall NE-SW strike of the region is related to D_2 deformation.

The overall structure of Carcass Bay, a first order anticline/syncline pair sitting on the southern end of the steep limb of the Hornby Anticline, is not dissimilar to the first order fold pair at Bold Cove, modified by refolding of the F_1 Many Branch Harbour Anticline, which lie at the northern end of the Hornby Anticline. The folding at Bold Cove, although modified by the interference folding of the F_1 fold appears to have been related to the dying out of the Hornby Anticline northwards and the north-eastward stepping of this NE-SW trend towards White Rock Bay. It is possible that this is related to an underlying structure, such as a fault, tailing off northwards and then stepping eastwards across the area of Bold Cove. Similarly it is possible at the

southern end of the Hornby Anticline, at Carcass Bay, that there is a termination of similar underlying structure southwards and a lateral stepping south-eastwards across Carcass Bay, so forming the localised zone of deformation in such a relatively undeformed region.

In summary, Carcass Bay is a complex area showing original D_2 structures related to NW-SE compression which has undergone later extensional events, both E-W and N-S. The full history of Carcass Bay is still not fully understood nor resolved from the present study of the area.

5.4 Formation of the Hornby Monocline

To understand the history of the deformation on West Falkland the question of how the Hornby Anticline formed needs to be addressed. In an attempt to understand this, three cross-sections have been constructed based on the geological map of Greenway (1972) and modified using data from this study. These sections, from mid West Falkland to the east side of the Falkland Sound on East Falkland (Fig. 5.32), show that the Hornby Anticline is half of an anticline/syncline pair, the syncline being under the Falkland Sound, which together form the Hornby Monocline. This monocline shows West Falkland to have been uplifted relative to East Falkland, giving a structural relief which increases southwards from 3 km in the north, to 6 - 8 km in the centre decreasing again to 6 km in the south. The Hornby Monocline is a large, isolated structure which deforms the Gran Malvina and Lower Lafonian Groups, the base of which, the Port Stephens Formation, sits unconformably on Precambrian metamorphic basement exposed at Cape Meredith. The isolated nature of this structure implies that it is related to an underlying fault and is not part of a train of folds related purely to horizontal compression. There is no definite continuous horizon which could be used as a décollement at the base of the sequence.

The timing of formation of the Hornby Monocline has been constrained from the fold interference patterns at Bold Cove. It post-dates the main E-W structures on the Falkland Islands, which are, by correlation to other Gondwanian fold-belts, Permo-Triassic in age. However, evidence from the sedimentary facies of the Lower Lafonian Group (Chapter 2.2.3.i) indicate that West Falkland was uplifted relative to

East Falkland in Late Carboniferous and Early Permian times. This implies that, although the main fold formation was post-Late Permian, a NE-SW trending structure was causing a relative uplift of West Falkland as far back as the Late or probably Early Carboniferous (Chapter 3, Hyam *et al.* 1997). This would imply that before the main fold formed, there was an existing fault between East and West Falkland.

To assess formation of the Hornby Monocline it is necessary to discuss how monoclines form. Reches & Johnson (1978) outline three main models by which monoclines can form: draping, buckling and kinking. Passive, drape or forced folding is thought by many (e.g. Kelley 1955) to be the main mechanism for the formation of monoclines. This is where a flat-lying layered sedimentary sequence is forced into a monoclinal fold by the movement of an underlying, steep fault, which is often reverse, although sometimes extensional in nature (e.g. Kelley 1955). It has also been shown (Reches 1978, Reches & Johnson 1978) that, in the Laramide Orogen of the western USA, significant horizontal compression has been involved in the formation of monoclines. Where this is involved, compressional structures occur in the aniticlinal part of the monocline whereas extensional structures occur where drape folding is the main mechanism. In addition, an existing discontinuity is required for asymmetric monoclines to form due to horizontal compression because its application to a flat-lying layered sedimentary sequence results only in buckling and the formation of a train of symmetric folds (Reches & Johnson 1978). Such a discontinuity need only be small (Abbassi & Mancktelow 1990) and may be caused by a fault or an existing flexure formed by passive or drape folding (Reches & Johnson 1978).

In examples from around the world where underlying faults are known to have formed monoclines, the faults are often inverted normal faults (Grand Canyon, Reches 1978; Negev, Shamir & Eyal 1995; Southern England, Chadwick 1993) or foreland-propagating thrust faults (Lake District, Kneller & Bell 1993; Italian Apennines, de Donatis & Mazzoli 1994). Oblique motion and transpression may also be involved (e.g. Dent Fault, Underhill *et al.* 1988). Reches and Johnson (1978) summarised earlier work on this subject and concluded that a fault may underlie either the anticlinal fold or the steep, inflexion limb or indeed lie behind the anticline (Fig. 5.33). However, Kelley (1955) concluded that the nature of an underlying fault cannot be elucidated simply from the form of the monocline above.

The examples in the previous paragraphs would suggest that the Hornby Monocline is a drape or forced fold and that an existing fault, which had formed by Late Carboniferous times, was reactivated during the main fold formation. The fold itself may have formed by a combination of fault movement and E-W horizontal compression. Evidence of horizontal compression is not seen to be related to the formation of the monocline and only veins and faults which cause sub-vertical extension (sections 5.2.2, 5.2.4) were observed on the anticline. However, although not seen at any scale across the Hornby Monocline itself, E-W compression is indicated by gentle N-S folds around Symonds Harbour on West Falkland (Fig. 5.1) which have been interpretted as coeval (Curtis & Hyam 1998). This compression may have amplified an existing monocline to its present 8 km structural relief. However, the evidence from extensional structures around Port Howard would suggest that the Hornby Monocline mainly formed by drape folding.

A thin-skinned model, with a low-angle reverse fault at the base of the sequence, cannot be the cause of the Hornby Monocline because, as noted earlier, there is no décollement horizon. However, by comparison to other monoclines (e.g. Chadwick 1993), a thick-skinned model with the involvement of a high-angle basement fault, located beneath or behind the anticlinal hinge, can be inferred. In many monoforms (e.g. Chadwick 1993) these faults are high-angle reverse faults. This is a good model for the Hornby Monocline as the steep to overturned limb of the fold is unlikely to have attained such an attitude above an extensional fault. However, it is possible that the fault began as extensional in the Early Carboniferous, forming a low amplitude monocline, and later reactivation and inversion of the fault caused amplification of the early formed monocline. Minor dextral faults, parallel to the fold hinge, and dextral offsets in the Coast Ridge at Port Howard and to the west of Bold Cove, suggest an element of dextral strike-slip. Wilcox *et al.* (1973) have shown that large anticlines may form sub-parallel to, and to the side of, large strike-slip faults if there is an element of vertical uplift associated with the fault movement. A strike-slip model for formation of the Hornby Monocline would infer that the fault lay beneath the Falkland Sound. Such a fault is difficult to trace between the islands in the Falkland Sound meaning it would have to lie close to the east coast of West Falkland (Marshall 1994a). In this model a contractional bend is necessary to the north of

Carcass Bay, however, the intensity of deformation at Carcass Bay does not support a model with large strike-slip displacement. So, although the evidence shows that there is not a major strike-slip fault, the strike-slip structures seen in the steep limb of the Hornby Monocline indicate that a steep reverse fault, cutting down into basement underneath West Falkland, may have had an element of oblique dextral movement.

Whatever the nature of the underlying fault, a feature to note about the Hornby Monocline is that it is periclinal in that amplitude decreases along strike to both the NE around Port Howard and to the SW to the north of Carcass Bay (Fig. 5.1). This is probably related to a displacement gradient along the length of the fault with the central dome of the anticline indicating the greatest displacement of the fault beneath (Shamir & Eyal 1995). The continuation of the NE-SW structural trend to the NE around White Rock Bay and offshore to the SW (see Chapter 6) would imply that the fault, which has caused the monocline to form, may be part of a series of fault segments rather than a single fault strand. If this is the case, then it is possible that the deformation at Bold Cove and Carcass Bay has, in part, been influenced by the interaction of the tips of these faults segments.

5.5 Conclusions

Evidence on West Falkland indicates that two clearly defined deformation phases have occurred in the formation of the folding around Port Howard. The first was a N-S compression resulting in gentle E-W striking folds and small scale top-to-the-south thrusting. The second deformation event involved the uplift of West Falkland along a steep reverse fault, with minor oblique dextral movement, located beneath the Hornby Mountains, coupled with minor E-W compression. This resulted in the formation of the Hornby Monocline, the refolding seen at Bold Cove and the deformation at Carcass Bay. The last definable event is an E-W extension. However, the deformation at Carcass Bay implies that there have been more complex, smaller events of extension and compression to give the deformation patterns seen there.

D_1 structures across the Hornby Anticline	*D_2 structures across the Hornby Anticline*
Top-to-the-south and north-west thrusts at Mt. Maria and Purvis Pond (Figs. 5.10, 5.11, 5.12).	Conjugate reverse faults causing extension of steep limb (Figs. 5.13, 5.14).
Bed parallel veins (refolded by D_2) (Figs. 5.18, 5.19).	Bed perpendicular veins causing bed parallel extension on steep limb (Figs. 5.18, 5.19).
	NW-SE striking veins and joints (cross joints) found uniformly across the fold (Figs. 5.18, 5.20).

Table 5.1: Summary of D_1 and D_2 structures across the Hornby Anticline.

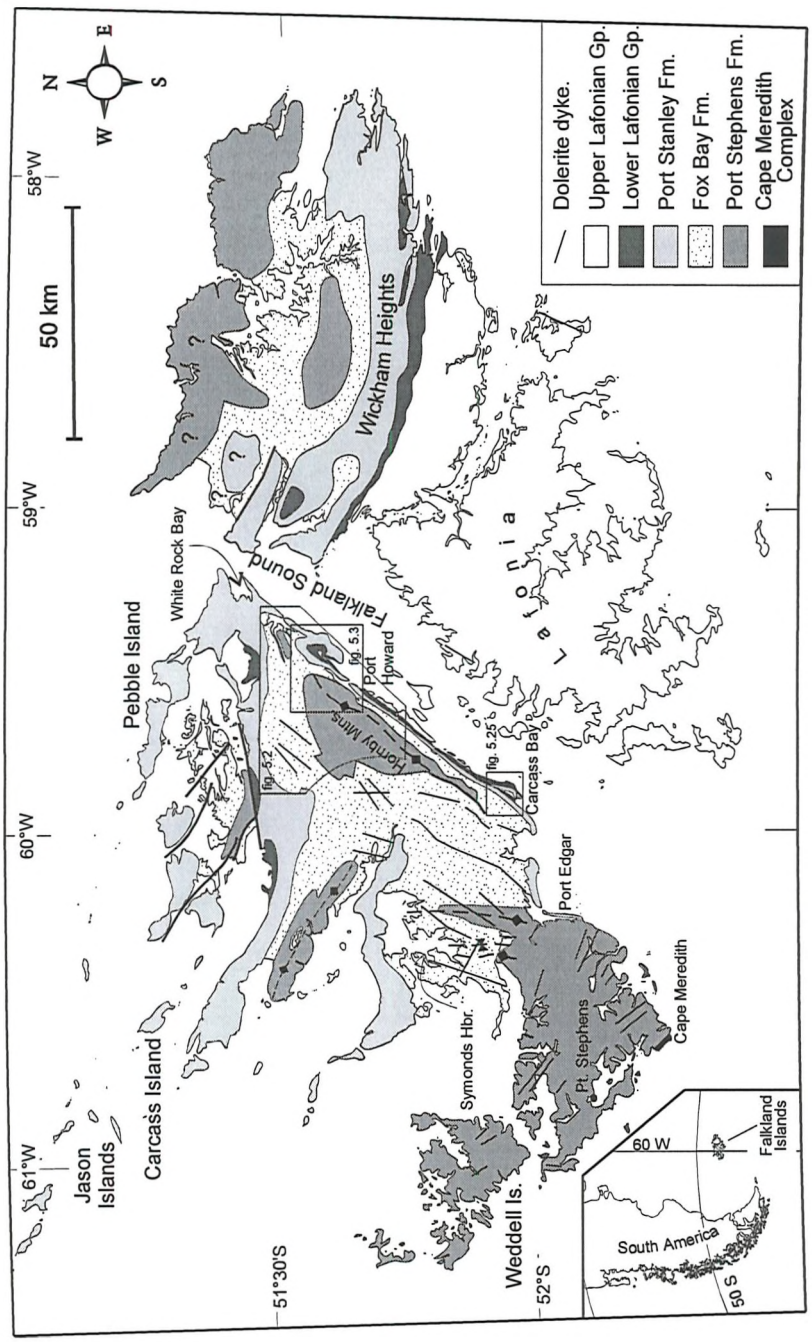

Figure 5.1: Geological map (modified from Greenway (1972)) showing areas mapped and relevant place names on West Falkland .

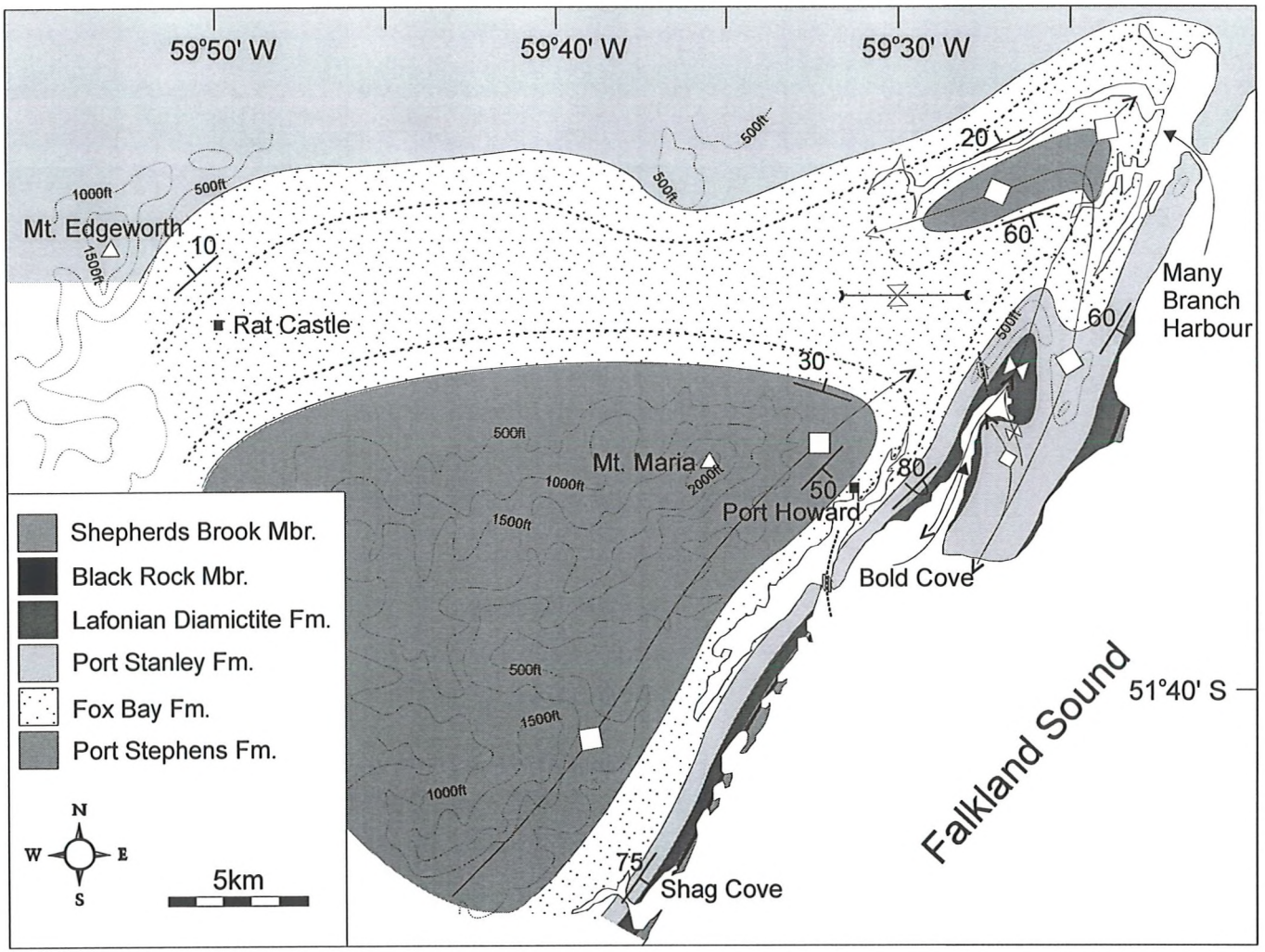

Figure 5.2: Summary geological map of north-east West Falkland (see Fig. 5.1) showing full extent of Hornby Anticline from Shag Cove in the east to Rat Castle in the west with closure at Port Howard.

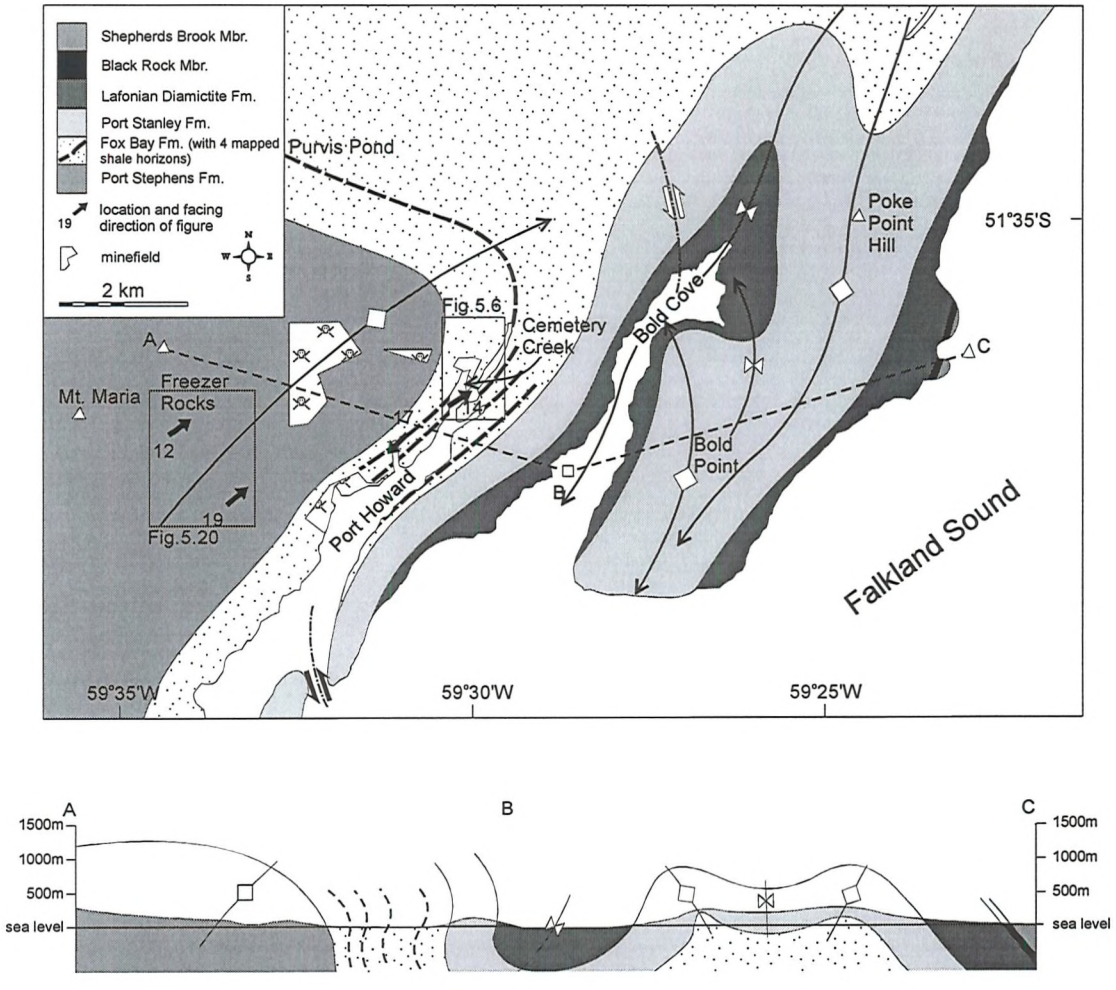

Figure 5.3: Summary geological map and cross-section from Port Howard.

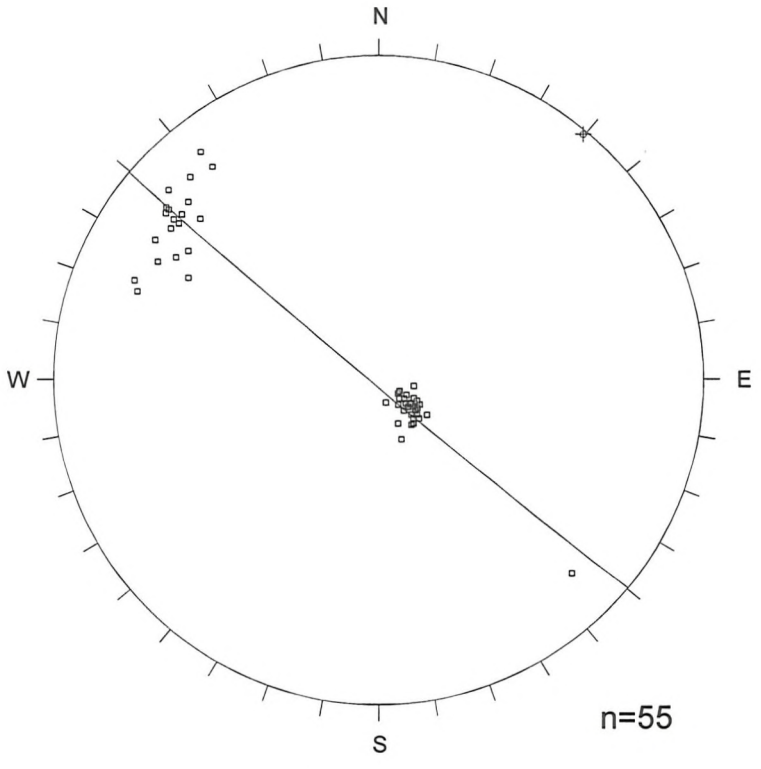

Figure 5.4: Equal-area lower hemisphere projection of poles to bedding from the Rat Castle and Shag Cove sections across the Hornby Anticline, West Falkland. Fold axis shown (plane and cross).

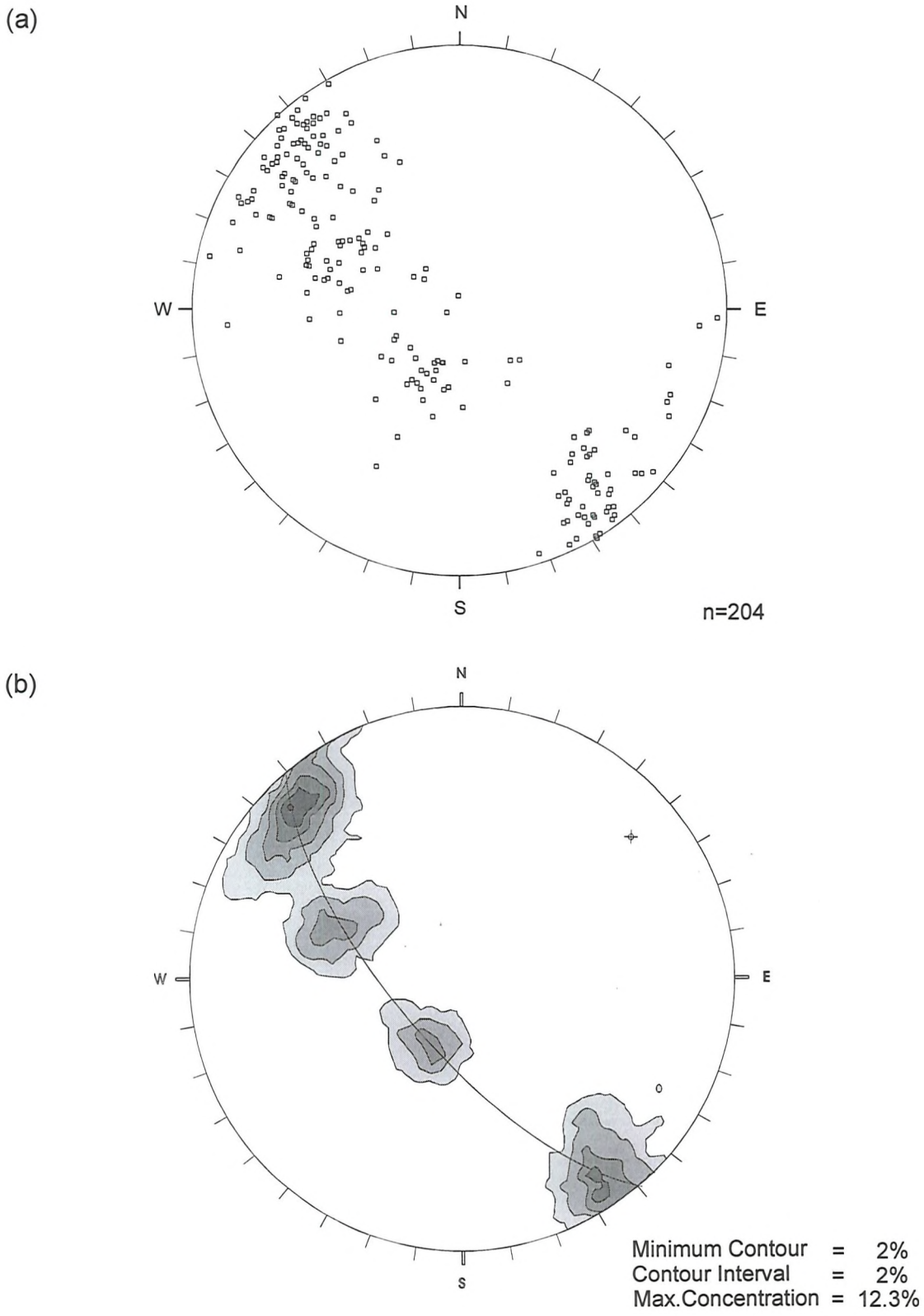

Figure 5.5: Equal-area lower hemisphere projections of: (a) poles to bedding; (b) contoured poles to bedding; from the Hornby Anticline, Port Howard. Fold axis shown (plane and cross).

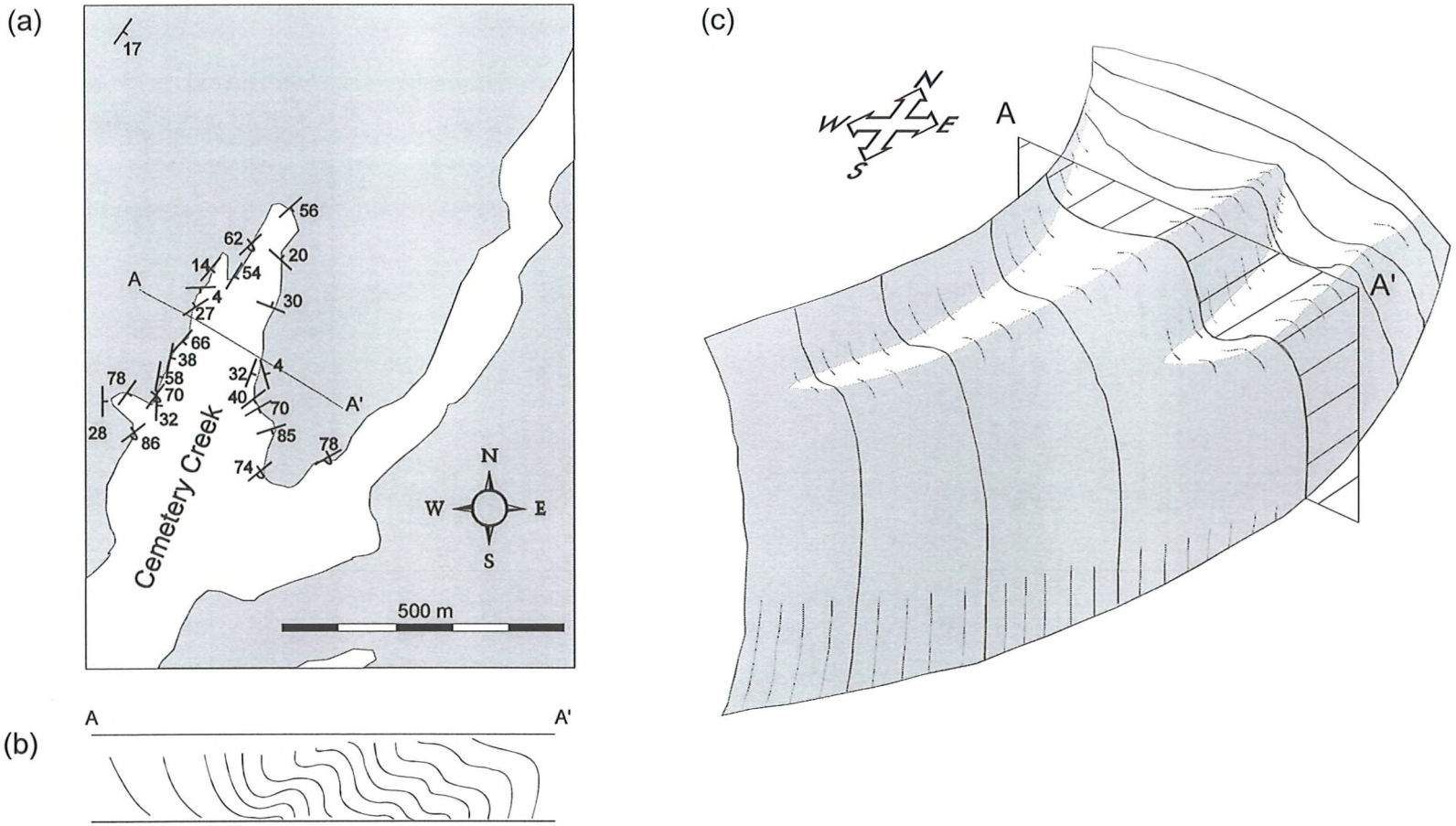

Figure 5.6: Detail of the area of folding at the head of Cemetery Creek. (a) map showing line of section A-A'; (b) schematic section along line A-A'; (c) theoretical plane showing the nature of folding, picked out as complete or partial contours, as accommodation folds between the shallow (light shade) and steep (dark shade) limbs of the fold.

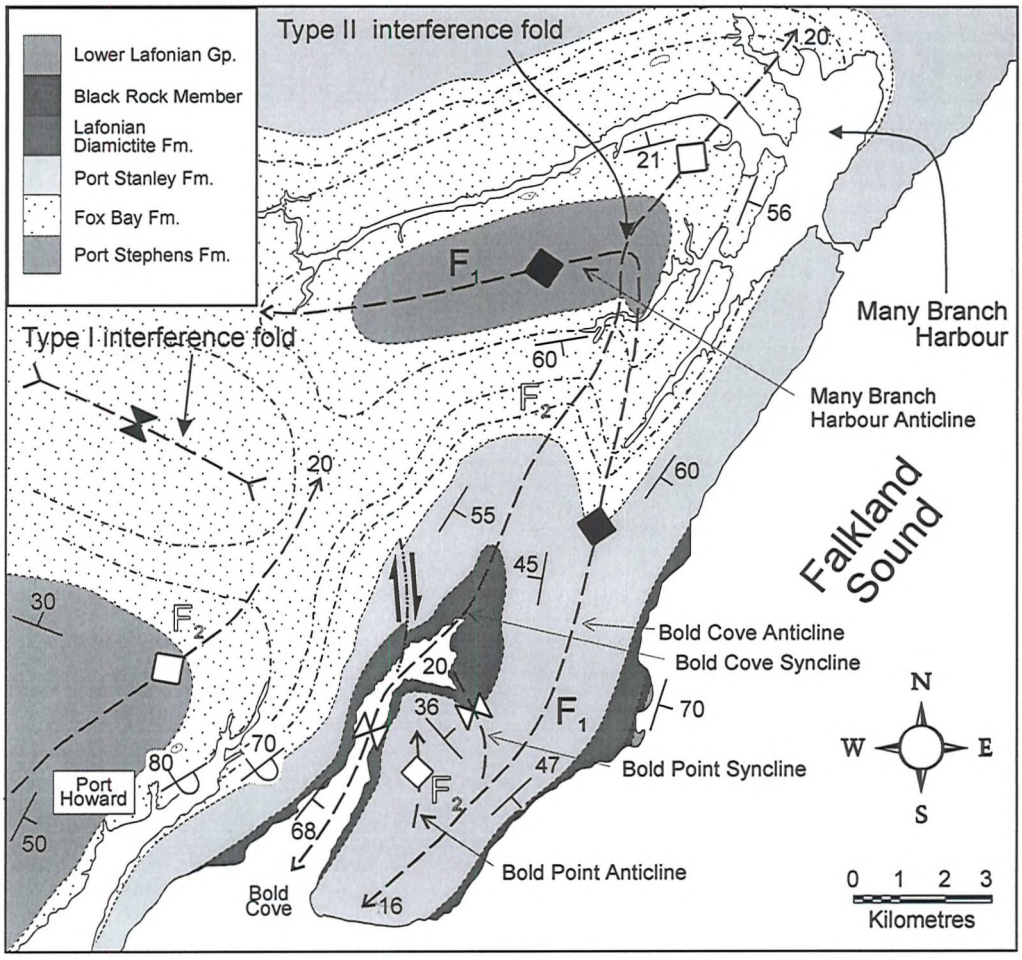

Figure 5.7: Map showing interference folding around Many Branch Harbour and to the north of Port Howard (after Curtis & Hyam *in press*).

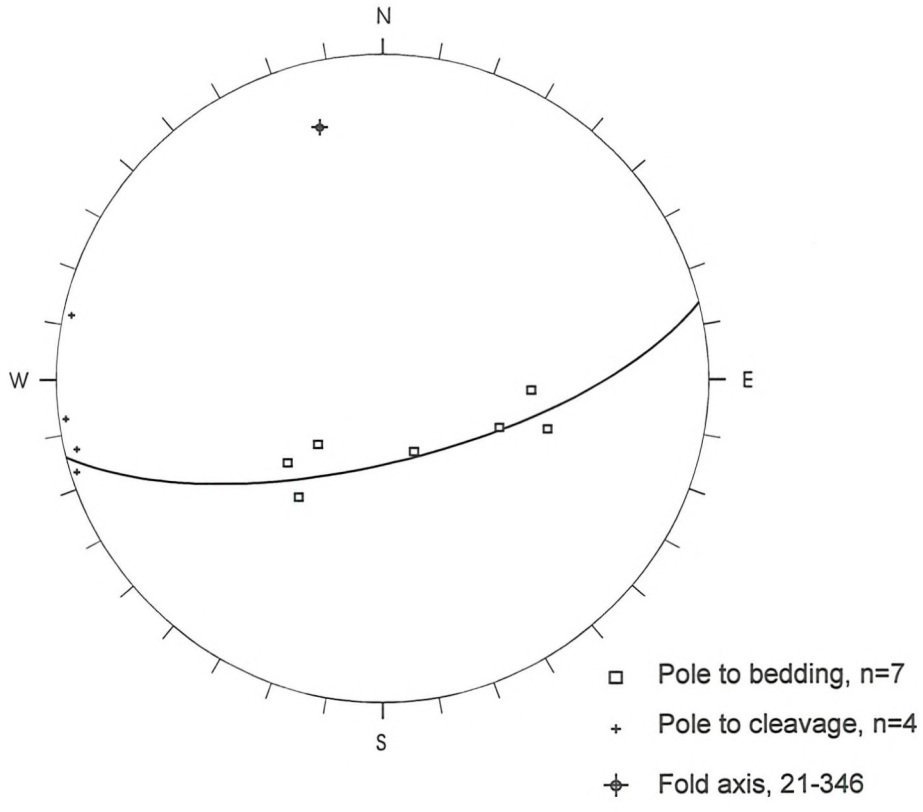

Figure 5.8: Equal-area lower hemisphere projection of poles to bedding and cleavage in the Bold Point syncline; fold axis shown to highlight axial planar nature of cleavage.

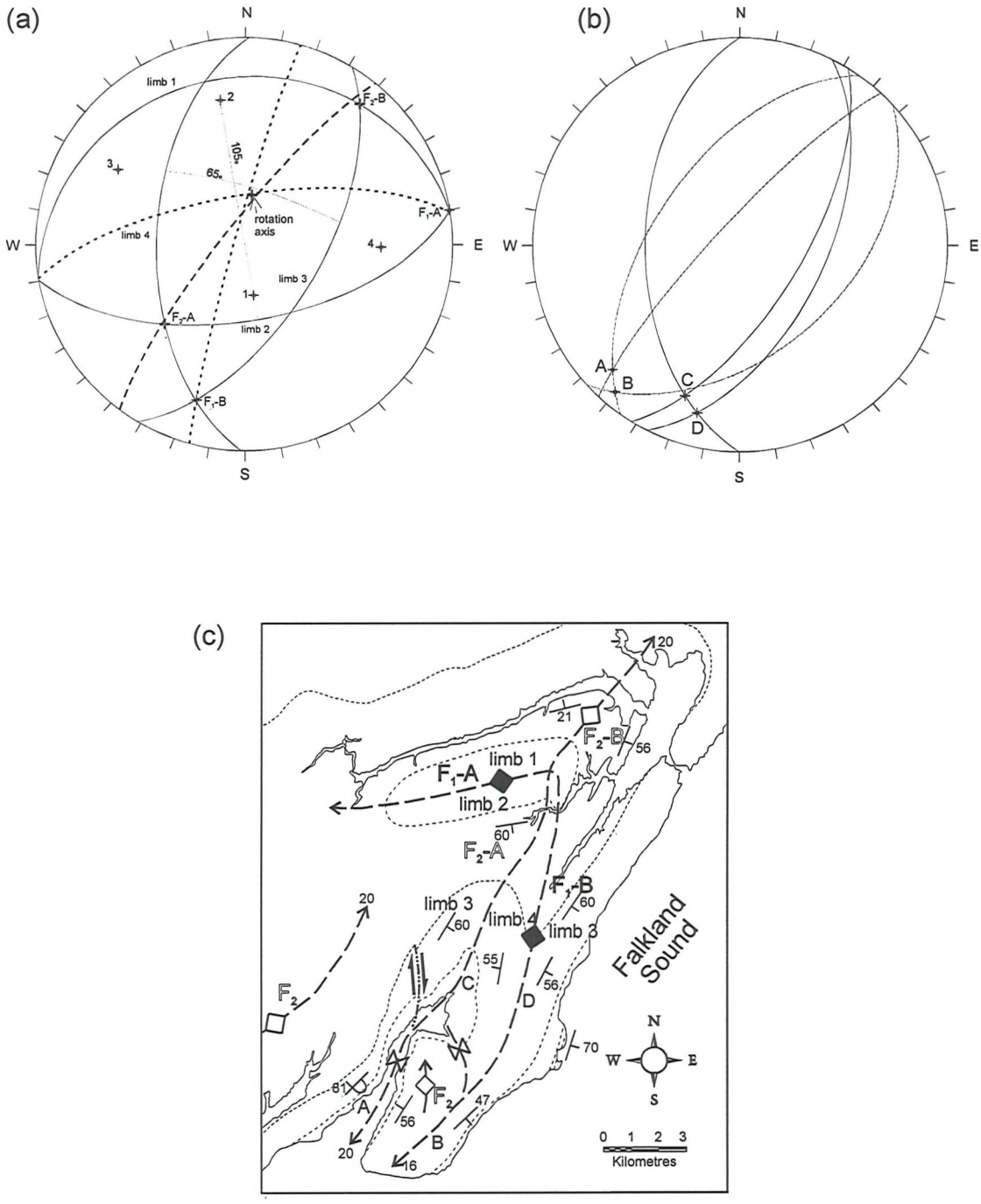

Figure 5.9:(a) Equal-area lower hemisphere projection showing the originally E-W F_1 fold (limbs 1 & 2, axis F_1-A) refolded around a steep NE-SW, F_2 fold axis (F_2-A/B) to form a NNE-SSW refolded F_1 axis (limbs 3 & 4, axis F_1-B). Note differences in plunge of F_2-A and B. (b) Equal-area lower hemisphere projection showing planes of bedding which form fold axes A-D (c.f. (c)) C being an F_2 axis and D being a refolded F_1 axis with A & B being the southerly continuations of axes C & D as F_2 folds. Note the close similarity of the refolded F_1 and the original F_2 folds. (c) relationship of folds and position of limbs 1 - 4 and axes F_1-A/B, F_2-A/B and A-D denoted in (a) & (b).

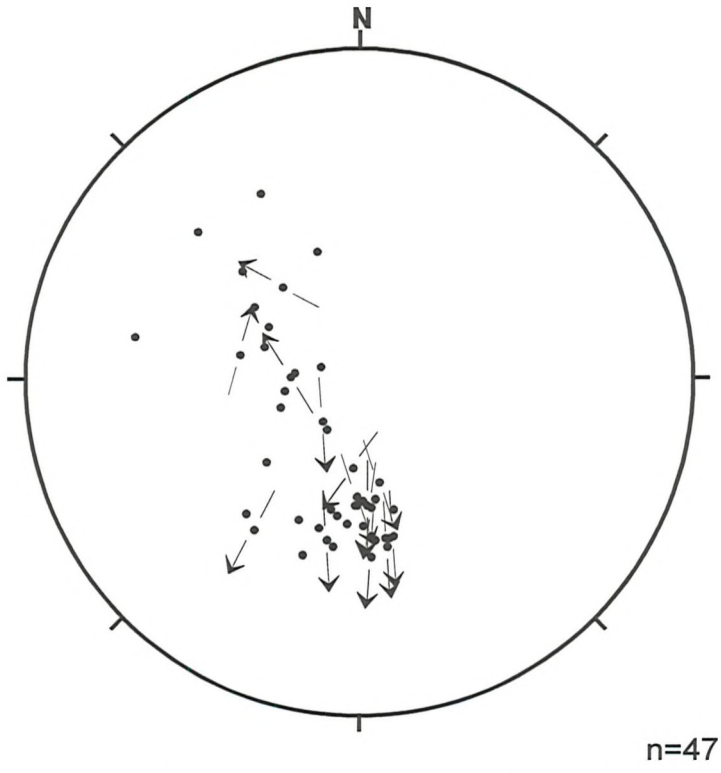

Figure 5.10: Hoepenor plot of thrusts in the Port Stephens and Fox Bay Formations from the shallow limb of the Hornby Anticline, Port Howard.

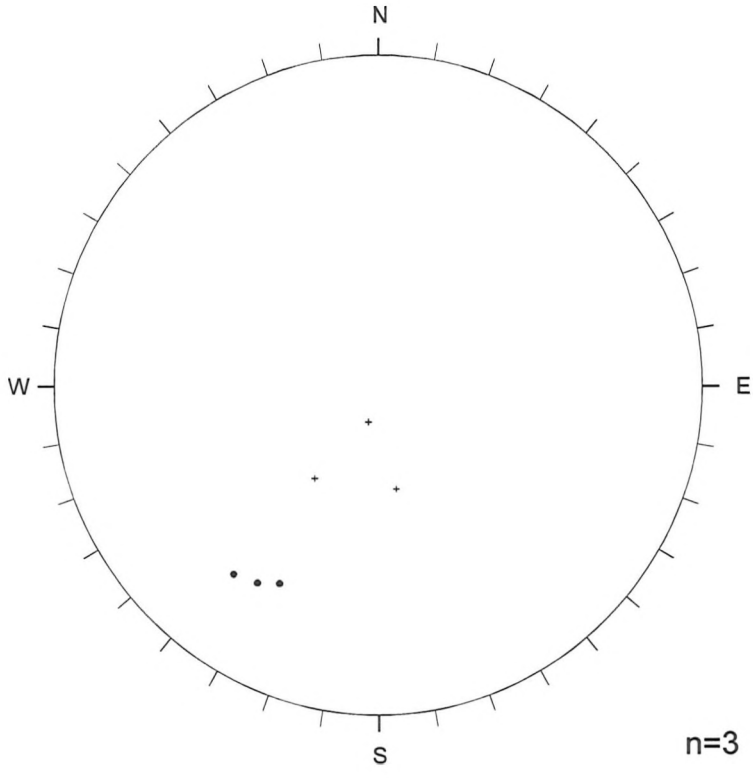

Figure 5.11: Equal-area lower hemisphere projection of poles to faults (crosses) and poles to cleavage within the fault planes (circles) from around Purvis Pond, Port Howard.

Figure 5.12: Photograph, looking north-east, of a pop-up structure in quartzites of the Port Stephens Formation at Freezer Rocks. The structure has been caused by the interaction of two top-to-the-south and top-to-the-north-west reverse faults. Notebook is 13 cm across. (UTM location 21UC793229).

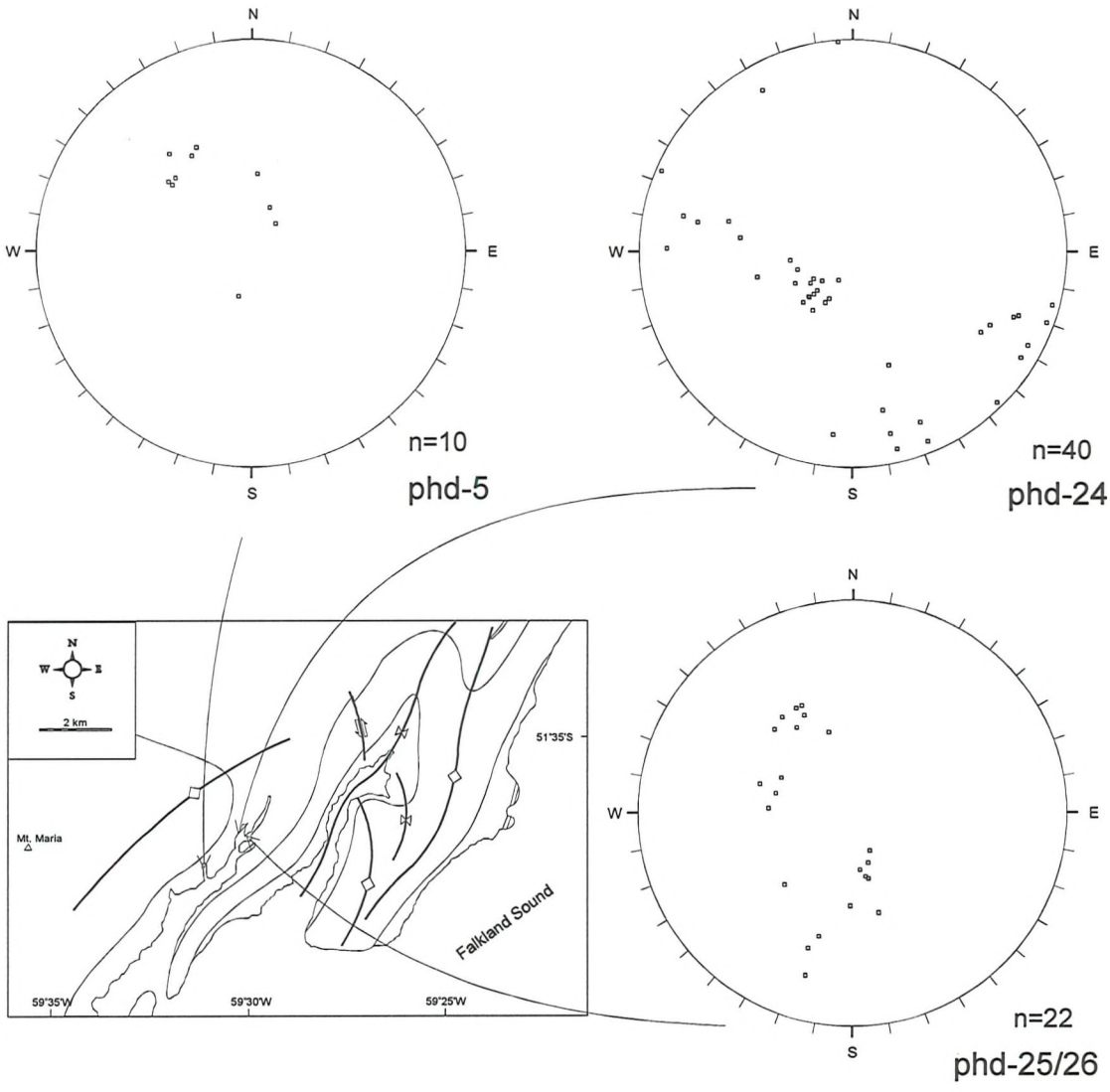

Figure 5.13: Equal-area lower hemisphere projections of poles to planes of reverse faults in the Fox Bay Formation from three locations on the steep limb of the Hornby Anticline, Port Howard.

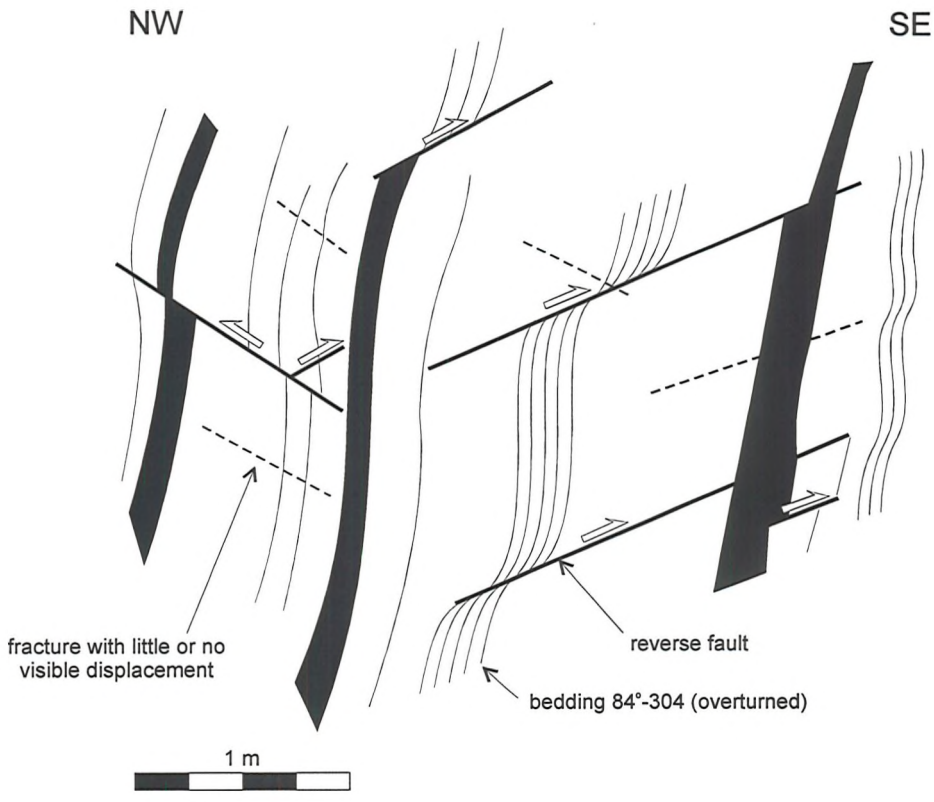

Figure 5.14: Line diagram, based on field sketches, showing the relationship of conjugate reverse faults to bedding in the shales of the Fox Bay Formation in the overturned limb of Hornby Anticline, Port Howard. (UTM 21FUC270797).

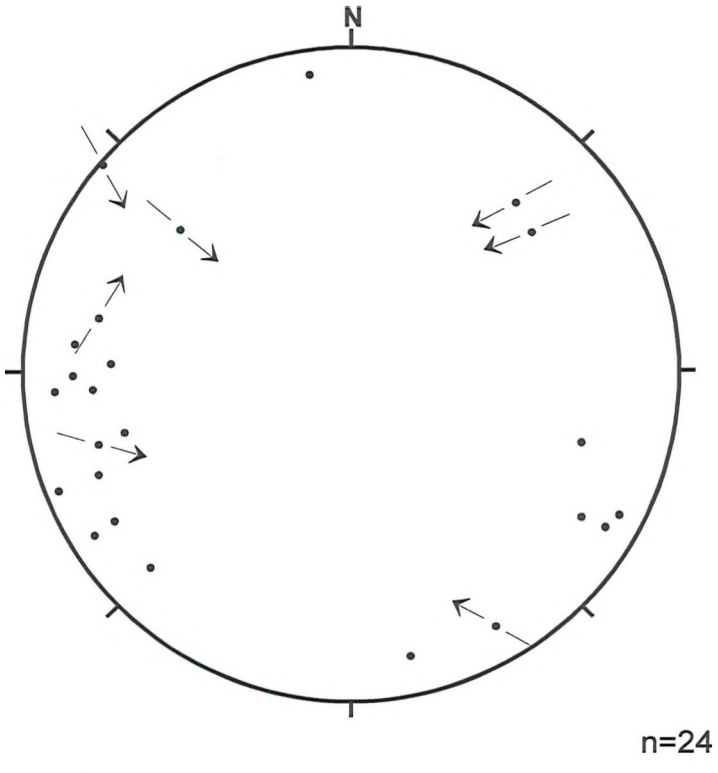

Figure 5.15: Hoeppenor plot of normal faults from the Port Stephens and Fox Bay formations from around the Hornby Anticline, Port Howard.

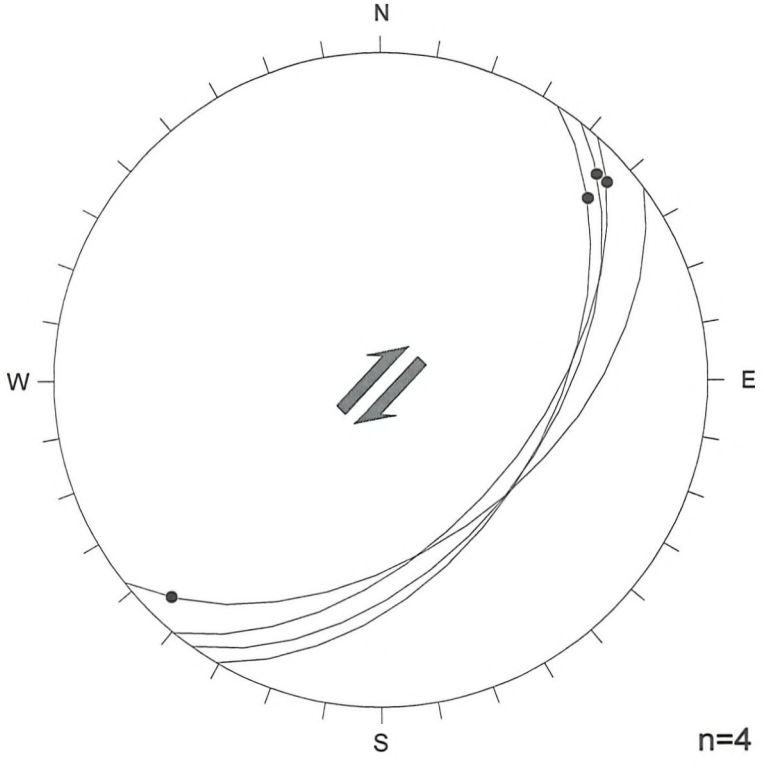

Figure 5.16: Equal-area lower hemisphere projection of planes to dextral strike-slip faults, with slickenside lineations marked. Data from the steep limb of the Hornby Anticline, Port Howard.

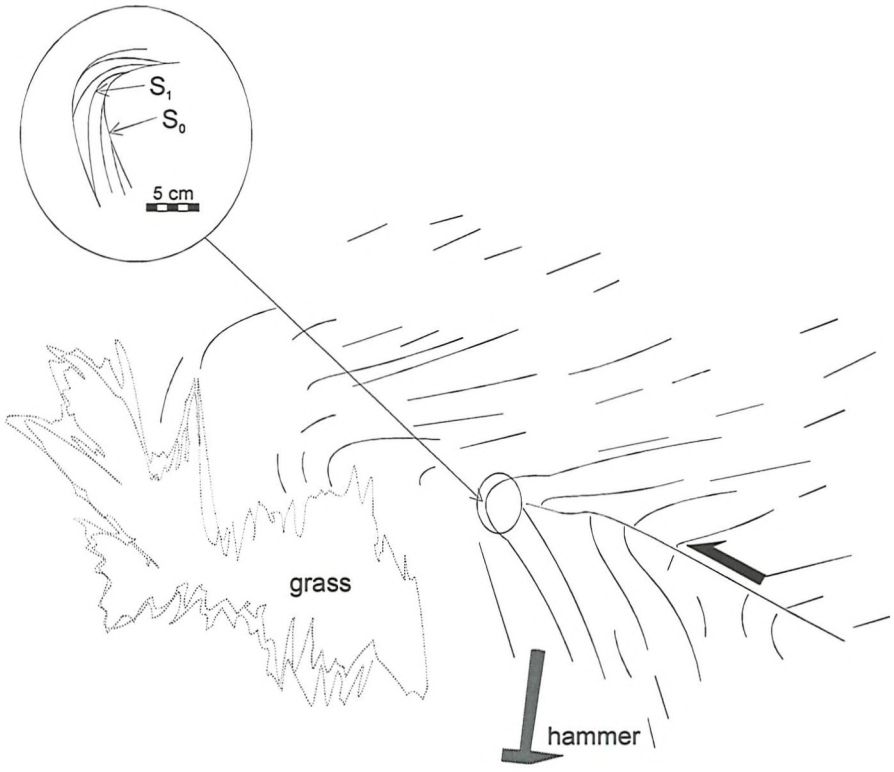

Figure 5.17: Line drawing, from field sketches, of bedding (S_0) and weakly developed cleavage (S_1) relationships in an area of localised folding and faulting, Port Howard. (UTM 21FUC256789).

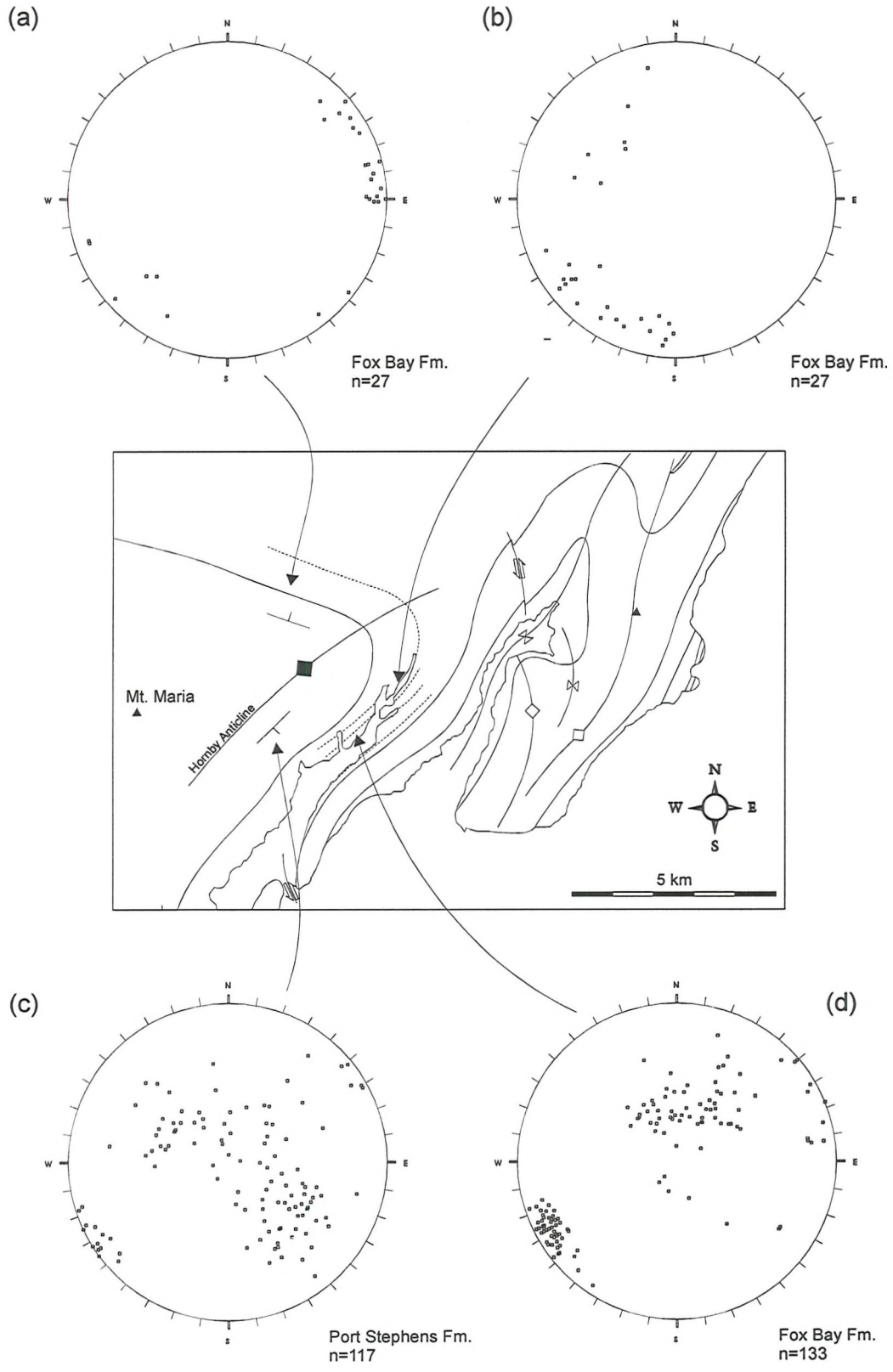

Figure 5.18: Equal-area lower hemisphere projections of poles to quartz veins from the Fox Bay and Port Stephens formations from across the Hornby Anticline, Port Howard.

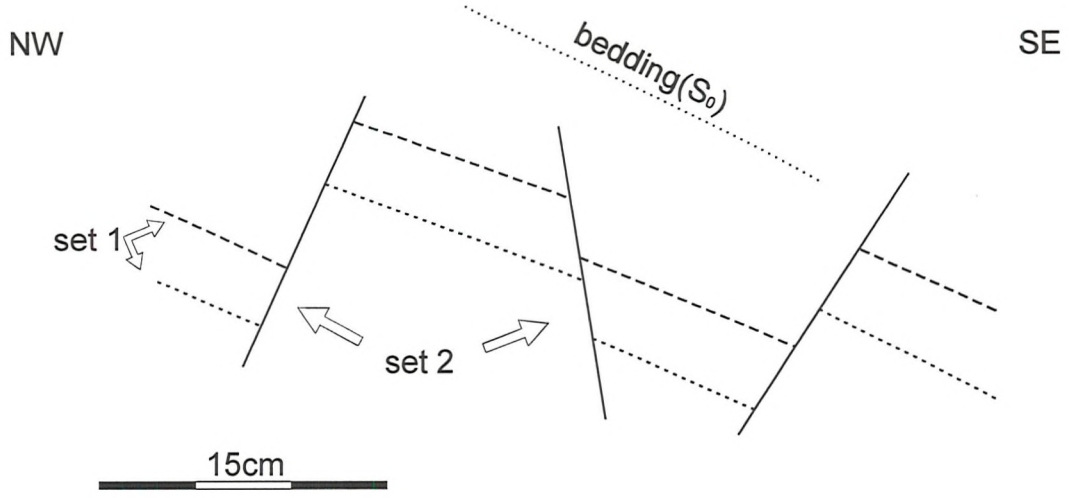

Figure 5.19: Diagram, taken from a field sketch, of cross-cutting relationship of two sets of quartz veins in the Port Stephens Formation on the steeper limb of the Hornby Anticline, Port Howard. (UTM 21FUC234787).

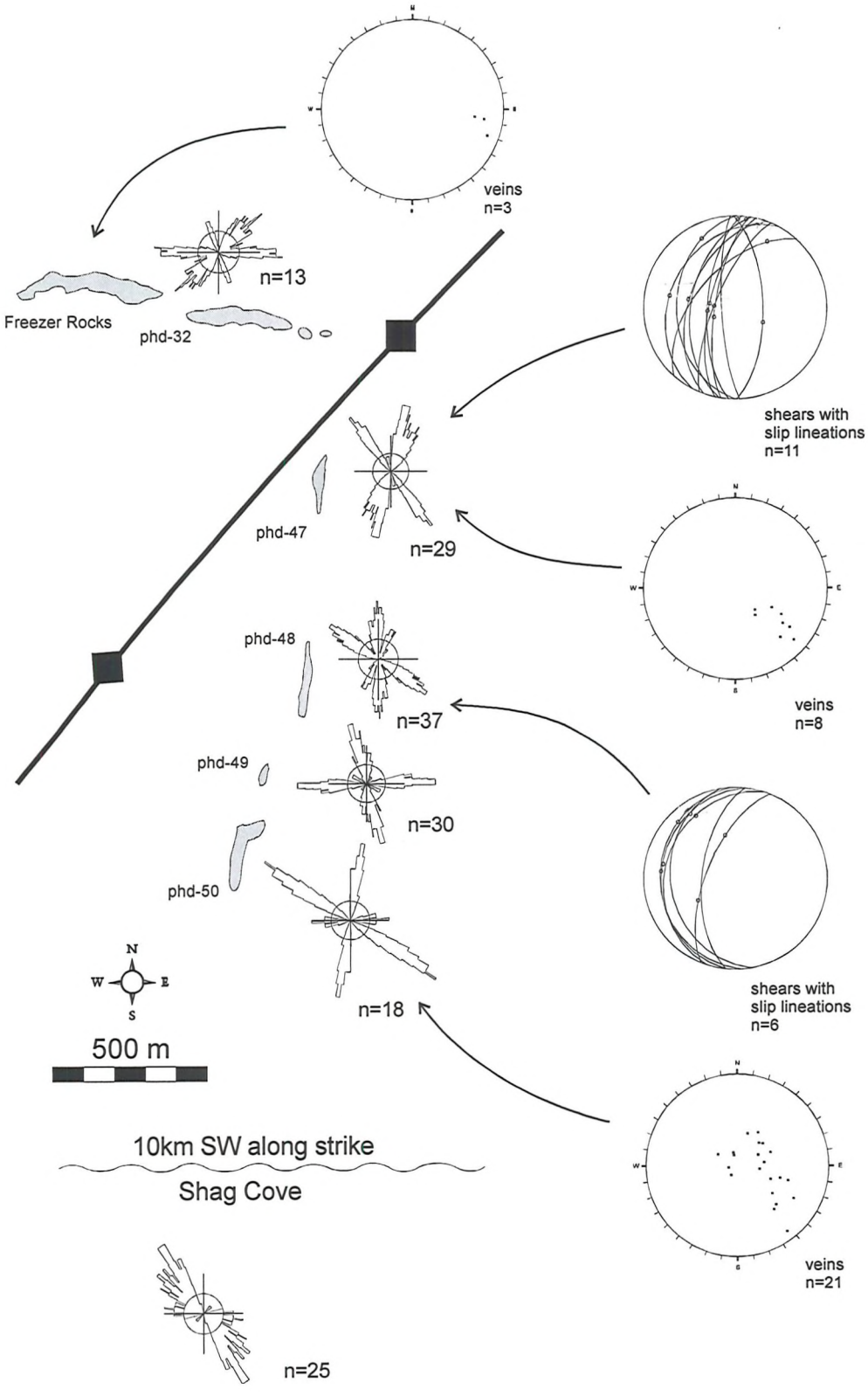

Figure 5.20: Outcrops of the Port Stephens Formation on the east side of Mount Maria showing deformation around the core of the Hornby Anticline. Jointing on rose diagrams, veining as poles and shears as planes and lineation directions, both on equal-area lower hemisphere projections. phd- denotes locality numbers.

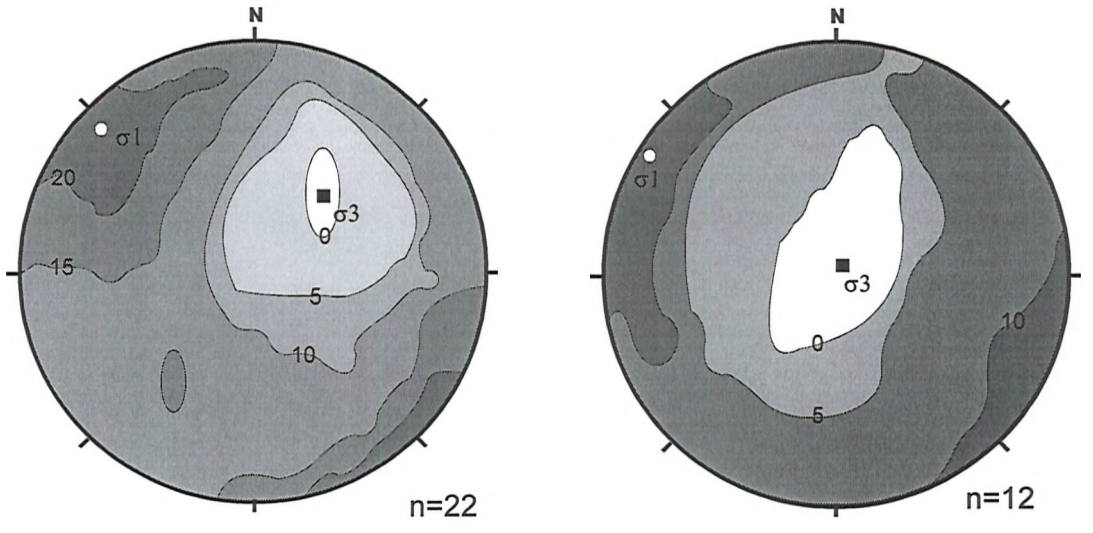

Figure 5.21: P/T dihedra plots of shears from locations phd-47 & 48 (c.f. Fig.5.20). Squares indicate most likely position of σ_3, circles indicate most likely position of σ_1. Both show σ_1 to be sub-horizontal and oriented NW-SE and σ_3 to be sub-vertical or dipping steeply SW. Contours denote concentrations of datapoints.

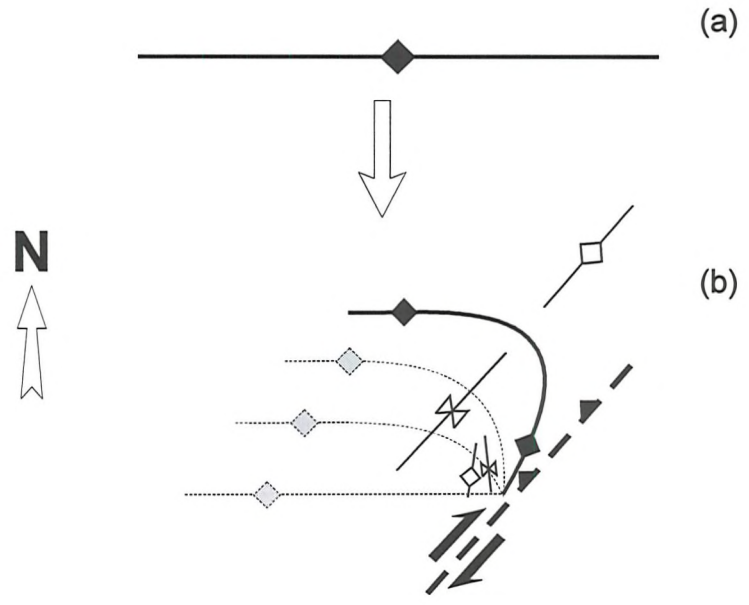

Figure 5.22: Model for the formation of the Bold Cove folds. (a) initially E-W fold. (b) E-W refolded around a vertical axis, probably indicating movement along a NE-SW oriented steep dextral fault within the Falkland Sound.

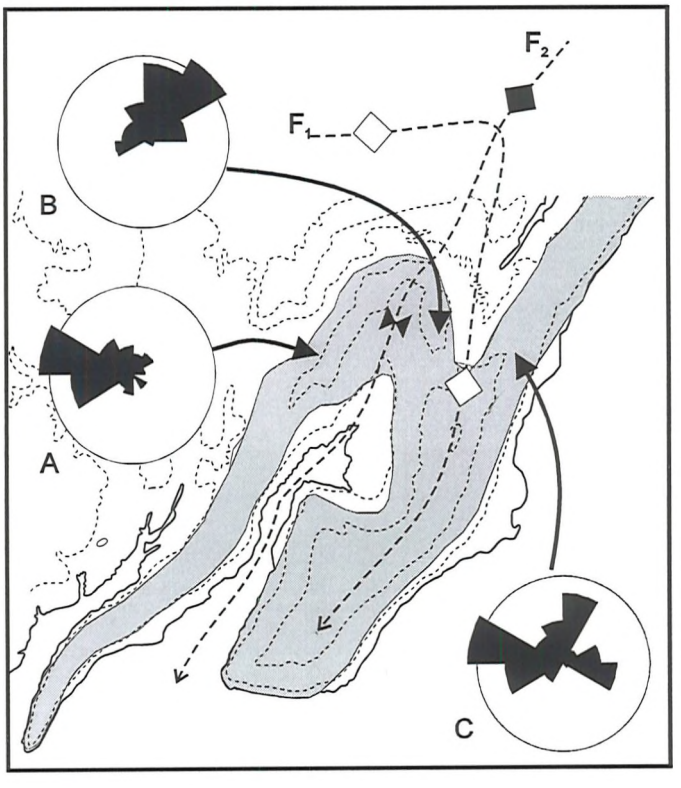

Figure 5.23: Rose diagrams of palaeocurrents from the Port Stanley Formation around Bold Cove which have been corrected for local tectonic tilt of bedding.

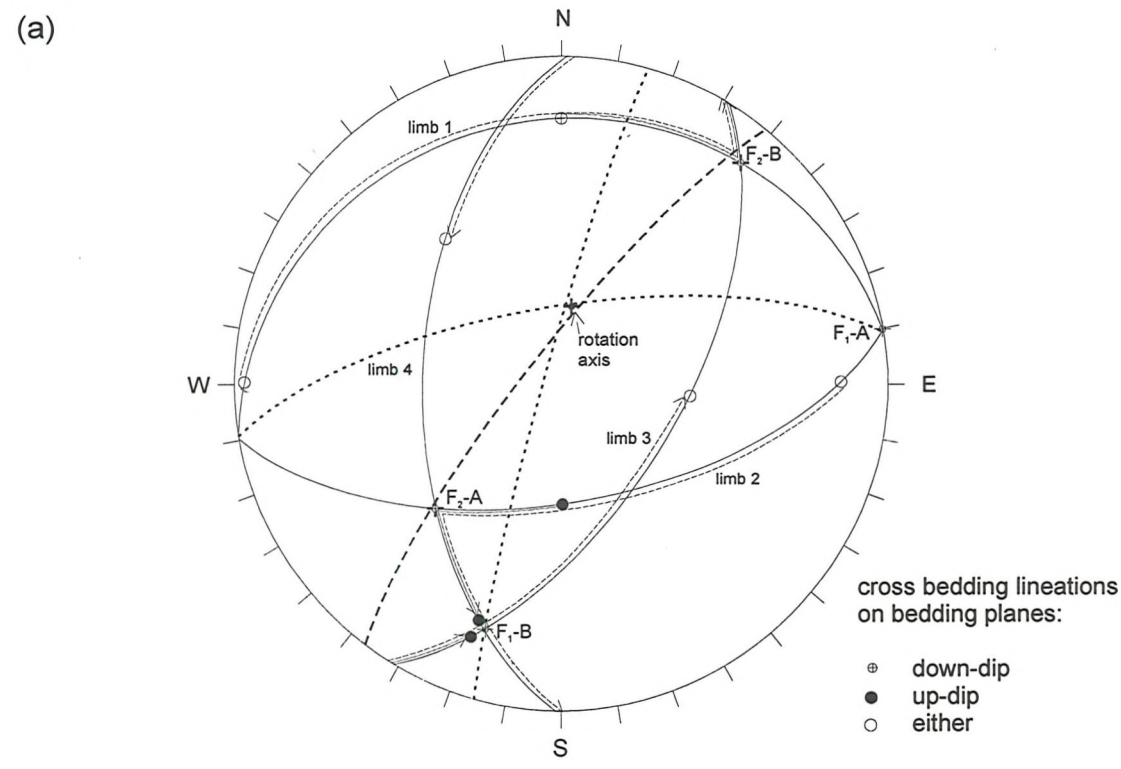

Figure 5.24: Equal-area lower hemisphere projection showing rotation around a shallowly plunging F_2 axis of cross-bedding foreset lineations from the Port Stanley Formation. Originally N palaeocurrents become NNE on easterly limbs and NE on westerly limbs, whereas originally E-W palaeocurrents become WNW-ESE. (c.f. Fig. 5.9c for locations of folds)

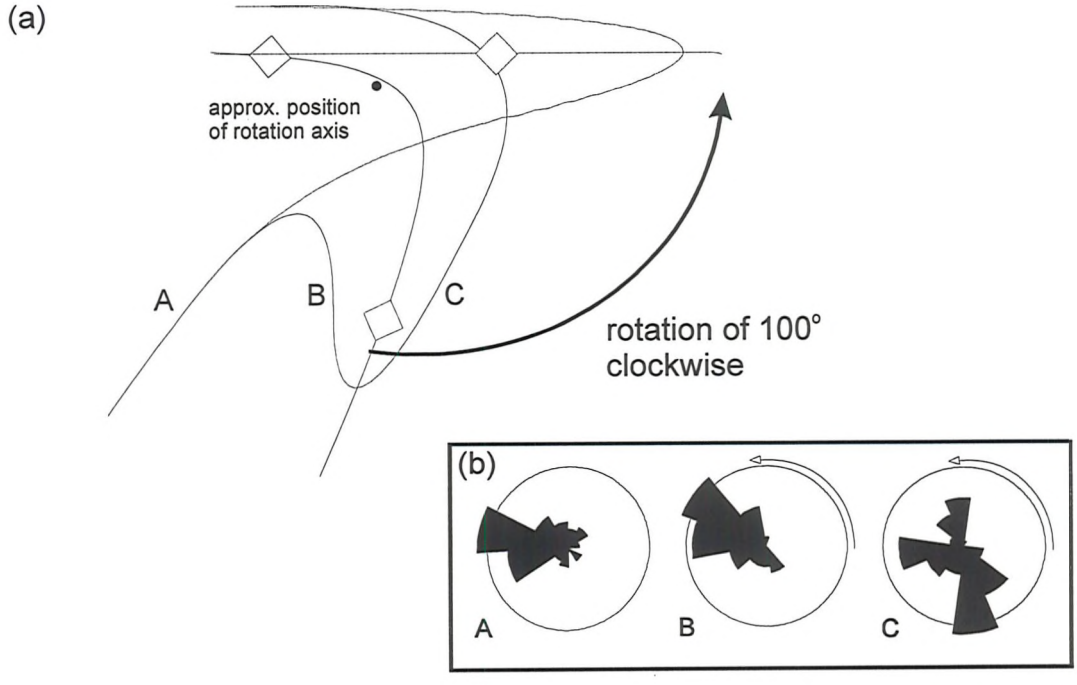

Figure 5.25: Rotation of palaeocurrents from the Port Stanley Formation by 100° about a vertical axis, so restoring an E-W strike to the refolded Bold Cove anticline. (a) schematic diagram showing restoration of E-W axis; (b) restored palaeocurrent directions after rotation.

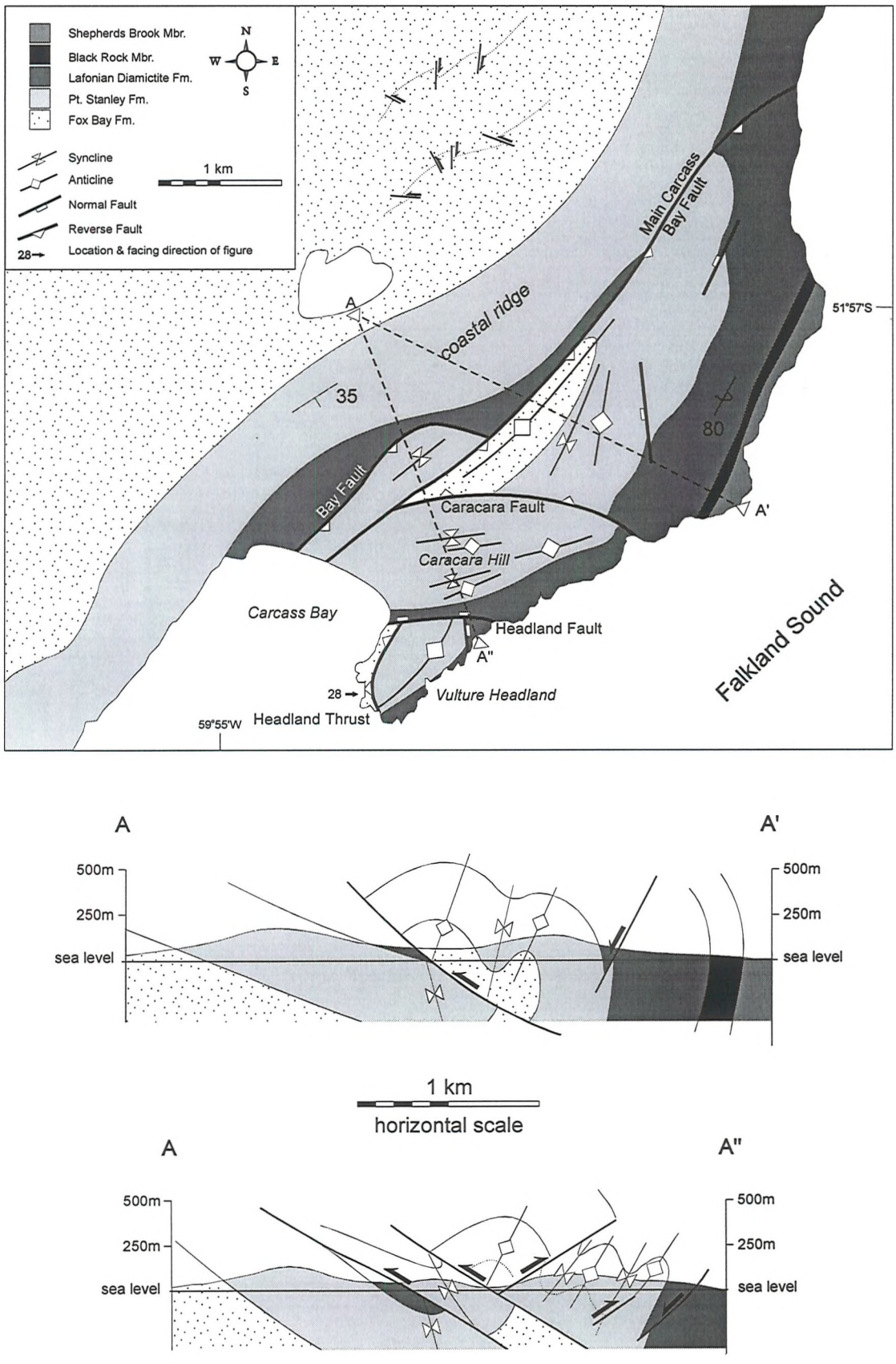

Figure 5.26: Summary geological map and cross-sections from Carcass Bay, West Falkland.

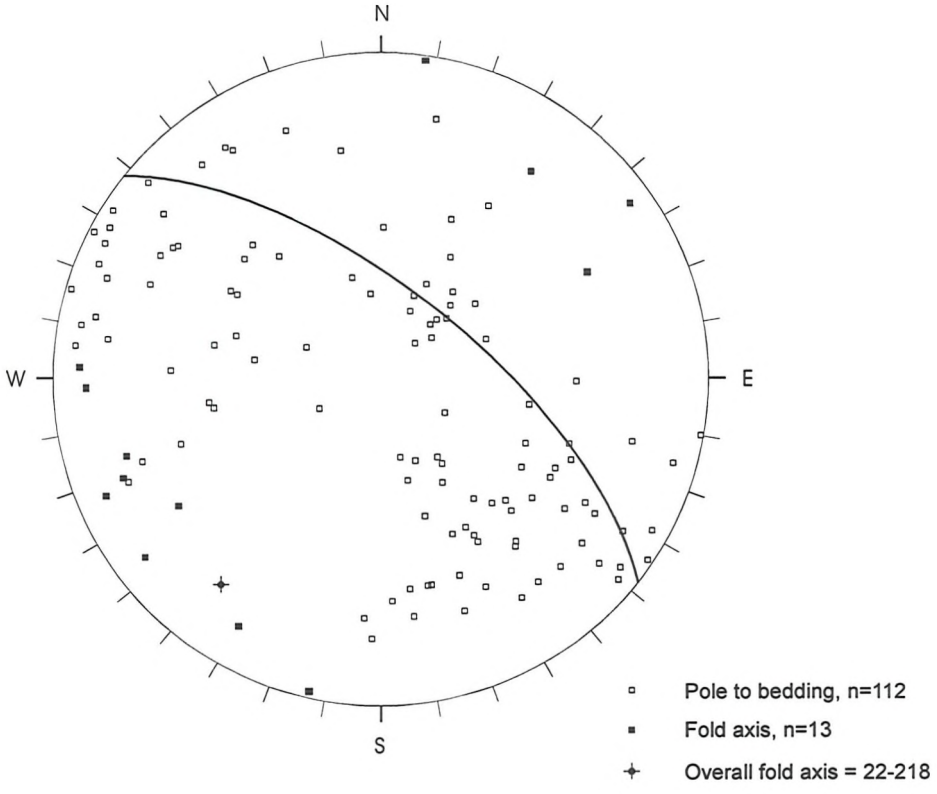

Figure 5.27: Equal-area lower hemisphere projection of poles to bedding and fold axes, Carcass Bay. Overall fold axis shown.

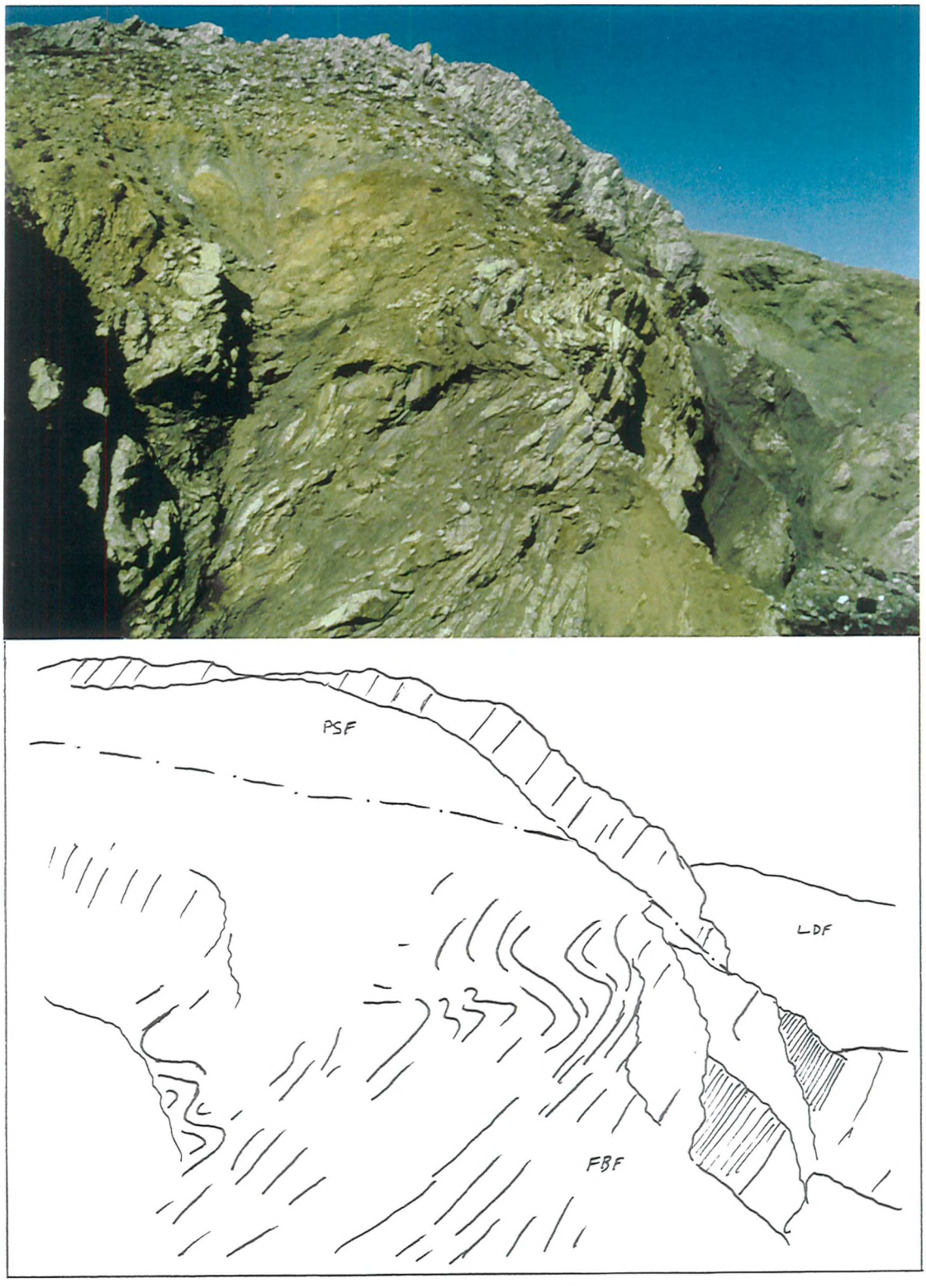

Figure 5.28: Photograph and line drawing, looking east, of the Headland Thrust, Carcass Bay. Lower brown exposure is of folded sandstones and shales of the Fox Bay Formation (FBF) dipping generally north-west, directly above are white quartzites of the Port Stanley Formation (PSF), dipping steeply north-west and in the distance is an outcrop of the Lafonian Diamictite Formation (LDF) overlying the Port Stanley Formation. The thrust is denoted by the dashed line between the lower FBF and upper PSF outcrops.

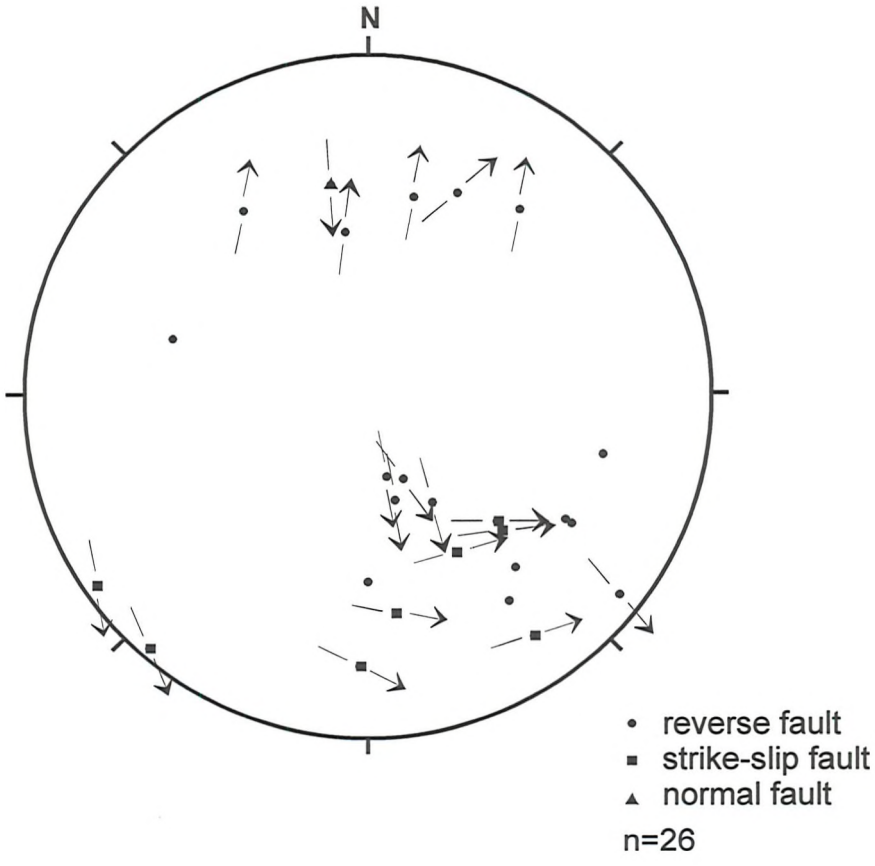

Figure 5.29: Hoeppenor plot of faults from Carcass Bay, West Falkland.

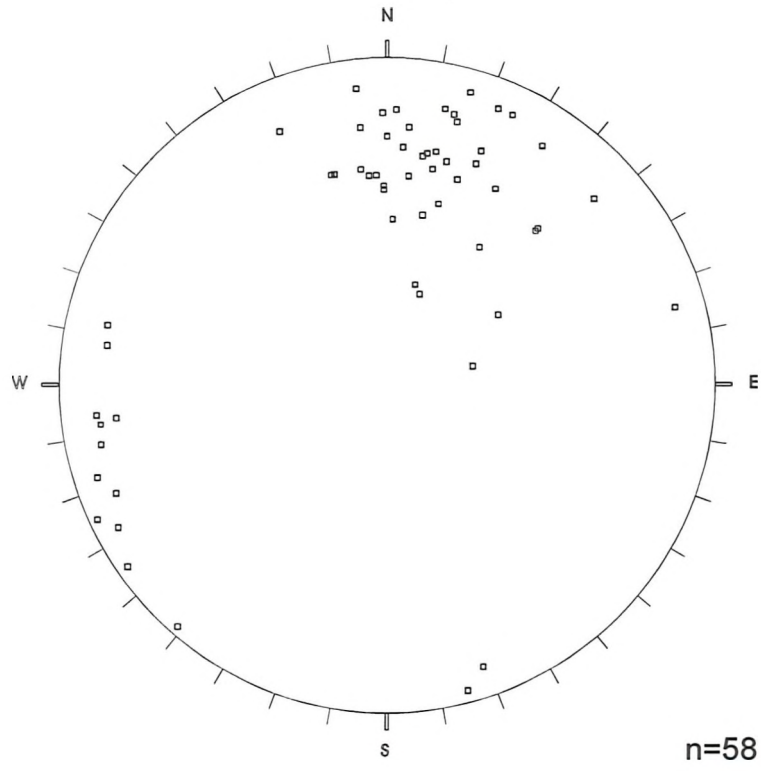

Figure 5.30: Equal-area lower hemisphere projection of poles to quartz veins, Carcass Bay.

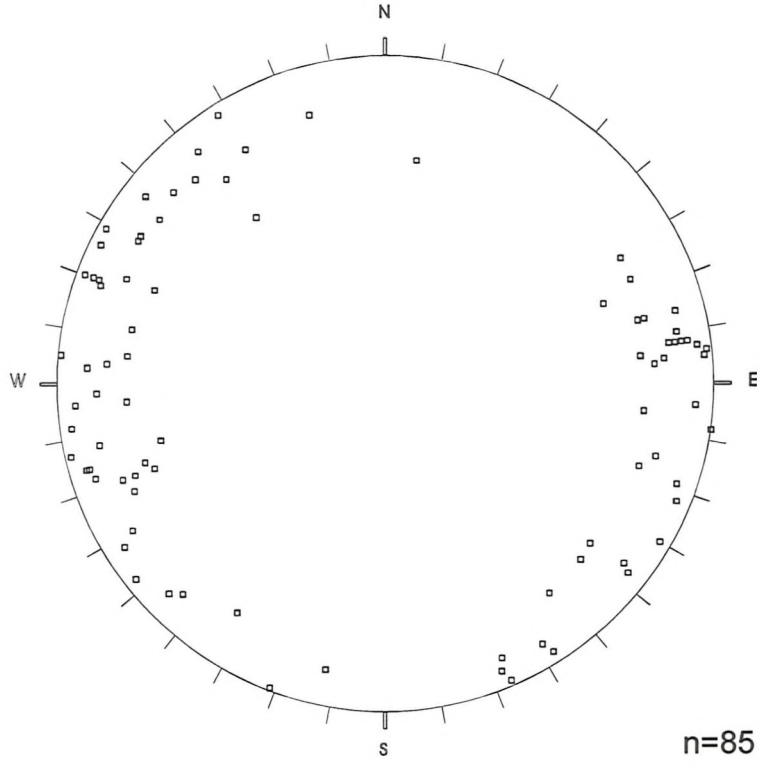

Figure 5.31: Equal-area lower hemisphere projection of poles to joints, Carcass Bay.

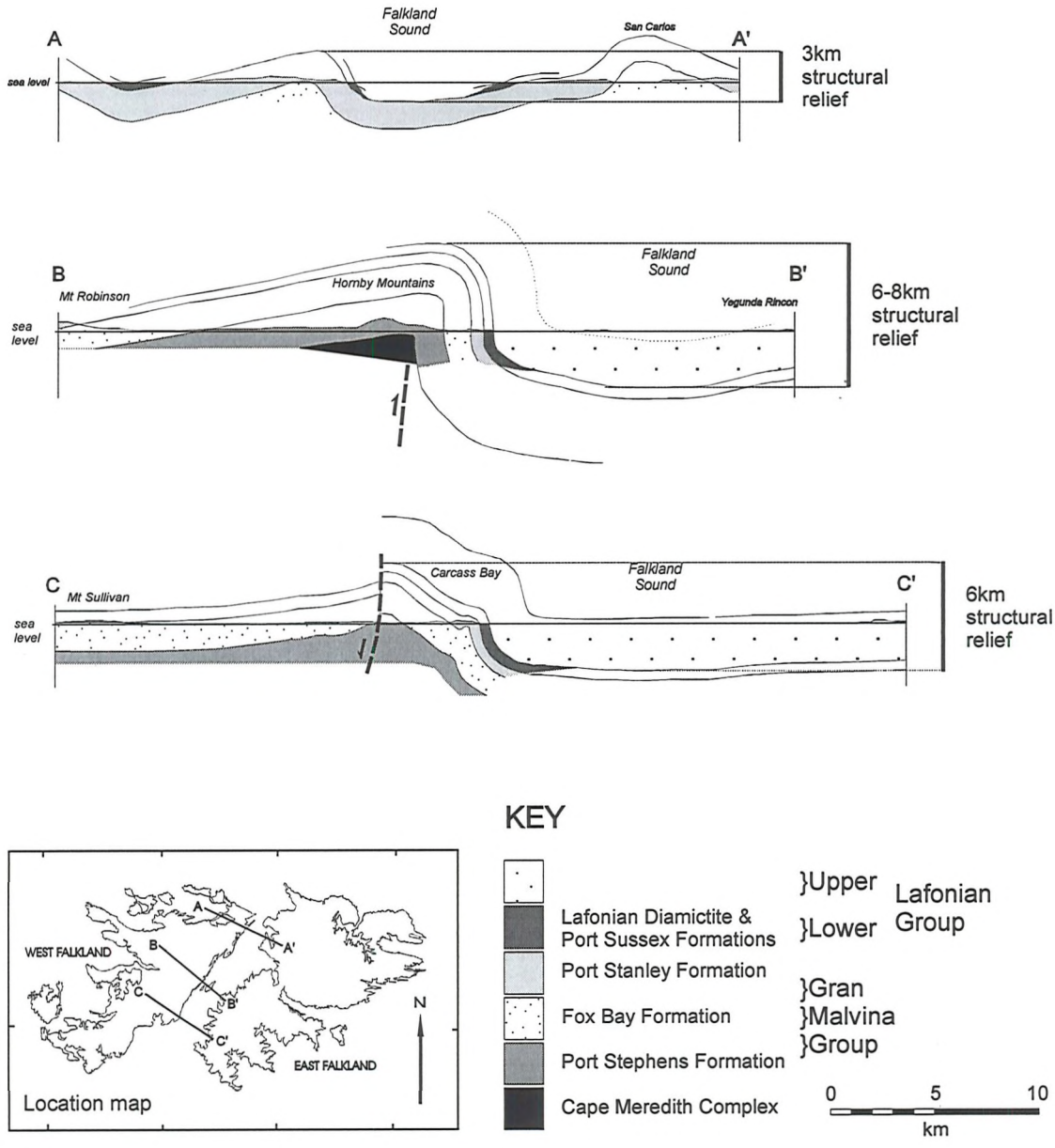

Figure 5.32: Three cross-sections across the Falkland Sound from NE (A-A') to SW (C-C') (see location map) showing the Hornby Monocline and structural relief across this fold. Vertical = horizontal scale.

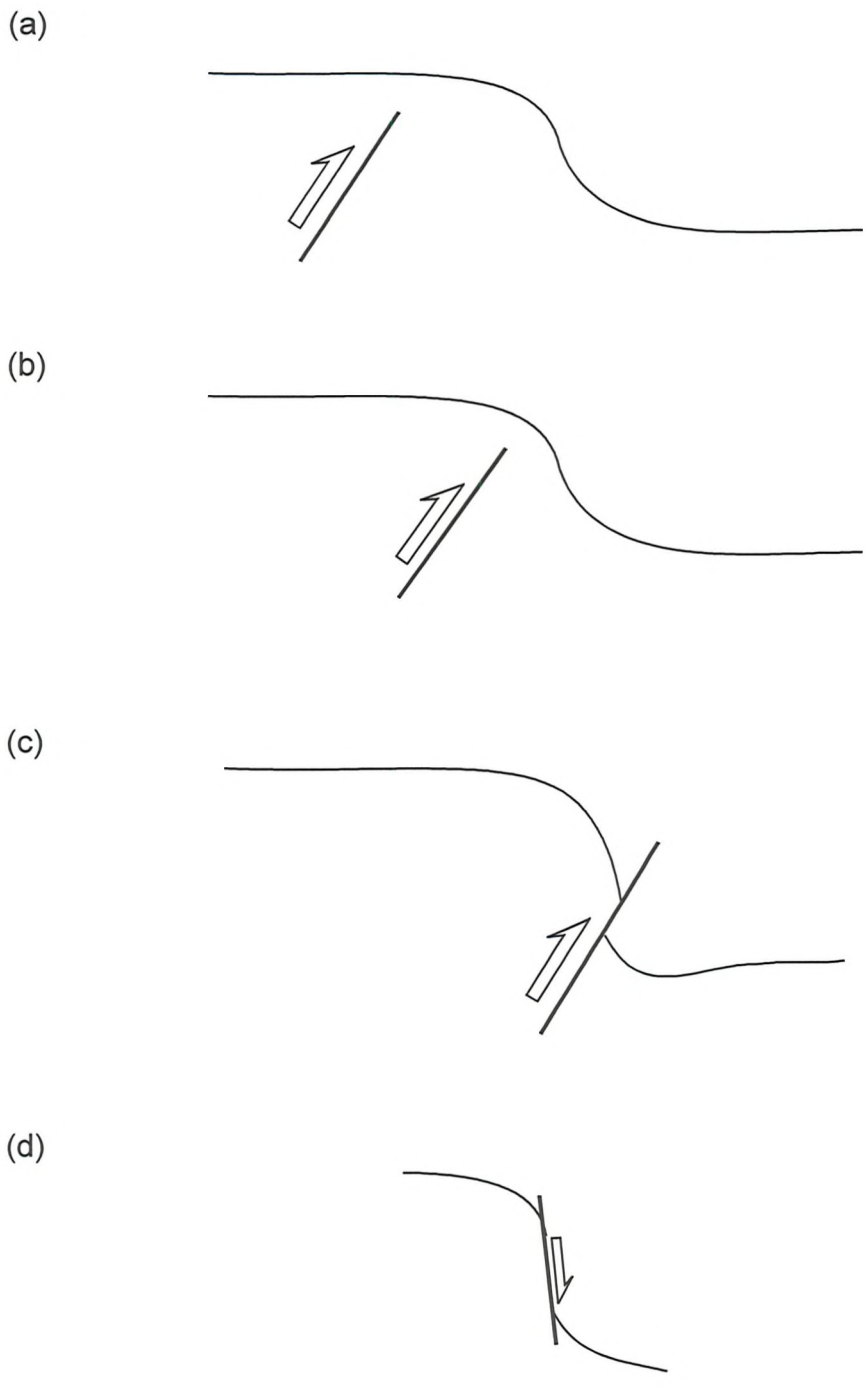

Figure 5.33: Diagrams to show the position of a high angle fault relative to the monocline it forms, (a)-(c) show a reverse fault, (d) shows a normal fault. (a) behind the anticlinal bend; (b) underneath the anticlinal bend; (c)&(d) under the inflexion point between the anticlinal and synclinal bends. (a)-(c) after Reches (1978), (d) after Kelley (1955).

Chapter 6: Geophysical studies to the SW of the Falkland Islands

Chapter 6: Geophysical studies to the SW of the Falkland Islands

6.1 Introduction

The onshore geology of the Falkland Islands shows a marked contrast between East and West Falkland. On West Falkland, Precambrian crystalline basement is exposed in the far south at Cape Meredith, and is overlain to the north and west by the mostly Devonian Gran Malvina Group. On East Falkland, the Gran Malvina Group is exposed in the north whilst the Permo-Carboniferous Lafonian Basin covers the south of the island. There are two distinct structural trends on the islands: (1) E-W/ESE-WNW exposed across the northern half of both islands and (2) NE-SW seen as the Hornby Monocline on West Falkland forming a major structural boundary between the two main islands (Fig. 6.1).

Little was known prior to 1994 about the offshore geology of the Falkland Islands, the only information coming from studies to the east, on the Falkland Plateau and Maurice Ewing Bank (Fig. 6.2) (Ewing *et al.* 1971, Barker *et al.* 1976a, Ludwig *et al.* 1979, 1983, Lorenzo & Mutter 1988). More recently work resulting from hydrocarbon exploration interests (Richards & Fannin 1994, 1997, Platt & Philip 1995, Richards *et al.* 1996) has concentrated on the offshore geology around the Falkland Islands. This work shows that there are four major basins; the North Falkland Basin (NFB) to the north, the Falkland Plateau Basin (FPB) to the east, the South Falklands Basin (SFB) to the south and the Malvinas Basin (MB) to the south-west (Fig. 6.2). The interpretation of all these basins has been based on DSDP holes from the Maurice Ewing Bank, 800 km to the east, and commercial exploration wells in the Argentine basins, such as the Magallanes Basin 500 km to west. This extrapolation is because, as yet, no direct evidence, such as from drilling, is available from any of the four basins themselves. The infill of the basins has been interpreted as syn-post rift sedimentation of Jurassic to Tertiary age (Richards & Fannin 1997), underlain by an economic basement which is the offshore continuation of the Palaeozoic rocks exposed on the Falkland Islands.

The two structural trends picked out on the Falkland Islands are only clearly seen offshore to the east where the western edge of the FPB trends NE-SW and to the

north-west where NW-SE trending faults bound the southern edge of the NFB (Richards & Fannin 1997). The lateral extent to the NE or SW of the fault or fault zone which has caused the NE-SW structural boundary between East and West Falkland is unclear. Richards & Fannin (1994) indicated a basement ridge extending south from Cape Meredith and again Richards *et al.* (1996) noted that gravity data implied there may be a continuation of the NE-SW structural trend to the SW. To the north, although faults bounding the NFB could possibly be a northern continuation of the structural trend, Richards *et al.* (1996) remained unconvinced.

This study uses data from a grid of seismic lines to the SW of the Falkland Islands which have come from a variety of non-exclusive proprietary surveys owned by Geco-Prakla (U.K.) Limited[1] (Fig. 6.3). The lines used in this study have been renumbered A - R in accordance with confidentiality agreements with Geco-Prakla. Bouguer gravity and magnetic data from ARK Geophysics has also been used. The aim of this chapter is to assess the lateral continuity of the structural boundary, seen onshore between East and West Falkland, in an area to the SW of the Falkland Islands encompassing the eastern edge of the Malvinas Basin and the western edge of the South Falkland Basin (Fig. 6.2).

6.2 Offshore geology to the SW of the Falkland Islands

In assessing the lateral continuation of a NE-SW structure the most useful seismic lines in this study have been lines A, B and C which strike NW-SE orthogonal to the NE-SW structure. Of these, the most informative has been line A which lies closest to the Falkland Islands.

6.2.1 Description of line A

The data from line A is of a poor quality for modern data and, although the upper strata are well imaged, the lower part of the section shows very little structure and is dominated by multiple reflections of the sea floor and scattering, probably due to the

[1] Permission to use this data is gratefully acknowledged.

uneven surface of the prominent unconformity seen clearly at around 1s two way time (TWT).

The line shows two distinct packages of strata (Fig. 6.4a, b);

1) an upper, well defined package of sub-horizontal strata of Jurassic to Tertiary age (Platt & Philip 1995). This package shows a relatively constant thickness across this line but pinches out to the NE and thickens to the SW.

2) a more poorly defined package of pre-late Jurassic strata (Platt & Philip 1995), probably mostly Palaeozoic and earlier in age, separated from the younger package by a clear unconformity.

The upper package of rocks are defined by clear, sub-horizontal, laterally continuous reflectors which onlap onto irregular highs (Fig. 6.4b at intersection with line O) and infill small depressions in the underlying unconformity (Fig. 6.4b at intersection with line M). The surface of the unconformity is irregular and somewhat broken, and indicates that there may be a series of small extensional faults which are causing some of the irregularity in this surface. Below this surface imaging is poor and only a few clear reflectors are identifiable lying at the NW end of the line picking out strata dipping gently to the NW, flattening out down dip. These reflectors can be seen to truncate up-dip against the unconformity surface especially around the intersection with line E. The remainder of the package below the unconformity consists of irregular and broken reflectors superimposed by multiples of the overlying unconformity and seabed surfaces. Only at deeper levels of 7 - 8s TWT do occasional dipping reflectors occur, the origin of which is unclear.

Little structure is seen below the unconformity except the shallowly dipping reflectors at the NW end of the seismic line. This lack of obvious structure imaged on the seismic line is probably due, in part, to the processing of the data, which will have concentrated on the upper suite of rocks which are of greater exploration interest, and also in part to scattering from the uneven surface of the unconformity which has obscured any true underlying reflectors. This lack of structure beneath the unconformity was also noted by Richards *et al.* (1996). However, despite the lack of direct evidence from the seismic data, both interval velocity and Bouguer gravity data show a major structure beneath the unconformity.

6.3 Interval Velocity Analysis

The interval velocities from the grid of seismic lines, taken at every 50th CDP with a spacing of 2 km, were determined across the area. These data were then contoured at 1000 ms^{-1} intervals along each line.

On line A (Fig. 6.4c) the 2000, 3000 and 4000 ms^{-1} contours are approximately horizontal, following a similar shape to the strata above the unconformity. In contrast, the 5000 ms^{-1} contour shows a marked step of approximately 3.3s from 4.3s TWT in the SE to 1s TWT in the NW between the intersections of lines J and K (Fig. 6.4c). On the NW side of this high the contour gradually dips to around 4s TWT at the NW end of the line. The dip of the 5000 ms^{-1} contour to the NW of the high point correlates closely to the lowermost of the dipping reflectors imaged on the seismic data below the unconformity against which they truncate.

Velocity profiles from line A (Fig. 6.5) show a velocity discontinuity close to the level of the 5000 ms^{-1} contour. As 5000 ms^{-1} approximates to the velocity of crystalline basement (McQuillin *et al.* 1984), this discontinuity in the velocity profiles indicates that the 5000 ms^{-1} contour is defining the top of crystalline basement and that the interval velocity data are imaging a sharp change in the depth to top of basement of 3 - 3.3s TWT. Using the depths from the seismic line the change in TWT indicates a structural relief of approximately 6.5 - 7.5 km and brings basement from between 8.3 and 7 km below the surface to 0.8 km, just below the unconformity, in the horizontal distance of 4 - 6 km. This is defining a sharp boundary between the lower velocity strata to the SE and the higher velocity, probably crystalline basement, to the NW.

A regional view of the 5000 ms^{-1} interval velocity contour (Fig. 6.6) shows that the marked high on the NW side of line A continues southwards dipping away to both the NW and SW. The sharp boundary for this high, imaged so clearly on line A, is not continuous to the SW where, on line B, no step is visible and the data shows the 5000 ms^{-1} contour at a relatively constant high level of 1.5 - 2.0s TWT. However, farther to the SW again, line C does show a marked, if somewhat muted, step up to the NW, along strike from that seen in line A.

Although it is appreciated that interval velocities are not the most accurate measurement, no borehole or refraction velocities are available as exploration is still in its early stages. This means that interval velocities are the only source of data available. Despite this uncertainty, the sharp change in the 5000 ms^{-1} interval velocity contour is clear, and strong enough to be considered reliable.

6.4 Bouguer Gravity Analysis

Regional Bouguer gravity data has been collected offshore on a ship-board survey by Geco-Prakla for ARK Geophysics (Fig. 6.7) and supplemented by known onshore data (McNaughton 1972, Martin & Sturgeon 1982). These data show a marked high across southern West Falkland and offshore to the SW and a marked low across southern East Falkland and offshore to the SW (Fig. 6.7). The transition between the high and low areas is imaged along line A where the gravity anomaly increases by between 38 - 44 mGals towards the NW reaching a maximum of approximately 51 mGals around the intersection of line J (Figs. 6.4d, 6.8d). The boundary of this anomaly is a linear structure running NE-SW, along strike, and parallel to, both the Hornby Monocline, with its inferred underlying fault (Chapter 5.4), and the Falkland Sound. To the north the gravity high continues onto the Falkland Islands themselves (Martin & Sturgeon 1982) (Fig. 6.7) where a similar, if somewhat damped, increase of 40 - 55 mGals in the Bouguer gravity anomaly occurs from East to West Falkland across the Falkland Sound (Fig. 6.8b). The shape of the curve from the onshore data is limited by the number of gravity points that were taken on West Falkland (Fig. 6.7), however, the increase from East to West Falkland is still clear. To the SW of line A, the sharp nature of the boundary only continues south-westwards as far as line B and no positive anomaly is apparent by line C (Fig. 6.7).

6.4.1 Gravity modelling

From the nature of the gravity anomaly along line A it is clear that the rocks on the NW side are of a higher density than on the SE side. To model this anomaly it is

necessary to correlate between the offshore and the known onshore geology of the Falkland Islands.

The clear structural boundary between East and West Falkland has resulted in West Falkland being uplifted relative to East Falkland by 6 - 8 km (Fig. 6.1). In the south of West Falkland, the Precambrian crystalline basement of granites, granite-gneisses and amphibolites is exposed at Cape Meredith and overlain to the N and W by the mostly Devonian Gran Malvina Group. Both are intruded by numerous dolerite dykes. This contrasts starkly with the Permian Lafonian Basin on East Falkland, which is up to 3.5 km thick and overlies 3 km of the Gran Malvina Group (Fig. 6.1). The juxtaposition of these two sequences causes an increase in the Bouguer gravity anomaly across the Falkland Sound from East to West Falkland. The cause of this anomaly is the change in rock density (Table 6.1) between the Permian Lafonian Basin and the Precambrian Cape Meredith Complex (CMC).

It is clear from the summary above that the 6 - 8 km structural relief and increase in the Bouguer gravity anomaly from East to West Falkland is identical to what is seen offshore in the interval velocity and Bouguer gravity data of line A (Fig. 6.8). Given this clear correlation it is possible to model the gravity anomaly seen offshore using the rock densities from the onshore geology.

Modelling of the gravity anomaly was initially undertaken using the Slab Formula (cf. McQuillin *et al.* 1984). Further to this, more detailed 2-dimensional modelling has been achieved using the programme 2DGM, which has been produced by the staff of the Oceanography Department at the University of Southampton.

i) The Slab Formula: The slab formula (equation 1) gives the gravity anomaly caused by an infinite horizontal slab of density ρ_2 inserted into a body of density ρ_1 (Fig. 6.9). In this case the slab is the Lafonian Basin placed against the Precambrian basement of the CMC.

The slab formula $\Delta g = 2\pi\Delta\rho Gt$ (1)

Δg = gravity contrast $g_1 - g_2$ (mGal), $\Delta\rho$ = density contrast $\rho_1 - \rho_2$ (kgm^{-3}), G = gravitational constant 6.672×10^{-11} (Nm^2kg^{-2}), t = thickness of the slab (m), (see Fig. 6.9).

Rearranging the equation for $\Delta\rho$ and given the gravity change of 38 - 44 mGals and the slab thickness of 6820 - 7380 m (Fig. 6.9) a negative density contrast of 123 - 154 kgm^{-3} is required to cause the anomaly. Onshore, the Cape Meredith Complex (CMC) has an average density, given the proportions of granitoids and amphibolites from known outcrop extent, of 2720±5 kgm^{-3}, and the Lafonian Basin has an average density, including the underlying Gran Malvina Group, of 2620±5 kgm^{-3}, a contrast of only 100±10 kgm^{-3}. This density contrast, given the slab thickness, would only create a gravity anomaly of 29 - 32 mGals; lower than that observed. As noted, the density for the CMC is calculated using known outcrop extent. To achieve the density contrast required there needs to be denser rocks at depth.

ii) 2DGM Modelling: This is a basic programme which allows interactive on-screen modelling of an observed gravity anomaly using the calculated anomaly for theoretical 2-d bodies, with known densities, emplaced into a medium of a given density. Parameters such as shape and density of the bodies can be adjusted to model a better fit of the theoretical to the observed data.

Two models have been generated for the observed data using this programme. The first accounts for the overall shape and increase from SE-NW. The second allows closer modelling of the two anomalous highs in the gravity data on the NW side of the line. The parameters for the models, such as thickness of Mesozoic/Cainozoic cover and depth to the top of the basement have been derived using the calculated depths from the velocity analyses on the seismic lines themselves. Further parameters such as the densities have, in part, been derived from onshore data (Table 6.1), however, as was shown by the simple Slab Formula, these densities do not give the contrast required to create the gravity anomaly observed. As the proportions of rock types in the basement are not well defined beneath the exposure at Cape Meredith, it is reasonable to vary the density of the basement block in the models to fit the observed data through the varying the proportions of amphibolite, granitoids and dolerite. By this means the density of 2788 kgm^{-3} was derived for the basement block.

Model 1. This model simply defines a basement block, similar to that imaged on the velocity analysis (Fig. 6.10). Although the velocity data defines a very sharp boundary, in order to closely correlate the slope of the gravity anomaly, the discontinuity in the basement has been modelled with a south-easterly slope (Fig. 6.10). This model allows a close match of the observed and theoretical anomaly across the major structure in the SE of the line. However, as the correlation is poor to the NW, other factors have influenced the Bouguer gravity anomaly. These are more closely modelled in Model 2.

Model 2. The overall configuration of the basement block used in this model is the same as in Model 1. Two elongate, vertical bodies with densities similar to basic igneous rocks have been inserted to the NW of the main anomaly to account for the two gravity highs seen between lines D and E and lines I and J (Fig. 6.11). The two bodies which have been modelled approximate to two negative anomalies in the magnetic data along line A (Fig. 6.12). Given that N-S dolerite dykes in the SW of the Falkland Islands have a reversed polarity (Mitchell *et al.* 1986, Taylor & Shaw 1989), these would be expected to produce negative magnetic anomalies. So, it may be possible that the two bodies which have been modelled approximate to dyke swarms, similar to the N-S dykes on West Falkland. Only with the inclusion of these two bodies do the theoretical and observed gravity anomalies correlate closely for the entire line.

iii) Discussion: Both the Slab Formula and the 2DGM modelling reveal a major inconsistency to the observed data in the density required of the basement block to cause the Bouguer gravity anomaly. In both models, the observed proportions of granites, amphibolites and dolerites from Cape Meredith give an overall density lower than that required. Several possibilities exist to explain this: (1) the more dense amphibolites and dolerites, which at present constitute approximately 20% of the CMC in outcrop (Thomas *et al.* 1995), become more abundant at depth. Increases in the proportion of deeper denser rocks to a total of 30 - 42% would result in density contrasts of 124 - 150 kgm^{-3} respectively which is similar to that required by the Slab Formula to cause the gravity anomaly seen. A ratio of approximately 50% granitoids

and 50% amphibolites would be required to cause the 170 kgm^{-3} density contrast used in the 2DGM modelling; (2) that there may be a separate, denser body at depth, causing the required increase in density contrast; (3) that there is a change to a more dense basement between Cape Meredith and line A to the south; and (4) that the sediments of the Lafonian Basin decrease in density southwards. This could be possible as density would decrease as the effects of the Gondwanian deformation and the associated metamorphism decrease away from the deformation front. This type of relationship is seen in the Karoo Basin in South Africa (Rowsell & de Swardt 1976).

As yet, it is unclear which, or any, of these hypotheses accounts for the required increase in density contrast.

It is appreciated that the modelled basement outline using 2DGM does not correlate exactly with the sharp boundary imaged on the interval velocity data. This may be an effect of the Palaeozoic sediments draping over the basement high as with the Hornby Monocline or to the basic nature of the gravity modelling programme. It is realised that, given more time and a more versatile modelling programme, the accuracy of the models could be improved. However, in spite of this, this modelling allows a first approximation for a model of the gravity anomaly along line A based on known geological constraints.

A further point of discussion is the magnetic data for line A. Although the negative anomalies roughly correlate to the theoretical bodies in Model 2, they do not correlate exactly. This may be due to one or both of two reasons; (1) that the modelling is inaccurate and, as with the slope of the basement, given a more versatile package, these may correlate more closely; or (2) that the magnetic data is imaging something unrelated to the gravity anomaly. Regional magnetic data by ARK Geophysics would imply the latter, however, small-scale local effects, such as a dyke swarm, could be overlooked on such regional data.

Finally, it has been noted from the Bouguer gravity data that the distinct structural boundary between East and West Falkland is not continuous all the way SW to line A (Fig. 6.7). This may be due the underlying structure, such as a fault, being segmented. In this model a fault under line A would have attained maximum displacement and that this tails off to the NE towards West Falkland and SW towards

line B. This is a very similar structural style to that which has been inferred beneath the Hornby Anticline on West Falkland (Chapter 5.4).

6.5 Conclusions

Using the evidence from the Falkland Islands it has been possible to interpret the geophysical data from line A offshore to the SW. Across this line, the 5000 ms^{-1} interval velocity contour, equivalent as the top of basement, shows a sharp structural relief of 6.5 - 7.5 km from NW-SE across a distance of 4 - 6 km, this is identical to what is seen across the Hornby Monocline with its inferred underlying fault. The Bouguer gravity data also show a sharp increase from SE-NW at the same position as the step in the 5000 ms^{-1} interval velocity contour, implying that they are imaging the same feature. Gravity modelling shows that a change in depth to the top of the basement, similar to that imaged on the velocity data, is an appropriate model for this anomaly. However, the density contrast derived from onshore exposures is too low for the gravity models and would imply more denser rocks at depth offshore. Using the onshore exposures as an analogue it is not unreasonable to imply that the interval velocity and Bouguer gravity data from line A are imaging the same juxtaposition of the Precambrian CMC against the Permian Lafonian Basin, both buried offshore beneath a Jurassic to Tertiary sedimentary cover. The cause of such a sharp boundary could be a major sub-vertical fault, and it is suggested here that the fault segments inferred beneath the Hornby Anticline on West Falkland continue along-strike to the SW, at least as far as 52°50'S.

Strata	*Average Density (kgm^{-3})*
Tertiary	2010*
Cretaceous	2225*
Jurassic	2330*
Permo-Trias (Lafonian Basin)	2620†
Devonian (Gran Malvina Gp.)	2610‡
Precambrian (Cape Meredith Complex)	2720 (granite = 2670‡, amphibolite = 2910‡)

Table 6.1: Average densities for the lithologies onshore and offshore the Falkland Islands. (*Barker *et al.* 1976a, †Rowsell & de Swardt 1976, ‡Martin & Sturgeon 1982).

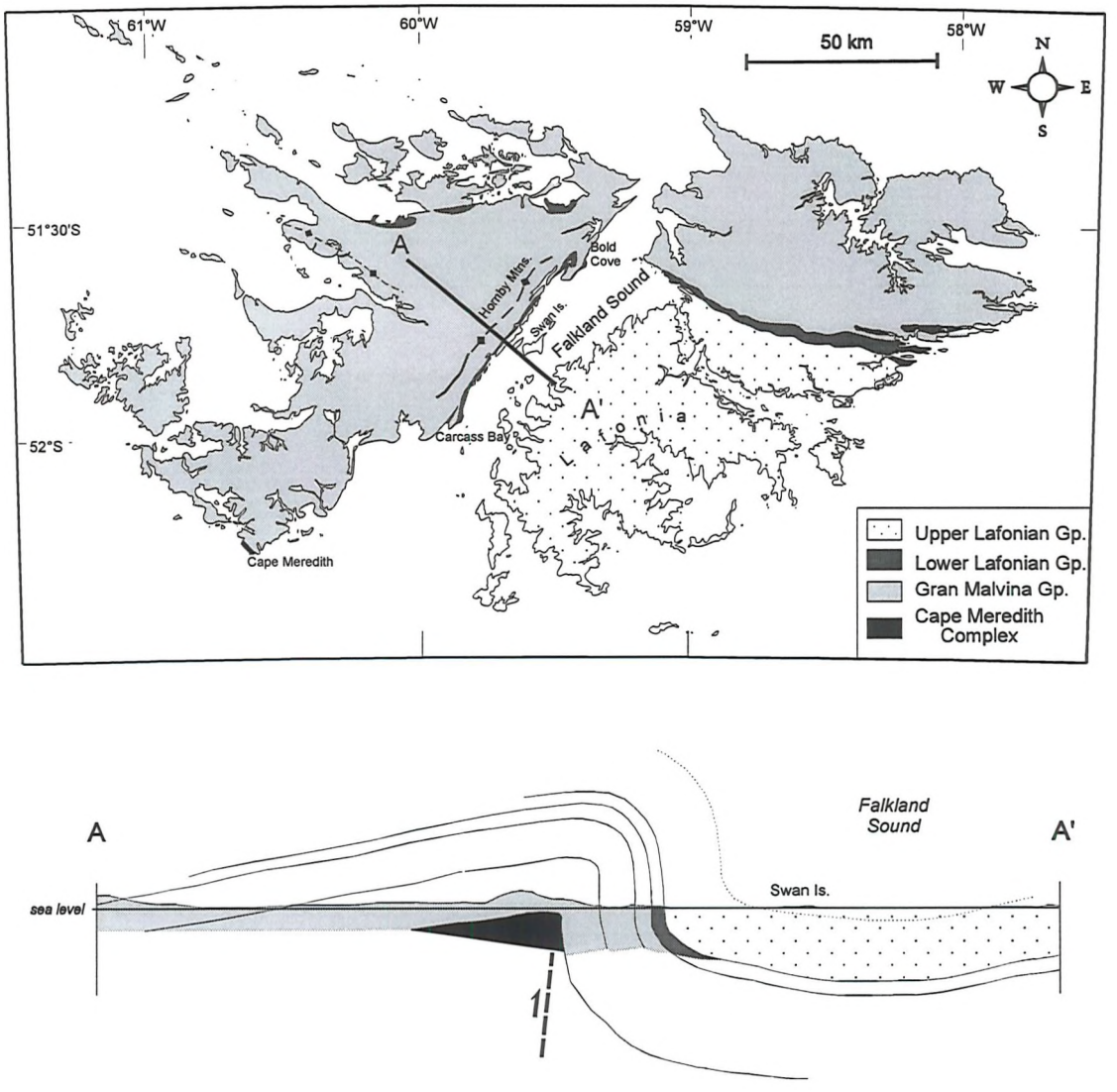

Figure 6.1: Summary geological map of the Falkland Islands (after Greenway 1972) and NW-SE cross-section showing the major NE-SW structural boundary between East and West Falkland.

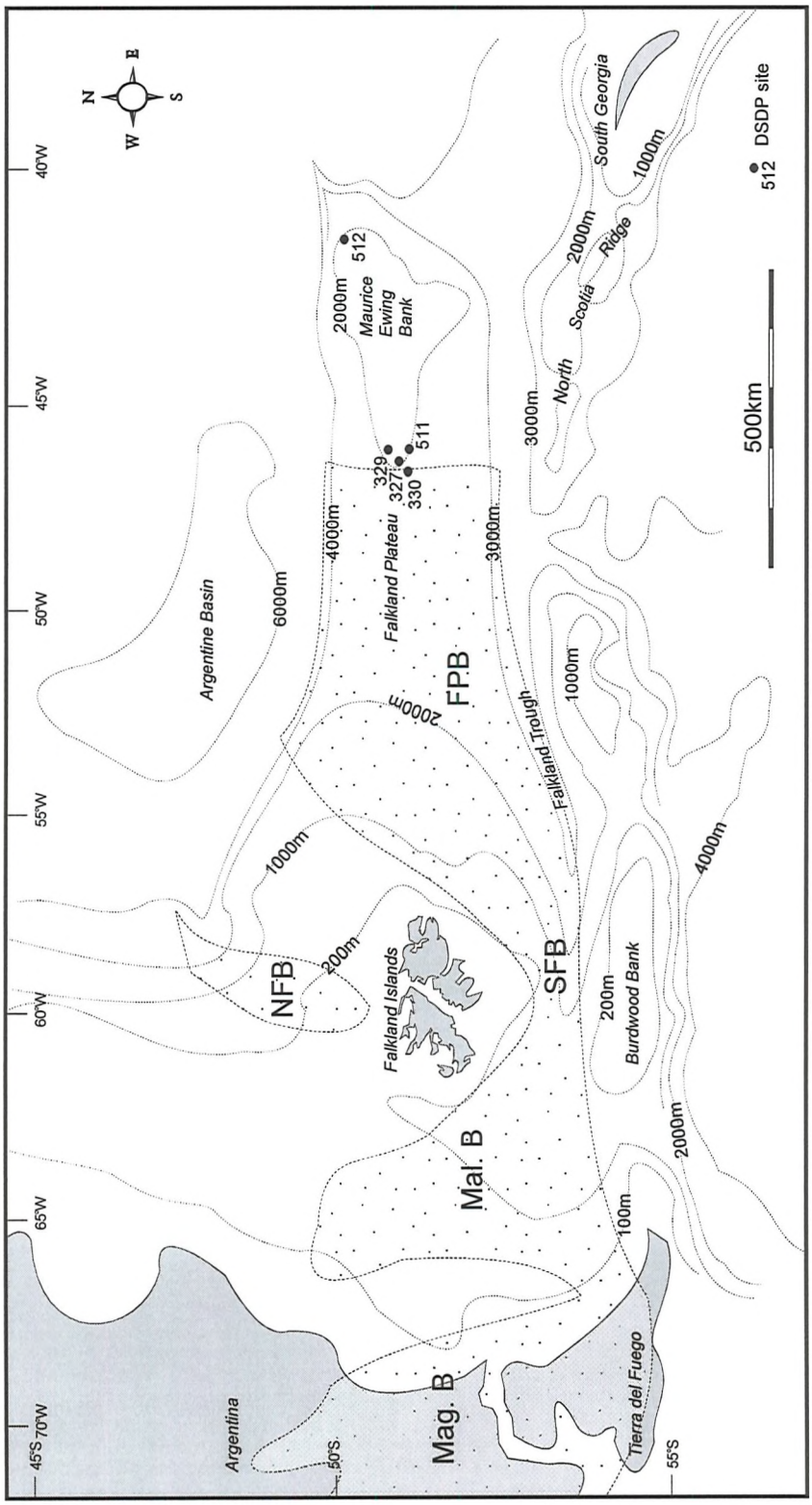

Figure 6.2: Summary of the bathymetry and offshore basins (stippled) around the Falkland Islands. NFB= North Falkland Basin; FPB=Falkland Plateau Basin; SFB=South Falkland Basin; Mal.B=Malvinas Basin; Mag.B=Magallanes Basin. (bathymetry after Ludwig *et al.* 1979, basin geometry after Platt & Philip 1995)

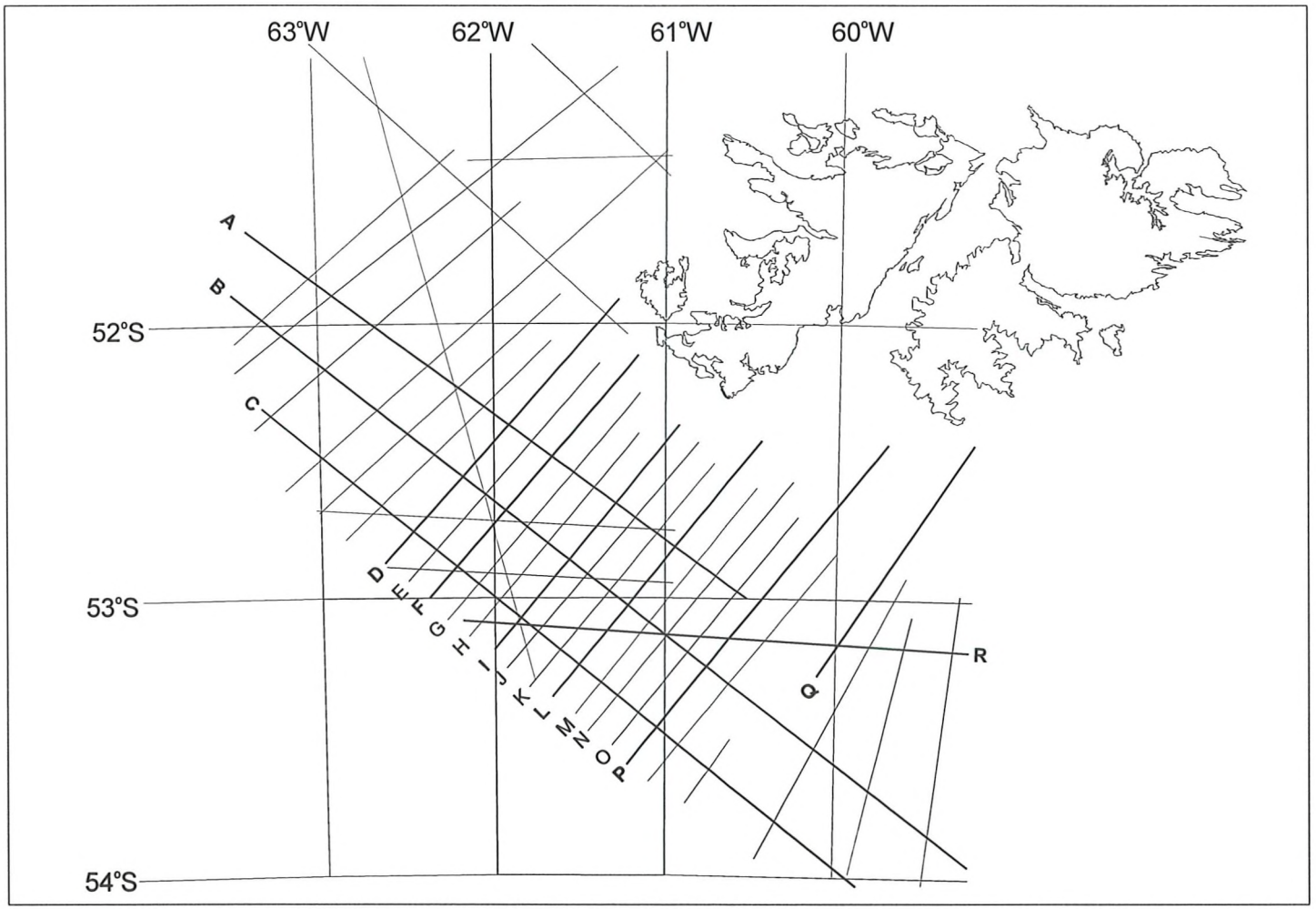

Figure 6.3: Grid of seismic lines to the SW of the Falkland Islands provided by Geco-Prakla. Lines in bold used in this study.

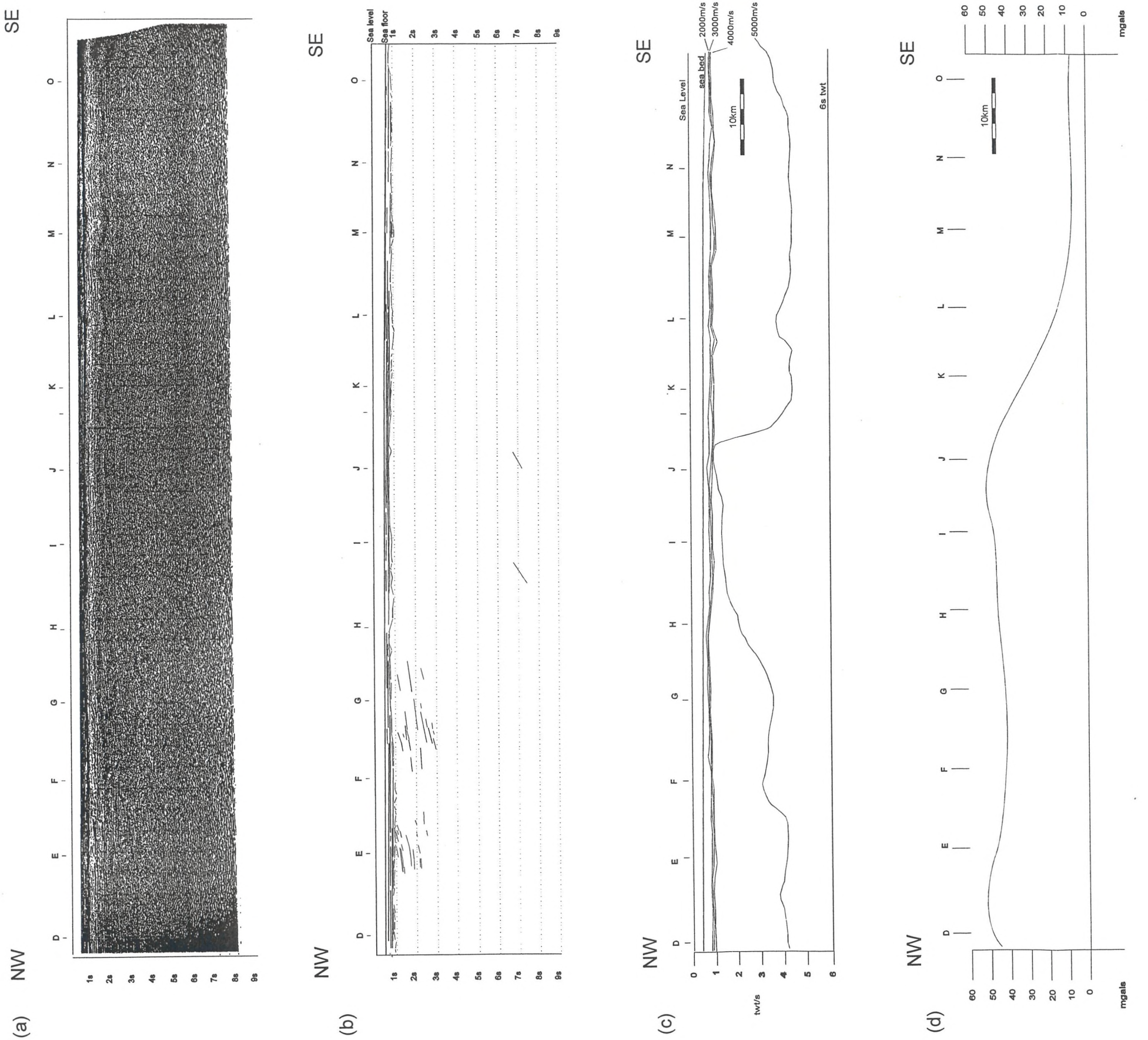

Figure 6.4: Line A ;(a) Seismic reflection data; (b) Seismic reflection interpretation; (c) Interval velocity contours at 1000ms^{-1} intervals; (d) Bouguer Gravity anomaly in mGals.

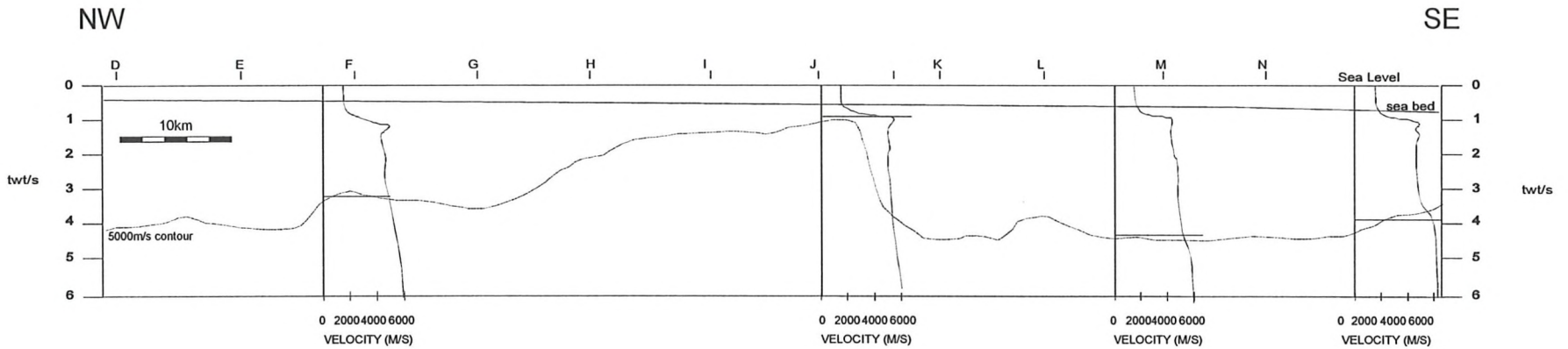

Figure 6.5: Line A showing the close correlation of the 5000ms^{-1} velocity contour, which approximates to the top of basement, and the lowermost velocity discontinuity, taken as the transition into basement, in the velocity profiles. The vertical line to the left of each velocity profile is the line along which the profile was taken.

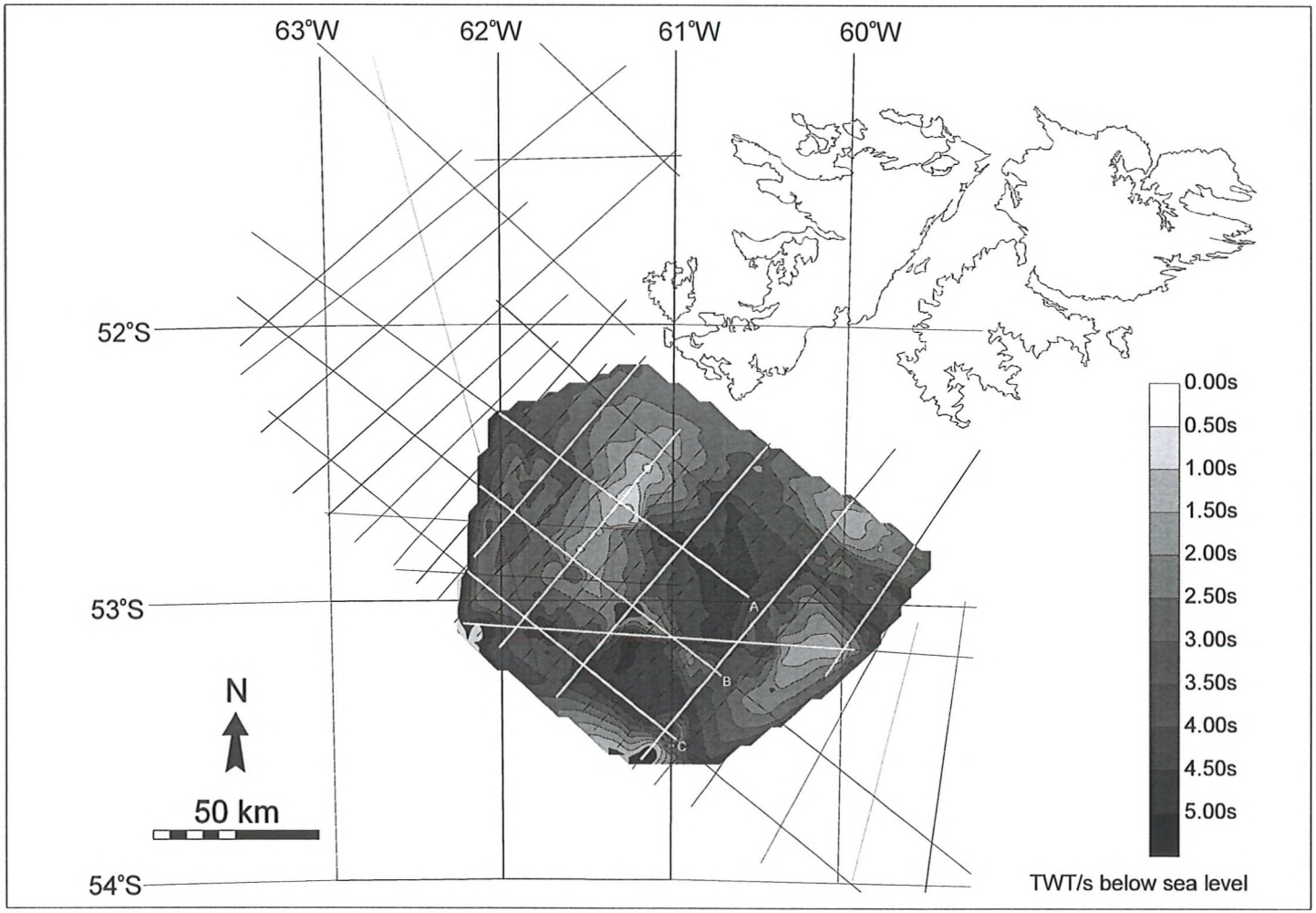

Figure 6.6: Regional contour map of the 5000ms^{-1} interval velocity contour in TWT/s below sea level. Data taken from interval velocity contours plotted by the author for each of the lines shown in white.

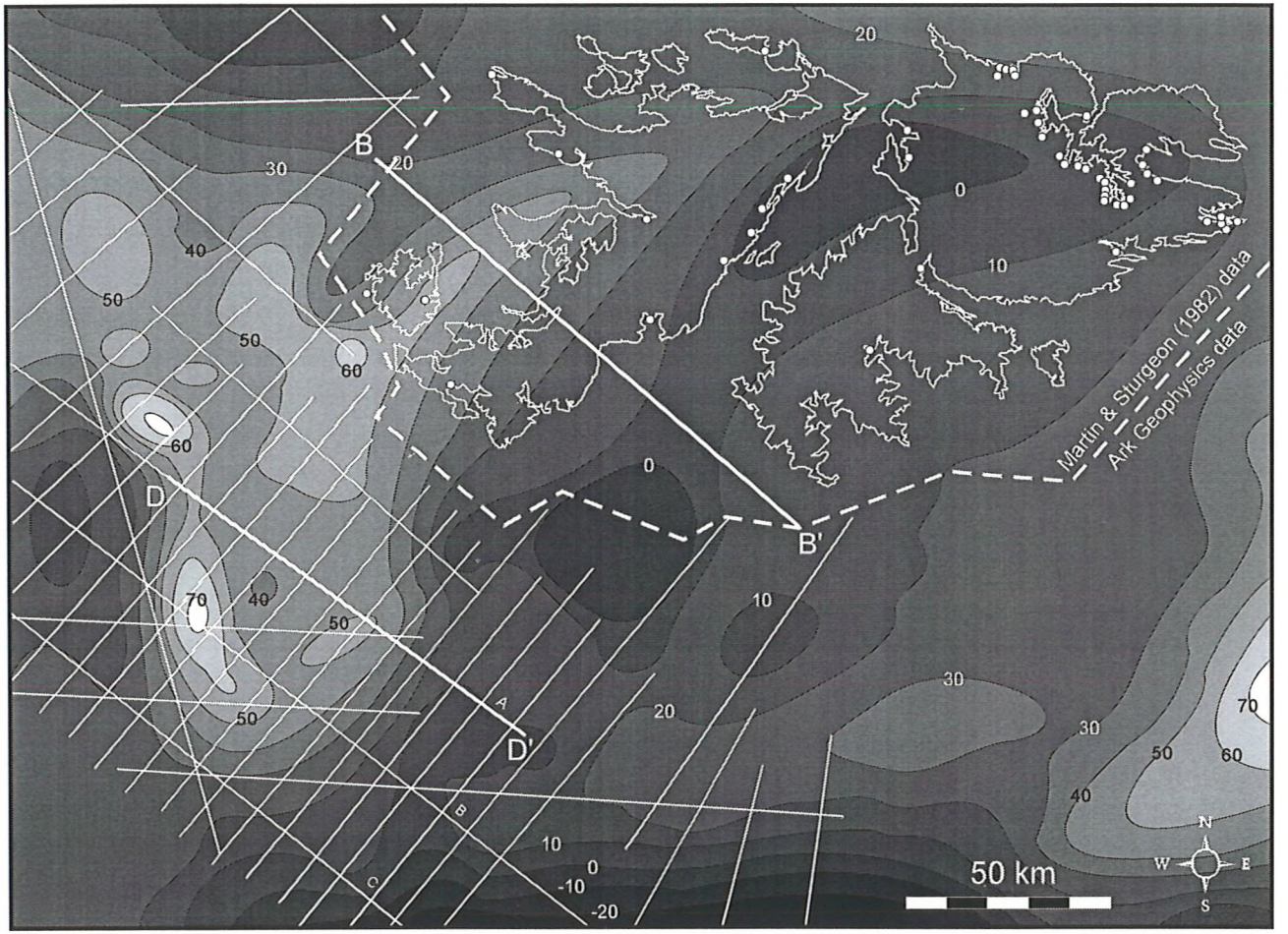

Figure 6.7: Bouger Gravity Anomaly map based on data from ARK Geophysics (1995) ship board offshore data and Martin & Sturgeon (1982) onshore data, (onshore gravity stations marked as white circles). Lines B-B' and D-D' refer to sections in Figure 6.8. Contours in 10 mGal intervals.

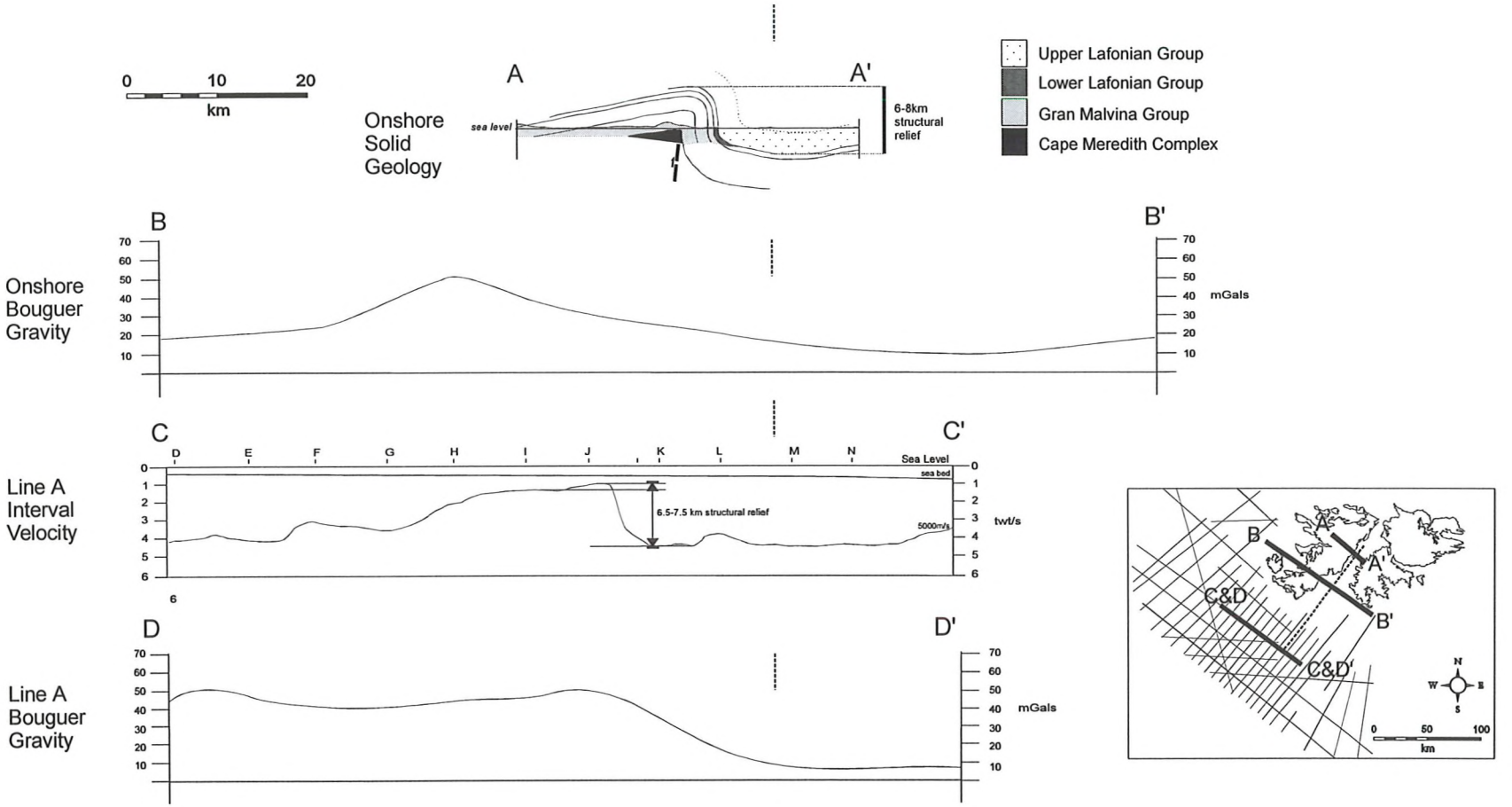

Figure 6.8: Correlation of the onshore and offshore geology along line A, both of which show an increase to the NW in structural relief of 6 - 8 km,(A-A' & C-C') and positive Bouguer gravity anomaly of 38 - 42 mGals (B-B' & D-D'). Onshore Bouguer gravity data has a poor resolution owing to scarcity of gravity points and therefore inadequate data coverage. Dashed line on map and above each section is an arbitary line used for correlation between the cross-sections. All sections (see map for locations) are to the same horizontal scale, section A-A' horizontal = vertical scale.

(a)

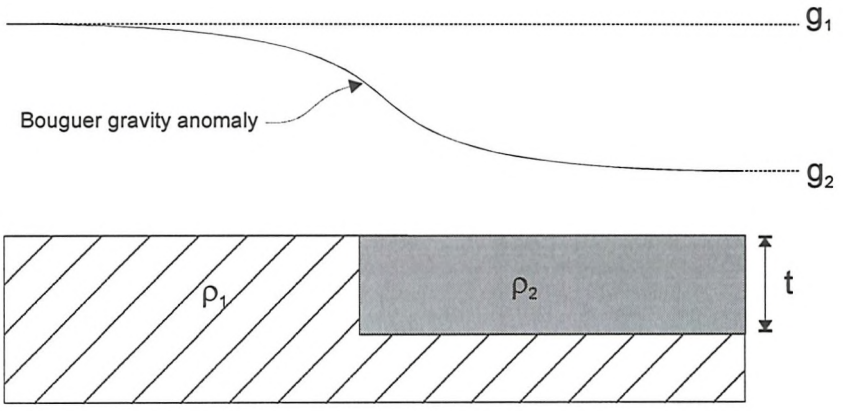

(b)

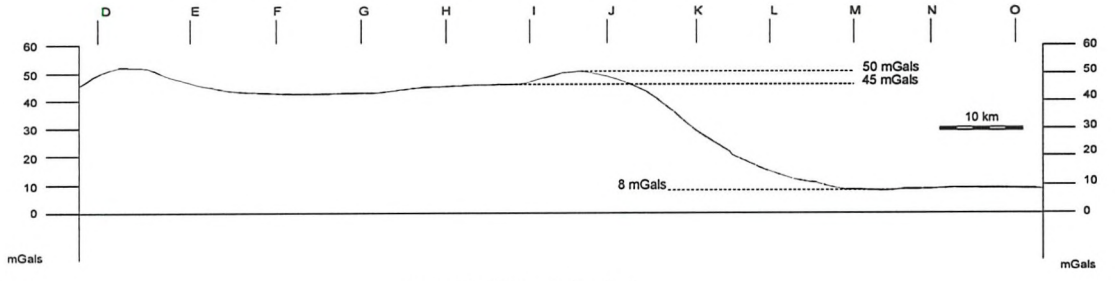

(c)

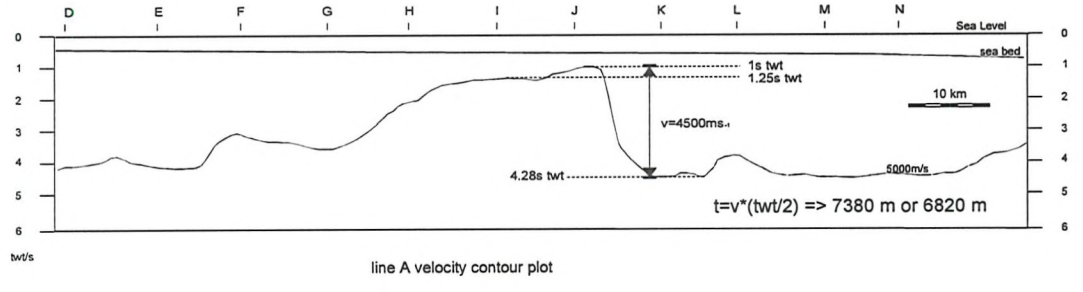

Figure 6.9:(a) Theoretical model for the slab formula where a slab causing a density contrast ρ_1-ρ_2 gives a gravity contrast of g_1-g_2. (b) The gravity anomaly across line A. (c) the thickness (t) for the slab in line A.

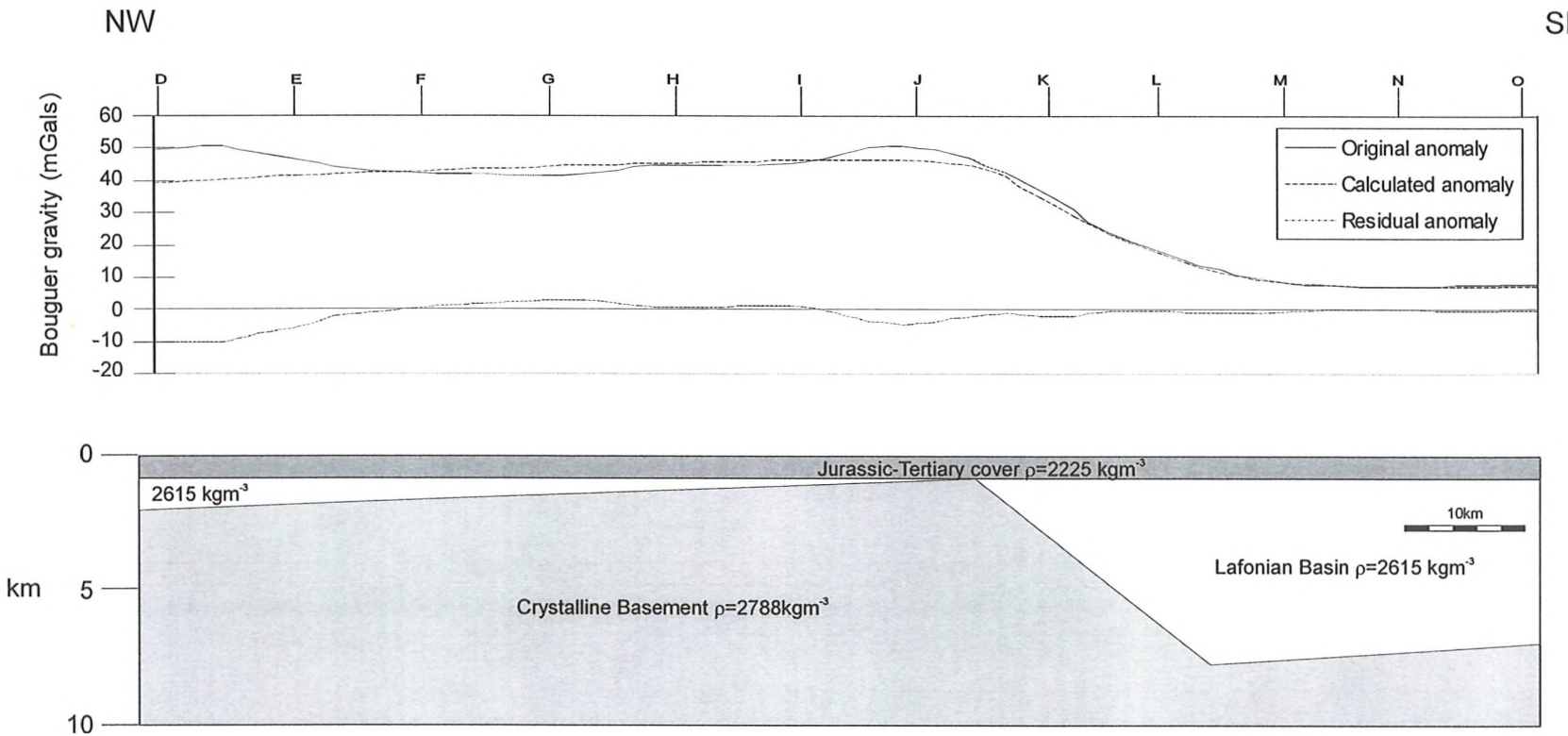

Figure 6.10: 2DGM Model 1for Line A; (a) Observed, theoretical and remnant Bouguer gravity anomaly obtained using the model shown in (b); (b) Model of a basement block of similar proportions to that imaged from the interval velocity data overlain by younger flat-lying Jurassic to Tertiary sediments. Densities based originally on those in Table 6.1, however, these have been varied in order to model the gravity curve accurately.

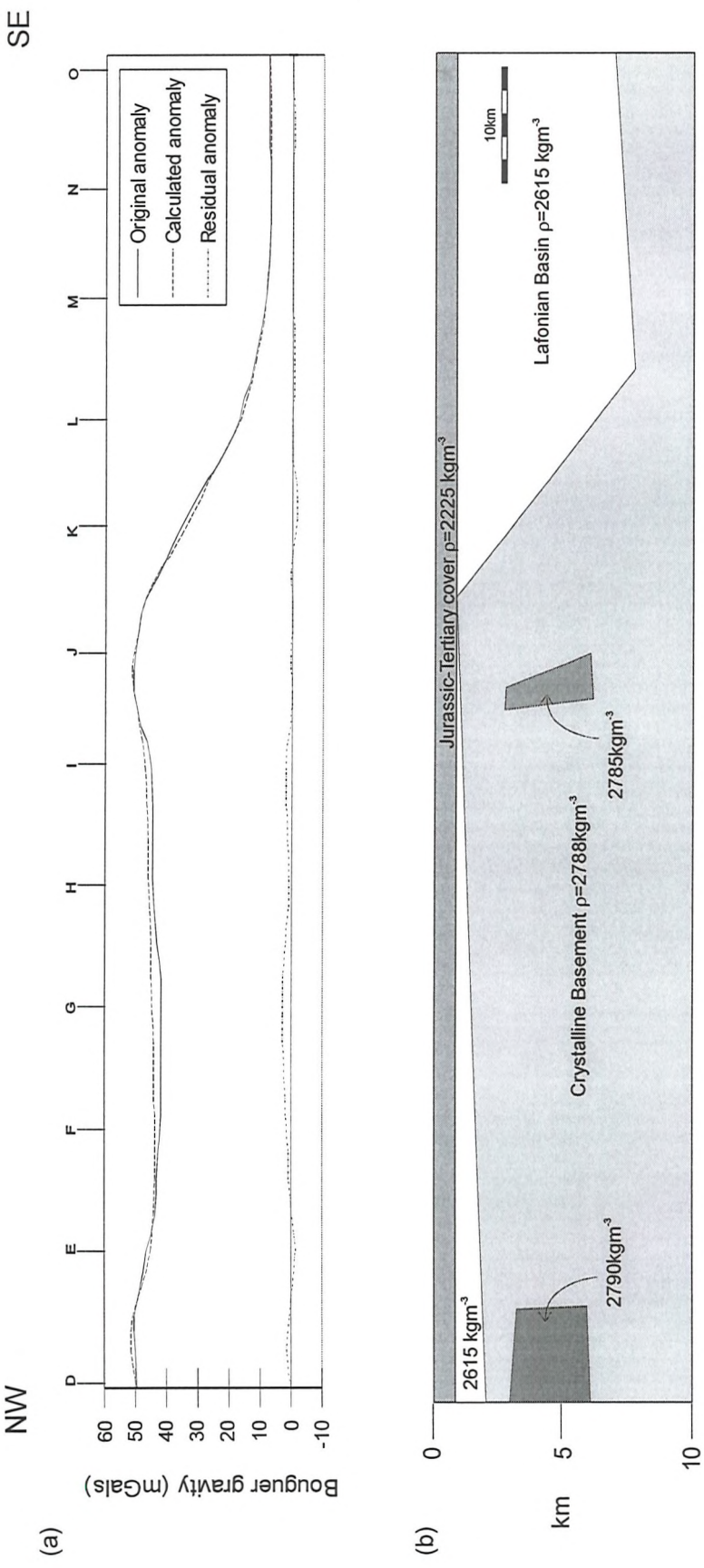

Figure 6.11: 2DGM Model 2 for Line A; (a) Observed, theoretical and remnant Bouguer gravity anomaly obtained using the model shown in (b); (b) Model 2, identical to Model 1 with the addition of two other bodies.

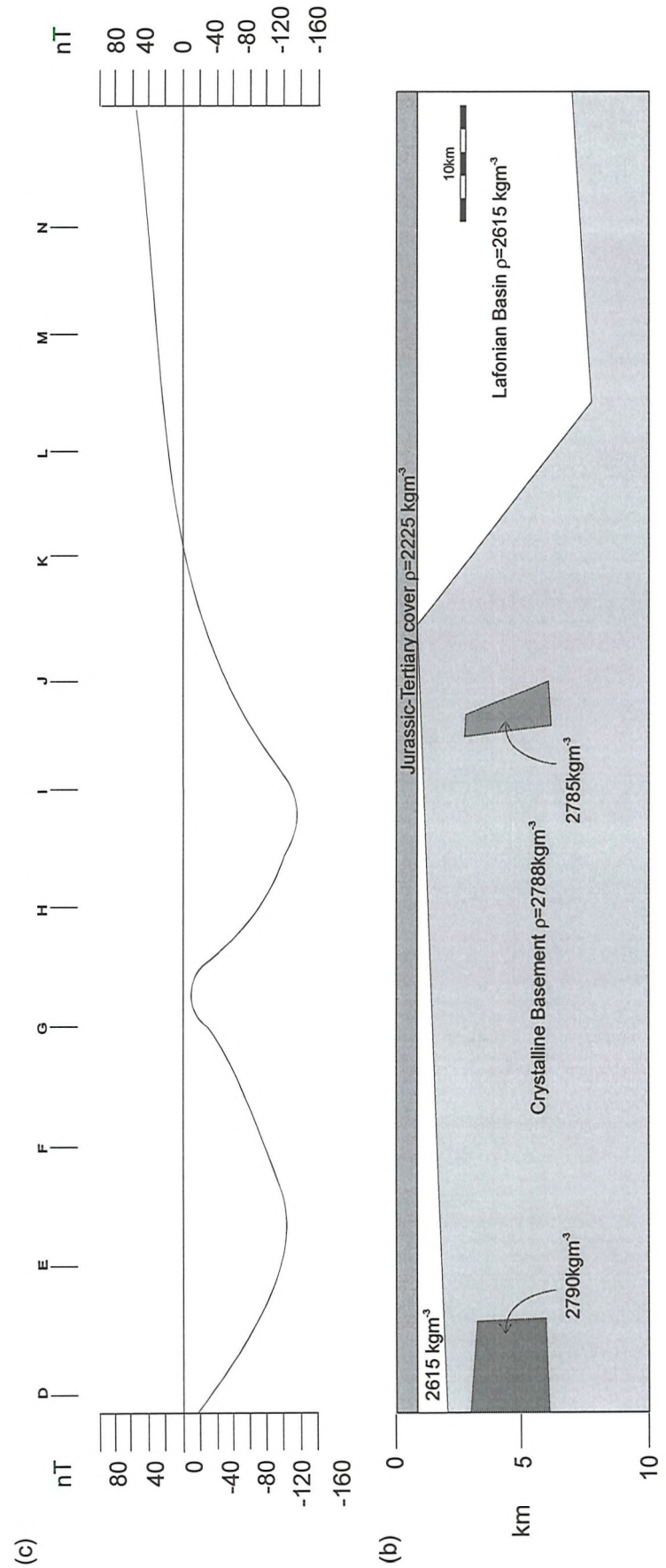

Figure 6.12: (a) Magnetic anomaly across line A, showing two marked magnetic low points; (b) 2DGM Model 2 showing rough correlation of inferred bodies and magnetic low points.

Chapter 7: Vitrinite Reflectance studies on the Falkland Islands

Chapter 7: Vitrinite Reflectivity studies on the Falkland Islands.

7.1 Introduction

Vitrinite reflectance (*Rv*) is a quantitative measure of the thermal maturity of sedimentary organic matter (e.g. Allen & Allen 1990, p 289). It is influenced by the effects of maximum temperature and duration of heating (Barker & Pawlewicz 1986), as well as locally, by the effects of deformation (e.g. Bustin 1983). The net effect of duration of heating on *Rv* is considered negligible compared to the effect of maximum temperature (Barker & Pawlewicz 1986, Barker & Goldstein 1990). However, high pressures can cause lower *Rv* values (Bustin 1983). Vitrinite reflectance data is therefore an invaluable tool as it allows, primarily, an assessment of maximum burial temperature, and, given a geothermal gradient, maximum depth of burial and secondly, can give an indication of intensity in localised deformation.

As yet, no in-depth, systematic study of *Rv* on the Falkland Islands has been undertaken. However, two studies, one by Marshall (1994b) the second by Marshall in a report by CASP (D.I.M. Macdonald *pers. comm.* 1996), have been carried out, both as additional parts of more thorough stratigraphical studies in the Fox Bay Formation and Lafonian Supergroup.

Although not a systematic study of *Rv* on the Falkland Islands, the data in this study is from a large area of the islands that had not been covered by the existing data set. The new data have been collected from the Fox Bay, Port Stanley, Bluff Cove and Port Sussex formations from both East and West Falkland during regional mapping across the islands. This spread of data across both islands allows the first substantial comparisons of *Rv* values, and therefore depth of burial, to be made for equivalent horizons between East and West Falkland.

7.2 Methodology

During mapping on the Falkland Islands shale samples were collected where available. Sedimentary organic matter was concentrated using demineralising techniques (HCl / HF) in accordance with standard palynological extraction

techniques, except for avoiding heating or oxidation treatments that could affect *Rv*. The concentrates were then mounted on polished thin sections using the method outlined by Hillier & Marshall (1988). Mean random vitrinite reflectance in oil (*Rv*) was measured at 546 nm using a Zeiss UMSP-50 (Universal Micro-Spectrophotometer) microscope fitted with a X40 oil immersion objective and using a 2.5 μm measuring spot. For the majority of samples *Rv* was calculated from 50+ individual reflectance measurements, although the leanest sample only gave 14 reflectance measurements. Once the measurements were obtained from each sample the data were edited and then a mean and standard deviation were calculated using a programme 'SLAP' (written by S.J. Hillier whilst at the Geology Department, University of Southampton).

7.3 Results

The *Rv* data from the samples collected are shown in Table 7.1 and summarised, along with other known data points from Marshall (1994b) and Macdonald (*pers. comm.* 1996), in Figure 7.1. It is significant that all data presented on Figure 7.1 were measured at Southampton University on the same UMSP-50 microscope by either J.E.A. Marshall or the author, under the supervision of J.E.A. Marshall. This gives an unique level of consistency between the three datasets.

7.3.1 West Falkland

Data points on West Falkland are, on the whole, restricted to the eastern coastline and the far west. Marshall (1994b) demonstrated an anomalous trend at the Port North section where *Rv* increases northwards from 1.0 %*Rv* in the Fox Bay Formation to 1.4 %*Rv* in the younger Port Stanley Formation. This trend has been extended by this study which shows 1.8 %*Rv* for the Permian Black Rock Member at West Lagoons. This is contrary to what would be expected simply for burial where *Rv* should decrease into younger strata. A value of 1.5 %*Rv* is recorded from the Fox Bay Formation at Rat Castle. Along the eastern coast of West Falkland in the steep limb of the Hornby Anticline, from Port Howard to Carcass Bay, the Fox Bay Formation

and Lower Lafonian Group show relatively constant values of 1.8 - 2.2 %*Rv*. This consistency across the stratigraphy indicates a non-stratigraphic, possibly structural, control in this area. Looking solely at the Fox Bay Formation, there is a general increase eastwards across West Falkland from Port North (1.0 %*Rv*) to Rat Castle (1.5%*Rv*), Carcass Bay (1.8 %*Rv*) and Port Howard (2.1 %*Rv*). The anomalously low value at South Harbour is from a diamictite dyke and is discussed more thoroughly in Chapter 3 (Hyam *et al.* 1997).

7.3.2 East Falkland

A large part of the data for East Falkland is unpublished and has been made available by Dr. D.I.M. Macdonald at CASP, further data is from Marshall (1994b).

East Falkland shows very high *Rv* values in the range of 2.8 - 5.3 %*Rv*. The lowest of these values are from the Fox Bay Formation in the north of the island. These show a slight change from 3.3 %*Rv* at Greenpatch in the east to 2.8 %*Rv* at San Carlos in the west. In the overlying stratigraphy, there is a general decrease southwards from a high of 5.3 %*Rv* in the Port Stanley Formation, from the Port Stanley region. A single result of 3.4 %*Rv* was obtained in the Bluff Cove Formation at Bluff Cove. The next horizon to have been sampled is the Black Rock Member from which a relatively large amount of data has been obtained. These data show *Rv* at a constant level of 3.7 - 4.1 %*Rv* across East Falkland from Port Fitzroy to Port Sussex. A low value of 3.0 %*Rv* at Port Sussex is probably reduced owing to the presence of bitumens (J.E.A. Marshall *pers. comm.* 1997). These values are markedly higher than for the older Fox Bay Formation to the north. Measurements across Lafonia, in the south of East Falkland, are relatively constant varying from 2.6 - 4.5 %*Rv* both vertically, through the stratigraphy, and laterally, as far south as Sea Lion and Speedwell Islands (Fig. 7.2). These *Rv* values indicate burial temperatures of 270 - 350°C (Barker & Goldstein 1990) which are in the anchi- to epi-metamorphism zone (Hälbich 1983). These values are also consistently lower than those obtained from the Black Rock Member to the north. The relatively high values obtained the Goose Green Isthmus (4.1 - 4.5 %*Rv*) are not highly anomalous if the 1σ standard deviation bar is considered (Fig. 7.2). However, the value of 4.1 %*Rv* from Lively Island was

taken close to a known dolerite dyke (c.f. Greenway 1972) and so has not been included on Figure 7.2.

7.3.3 Comparison of East and West Falkland

It is clear from the data that there is a marked difference in the *Rv* values from East and West Falkland. West Falkland shows values that are consistently lower for each horizon where direct comparison can be made (Table 7.2).

7.4 Illite Crystallinity

Further to the vitrinite reflectance data presented above, limited illite crystallinity data is available for the Falkland Islands (D.I.M. Macdonald *pers. comm.* 1996) (Fig. 7.3).

Illite crystallinity (IC) is a quantitative method, independent of *Rv*, which uses the the amount of the clay mineral illite to measure burial temperatures and therefore depth of burial. Illite grows in conditions of low-level metamorphism in response to a number of factors including time, porosity and chemistry, but, most importantly, increasing temperature (Frey 1987). IC is calculated using X-ray diffraction, in this case using the Kübler index, by measuring the half height width of the 10 Å diffraction peak (e.g. Frey 1987). So, as IC increases, the peak becomes sharper and more defined and the value of half height width decreases, meaning that lower values indicate higher IC and therefore higher temperatures and metamorphic grade.

The IC data across Lafonia is variable, ranging from 2.9 - 1.2 °2θ indicating anchi- to epizonal metamorphism. Using a correlation based on the work of Tricker (1991) (Fig. 7.4) the IC data shows a similar level of thermal maturity on East Falkland to that indicated from the *Rv* data.

7.5 Discussion / Interpretation

In order to develop a model for the thermal or metamorphic history of the Falkland Islands it is necessary to consider analogues. On East Falkland, the Lafonian Basin in the south is a foreland basin to the fold-belt in the north. Of the many foreland basins

which have been studied in the world there is little work on their thermal history. Those studies that exist on foreland basins in Europe indicate a low geothermal gradient (Robert 1988) with *Rv* values as low as 0.6 %*Rv* at depths of 6 km (Robert 1988, p206). These basins also show significant thrusting from the mountain belt onto the foreland, so are not a good analogue for the Falkland Islands. The closest analogue to the Falkland Islands is the South African Karoo Basin which is a foreland basin to the Cape Fold Belt in the south. The use of this basin as an analogue is justified considering that Lafonia was once part of it (e.g. Adie 1952b).

7.5.1 Comparison to the South African Karoo foreland basin

The Karoo Basin is a vast foreland basin lying to the north of the Permo-Triassic Cape Fold Belt. The Karoo basin consists of approximately 12 km of sedimentary rocks showing facies changes typical of foreland basins (e.g. Allen & Allen 1990, p246 - 250) from basinal to flysch (Ecca Group), deltaic, flood plain (Beaufort Group, Molteno Formation) and aeolian (Clarens Formation), these are capped by thick basalts (Draakensberg Formation), (Fig. 7.5a), (Cole 1992). Johnson (1991) and Cole (1992) have shown that by the time the late Ecca or early Beaufort Groups were being deposited the fold belt to the south had been uplifted enough to become a source for the Karoo foreland basin.

The thermal history of the basin is still poorly known, however, from the work carried out in the basin using illite crystallinity and vitrinite reflectance (Rowsell & de Swardt 1976, Hälbich & Cornell 1983, Department of Minerals & Energy Affairs 1992) certain regional trends can be seen (Fig. 7.5). There is an overall decrease northwards in the level of metamorphism from lower epi-metamorphism in the Cape Fold Belt to diagenetic/unmetamorphosed in the northern Karoo. This is seen from *Rv* data from the Ecca Group which decrease northwards from 3.8 %*Rv* to 1.7 %*Rv* (Fig. 7.5) and from illite crystallinity data from the Bokkeveld Group of the Cape Supergroup which decreases northwards in spite of increasing depth of burial (Rowsell & de Swardt 1976). There is also an overall decrease in illite crystallinity away from the fold-belt and up the stratigraphy from the Bokkeveld to the Beaufort Group (Fig. 7.5a). The *Rv* values for the Ecca and Beaufort in the area in front of the

fold-belt are relatively constant around 3.5 %*Rv* both vertically and laterally. Hälbich & Cornell (1983) have shown from borehole illite crystallinity data that the temperature gradient in the central area of the southern Karoo basin was no more than 30 - 35°C km^{-1} which is a relatively normal geothermal gradient (Allen & Allen 1990, p300).

7.5.2 East Falkland

When the model from South Africa is compared to a rotated East Falkland the following similarities come to light: (1) an overall decrease in metamorphism away from the fold belt seen as decreasing vitrinite reflectance (Port Stanley Formation to Upper Lafonian Group) and illite crystallinity trends; and (2) relatively consistent *Rv* values vertically and laterally across the Upper Lafonian Group within 100 km of the fold-belt. However, despite these close similarities between thermal maturity indicators, the top of the preserved stratigraphy on the Falkland Islands is Late Permian, which is truncated relative to the Triassic age for the top Karoo Supergroup in South Africa (Cole 1992). This would imply that to have achieved the same thermal history as South Africa a significant thickness has been eroded from East Falkland. An estimate of how much can be made using the geothermal gradient of 30 - 35°C km^{-1} for the Karoo basin calculated by Hälbich & Cornell (1983). Given this gradient and the burial temperatures inferred from the *Rv* values on East Falkland, a burial depth of ~8 - 9 km can be estimated for most of Lafonia. This excess overburden can only be accounted for, if equivalents of the Beaufort Group and Stormberg Series of the Karoo Basin (a total of ~8 km in the Karoo Basin, (Cloetingh *et al.* 1992)) were also deposited on East Falkland, being eroded and removed since the Triassic.

The comparison to South Africa also gives an explanation for the *Rv* values in the Fox Bay Formation on East Falkland which are lower than for the overlying Lafonian Supergroup. In the Karoo Supergroup it is known that the provenance was from the south (Johnson 1991, Cole 1992) and that as Cape Fold Belt formed so the Cape Supergroup began to be uplifted, eroded and become a source for the Beaufort Group (Johnson 1991) or possibly even the Ecca Group (Cole 1992). This would

infer that not all the Karoo Supergroup was deposited across the Cape Fold Belt. This model is exactly what is seen in the Falkland Islands. On East Falkland *Rv* values in the Fox Bay Formation indicate burial temperatures of ~300°C which equates to only around 8 km overburden given the estimated geothermal gradient of 30 - 35°C km^{-1}. Considering that the stratigraphy preserved on the Falkland Islands above the Fox Bay Formation is ~4 - 4.5 km, the total thickness of the Lafonian Supergroup, inferred in the previous section from the *Rv* values in Lafonia, was not deposited across northern East Falkland. This reduced stratigraphy would indicate that, although the strata preserved in the Lafonian Basin would have initially been deposited across northern East Falkland, as the fold-belt began to form, so northern East Falkland was uplifted, becoming an area of erosion and a source area for the developing Lafonian Basin. This is supported by palaeocurrent data from the Upper Lafonian Group which is predominantly south-westerly (Curtis & Hyam 1998) shedding off the fold-belt. The *Rv* data therefore imply that the ~8 km equivalents of the Beaufort Group and Stormberg Series were not deposited on northern East Falkland, however, as implied earlier, they were deposited on Lafonia and have since been eroded.

There is a close comparison between the estimates of strain (Chapter 4.6) and *Rv* values across East Falkland. There is a slight, but overall, decrease westwards across East Falkland in the *Rv* of the Fox Bay Formation which is the same as the decrease in strain seen from Port Stanley to San Carlos in the bed-length and vein data. Also there is a decrease in *Rv* between Port Stanley and Greenpatch which is also seen in the bed-length strain data.

7.5.3 West Falkland

Given the model from South Africa of decreasing metamorphism away from the fold-belt, it is possible to interpret the data from Port North and West Lagoons. These data show an anomalous trend of *Rv* values increasing northwards into younger strata contrary to what would be expected simply from the effects of burial where *Rv* should decrease into younger strata. Marshall (1994b) interpreted this trend to be showing the effect of the fold-belt in the north of West Falkland. If these *Rv* values have been

overprinted by the fold-belt it indicates that West Falkland has undergone very shallow burial compared to East Falkland.

In the east of West Falkland, *Rv* values are consistently ~2.0 % across the stratigraphy from the Fox Bay Formation to the Lower Lafonian Group. These values are clearly related to the effects of the NE-SW Hornby Monocline and its underlying structure. Two models can be presented for these data: (1) increased strain in the steeper limb of the fold; and (2) the underlying fault has acted as a conduit to possible fluid flow, allowing overprinting of the regional *Rv* values with those related to the structure. In the first model, higher *Rv* values would be expected on the steeper limb, however, there is no change in *Rv* data between the limbs of the fold (phd-40 and phd-60, Table 7.1) indicating that increased strain on the steeper limb is not the cause. This would infer that the consistently higher *Rv* data is related to the second model, of an elevated heat flow relative to the regional geothermal gradient, associated to fluid low in the fault beneath the Hornby Monocline.

The value recorded at South Harbour is explained in more detail in Chapter 3. However, in summary the value is from rocks of Early Carboniferous age (pre-Lafonian Supergroup) and only shows a burial temperature of ~100°C (Barker & Goldstein 1990). This would infer that only a fraction of the 3.5 km of the Lafonian Supergroup preserved, and further 8 km inferred, for the Lafonian Basin was ever deposited on West Falkland.

7.5.4 Comparison of East and West Falkland

Where direct comparisons can be made, such as in the Fox Bay and Port Sussex formations, it can be seen that there is an increase in the *Rv* values from West to East Falkland (see Fig 7.1, Table 7.2) which indicate a difference of ~100°C burial temperature between the two islands. If this temperature is taken to have resulted primarily from burial rather than from deformation, then this would imply that West Falkland has been uplifted relative to East Falkland and that the Lafonian Supergroup, exposed only as thin sequences on West Falkland, was not deposited in its entirety on this island (Chapter 3, Hyam *et al.* 1997). This is consistent with changes in sedimentary facies in both the Lafonian Diamictite and Port Sussex Formations

(Chapter 2.2.3.i). The reason for this westward thinning of the Lafonian Supergroup across the Falkland Islands is the presence of a basement fault under the eastern margin of West Falkland (Chapter 5.4) which has caused the island to be uplifted relative to East Falkland since Early Carboniferous times (Chapter 3, Hyam *et al.* 1997). Hyam *et al.* (1997) estimate that only 2 - 3 km have been deposited over SW West Falkland since the Carboniferous, a much thinner succession to that preserved or postulated for East Falkland. However much of a thinned Lafonian Supergroup was deposited on West Falkland, it has now been eroded and removed.

7.6 Conclusions

New vitrinite reflectance data from the Falkland Islands shows that there has been a markedly different burial history between East and West Falkland. The low values on West Falkland indicate that it has been a relatively uplifted block and was never covered by the full sequence of the Lafonian Supergroup. On East Falkland the variation in *Rv* values implies that (1) the Lafonian Supergroup was a lot thicker (by up to 8 - 9 km) and that this thickness has since been eroded; and (2) that northern East Falkland may have become a source for the Lafonian Basin in the Late Permian so that it was never covered by much more of the Lafonian Supergroup than is presently exposed in Lafonia.

Sample	*Location*	*Formation*	Rv	1σ	*n*
scp-1	Shag Cove	Shepherds Brook Member	1.8	0.4	56
cb-19-1	Carcass Bay	Shepherds Brook Member	2.1	0.3	56
cb-19-2	Carcass Bay	Shepherds Brook Member	2.4	0.23	73
hc-e	West Lagoons	Black Rock Member	1.8	0.18	54
hc-a	West Lagoons	Black Rock Member	1.9	0.3	54
hc-b	West Lagoons	Black Rock Member	1.8	0.27	55
2hc-1-2	West Lagoons	Black Rock Member	1.9	0.16	54
2hc-1-3	West Lagoons	Black Rock Member	1.9	0.19	64
2hc-1-6	West Lagoons	Black Rock Member	1.7	0.25	58
cb-20-1	Carcass Bay	Black Rock Member	2.3	0.27	53
cb-20-2	Carcass Bay	Black Rock Member	2.2	0.34	59
cb-20-3	Carcass Bay	Black Rock Member	2.2	0.18	54
cb-20-4	Carcass Bay	Black Rock Member	1.9	0.19	49
cb-20-5	Carcass Bay	Black Rock Member	1.9	0.2	52
pfz-1	Port Fitzroy	Black Rock Member	3.8	0.41	53
pst-65	Bluff Cove	Bluff Cove Formation	3.4	0.59	55
pst-11	Port Stanley	Port Stanley Formation	5.3	0.9	25
pst-45	Port Stanley	Port Stanley Formation	4.1	0.85	55
phd-40	Port Howard	Fox Bay Formation	2.3	0.31	55
phd-60	Port Howard	Fox Bay Formation	1.9	0.34	59
rat-1	Rat Castle	Fox Bay Formation	1.5	0.31	59
cb-2a	Carcass Bay	Fox Bay Formation	2.3	0.41	30
cb-12a	Carcass Bay	Fox Bay Formation	1.8	0.26	46
cb-12b	Carcass Bay	Fox Bay Formation	1.8	0.35	14
cb-14	Carcass Bay	Fox Bay Formation	2.2	0.31	55
scr-13	San Carlos	Fox Bay Formation	3.0	0.33	49
scr-14	San Carlos	Fox Bay Formation	2.6	0.34	51
gp-8	Greenpatch	Fox Bay Formation	3.0	0.65	51
gp-9	Greenpatch	Fox Bay Formation	3.7	0.96	50
gp-19	Greenpatch	Fox Bay Formation	3.0	0.62	49
gp-30	Greenpatch	Fox Bay Formation	3.7	0.63	55
gp-37	Greenpatch	Fox Bay Formation	2.4	0.59	54
gp-38	Greenpatch	Fox Bay Formation	4.6	0.64	55
gp-43	Greenpatch	Fox Bay Formation	3.0	0.77	51
gp-45	Greenpatch	Fox Bay Formation	2.3	0.36	51
gp-52	Greenpatch	Fox Bay Formation	3.8	0.8	51
gp-53	Greenpatch	Fox Bay Formation	3.8	0.89	47

Table 7.1: Vitrinite Reflectance (*Rv*) values obtained from shale samples collected across the Falkland Islands during regional mapping (see Fig. 7.1 for locations).

Formation	Rv *West Falkland*	*Max. burial Temperatures*	Rv *East Falkland*	*Max. burial Temperatures*
Shepherds Brook Member / Terra Motas Sandstone	1.8 - 2.2%	200 - ~230°C	2.6 - 3.5%	270 - 320°C
Black Rock Member	1.8 - 2.1%	200 - ~230°C	3.0 - 4.1%	300 - 350°C
Fox Bay Formation	1.0 - 2.2%	150 - 230°C	2.8 - 3.3%	300 - 320°C

Table 7.2: Comparison of *Rv* data and burial temperatures across East and West Falkland.

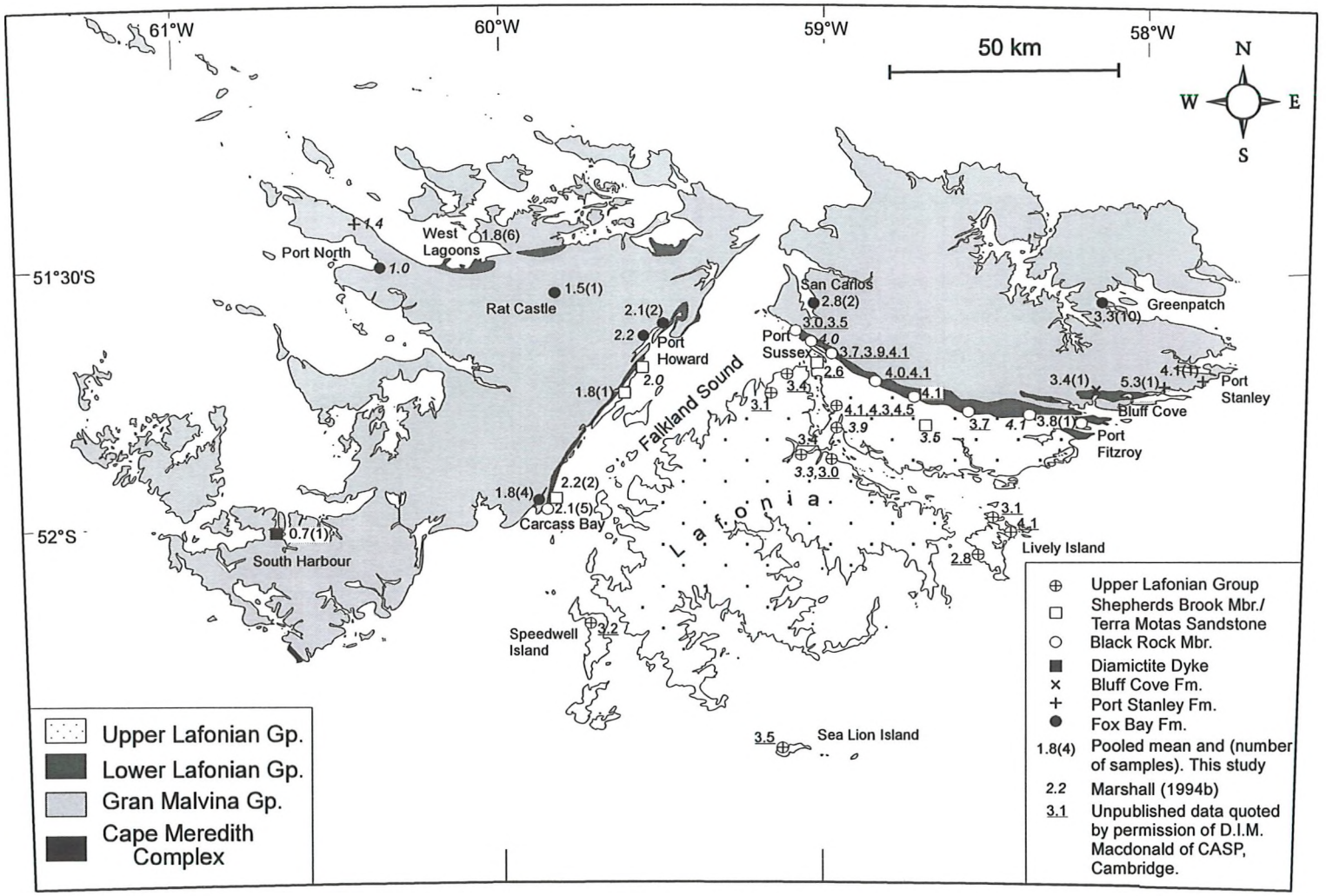

Figure 7.1: Simplified geological map of the Falkland Islands showing all known vitrinite reflectance values (%*Rv*).

(a)

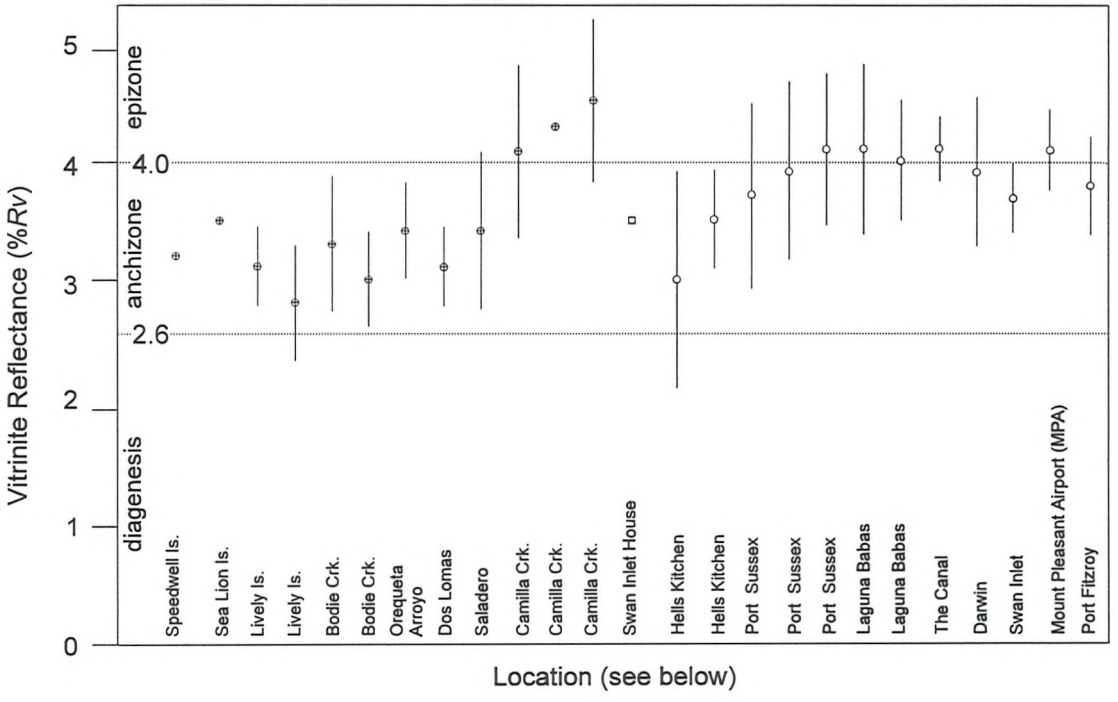

(b)

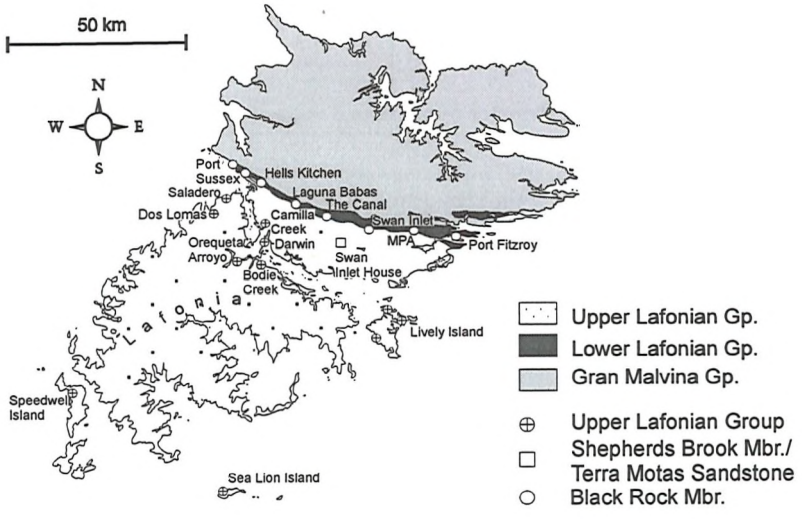

Figure 7.2: (a) Graph showing *Rv* values with standard deviation ($\sigma 1$), where known, across Lafonia. Data courtesy of Marshall (*pers. comm.* 1997) except Port Fitzroy (see Table 7.1). (b) map showing locations of datapoints.

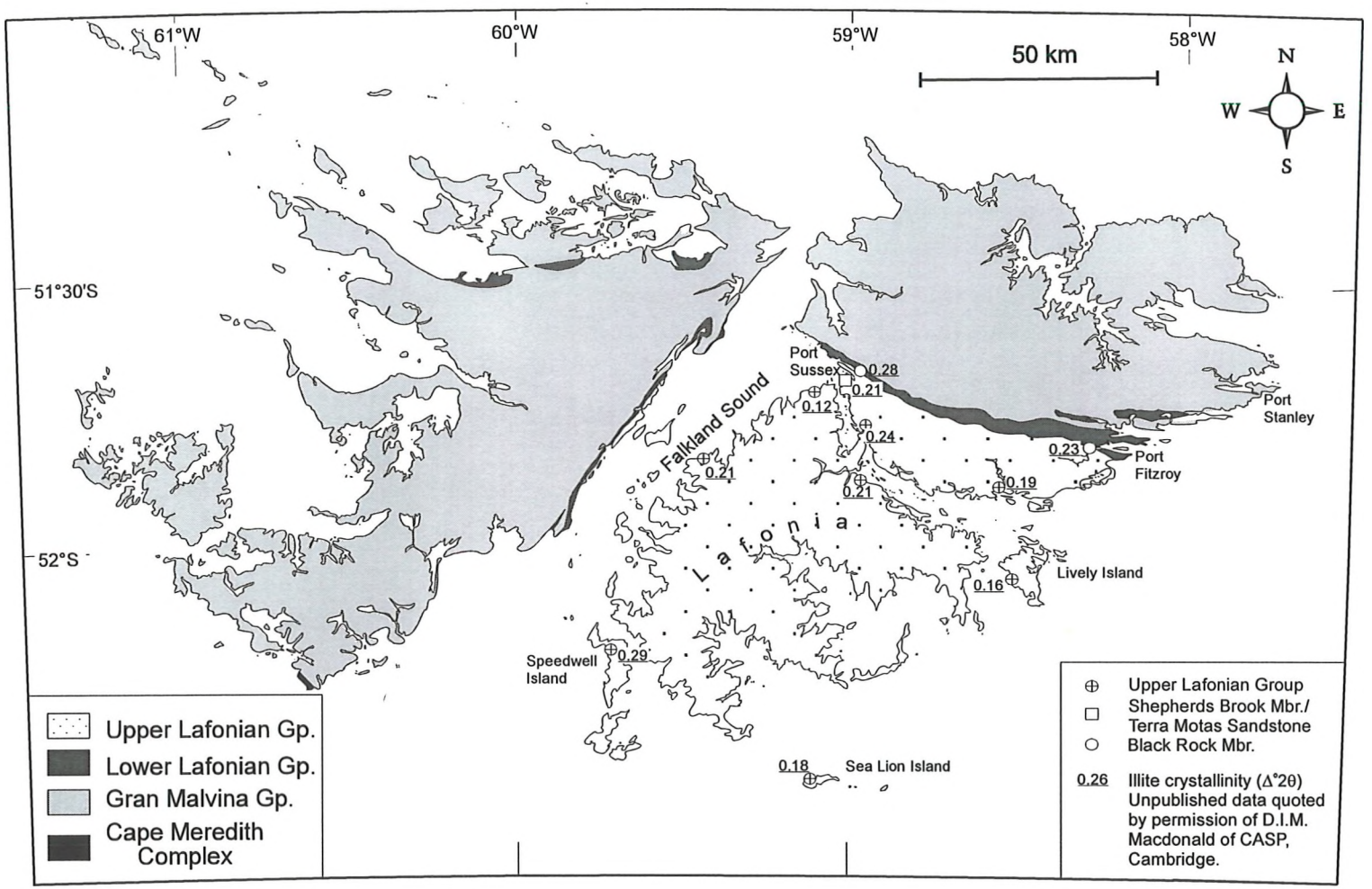

Figure 7.3: Simplified geological map of the Falkland Islands showing known illite crystallinity (Δ°2θ) data

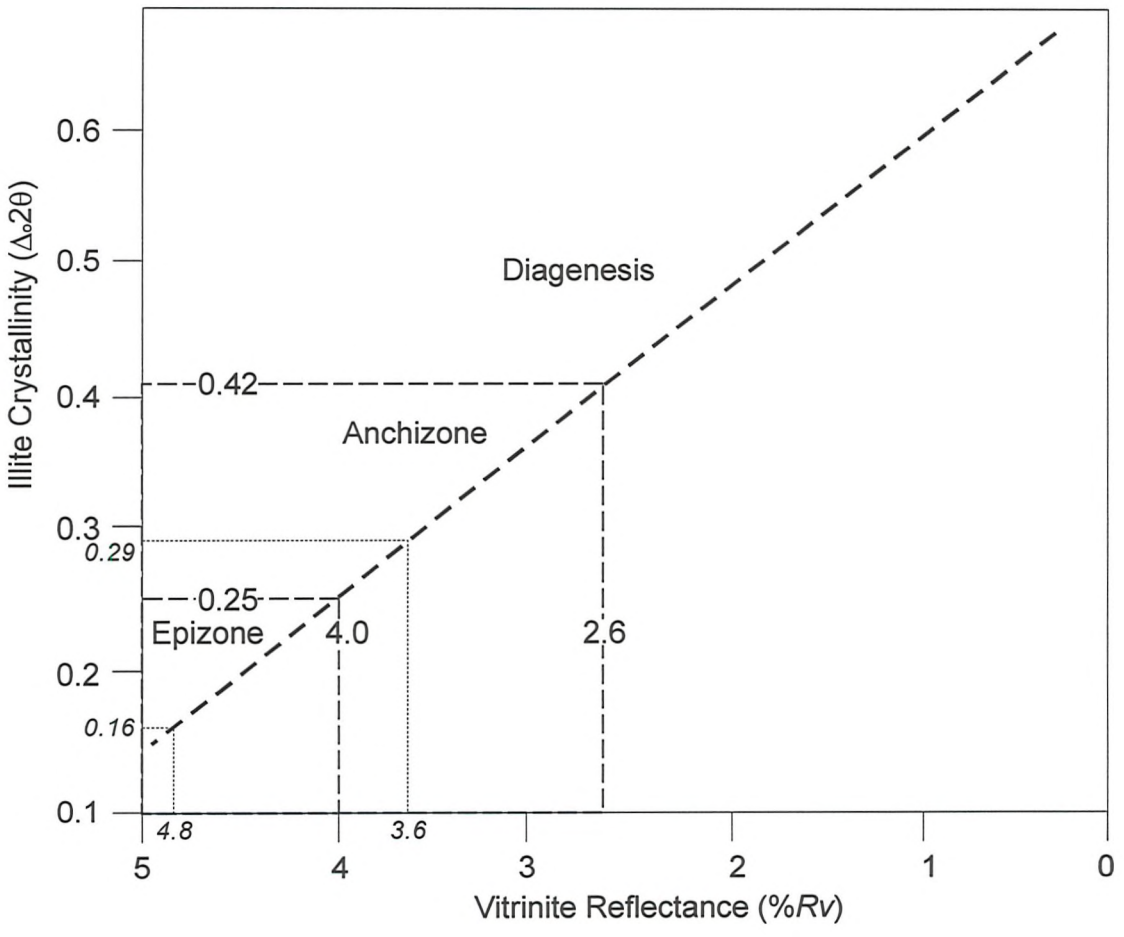

Figure 7.4: Graph showing approximate correlation of illite crystallinity to vitrinite reflectance (after Tricker 1991). Maximum and minimum illite crystallinity data for the Falkland Islands shown in italics with corresponding *Rv* values. Note the close correlation between the two independent data sets (c.f. Figure 7.1, 7.2 for original *Rv* data).

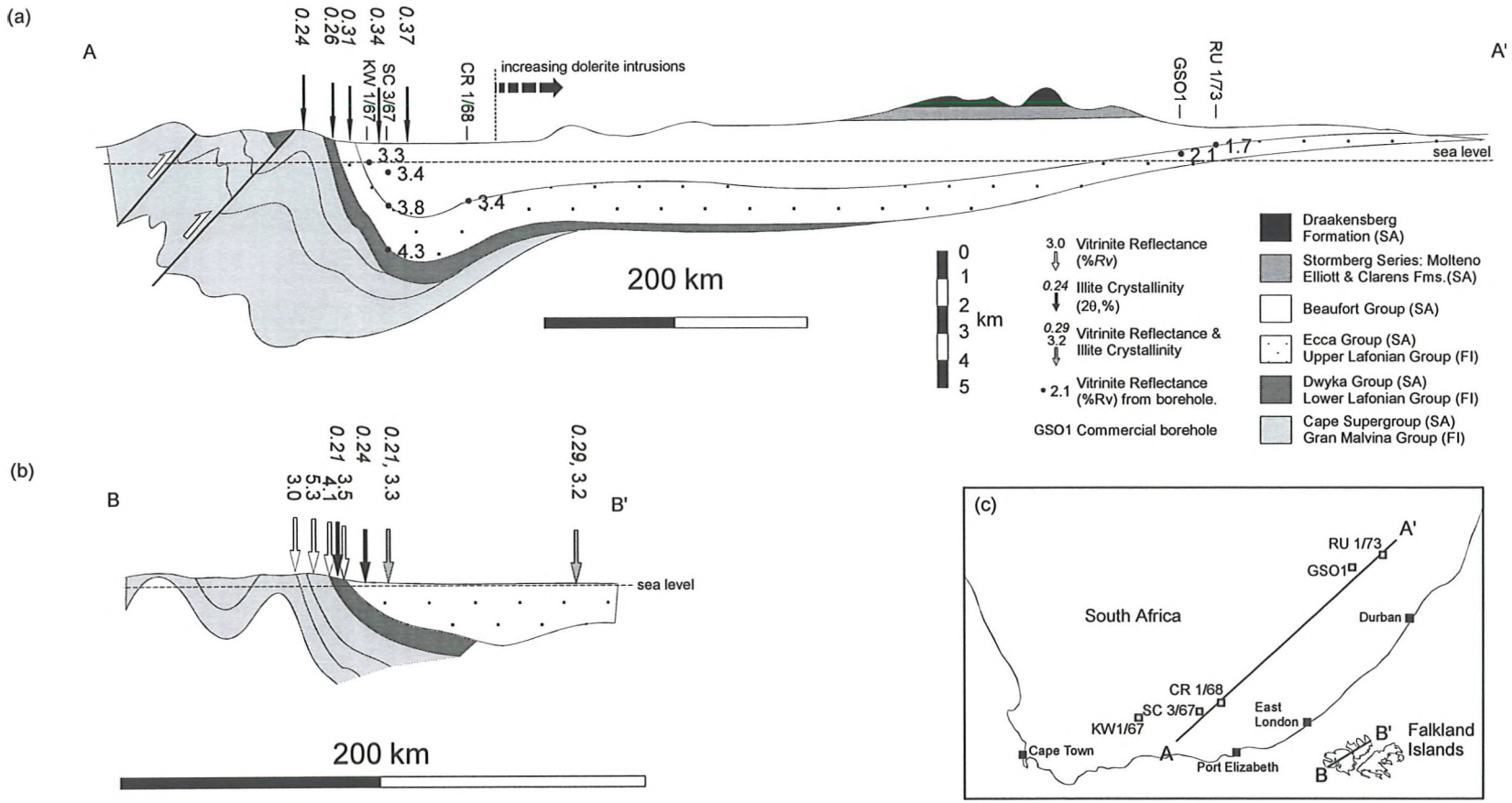

Figure 7.5: NE-SW cross-sections across (a) the Karoo and (b) Lafonian basins showing known vitrinite reflectance (%*Rv*) and illite crystallinity data (Kübler index). Note scale difference between the two sections. South Africa vitrinite data from Rowsell & de Swardt (1976) and illite data from Hälbich & Cornell (1983). Falkland Island vitrinite data from Fig. 7.1, illite data from Fig. 7.3. (c) location map for South Africa and the restored Falkland Islands showing cross-sections and boreholes.

Chapter 8: The evolution of the Falkland Islands: a discussion

Chapter 8: The evolution of the Falkland Islands: a discussion

8.1 Introduction

This discussion will look firstly at the structural evolution of the Falkland Islands drawing on the data presented in the previous six chapters and a paper by the author (Appendix 1, Curtis & Hyam 1998). The context of the Falkland Islands within Gondwana will then be reviewed, looking at the evidence, both structural and stratigraphical, for their fit against the Eastern Cape of South Africa. Finally, there will be a review of the current models regarding the break-up of Gondwana, and how the Falkland Islands rotated by the 180° required by the match of the geology to eastern South Africa.

8.2 The structural evolution of the Falkland Islands

From the data presented in the preceding chapters it is clear that there have been two major structural episodes on the Falkland Islands, D_1 and D_2. The earlier of these (D_1) is the E-W to ESE-WNW fold-belt, seen across northern East and West Falkland (Fig. 8.1), which has long been considered to be part of the Gondwanian fold-belt, now fragmented and scattered across the southern continents (the 'Samfrau Geosyncline' of du Toit (1937)). The later event (D_2) is seen primarily as the NE-SW Hornby Monocline and N-S folds around Symonds Harbour on West Falkland (Fig. 8.1). Recent satellite imagery (mid summer 1997) over both East and West Falkland has also shown there to be NE-SW folds on the western coast of East Falkland and on the Swan Islands (see Fig. 8.1).

8.2.1 D_1 deformation

i) Summary: On eastern East Falkland, southerly fold vergence, top-to-the-south thrusting, northerly dipping cleavage and the southward decline in deformation all indicate a southward vergence for the fold-belt. The gradual change in the strike of the fold-belt westwards across East Falkland, from E-W at Port Stanley to WNW-ESE

at San Carlos, is coupled by a marked decrease and change in orientation of principal strain axes. This trend continues onto West Falkland where gentle WNW-ESE folds are exposed on the western side of the island, the folds becoming tighter in the north on Carcass Island and Pebble Island. The general lack of cleavage on West Falkland infers low strain associated with this folding.

On East Falkland, the southern limit of deformation is approximately the line of Choiseul Sound in the east, being displaced north to Port Sussex in the west across the Goose Green Isthmus (Fig. 8.1). In contrast, on West Falkland the southern limit of the D_1 deformation is farther south than on East Falkland, around King George Bay (Fig. 8.1).

Discounting, for the moment, the effects of the D_2 deformation at Port Howard, the D_1 structures on East Falkland continue onto West Falkland describing an arcuate nature to the fold-belt. As inferred from strain data on East Falkland (Chapter 4.7.3), the overall change in strike from east to west across East Falkland, extended here to include West Falkland, is due to decreasing deformation, associated with the lateral tip of the E-W striking, southerly vergent fold-belt, exposed most fully around Port Stanley.

A late stage of localised, post-cleavage, N-S extension is implied from normal faults and small-scale kink bands (Curtis & Hyam 1998). It has also been shown that although this extensional event post-dates cleavage formation, it occurred prior to the termination of N-S compression and represents a small relaxation period in the overall compressional event (Curtis & Hyam 1998).

ii) Timing: Data from the Lafonian Diamictite Formation and its relationship to the overlying Black Rock Member of the Port Sussex Formation reveal that D_1 deformation started towards the end of glaciogenic sedimentation (Curtis & Hyam 1998) in the Early Permian. The timing of deformation is also seen in the palaeocurrent directions on the Falkland Islands which change from being consistently northerly in the Devonian Gran Malvina Group (Chapter 2.2.2.iii), to easterly in the Permo-Carboniferous Lower Lafonian Group (Dawson 1967) and south-westerly in the Permian Upper Lafonian Group (Curtis & Hyam 1998). This switch in provenance, owing to the onset of deformation and uplift of the fold-belt, is coupled

with the first appearance of volcanism where, at Shag Cove, pyroclastic interbeds have been found in the uppermost Lower Lafonian Group (Scasso & Mendia 1985). These features are comparable to the Karoo basin in South Africa where (1) the Dwyka Group, the South African lithostratigraphic correlative of the Lafonian Diamictite Formation, shows deformation initiating in the final stages of its deposition in Early Permian times (Hälbich *et al.* 1983); (2) a change in provenance occurs associated with the onset of Cape Fold Belt deformation (Johnson 1991); and (3) there is the appearance of volcanism in the lowermost Ecca Group (Cole 1992). It can be inferred from these similarities that the reason for this change in provenance and appearance of volcanism in the Falkland Islands is the same as in South Africa, being related to the development of a magmatic arc along the palaeo-Pacific margin of Gondwana coupled with the onset of Cape Fold Belt deformation (Cole 1992).

It has been inferred (Curtis & Hyam 1998), that the syntectonic nature of the Lafonian Supergroup is also the cause of the difference in observed southerly extent of the D_1 deformation on East and West Falkland. On West Falkland the Lafonian Supergroup has been all but removed revealing the full extent of deformation in the pre- D_1 Gran Malvina Group. In contrast, the full extent of D_1 deformation in the Gran Malvina Group in southern East Falkland is hidden beneath the thicker and significantly less deformed, syn-tectonic Lafonian Supergroup.

8.2.2 D_2 deformation

i) Summary: The NE-SW trend of the D_2 deformation is seen clearly as; the Falkland Sound between East and West Falkland; faulting offshore; and folding on both islands, close to the Falkland Sound.

Offshore, the NE-SW structural trend is seen clearly to the SW, as a steep basement fault with ~ 6.5 - 7.5 km vertical movement (Chapter 6). The same trend is seen through the Jason Islands in the NW (Fig. 8.1), and to the east where a NE-SW extensional basement fault forms the continental margin of the Falkland Islands (Platt & Philip 1995).

On East Falkland, D_2 structures are uncommon, being restricted mainly to the western side of the island. These structures include; a NE-SW structural grain and the

development of open folds along the NW coast of Lafonia (Fig. 8.1); prominent NE-SW joints showing dextral shear sense at Egg Harbour (c.f. Chapter 4.5, Fig. 4.41); and dextral kink bands which change in strike from N-S to NE-SW across East Falkland towards the Falkland Sound (Curtis & Hyam 1998).

On West Falkland the SE-facing Hornby Monocline is the primary D_2 structure striking NE-SW, parallel to the coast of the Falkland Sound. Curtis & Hyam (1998) have also interpreted the gentle, N-S to NE-SW folds at Port Edgar and Symonds Harbour to be related to D_2 deformation. The Hornby Monocline formed primarily as a drape fold over a high angle, oblique (reverse-dextral) basement fault (Chapter 5.4). Evidence from facies changes in the Lower Lafonian Group (Chapter 2.2.3) and vitrinite reflectance values (Chapter 7.4.3) indicate that this structure has been a long standing basement feature since, at least, Early Carboniferous times (Chapter 3, Hyam *et al.* 1997). The Hornby Monocline dies out along strike at Blue Mountain in the SW and Port Howard in the NE, however, the structural trend carries on to the NE as an anticline through White Rock Bay and offshore to the SW (Chapter 6). Anomalous structures are seen at both the northern and southern terminations of the Hornby Monocline. The interference structures at the northern end, around Bold Cove, have formed from the refolding of the earlier E-W structures around the NE-SW, D_2 axis (see discussion in Chapter 5.2.5.i) whereas the structures at Carcass Bay are related to a large parasitic fold-pair cut by coeval thrusting (Chapter 5.3). Dextral strike-slip structures occur at Port Howard, Carcass Bay and Hill Gap along the steep limb of this fold (Curtis & Hyam 1998).

ii) Timing: The interference folds at Bold Cove unequivocally demonstrate that the main phase of D_2 deformation post-dates the D_1 structures. Although the D_1 deformation has been shown to have started in the Permian (Curtis & Hyam 1998), correlation to the South African Cape Fold Belt suggests it may have continued until Early Triassic times (Hälbich *et al.* 1983), providing a maximum age for the D_2 deformation. However, vitrinite reflectance values across the Falkland Islands (Chapter 7) indicate that West Falkland has been a positive structure relative to East Falkland since Early Carboniferous times (Chapter 3, Hyam *et al.* 1997) and that only 2 - 3 km of the Upper Lafonian Group was deposited on West Falkland (as opposed to

the ~ 10 - 11 km postulated to have been deposited on East Falkland, Chapter 7.4.2). This would imply that the fault beneath the eastern margin of West Falkland must have been active at some time during the deposition of the syn-tectonic, Permian age Lafonian Supergroup. This early fault movement may have been extensional, related to basin development or compressional, related to N-S compression. If extensional, the movement was probably not contemporaneous to compressional phases of D_1 deformation as the kinematics of N-S compression and extension across a NE-SW structure are difficult to resolve. If compressional and related to N-S compression then there must have been associated sinistral strike-slip movement. As all the strike-slip structures related to this fault are dextral it would seem that the early movement was extensional and before the main N-S D_1 compressional events.

However, although the fault must have been active during the Permian giving rise to the differences in thickness of the Lafonian Supergroup, the main structure associated with the fault, the D_2 Hornby Monocline, formed after the Permo-Triassic D_1 deformation event, as indicated by the interference fold pattern around Port Howard. A minimum age for the D_2 deformation can be inferred if the interpretation of the Port Edgar/Symonds Harbour folds as coeval with the Hornby Monocline (Curtis & Hyam 1998) is correct. This is because dolerite dykes, known to be c. 190 Ma (Early Jurassic) (Mussett & Taylor 1994), cross-cut these folds without any effect, implying that they post-date the D_2 deformation.

iii) Models for D_2 deformation: It has been shown (Chapter 5.4) that the Hornby Monocline, the main structure of the D_2 deformation on West Falkland, is related to a steep, NW dipping, oblique (reverse-dextral) fault. This fault lies beneath or behind the anticlinal part of the fold and shows up to 6 - 8 km of vertical displacement and a small amount of dextral strike-slip. In considering the Port Edgar/Symonds Harbour folds as coeval with the Hornby Monocline, Curtis & Hyam (1998) have suggested a transpressional model for D_2 involving an E-W compression being applied across a pre-existing NE-SW basement discontinuity forming the Hornby Monocline and the dextral strike-slip structures seen (Fig. 8.2). The model indicates that the E-W compression across the NE-SW fault resulted in 3.9 km of shortening perpendicular to

strike across the Hornby Monocline and 3.3 km of right-lateral displacement parallel to it.

Although the presence of N-S folds at Port Edgar/Symonds Harbour and thrust faults at Carcass Bay suggests E-W compression for D_2 there is no evidence for compressional structures (e.g. thrust faults) across the anticlinal part of the Hornby Monocline related to its formation. In contrast the Hornby Monocline shows veins and faults which have caused extension across the anticline. Compressional features are characteristic in monoclines formed by lateral compression whereas extensional structures characterise drape folding (Reches 1978). This would infer that, although E-W lateral compression is evident, it was not the main driving force for the formation of the fold and that it formed primarily by drape folding caused by significant vertical movement on the basement fault.

The E-W transpression model of Curtis & Hyam (1998) fits the evidence of a small amount of dextral strike-slip across the steep limb of the fold and the N-S folds at Port Edgar/Symonds Harbour. However the 3.9 km of strike-perpendicular lateral shortening across the structure does not wholly comply with the 6 - 8 km vertical movement on the underlying fault nor the non-compressional, drape fold nature of the Hornby Monocline. What is proposed here is that pre-D_2, a low amplitude monoclinal flexure existed owing to Permo- Carboniferous vertical movement on the basement fault. This early formed monoclinal flexure was then amplified by D_2 deformation, which involved further vertical movement on the fault and E-W compression. This model implies that the primary cause of the Hornby Monocline was by vertical movement on the underlying fault and subsequent drape folding giving rise to the sub-vertical extension across the anticlinal part of the monocline. Although evident in forming the Port Edgar/Symonds Harbour folds, E-W compression probably played a minor role during the formation of the Hornby Monocline in aiding to amplify an existing monoclinal flexure to the present 6 - 8 km structural relief. An element of E-W compression causing amplification of an existing low amplitude monoclinal flexure also explains why, although several D_2 folds exist, the Hornby Monocline is the largest single D_2 structure on the Falkland Islands.

One aspect of the D_2 deformation which still remains unclear, is the cause of the E-W compression. As the source of the compression is not apparent on the

Falkland Islands, a broader view within the context of Gondwana is required. The major events in Gondwana break-up did not start until ~ 190 Ma (Cox 1992). As noted in section 8.2.2.i, D_2 deformation was over by c.190 Ma indicating that it is not related directly to major Gondwanian events. It is possible, however, that the E-W compression may be related to stresses associated with the early anticlockwise rotation of the Ellsworth-Whitmore Mountains (EWM) block. The timing of this also fits as it is known that the rotation of the EWM occurred after the Gondwanian Orogeny (Schopf 1969) and before 175 Ma (Grunow *et al.* 1991). This shall be reviewed again later after discussion of Gondwana break-up models

iv) Structural boundary between East and West Falkland: Previous workers on the Falkland Islands have inferred the boundary between East and West Falkland to be either; an undefined structure (Greenway 1972); the Falkland Sound Fault, a major structural discontinuity between East and West Falkland (Marshall (1994a); a strike-slip fault with up to 300 km dextral displacement (Thomas *et al.* 1995) or; a steep fault beneath eastern West Falkland (Curtis & Hyam 1998). As the discussion in Chapter 5.4 and in the previous sections shows, present understanding does not support the model of strike-slip motion, or of a fault within the Falkland Sound. Instead, the morphology of the Hornby Monocline infers a basement fault lying beneath the eastern margin of West Falkland. Data from vitrinite and facies analysis indicates that the NE-SW structure is long-lived, that there was early movement in the Permo-Carboniferous and that it was reactivated during D_2 deformation to become the steep, oblique (reverse-dextral) fault presently inferred beneath West Falkland. Given the long-standing nature of this basement structure, this fault probably represents a primary block boundary between East and West Falkland. It is possible that the NE-SW structures around the Jason Islands and along the eastern boundary of the Falkland Island continental margin represent similar structures.

It has been inferred that distribution of displacement on the basement fault beneath the eastern margin of West Falkland is similar to that of the overlying periclinal Hornby Monocline, being at its greatest around Shag Cove and dying out laterally to the NE and SW (Chapter 5.4). The eastward shift of the D_2 fold axes at the NE end of the Hornby Anticline to the anticline through White Rock Bay (Fig.

8.1) indicates that an underlying fault also steps eastwards. Similarly, at Carcass Bay, the isolated nature of the deformation has been interpreted as being related to an eastward stepping of basement faults (Chapter 5.3.5). Cross-sections across the Falkland Sound show that displacement across this structural boundary peters out northwards, so that in the North Falkland Basin, located to the north of the Falkland Islands (Fig. 6.1), there is no evidence of a NE-SW structural trend. In contrast, offshore seismic and gravity data to the SW of the Falkland Islands show that there is a major NE-SW basement structure, probably a fault, with up to 7.5 km vertical displacement (Chapter 6.3) as far south as 52°30'S. Given the discontinuous nature of the positive gravity anomaly to the NE of this structure (Fig. 6.6) it is likely that the segmented nature of the faults beneath West Falkland also continues offshore to the SW.

8.3 The position of the Falkland Islands within Gondwana

As discussed in Chapter 2.1 there has been controversy over the position of the Falkland Islands in Gondwana reconstructions. It was recognised by du Toit (1937), that the Falkland Islands were a displaced part of the Cape Fold Belt of South Africa and, in attempting to resolve this, he placed them to the west of South Africa, between the Cape Fold Belt and Sierra de la Ventana. Fifteen years later, Adie (1952b) suggested that the Falkland Islands lay to the east of South Africa, rotated by 180° relative to their present position, based on close correlation of the stratigraphy. In contrast others (e.g. de Wit *et al.* 1988) place the Falkland Islands 500 km south of Cape Town which infers a significant 'Z' bend in the Cape Fold Belt to accommodate the correlation to the fold-belt on the Falkland Islands. In recent years, further stratigraphic correlations between the Falkland Islands and eastern South Africa including; the Precambrian (Thomas *et al.* 1995); Devonian (Marshall 1994a, Chapter 2 *this study*); and Permian (Chapter 2) sequences, coupled with palaeomagnetic evidence from Jurassic dolerite dykes (Mitchell *et al.* 1986, Taylor & Shaw 1989) have confirmed the hypothesis of Adie (1952b). One area of correlation, that of the structural geology, has, until recently (Curtis & Hyam 1998), remained largely unstudied.

The structure of the Falkland Islands and the Cape Fold Belt is, at a broad scale, quite similar. This was first seen by Adie (1952b) who noted the common features of the E-W fold-belt dying out into the Permian foreland basin across a relatively sharp deformation front. However, a more detailed comparison of the two areas does not, at first glance, give such a clear correlation. This is because the majority of published work is from the central and western Cape Fold Belt rather than the Eastern Cape. In the central Cape Fold Belt there are four phases of compressional deformation dated at 278, 258, 247 and 230 Ma from micas in cleavages (Hälbich *et al.* 1983). In contrast, the Falkland Islands show only one main deformation phase with one associated cleavage. Comparison to the eastern end of the Cape Fold Belt is restricted by the lack of published literature, so some reconnaissance fieldwork was undertaken in the area with M.L. Curtis (BAS) in September 1996. This work revealed that the polyphase deformation of the central Cape Fold Belt is replaced in the Eastern Cape by a single phase of deformation with NNE verging folds and thrusts, the development of a single, southerly dipping cleavage, and a rapid northward decline in deformation into the Karoo Supergroup around Ecca Pass (Fig. 8.3a). Recent work near Steytlerville has also revealed post-Cape Fold Belt, NE-SW dextral faulting (Booth 1996).

If the observed structural characteristics of East Falkland and the eastern part of the Cape Fold Belt are compared (Table 8.1), it becomes clear that the structural styles are very similar and that the Falkland Islands need to be rotated by 180° for the structures to correlate (Fig. 8.3b-g). Thus, this comparison strengthens the conclusions derived from the stratigraphic correlation and palaeomagnetic evidence, confirming once again, that the position of the Falkland Islands in pre-break-up Gondwana was against the Eastern Cape of South Africa.

A further point is that, although the arcuate nature of the Falkland Islands fold-belt is similar to that of the South African Cape Fold Belt, the decrease in deformation seen across the Falkland Islands would indicate that the islands represent an eastward lateral termination to the South African segment of the Gondwanide Orogeny.

8.4 Break-up of Western Gondwana and the rotation of the Falkland Islands

Having looked at the evidence for the position of the Falkland Islands in Gondwana, it is necessary to discuss how the Falkland Islands broke away and were rotated. The youngest pre-Pleistocene event which can be defined on the Falkland Islands is the intrusion of Early to Middle Jurassic dolerite dykes which are known to have formed before rotation began (Taylor & Shaw 1989). Therefore, as there is little structure that can be confirmed as being Mesozoic on the Falkland Islands, models regarding the rotation of the Falkland Islands block cannot be tested using structural evidence from the islands themselves. Instead, rotation models for the Falkland Islands have been based on the geology from other parts of Gondwana.

As detailed above, the pre-break-up position of the Falkland Islands is well constrained against the eastern coast of South Africa. Marshall (1994a), using the gravity data of Sandwell & Smith (1992), defined the Falkland Islands microcontinent as being a rectangular block with the islands lying in the southern half (in their present orientation). However, as Gondwana reconstructions highlight, it is important to consider that the Falkland Islands are only one of several continental fragments in this part of Gondwana (Fig. 8.4a) (Dalziel & Elliot 1982) which have nearly all undergone long-lived and complex movements since the initiation of break-up. Several aspects of the fragmentation of Gondwana need to be considered regarding the Falkland Islands; timing, relative motions of other plates; and possible causes.

8.4.1 Timing

The timing of the fragmentation of Gondwana into its constituent parts is crucial to constraining the movements of the Falkland Islands microcontinent. Although the main events in the break-up of Gondwana are well documented, the timing of rotation of the Falkland Island microplate is still poorly defined (Fig. 8.5). There are several constraints and estimates on the timing of rotation of the Falkland Islands:

(1) Palaeomagnetic results from c. 190 Ma dykes on the Falkland Islands indicate a rotation of 180° (Taylor & Shaw 1989) implying that the dykes were emplaced before rotation began. Other dolerite dykes show palaeomagnetic data indicating a lower

angle of rotation (Taylor & Shaw 1989) possibly related to emplacement during rotation. These may correlate to younger dolerite dykes on the Falkland Islands dated by Thistlewood *et al.* (1997) at 176±7 Ma and 162±6 Ma, however, this correlation is untested.

(2) The Gastre Fault System (GFS) in Patagonia, interpreted as a dextral strike-slip fault which translated Patagonia westwards by c. 500 km, is known to have been active between 208 Ma and 172 Ma (Rapela & Pankhurst 1992). The Falkland Fracture Zone, the lateral equivalent of the GFS, finished movement by the Mid Jurassic (Lorenzo & Mutter 1988) at around 165 Ma (South Atlantic Geological Research Group 1997). The westward movement of this block has been related to rotation of the Falkland Islands microcontinent (Marshall 1994a).

(3) Ben-Avraham *et al.* (1993), in correlating the opening of the Falkland Plateau Basin to the Outeniqua Basin estimated that the microcontinental block rotated between 175 Ma and 155 Ma.

(4) Marshall (1994a) placed the rotation during the mid - late Jurassic (c. 150-180 Ma) based on the need to open the Falkland Plateau Basin and for the Falkland Islands to clear the Agulhas Plateau before rotating.

(5) Richards *et al.* (1996) find no evidence for rotation in the Late Jurassic to Early Cretaceous offshore basins around the Falkland Islands. However, Richards & Fannin (1997) admit that rotation could have taken place before the opening of the basins.

(6) From analysis of the faults along the Natal coastline, Watkeys & Sokoutis (1997) interpreted a transtensional event around 175-155 Ma and related this to the rotation of the Falkland Island microplate.

(7) The emplacement of a magmatic plume (White & McKenzie 1989) at around 180 Ma under Mozambique (Cox 1992) is thought to have been related to the formation and rotation of the many microplates in western Gondwana (Storey *et al.* 1996).

(8) The EWM block had rotated by 90° (Schopf 1969, Watts & Bramall 1981) by 175 Ma (Grunow *et al.* 1987), and it has been considered that the Falkland Islands microplate also completed its rotation by this time (Grunow *et al.* 1987).

A summary of these controls on the timing of rotation of the Falkland Islands microplate suggests that; it must have started after initial dyke emplacement on the

Falkland Islands at c.190 Ma; it probably started with the emplacement of a plume at 180 Ma under Mozambique (Cox 1992); it was occurring around 155 - 175 Ma, based on interpretation of faults in Natal (Watkeys and Sokoutis 1997) and offshore basins in South Africa (Ben-Avraham *et al.* 1993); it may have terminated by the Late Jurassic (165 Ma) with the last movements on the Falkland Fracture Zone (Lorenzo & Mutter 1988). From this it would seem that 120° rotation of the Falkland Islands occurred in a time window of ~ 20 My between ~180 and ~160 Ma. This would imply rotation rates of ~6° My^{-1} which is not an unreasonable estimate for rotation related to continental deformation as similar rates of 3 - 10° My^{-1} (Israel, Ron *et al.* 1984), 6° ± 2° My^{-1} (California, Molnar & Gipson 1994) and ~5° My^{-1} (Central Asia, Thomas *et al.* 1994) are known for rotation of continental blocks.

8.4.2 Relative plate motions in western Gondwana

In considering the movements of the Falkland Islands microplate, it is necessary to review the relative motions of the surrounding plates at around the time of the Falkland Island rotation. This is done in an African reference frame and is summarised in Figure 8.6.

i) Early Jurassic: Movement occurred along the Gastre Fault System with the westward escape of Patagonia between 208 and 172 Ma (Rapela & Pankhurst 1992). At around 190 Ma, East Antarctica moved westwards relative to West Gondwana along an E-W sinistral zone (Cox 1992). The EWM block, part of the Gondwanide fold-belt, rotated anticlockwise by 90° (Schopf 1969) away from a position SW of the Falkland Islands and southern Africa (Curtis & Storey 1996) before 175 Ma (Grunow *et al.* 1987).

ii) Middle Jurassic: Patagonia's westward escape continued until 165 Ma with movement along the Falkland Fracture Zone (Lorenzo & Mutter 1988). About 170 Ma the relative motion of East Antarctica and West Gondwana changed so that East Antarctica began moving southwards (Cox 1992). The Falkland Islands microplate rotated by 120° between around 180 Ma and 160 Ma. The Outeniqua and

Falkland Plateau Basins began opening around ?170 - 165 Ma (Barker *et al.* 1976b, Ben-Avraham *et al.* 1993). The Antarctic Peninsula began to rotate clockwise, towards the palaeo-Pacific margin (Grunow 1993a, b)

iii) Late Jurassic: The Antarctic Peninsula continued its anticlockwise rotation (Grunow 1993a, b). Sedimentation in the Outeniqua and Falkland Plateau Basins was slow and anoxic black shales accumulated. The North Falkland Basin is thought to have opened around this time (Richards *et al.* 1996)

iv) Cretaceous: By 125 Ma the South Atlantic began to open (e.g. Martin *et al.* 1982) and the Falkland Islands were rotated by a further 60°.

8.4.3 Causes of rotation

Several models have been proposed for the causes of rotation of the microplates, especially the Falkland Islands, in Western Gondwana. These will be discussed below.

(1) Emplacement of the mantle plume in Mozambique (Fig. 8.4b) (e.g. Storey *et al.* 1996). This model, suggests a mechanism by which West Gondwana broke-up into microcontinents and provides an initiation process for rotation due to doming related to the emplacement of the plume. It is also possible that movements in the lower crust / upper mantle, related to the plume, also provided an underlying driving force for the rotation of the microcontinental blocks (c.f. Molnar & Gipson 1994).

(2) Rotation along strike-slip faults (e.g. Taylor & Shaw 1989, Storey *et al.* 1996). Although the specific faults required for this model are not identified, the strike-slip movements along the GFS and between East and West Gondwana, combined with the extensional regime of continental break-up, created transtension in which the blocks could rotate without locking up. In this model, the space created by rotation of the EWM and Falkland Island blocks is accommodated by crustal extension of the Filchner block and basin development in the Antarctic Peninsula and South Atlantic (Storey *et al.* 1996) (Fig. 8.7c). It is unclear whether the extension in these basins

completely accounts for the amount of stretching involved in the rotation of the EWM.

(3) Differential movement between spreading ridges (Marshall 1994a) (Fig. 8.7a). This is the only model that suggests a method for the opposite senses of rotation of the EWM and the Falkland Islands (1994a) through differential strike-slip movement between spreading ridges. Development of the Falkland Plateau Basin (FPB) and oceanic crust in the southern Weddell Sea (Fig. 8.7a) is suggested to have accommodated the space created by the rotations. However, in this model, the Falkland Islands would have to cross several ridge transforms during rotation and, although the timing of the opening of the FPB at 170? -160 Ma (Barker *et al.* 1976b) is likely to have accommodated the space made by the Falkland Islands rotating, the model of ocean crust development and subsequent subduction in the southern Weddell Sea has been shown to be implausible as there is no related subduction complex (Storey *et al.* 1996).

(4) Rotation related to the westward movement of Patagonia and the synchronous development of the Outeniqua and Falkland Plateau basins (Fig. 8.7b), (Ben-Avraham *et al.* 1993). This model suggests that the FPB opened synchronously with rotation of the Falkland Islands accommodating the space created.

(5) Re-adjustment of microplates within Gondwana along strike-slip faults following the Gondwanide Orogeny (Dalziel & Grunow 1992). This model is improbable as; (i) rotation occurred ~40 Ma after the last pulse of deformation in the Cape Fold Belt during extension and break-up of Gondwana and; (ii) a compressional regime would allow no room to rotate the elongate EWM and Falkland Island blocks.

From the above models it would seem that plume emplacement provides the most plausible explanation for the initial break-up, initiation and driving force behind the microplate rotations. A transtensional strike-slip regime was the most likely mechanism for the rotations, and extension of the Filchner block and the development of the FPB and basins in Antarctica accommodated the space created by the rotations. As the model of Marshall (1994a) for opposite senses of rotation is unlikely, another model is suggested, whereby different stress regimes across Gondwana controlled the rotations of the two blocks (Fig. 8.8). In this model, the pre-175 Ma anticlockwise rotation of the EWM would be related to the sinistral motion between East Antarctica

and Africa (e.g. Cox 1992) and the 160 - 180 Ma clockwise rotation of the Falkland Islands would be related to the westward escape of Patagonia through dextral movement along the GFS (e.g. Marshall 1994a) and N-S movement between East Antarctica and Africa (c.f. Figure 8.6).

8.4.4. Break-up models and the cause of D_2 deformation on the Falkland Islands

The D_2 deformation event on the Falkland Islands is characterised by E-W compression and the formation of fold structures which die out from E-W (in a pre-break-up orientation of the Falkland Islands) and occurred after the Permo-Triassic D_1 Gondwanian event and prior to the break-out of the Falkland Islands from South Africa around 160-180 Ma (c.f. chapter 8.2.2). This leaves the problem of what caused D_2. As the deformation occurred prior to break-up of the Falkland Islands it can not be related simply to their clockwise rotation, however, as mentioned in chapter 8.2.2.iii the anticlockwise rotation of the EWM block before 175 Ma, prior to the rotation of the Falkland Islands block, may have been the cause of D_2 deformation on the Falkland Islands. Several elements support this model, (i) the EWM block is postulated to have lain to the east of the Falkland Islands in Gondwana reconstructions (e.g. Curtis *et al.* 1996), and, given that there is a decrease from West to East Falkland in D_2 structures, the EWM block is sitting in the region where the D_2 stress would have originated from; (ii) the rotation of the EWM block occurred before the rotation of the Falkland Islands block, this would allow for D_2 to occur before rotation of the Falkland Islands; (iii) the anticlockwise rotation of the EWM block during E-W sinistral motion of East and West Gondwana could have caused compression across the Falkland Islands to the west. The related deformation would have been most intense in the east, near the EWM block, dying out westwards towards South Africa, exactly what is seen across the Falkland Islands when in pre-break-up position.

In summary (Fig. 8.8), this model infers that anticlockwise rotation of the EWM block due to sinistral motion between East and West Gondwana prior to 175 Ma (Cox 1992) caused E-W compressive stress across the Falkland Islands which lay to the palaeo-west. Deformation caused by this was recorded as the D_2 structures on

West Falkland which peter out towards East Falkland and South Africa. Following this event the stresses across Gondwana changed and East and West Gondwana underwent N-S strike-slip movement, during which time the Falkland Islands broke away from South Africa and began rotating.

8.4.5 Summary

In summary it would appear that the rotation of the Falkland Islands occurred between ~180 and ~160 Ma and that it was related to the extensional and strike-slip regime created by the westward escape of Patagonia and the N-S movement of East and West Gondwana. Emplacement of a mantle plume provided both the initiation and the underlying mechanism for the rotation.

	East Falkland, Falkland Islands	*Eastern Cape Fold Belt, South Africa*
Fold vergence	South.	North-north-east.
Reverse fault transport direction	South.	North-north-east.
Cleavage	One, dipping north.	One, dipping south.
Deformation front	Dies out south into Permian aged Lafonian Basin.	Dies out north into Permo-Triassic Karoo Basin.
Change in provenance	Switches from S to NE.	Switches from N to S.
Initiation of deformation	Early Permian in the late stages of deposition of the glacial Lafonian Diamictite Formation.	Early Permian in the late stages of deposition of the glacial Dwyka Group.

Table 8.1: Comparison of the structures of East Falkland, Falkland Islands and the Eastern Cape Fold Belt, South Africa

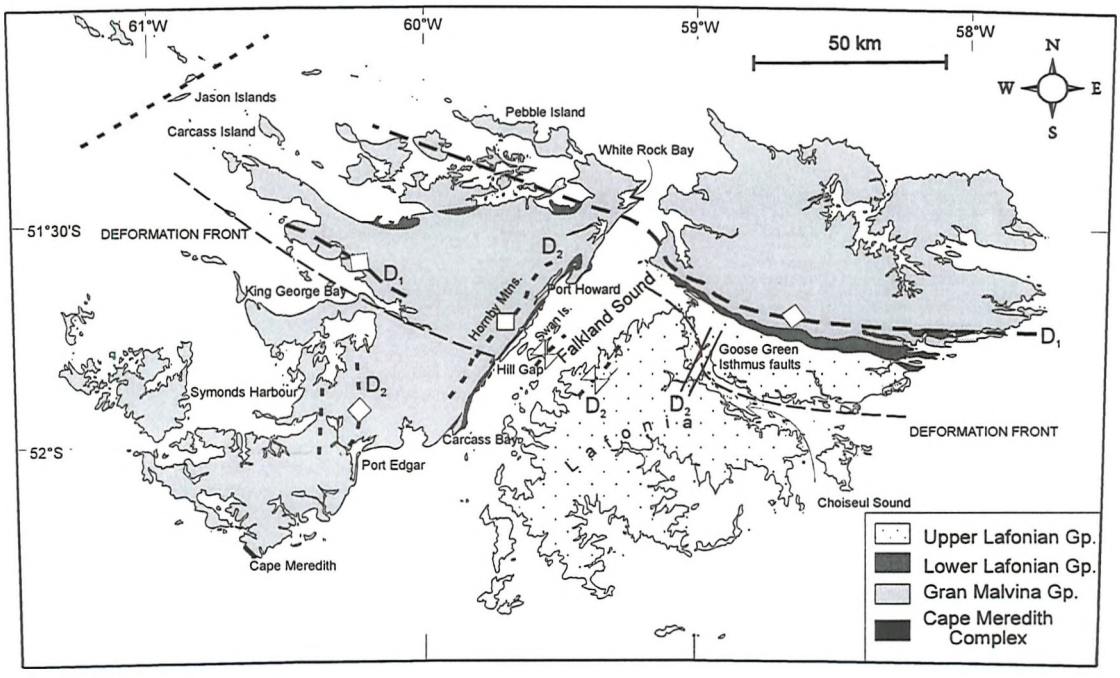

Figure 8.1: Simplified geological map of the Falkland Islands showing D_1 and D_2 deformation trends and the deformation front.

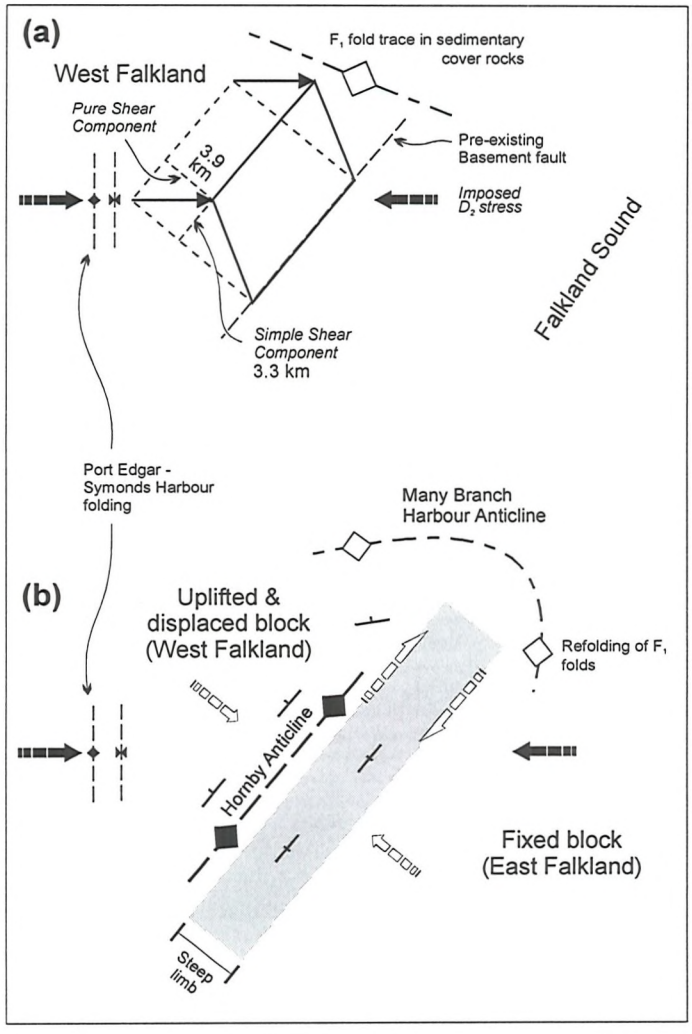

Figure 8.2: Curtis & Hyam (*in press*) transpression model for the formation of the Hornby Monocline by E-W D_2 compression. (a) E-W compression across the existing NE-SW basement fault beneath West Falkland, resulting in fault-perpendicular pure shear and fault-parallel simple shear. (b) The E-W compression results in oblique (reverse-dextral) movement on the underlying fault and the formation of the Hornby Monocline with NE-SW dextral strike-slip parallel to the fault and NW-SE shortening perpendicular to the fault.

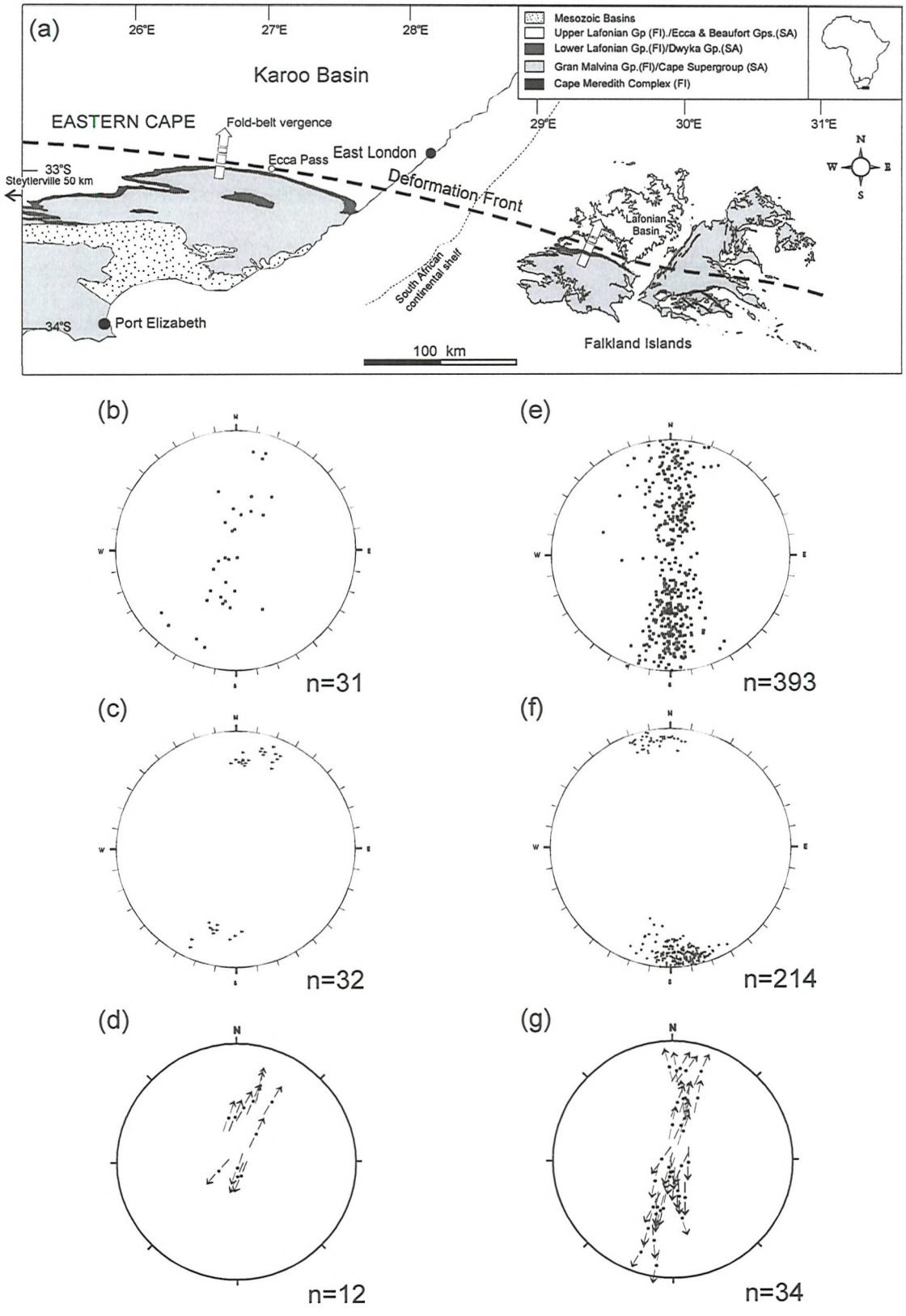

Figure 8.3: Structural comparison between East Falkland and the South African Eastern Cape. (a) pre-break-up position of the Falkland Islands against eastern South Africa; (b-d) poles to bedding, poles to cleavage and hoepenor plot of reverse faults for East Cape; (e-g) poles to bedding, poles to cleavage and hoepenor plot of reverse faults for East Falkland (present orientation).

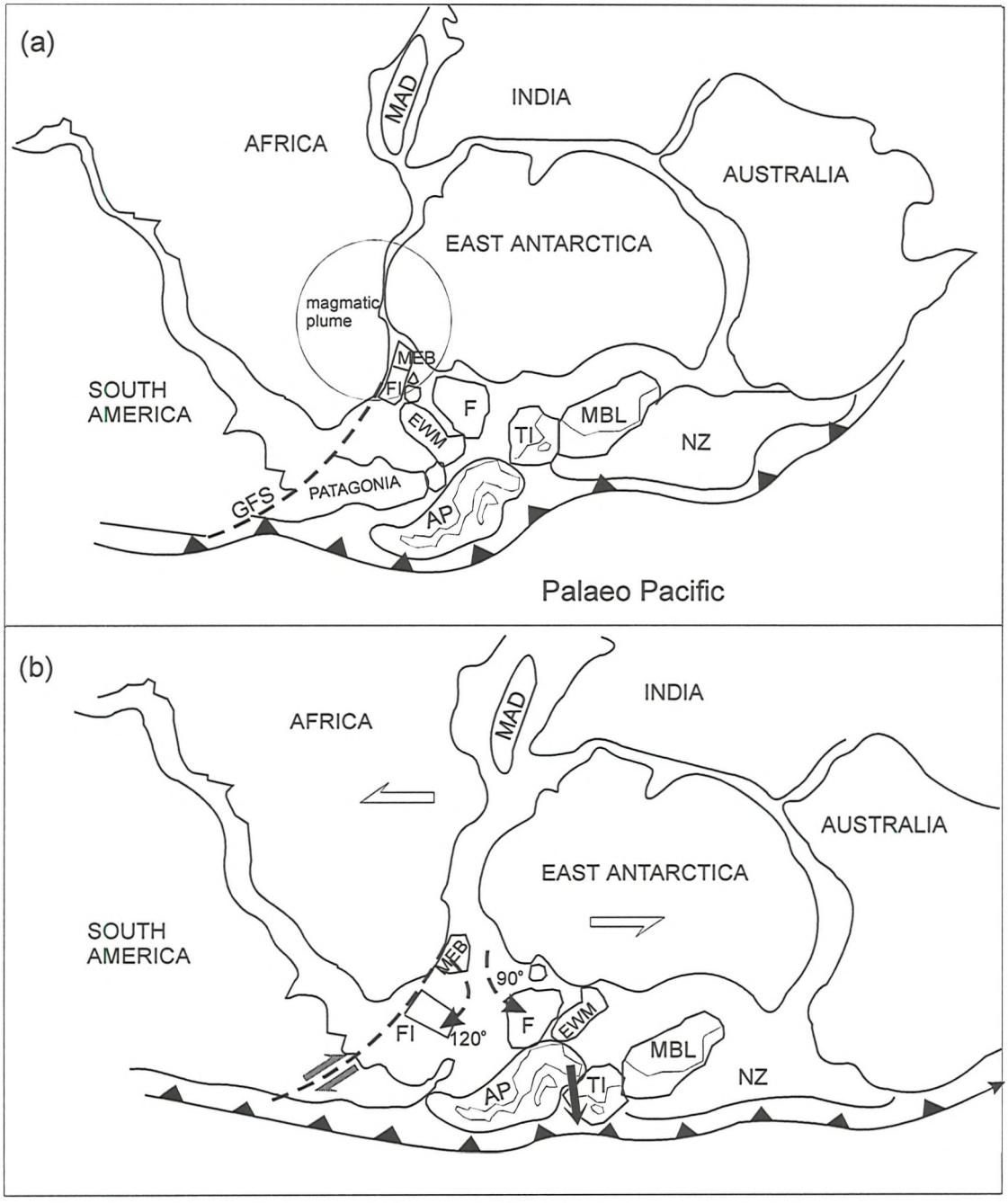

Figure 8.4: (a) Pre-break-up Gondwana reconstruction after Storey *et al.* (1996). Microcontinent positions after Rapela & Pankhurst (1992) and Storey *et al.* (1996). (b) Initial break-up model showing rotations of EWM and FI, rifting of East and West Gondwana and the dextral translation of Patagonia along the GFS. AP= Antarctic Peninsula, EWM= Ellsworth Whitmore Mountains, F= Filchner block, FI= Falkland Islands, GFS= Gastre Fault System, MAD= Madagascar, MEB= Maurice Ewing Bank, MBL= Marie Byrd Land, NZ= New Zealand, TI= Thurston Island.

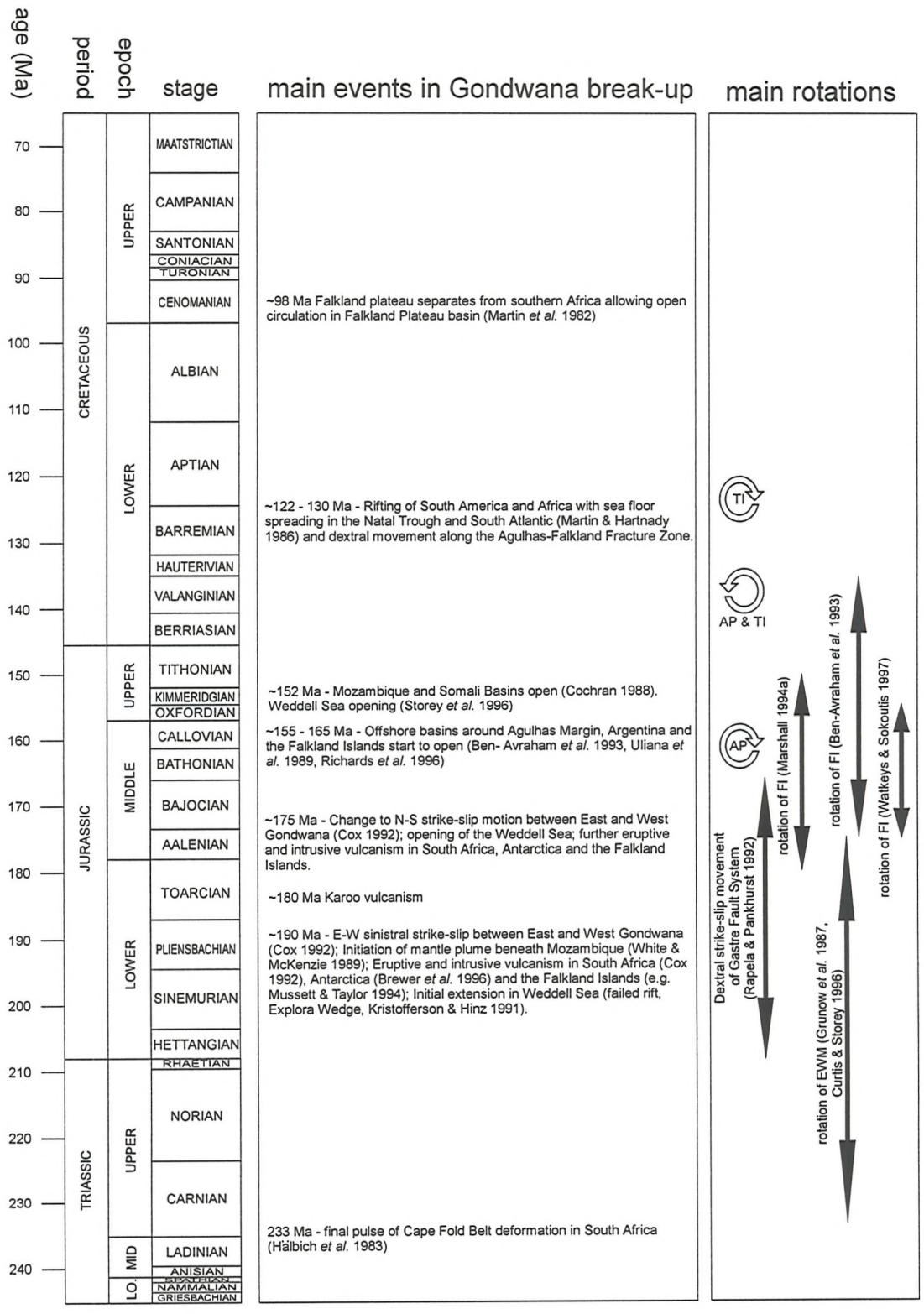

Figure 8.5: Correlation chart showing main events in the break-up of western Gondwana. AP= Antarctic Peninsula, EWM= Ellsworth Whitmore Mountains, FI= Falkland Islands, TI=Thurston Island AP & TI rotations after Grunow *et al.* (1991) and Grunow 1993a. Other events as referenced.

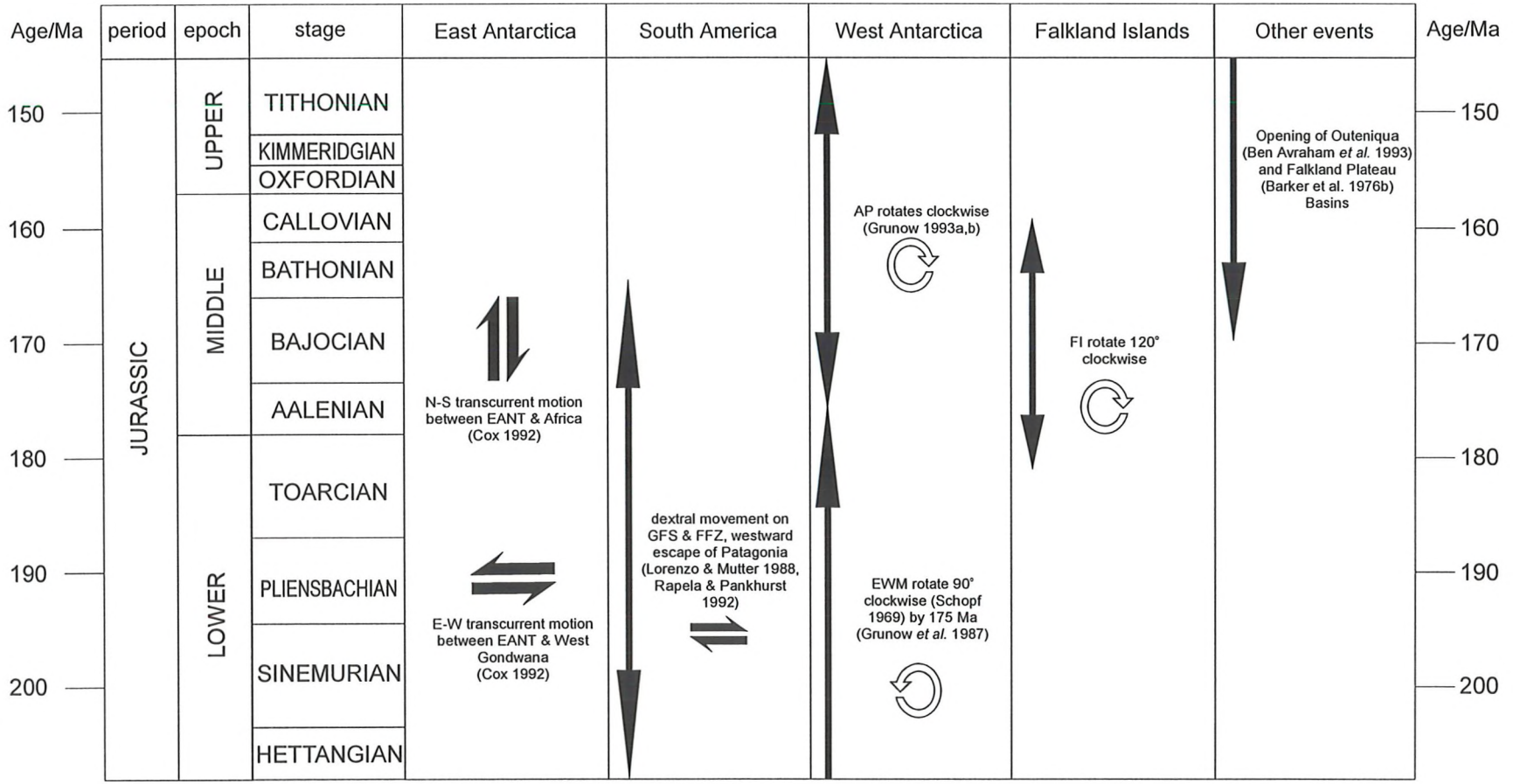

Figure 8.6: Correlation chart showing the relative motions (in an African reference frame) of the plates surrounding the Falkland Islands for the Jurassic Period. AP= Antarctic Peninsula, EANT= East Antarctica, FFZ= Falkland Fracture Zone, FI=Falkland Islands, GFS=Gastre Fault System.

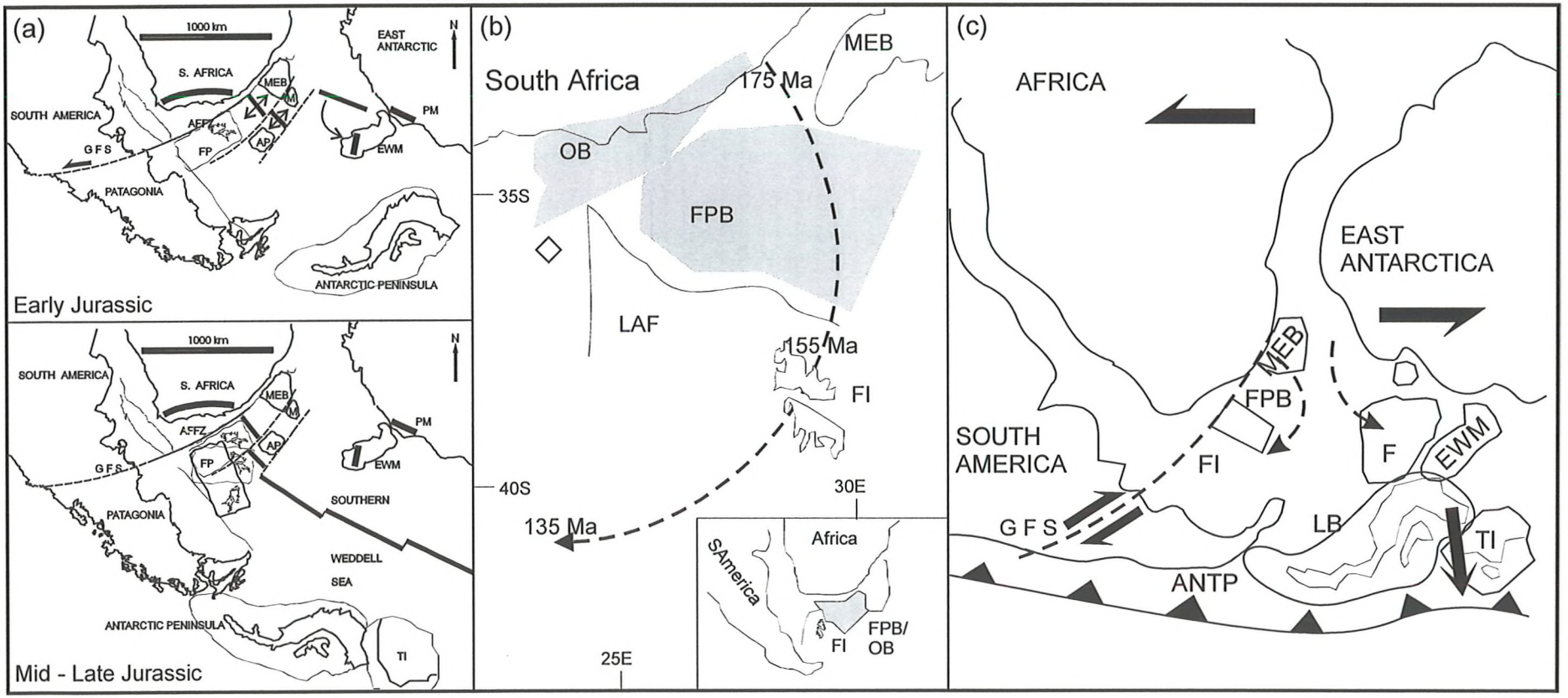

Figure 8.7: Models for rotation of the Falkland Islands; (a) after Marshall (1994a); (b) after Ben-Avraham *et al.* (1993); (c) after Storey *et al.* (1996). AFFZ= Agulhus Falkland Fracture Zone, ANTP=Antarctic Peninsula, AP=Agulhas Plateau, EWM= Ellsworth Whitmore Mountains, F=Filchner Block, FI=Falkland Islands, FP=Falkland Plateau, FPB=Falkland Plateau Basin, GFS=Gastre Fault System, LAF=Lafonian Plate, LB= Latady Basin, OB=Outeniqua Basin, M=Mozambique Ridge, MEB=Maurice Ewing Bank PM=Pensacola Mountains, TI=Thurston Island.

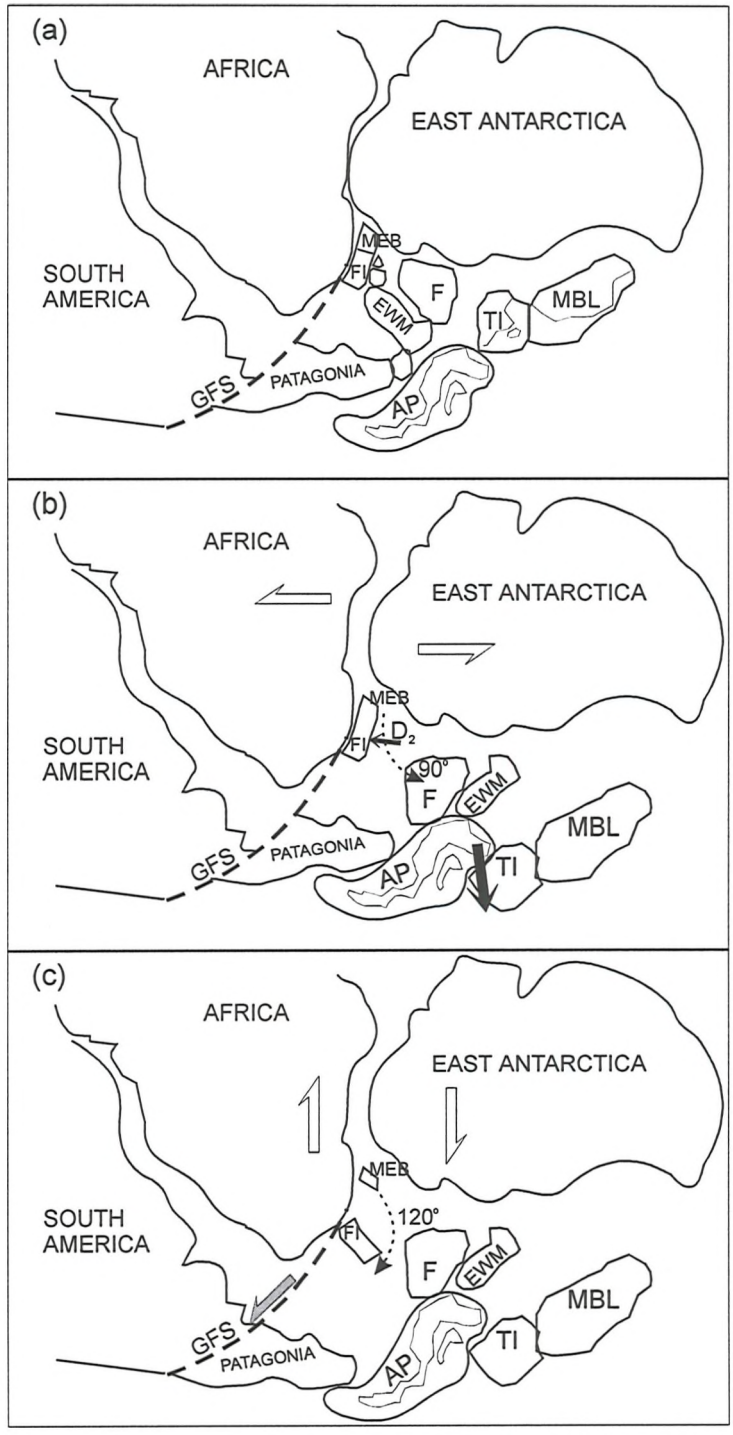

Figure 8.8: Revised break-out model for the Falkland Islands. (a) Pre-break-up Gondwana reconstruction after Storey *et al.* (1996). Microcontinent positions after Rapela & Pankhurst (1992) and Storey *et al.* (1996). (b) Initial break-up showing sinistral E-W motion between East and West Gondwana giving rise to a 90° rotation of the EWM block which in turn causes D_2 deformation across the Falkland Islands. (c) Secondary break-up with dextral N-S motion between East and West Gondwana coupled with 120° rotation of the FI block and the dextral translation of Patagonia along the GFS. AP= Antarctic Peninsula, EWM= Ellsworth Whitmore Mountains, F= Filchner block, FI= Falkland Islands, GFS= Gastre Fault System, MEB= Maurice Ewing Bank, MBL= Marie Byrd Land, TI= Thurston Island.

Chapter 9: Conclusions

Chapter 9: Conclusions

The Falkland Islands are unequivocally a displaced part of the South African Cape Fold Belt which originally lay to the east of South Africa as suggested by Adie (1952b). This model has been confirmed through (i) new data from the stratigraphy; (ii) detailed analysis of the structure and; (iii) assessment of the burial history of the foreland basin on both the Falkland Islands and in the Eastern Cape of South Africa.

Stratigraphic correlations include: (1) the matching of new palaeocurrent data from the Gran Malvina Group with known data from the Cape Supergroup, only when the islands are rotated by 180°; (2) correlation of the sedimentary facies of the Black Rock Member, based on kerogen analysis, to identical facies of the Whitehill Formation and equivalents in the Eastern Cape; (3) correlation of the Bluff Cove Formation, to its lithostratigraphic equivalent the Kommadagga Subgroup, only found in the Eastern Cape and; (4) discovery of outcrops of the Port Stephens Formation in north East Falkland and its match to outcrops of its lithostratigraphic equivalent, the Table Mountain Group, in the Eastern Cape, only when rotated by 180°.

Two, almost orthogonal, structural trends exist on the Falkland Islands; an E-W to WNW-ESE trending fold-belt across the northern part of both East and West Falkland; and a NE-SW trending set of structures dominated by the Hornby Monocline on West Falkland. From interference fold patterns on West Falkland these have been defined as D_1 and D_2 respectively.

Analysis across East Falkland has shown that D_1 started in the Early Permian and is dominated by a train of upright to southerly inclined, open to isoclinal folds, with minor top-to-the-south thrusting and the development of one, northerly dipping cleavage. D_1 deformation dies out rapidly to the south, into the Permo-Carboniferous Lafonian foreland basin. The style of D_1 deformation changes westward across East Falkland and onto West Falkland, with a change in strike from E-W to WNW-ESE, coupled with a marked decrease in strain (calculated from quartz vein analysis, cross-section balancing and intensity of cleavage). This westward decrease in deformation is modelled as a lateral tip to the fold-belt. Localised changes in strike on western East Falkland are the result of differential movement along faults sub-orthogonal to

the fold-belt. Given present knowledge D_1 resulted from N-S compression and thick-skinned deformation without the development of a basal décollement.

The NE-SW structures, including the Hornby Monocline, on West Falkland, and N-S folds in mid West Falkland are related to D_2. From interpretation of dextral strike-slip structures and shortening estimates across the Hornby Monocline on West Falkland, D_2 can be seen to have been an E-W compressional event.

Interpretation of the Hornby Monocline and the sub-vertical extension structures in the steep limb of the fold show that, although E-W compression (D_2) was probably involved in amplifying the monocline to its present size, the monocline formed primarily by drape folding caused by movement along a major oblique (reverse-dextral) basement fault, inferred beneath the eastern margin of West Falkland, causing West Falkland to be uplifted by 6 - 8 km relative to East Falkland. A marked step in the 5000 ms^{-1} interval velocity contour (equivalent to the top of crystalline basement) and a corresponding step in the Bouguer gravity data to the SW of the Falkland Islands reveal a similar NE-SW structure, with 6.5 - 7.5 km structural relief, continuing for at least 60 km along strike of the southern end of the Falkland Sound, between East and West Falkland.

Vitrinite reflectance data from downwardly injected sedimentary dykes of Early Carboniferous age and; a change from proximal to basinal facies in the Lower Lafonian Group from West to East Falkland show that West Falkland was uplifted relative to East Falkland from the Early Carboniferous. The marked increase in vitrinite reflectance in the Gran Malvina Group from West to East Falkland suggests that the Lafonian Supergroup was only ever deposited as a thin sequence on West Falkland and that the relative uplift of West Falkland seen in the Early Carboniferous continued through the Permian, and the D_1 deformation event. The pre and syn-D_1 movement on this basement fault resulted in the formation of a low amplitude monocline, which was amplified to become the Hornby Monocline when the fault was reactivated as an oblique reverse-dextral fault during the E-W D_2 deformation event.

Analysis of the structures in the Eastern Cape and East Falkland has revealed, that when the Falkland Islands are rotated by 180°, both show a northward verging fold-belt, with north facing folds, top-to-the-north thrusts, one southward dipping cleavage, and a foreland basin to the north. Using vitrinite reflectance and illite crystallinity as

measures of low-level metamorphism this study has shown that the burial histories of East Falkland and the Cape Fold Belt are almost identical. Both these new lines of evidence confirm the connection between the Falkland Islands and the Eastern Cape of South Africa.

References

References

ABBASSI, M.R. & MANCKTELOW, N.S. 1990. The effect of initial perturbation shape and symmetry on fold development. *Journal of Structural Geology* **12,** 273-282.

ADIE, R.J. 1952a. Representatives of the Gondwana system in the Falkland Islands. *International Congress, 19th Algeria Syposium sur les series de Gondwana.* 385-392.

———, 1952b. The Position of the Falkland Islands in a Reconstruction of Gondwanaland. *Geological Magazine* **89,** 401-410.

———, 1958. Falkland Islands. *Lexique Stratigraphique Internationale* **5,** 33-55.

ALLEN, P.A. & ALLEN, J.R. 1990. *Basin Analysis.* 451 pp. Blackwell Scientific Publications, Oxford.

ALPERT, S.P. 1977. Trace fossils and the basal Cambrian boundary. *In:* CRIMES T.P. & HARPER, J.C. (eds) *Trace Fossils 2,* Geological Journal Special Issue **9,** 1-8.

ANDERSON, J.M. 1977. The biostratigraphy of the Permian and Triassic Part 3. A review of Gondwana Permian palynology with particular reference to the northern Karoo Basin South Africa. *Memoirs of the Botanical Survey of South Africa* **41**, 1-133.

ANGELIER, J. 1984, Tectonic analysis of fault slip data sets. *Journal of Geophysical Research* **89,** 5835-5848.

ASHLEY, J. 1961. A magnetic survey in the vicinity of Port Stanley, Falkland Islands. *Falkland Island Dependencies Survey Preliminary Geological Report* **10.**

AZCUY, C.L. 1981. A review of early Gondwana palynology of Argentina and South America. *Proceedings of the IV International Palynological, Conference, Lucknow (1976-77)* **2**, 175-185.

BACKHOUSE, J. 1991. Permian palynostratigraphy of the Collie Basin, Western Australia. *Review of Palaeobotany and palynology* **67,** 237-314.

BAGNOLD, R.A. 1954. Experiments on a gravity-free dispersion of large solid spheres in a Newtonian fluid under shear. *Proceedings of Royal Society of London, Series A* **225,** 49-63.

BAKER, H.A. 1924. *Final report on geological investigations in the Falkland Islands.* (1920-22). 47 pp. Government Printer, Stanley.

BARKER, C.E. & GOLDSTEIN, R.H. 1990. Fluid-inclusion technique for determining maximum temperature in calcite and its comparison to the vitrinite reflectance geothermometer. *Geology* **18,** 1003-1006.

——— & PAWLEWICZ, M.J. 1986. The correlation of vitrinite reflectance with maximum temperature in humic organic matter. *In:* BUNTEBARTH, G. & STEGENA, L. (eds) *Paleogeothermics*. Lecture notes in Earth Sciences **5,** 79-93.

BARKER, P.F., DALZIEL, I.W.D. ET AL. 1976a. *Initial Reports of the Deep Sea Drilling Project* **36,** 1080 pp.Washington. (U.S. Government Printing Office).

BARKER, P.F. ET AL. 1976b. Site 330. *In:* BARKER, P.F., DALZIEL, I.W.D. ET AL. (eds) *Initial Reports of the Deep Sea Drilling Project* **36,** 207-258.

BEN-AVRAHAM, Z., HARTNADY, C.J.H. & MALAN, J.A. 1993. Early tectonic extension between Aghulas Bank and the Falkland Plateau due to rotation of the Lafonia microplate. *Earth and Planetary Science Letters* **117,** 43-58.

BOOTH, P.W.K. 1996. The relationship between folding and thrusting in the Floriskraal Formation (Upper Witteberg Group), Steytlerville, Eastern Cape. *South African Journal of Geology* **99,** 235-243.

BORRELLO, A.V. 1963. *Sobre la geología de las Islas Malvinas*. 70 pp. Educiones Cultura, Argentina, Ministerio de Educióne y Justica, Buenos Aires.

BREWER, T.S., REX, D., GUISE, P.G. & HAWKESWORTH, C.J. 1996. Geochronology of Mesozoic tholeiitic magmatism in Antarctica: implications for Gondwana break-up. *In:* STOREY, B.C., KING, E.C. & LIVERMORE, R.A. (eds) *Tectonic evolution of the Weddell Sea and surrounding regions*. Special Publication of the Geological Society of London **108,** p45-62.

BUSTIN, R.M. 1983. Heating during thrust faulting in the Rocky Mountains. Friction or Fiction? *Tectonophysics* **95,** 309-328.

CAIRNCROSS, B. 1989. Paleodepositional environments and tectonosedimentary controls of the post-glacial Permian coals, Karoo Basin, South Africa. *In:* LYONS, P.C. & ALPERN, B. (eds) *Peat and Coal: Origin, Facies and Depositional Models*. International Journal of Coal Geology **12,** 365-380.

CHADWICK, R.A. 1993. Aspects of Basin Inversion in southern Britain. *Journal of the Geological Society of London* **150,** 311-322.

CHOWN, E.H. & GOBIEL, A. 1990. Clastic dykes in the Chibougamau Formation: distribution and origin. *Canadian Journal of Earth Sciences* **27,** 1111-1114.

CINGOLANI, C.A. & VARELLA, R. 1976. Investigaciones geologicas y geocronologicas en el extremo Sur de la Isla Gran Malvina, sector de Cabo Belgrano (Cabo Meredith), Islas Malvinas. *Actas del Sexto Congresso Geologico Argentino, La Asociacion Geologica Argentina, Bahia Blanca, Buenos Aires.* **Vol. 1,** 457-473.

CLARKE, J.M. 1913. Fossies Devonianos do Paraná. *Monographias Serviço Geologico e Mineralogico do Brasil* **1,** 1-353, (in both English and Portuguese), Typografia Annexa á Directoria do Serviço de Estatistica, Rio de Janeiro.

CLIFFORD, P., FLEUTY, M.J., RAMSAY, J.G., SUTTON, J. & WATSON, J. 1957. The development of Lineation in Complex Fold Systems. *Geological Magazine* **94,** 1-24.

CLOETINGH, S., LANKREJER, A., DE WIT, M.J. & MARTINEZ, I. 1992. Subsidence history analysis and forward modelling of the Cape and Karoo Supergroups. *In:* DE WIT, M.J. & RANSOME, I.G.D. (eds) *Inversion Tectonics of the Cape Fold Belt, Karoo and Cretaceous Basins of Southern Africa.* 239-248.

COCHRAN, J.R. 1988. Somali Basin, Chain Ridge, and origin of the northern Somali Basin gravity and geoid low. *Journal of Geophysical Research* **93,** 11985-12008.

COCKS, L.R.M. & FORTEY, R.A. 1986. New evidence on the South African lower Palaeozoic age and fossils reviewed. *Geological Magazine* **123,** 437-444.

COETZEE, 1983. The deformation style between Meiringspoort and Beaufort West. *In:* SÖHNGE, A.P.G. & HÄLBICH, I.W. (eds) *Geodynamics of the Cape Fold Belt.* Special Publication of the Geological Society of South Africa **12,** 101-113.

COLE, D.I. 1992. The evolution and development of the Karoo Basin. *In:* DE WIT, M.J. & RANSOME, I.G.D. (eds) *Inversion Tectonics of the Cape Fold Belt, Karoo and Cretaceous Basins of Southern Africa.* 87-99

——— & MCLACHAN, I.R. 1991. Oil Potential of the Permian Whitehill Shale Formation in the main Karoo Basin, South Africa. *Gondwana Seven Proceedings, Sao Paulo, Brazil*, p379-390.

COOK, R.A. 1978. A relationship between strike-slip faults and the process of drape folding of layered rocks. *In:* MATTHEWS III, V. (ed) *Laramide Folding and*

Faulting in the Western United States. Memoir of the Geological Society of America **151,** 197-214

COWARD, M.P. & KIM, J.H. 1981. Strain within thrust sheets. *In:* MCCLAY, K.R. & PRICE, N.J. (eds) *Thrust and Nappe Tectonics*. Geological Society of London Special Publication **9,** 275-292.

——— & POTTS, G.J. 1983. Complex strain patterns developed at the frontal and lateral tips of shear zones and thrust zones. *Journal of Structural Geology* **5,** 383-399.

COX, K.G. 1992. Karoo igneous activity and the early stages of the break-up of Gondwanaland. *In:* STOREY, B.C., ALABASTER, T. & PANKHURST, R.J. (eds) *Magmatism and the Causes of Continental Break-up*. Geological Society of London Special Publication **68,** 137-148.

CREANEY, S. 1989. Reaction of Organic Material to Progressive Geological Heating. *In:* NAESER N.D. & MCCULLOH, T.H. (eds) *Thermal History of Sedimentary Basins: Methods and Case Histories*, 37-52, New York, Springer-Verlag.

CRIMES, T.P., LEGG, I., MARCOS, A. & ARBOLEYA, M. 1977. ?Late Precambrian-low Lower Cambrian trace fossils from Spain. *In:* CRIMES T.P. & HARPER, J.C. (eds) *Trace Fossils 2*, Geological Journal Special Issue **9,** 91-138.

CURTIS, M.L. & STOREY, B.C. 1996. A review of geological constraints on the pre-break-up position of the Ellsworth Mountains within Gondwana: implications for Weddell Sea evolution. *In:* STOREY, B.C., KING, E.C. & LIVERMORE, R.A. (eds) *Tectonic evolution of the Weddell Sea and surrounding regions*. Special Publication of the Geological Society of London **108,** 11-30.

——— & HYAM, D.M. 1998. Late Palaeozoic to Mesozoic structural evolution of the Falkland Islands: a displaced segment of the Cape Fold Belt. *Journal of the Geological Society of London* **155**, 115-130.

DALZIEL, I.W.D. & ELLIOT, D.H. 1982. West Antarctica: problem child of Gondwanaland. *Tectonics* **1,** 3-19

——— & GRUNOW, A.M. 1992. Late Gondwanaide Tectonic Rotations within Gondwanaland. *Tectonics* **11,** 603-606.

DARWIN, C. 1846. The Geology of the Falkland Islands. *Quarterly Journal of the Geological Society of London* **2,** 267-274.

DAWSON, J.C. 1967. *The Geology of the Bluff Cove Area, Falkland Islands*. Masters Thesis, 99 pp. UCLA, U.S.A..

DEBELMAS, J., ESCHER, A. & TRUMPY, R. 1983. Profiles through the western Alps. - *In:* RAST, N. & DELANY, F.M. (eds) *Profiles of Orogenic Belts*. American Geophysical Union Geodynamic series **10,** 83-96

DE DONATIS, M. & MAZZOLI, S. 1994. Kinematic evolution of thrust-related structures in the Umbro-Romagnan parautochthon (northern Apennines, Italy). *Terra Nova* **6,** 563-574.

DEPARTMENT OF MINERALS AND ENERGY AFFAIRS 1992. *Metamorphic map of the Republics of South Africa, Transkei, Boputhaswana, Venda & Ciskei and the kingdoms of Lesotho & swaziland.* 1:10,000,000 Scale.

DE WIT, M.J., JEFFERY, M., BERGH, H. & NICOLAYSEN, L. 1988. *Geological Map of sectors of Gondwana reconstructed to their disposition 150Ma ago.* American Association of Petroleum Geologists, Tulsa, Oklahoma.

DIXON, R.J., SCHOFIELD, K., ANDERTON, R., REYNOLDS, A.D., ALEXANDER, R.W.S., WILLIAMS, M.C. & DAVIES, K.G. 1995. Sandstone Diapirism and clastic intrusion in the Tertiary submarine fans of the Bruce-Beryl Embayment, Quadrant 9, UKS. *In:* HARTLEY, A.J. & PROSSER, D.J. (eds) *Characterisation of Deep Marine Clastic Systems*. Geological Society Special Publication **94,** 77-94.

DU TOIT, A.L. 1927. *A geological comparison of South America with South Africa.* 158 pp. Carnigie Institution of Washington Publication **381.**

———, 1937. *Our Wandering Continents - an hypothesis of continental drifting.* 366 pp. Oliver Boyd.

EDGECOMBE, G.D. 1994. Calimonid trilobites from the Devonian Fox Bay Formation, Falkland Islands: Systematics and biogeography. *In:* LANDING, E. (ed) *Studies in Stratigraphy and Paleontology in Honour of Donald W. Fisher, New York State Museum Bulletin* **481,** 55-68.

ELLIOTT, D. 1976. The energy balance and deformation mechanism of thrust sheets. *Philosophical Transactions of the Royal Society of London* **283,** 289-312.

ERIKSON, S.G. 1991. Structure of the Kelley Mountain culmination, central Alabama, and implications for the evolution of the southern Appalachian foreland thrust belt. *Geological Society of America Bulletin* **103,** 136-143.

EWING, J.L., LUDWIG, W.J., EWING, M. & EITTREIM, S.L. 1971. Structure of the Scotia Sea and Falkland Plateau. *Journal of Geophysical Research* **75,** 7118-7137.

EYAL, Y. 1988. Sandstone dykes as evidence of localised transtension in a transpressive regime, Bir Zreir Area, Eastern Sinai. *Tectonics* **7,** 1279-1289.

FLINT, R.F., SANDERS, J.E. & RODGERS, J. 1960a. Symmictite: A name for nonsorted terrigenous sedimentary rocks that contain a wide range of particle sizes. *Bulletin of the Geological Society of America* **71,** 507-510.

———, ———, & ——— 1960b. Diamictite: A substitute term for Symmictite. *Bulletin of the Geological Society of America* **71,** 1809-1810.

FRAKES, L.A. & CROWELL, J.C. 1967. Facies and paleogeography of Late Paleozoic diamictite, Falkland Islands. *Geological Society of America Bulletin* **78,** 37-58.

FREY, M. 1987. Very low-grade metamorphism of clastic sedimentary rocks. *In:* FREY, M. (ed) *Low Temperature Metamorphism*, 9-58. Blackie.

FREY, R.W. & HOWARD, J.D. 1970. Comparison of Upper Cretaceous ichnofaunas from siliceous sandstones and chalk, Western Interior Region, U.S.A.. *In:* CRIMES, T.P. & HARPER, J.C. (eds) *Trace Fossils*. Geological Journal Special Issue **3,** 141-166.

GHOSH, S.K. & RAMBERG, H. 1968. Buckling experiments on intersecting folds. *Tectonophysics* **5,** 89-105

GONZÁLEZ-BONORINO, G. 1992. Carboniferous glaciation in Gondwana. Evidence for grounded marine ice and continental glaciation in Southwestern Argentina. *Palaeogeography, Palaeoclimatology, Palaeoecology*, **91,** 363-375.

——— & EYLES, N. 1995. Inverse relation between ice extent and the late Paleozoic glacial record of Gondwana. *Geology*, **23,** 1015-1018.

GREENWAY, M. E. 1972. The geology of the Falkland Islands. 42 pp. *British Antarctic Survey Scientific Report* **76.**

GRUJIC, D. 1993. The influence of initial fold geometry on Type 1 and Type 2 interference patterns: an experimental approach. *Journal of Structural Geology* **15,** 293-307.

GRUNOW, A.M. 1993a. Creation and destruction of Weddell Sea floor in the Jurassic. *Geology* **21,** 647-650.

———, 1993b. New Paleomagnetic Data From the Antarctic Peninsula and Their Tectonic Implications. *Journal of Geophysical Research* **98,** 13815-13833.

———, KENT, D.V. & DALZIEL, I.W.D. 1987. Mesozoic evolution of West Antactica and the Weddell Sea Basin: new paleomagnetic constraints. *Earth and Planetary Scvience Letters* **86,** 16-26.

———, ——— & ——— 1991. New Paleomagnetic Data From Thurston Island: Implications for the Tectonics of West Antarctica and Weddell Sea Opening. *Journal of Geophysical Research* **96,** 17935-17954.

HÄLBICH, I.W. 1983. Geodynamics of the Cape Fold Belt in the Republic of South Africa: A summary. *In:* RAST, N. & DELANY, F.M. (eds) *Profiles of Orogenic Belts*. American Geophysical Union Geodynamic series **10,** 21-29.

——— & CORNELL, D.H. 1983. Metamorphic history of the Cape Fold Belt. *In:* SÖHNGE, A.P.G & HÄLBICH, I.W. (eds) *Geodynamics of the Cape Fold Belt,* Special Publication of the Geological Society of South Africa **12,** 138-148.

———, FITCH, F.J. & MILLER, J.A. 1983. Dating the Cape Orogeny. *In:* SÖHNGE, A.P.G & HÄLBICH, I.W. (eds) *Geodynamics of the Cape Fold Belt*. Special Publication of the Geological Society of South Africa **12,** 149-164.

HALLE, T.G. 1912. On the geological structure and history of the Falkland Islands. *Bulletin of the Geological Institute of Upsala* **11,** 115-229.

HAMBREY, M.J. 1994. *Glacial Environments*. 296 pp. UCL Press.

HANCOCK, P.L., DUNNE, W.M. & TRINGHAM, M.E. 1983. Variscan Deformation in Southwest Wales. *In:* HANCOCK, P.L. (ed) *The Variscan Fold Belt in the British Isles*. 47-73. Adam Hilger.

HAUGHTON, S.H. 1928. *The geology of the country between Grahamstown and Port Elizabeth. Explanation of Cape Sheet No.9 Port Elizabeth.* Union of South Africa Department of Mines and Industries Geological Survey.

HAYASHI, T. 1966. Clastic dykes in Japan. *Transactions of Japanese Journal of Geology and Geography* **37,** 1-20.

HILLER, N. & TAYLOR, F.F. 1992. Late Devonian shoreline changes: an analysis of Witteberg Group stratigraphy in the Grahamstown area. *South African Journal of Geology* **95,** 203-212.

HILLIER, S. & MARSHALL, J. 1988. A rapid technique to make polished thin sections of sedimentary organic matter concentrates. *Journal of Sedimentary Petrology* **58,** 754-755.

HISCOTT, R.N. 1979. Clastic Sills and Dikes associated with deep-water sandstones, Tourelle Formation, Ordovician, Quebec. *Journal of Sedimentary Petrology* **49,** 1-9.

HOBSON, D.M. & SANDERSON, D.J. 1983. Variscan deformation in Southwest England. *In:* HANCOCK, P.L. (ed) *The Variscan Fold Belt in the British Isles.* 108-129. Adam Hilger.

HYAM, D.M., MARSHALL, J.E.A. & SANDERSON, D.J. 1997. Carboniferous diamictite dykes on the Falkland Islands. *Journal of African Earth Sciences* **26**, 505-517

HYETT, A.J. 1990. Deformation around a thrust tip in Carboniferous limestone at Tutt head, near Swansea, South Wales. *Journal of Structural Geology* **12,** 47-58.

IIJIMA, A., MATSUMOTO, R. & TADA, R. 1985. Mechanisms of sedimentation of rhythmically bedded chert. *Sedimentary Geology* **41,** 221-233.

JOHNSON, M.R. 1976. *Stratigraphy and sedimentology of the Cape and Karoo Sequences in the Eastern Cape Province.* PhD Thesis (Unpublished), 336 pp. Rhodes University, Grahamstown, South Africa.

———, 1991. Sandstone petrography, provenance and plate tectonic setting in the Gondwana context of the southeastern Cape-Karoo Basin. *South African Journal of Geology* **94,** 137-154.

——— & LE ROUX, F.G. 1994. *The geology of the Grahamstown area.* Explanation of sheet 3326. 40 pp. South African Council for Geoscience.

JONES, M.J. & TRUSWELL, E.M. 1992. Late Carboniferous and early Permian palynostratigraphy of the Joe Joe Group, southern Galilee Basin, Queensland, and implications for Gondwanian stratigraphy. *BMR Journal of Australian Geology and Geophysics* **13**, 143-185.

KELLEY, V.C. 1955. Monoclines of the Colorado Plateau. *Geological Society of America Bulletin* **66,** 789-804.

KNELLER, B.C. & BELL, A.M. 1993, An Acadian mountain front in the English Lake District: the Westmoreland Monocline. *Geological Magazine* **130,** 203-213.

KRISTOFFERSON, Y. & HINZ, K. 1991. Evolution of the Gondwana plate boundary in the Weddell Sea area. *In:* THOMSON, M.R.A., CRAME, J.A. & THOMSON, J.W. (eds) *Geological evolution of Antarctica.* Cambridge University Press, Cambridge. 225-230.

LOOCK, J.C. 1967. *The Stratigraphy of the Witteberg-Dwyka contact beds.* Masters Thesis, 139 pp. University of Stellenbosch, South Africa.

——— & VISSER, J.N.J. 1992. South Africa. *In:* DIAZ, C. (ed) *Carboniferous of the world, Volume II. Australia, Indian sub-continent, South Africa, South America and North America.* Institute Geologico y Minero Espana. 197-174.

LOPEZ-GAMUNDI, O.R., ESPEJO, I.S., CONAGHAN, P.J. & POWELL, C.MCA. 1994. Southern South America. *In:* VEEVERS, J.J & POWELL, C.MCA. (eds) *Permian-Triassic Basins and Fold belts along the Panthalassan Margin of Gondwanaland,* Boulder Colorado, Geological Society of America Memoir, **184,** 281-329.

LORENZO, J.M. & MUTTER, J.C. 1988. Seismic stratigraphy and tectonic evolution of the Falkland/Malvinas Plateau. *Revista Brasileira de Geociências* **18,** 191-200.

LUDWIG, W.J., WINDISCH, C.C., HOUTZ, R.E. & EWING, J.L. 1979. Structure of the Falkland Plateau and offshore Tierra del Fuego, Argentina. *In:* WATKINS, J.S., MONTADERT, L. & WOOD DICKERSON, P. (eds) *Geological and Geophysical Investigations of Continental Margins.* American Association of Petroleum Geologists Memoir **29,** 125-137.

———, KRASHENINIKOV, V.A. ET AL. 1983. *Initial Reports of the Deep Sea Drilling Project,* **71.** 1187 pp.Washington. (U.S. Government Printing Office).

MCNAUGHTON, N.C. 1972. Gravity Survey of the Falkland Islands. *British Antarctic Survey Scientific Report* **76,** 39-42.

MCQUILLIN, R., BACON, M. & BARCLAY, W. 1984. *An Introduction to Seismic Interpretation.* 287 pp. Graham & Trotman.

MCRAE, C.S. 1988. Palynostratigraphic correlation between the Lower Karoo sequence of the Waterberg and Pafuri coal-bearing basins and the Hammanskraal plant macrofossil locality, Republic of South Africa. *Memoir of the Geological Survey, South Africa* **75,** 1-217.

MARSHALL, J.E.A. 1994a. The Falkland Islands: A key element in Gondwana paleogeography. *Tectonics* **13,** 499-514.

———, 1994b. The Falkland Islands and the early fragmentation of Gondwana: implications for hydrocarbon exploration in the Falkland Plateau. *Marine and Petroleum Geology* **11,** 631-636.

MARTIN, A.K., GOODLAD, S.W., HARTNADY, C.J.H. & DU PLESSIS, A. 1982. Cretaceous palaeopositions of the Falkland Plateau relative to southern Africa using Mesozoic seafloor spreading anomalies. *Geophysical Journal of the Royal Astrological Society* **71,** 567-579.

——— & HARTNADY, C.J.H. 1986. Plate tectonic development of the south west Indian Ocean: a revised reconstruction of East Antarctica and Africa. *Journal of Geophysical Research* **91,** 4767-4786.

MARTIN, J.L. & STURGEON, L.J.S. 1982. Gravity measurements on the Falkland Islands. *British Antarctic Survey Bulletin* **51,** 137-143.

MATTE, P. 1983. Two Geotraverses across the Ibero-Amorican Variscan Arc of Western Europe. *In:* RAST, N. & DELANY, F.M. (eds) *Profiles of Orogenic Belts.* American Geophysical Union Geodynamic series **10,** 53-81.

MITCHELL, C., TAYLOR, G.K., COX, K.G. & SHAW, J. 1986. Are the Falkland Islands a rotated microplate? *Nature* **319,** 131-134.

MOLNAR, P. & GIPSON, J.M. 1994. Very long baseline interferometry and active rotations of crustal blocks in the Western Transverse Ranges, California. *Geological society of America Bulletin* **106,** 594-606.

MOORES, E.M. & TWISS, R.J. 1995. *Tectonics.* 415 pp.W.H. Freeman & Co.

MORRIS, J. & SHARPE, D. 1846. Description of eight species of Brachiopod shells from the Palaeozoic Rocks of the Falkland Islands. *Quarterly Journal of the Geological Society of London* **2,** 274-278.

MOUNTAIN, E.D. 1945, Problems of Eastern Province geology. *Proceedings of the Geological Society of South Africa* **48,** 21-37.

———, 1962. *The geology of the country around Port Alfred, Cape Province. An explanation of sheets 3326D (Port Alfred) and 3327C.* Republic of South Africa Department of Mines Geological Survey.

MUSSETT, A.E. & TAYLOR, G.K. 1994. ^{40}Ar-^{39}Ar age for dykes from the Falkland Islands with implications for the break up of southern Gondwana. *Journal of the Geological Society of London* **151,** 79-81.

MUSTARD, P.S. 1989. Bed-Tilt, Fold-Plunge Correction and Statistical Analysis of Paleocurrents Using Lotus 1-2-3. *Geobyte* **4,** 15-26.

NAYLOR, D., REILLY, T.A., SEVASTOPULO, G.D. & SLEEMAN, A.G. 1983. Stratigraphy and structure in the Irish Variscides. *In:* HANCOCK, P.L. (ed) *The Variscan Fold Belt in the British Isles*. 20-46. Adam Hilger.

NEATHERY, T.L. & THOMAS, W.A. 1983. Geodynamics transect of the Appalachian Orogen in Alabama. *In:* RAST, N. & DELANY, F.M. (eds) *Profiles of Orogenic Belts*. American Geophysical Union Geodynamic series **10,** 301-307.

NEWTON, A.R. 1993. Thrusting on the northern margin of the Cape Fold Belt near Laingsburg. *South African Journal of Geology* **96,** 22-30.

OELOFSEN, B.W. 1987. The biostratigraphy and fossils of the Whitehill and Irati shale formations of the Karoo and Paraná basins. *In:* MCKENZIE, G.D. (ed) *Gondwana Six: Stratigraphy, Sedimentology and Palaeontology*. Geophysical Monographs Series **41,** 131-138.

PEACOCK D.C.P. & SANDERSON D.J. 1993. Estimating strain from fault slip using a line sample. *Journal of Structural Geology* **15,** 1513-1516.

PLATT, N.H. & PHILIP, P.R. 1995. Structure of the southern Falkland Islands continental shelf: initial results from new seismic data. *Marine and Petroleum Geology* **12,** 759-771.

PLAYFORD, G. 1983. Two new genera of trilete *sporae dispersae* from the Lower Carboniferous of Queensland. *Pollen et Spores* **25**, 265-278.

———, 1990. Australian Lower Carboniferous miospores relevant to extra-Gondwanic correlations: an evaluation. *Courier Forschungsinstitut Senckenberg* **130**, 85-125.

——— & HELBY, R. 1968. Spores from a Carboniferous section in the Hunter Valley, New South Wales. *Journal of the Geological Society of Australia* **15**, 103-119.

POWIS, G.D. 1984. Palynostratigraphy of the Late Carboniferous sequence, Canning Basin, W.A. *In:* PURCELL, P.G. (ed) *The Canning Basin, W.A.: Proceedings of the Geological Society of Australia/ Petroleum Exploration Society of Australia Symposium, Perth.* 429-437.

PRICE, N.J. & COSGROVE, J.W. 1992. *Analysis of Geological Structures*. 502pp. Cambridge University Press.

PRICE, R.A. 1981. The Cordilleran foreland thrust and fold belt in the southern Canadian Rocky mountains. *In:* MCCLAY, K.R. & PRICE, N.J. (eds) *Thrust and Nappe Tectonics*. Geological Society of London Special Publication **9,** 427-428.

PUSCH, R., BÖRGESSON, L. & KNUTSSON, S. 1990. Origin of silty fracture fillings in crystalline bedrock. *Geologiska Föreningens I Stockholm Förhandlingar* **112,** 209-213.

RAMSAY, J.R. 1967. *Folding and Fracturing of Rocks*. 568 pp. New York, McGraw-Hill.

RAPELA, C.W. & PANKHURST, R.J. 1992. The granites of northern Patagonia and the Gastre Fault System in relation to the break-up of Gondwana. *In:* STOREY, B.C., ALABASTER, T. & PANKHURST, R.J. (eds) *Magmatism and the Causes of Continental Break-up*. Geological Society of London Special Publication **68,** 209-220.

RATTEY, P.R. & SANDERSON, D.J. 1982. Patterns of folding within nappes and thrust sheets: examples from the Variscan of southwest England. *Tectonophysics* **88,** 247-267.

RECHES, Z. 1978. Development of Monoclines Pt.I: Structure of the Palisades Creek branch of the East Kaibab Monocline, Grand Canyon, Arizona. *In:* MATTHEWS III, V. (ed) *Laramide Folding associated with Basement Block Faulting in the Western United States*. Memoir of the Geological Society of America **151,** 235-271.

——— & JOHNSON, A.M. 1978. Development of Monoclines : Theoretical Analysis of monoclines. *In:* MATTHEWS III, V. (ed) *Laramide Folding associated with Basement Block Faulting in the Western United States*. Memoir of the Geological Society of America **151,** 273-311.

REX, D.C. & TANNER, P.W.G. 1982. Precambrian age for gneisses at Cape Meredith in the Falkland Islands. *In:* CRADDOCK, C. (ed) *Antarctic Geoscience Syposium on Antarctic Geology and Geophysics, Madison Wisconsin, U.S.A.* 107-110.

RICHARDS, P.C. & FANNIN, N.G.T. 1994. Falkland Islands offshore offers high risks-costs, good potential. *Oil & Gas Journal* **January 17th,** 67-70.

——— & ——— 1997. Geology of the North Falklands Basin. *Journal of Petroleum Geology* **20,** 165-183.

———, GATLIFF, R.W., QUINN, M.F., WILLIAMSON, J.P. & FANNIN, N.G.T. 1996. The geological evolution of the Falkland Islands continental shelf. *In:* STOREY, B.C., KING, E.C. & LIVERMORE, R.A. (eds) *Tectonic evolution of the Weddell Sea and surrounding regions*. Special Publication of the Geological Society of London **108,** 105-128

ROBERT, P. 1988. *Organic Metamorphism and Geothermal History: Microscopic Study of Organic Matter and Thermal Evolution of Sedimentary Basins*. 311 pp. Elf-Aquitaine and Reidel Publishing Company.

ROBERTS, J., JONES, P.J. & JENKINS, T.B.H. 1993. Revised correlations for Carboniferous marine invertebrate zones of eastern Australia. *Alcheringa* **17,** 353-376.

RON, H., FREUND, R. & GARFUNKEL, Z. 1984. Block rotation by strike-slip faulting: structural and paleomagnetic evidence. *Journal of Geophysical Research* **89,** 6256-6270.

RONIEWICZ, P. & PIENKOWSKI, G. 1977. Trace fossils of the Podhale Flysch Basin. *In:* CRIMES, T.P. & HARPER, J.C. (eds) *Trace Fossils 2*, Geological Journal Special Issue **9,** 273-288.

ROWSELL, D.M. & DE SWARDT, A.M.J. 1976. Diagenesis in Cape and Karroo sediments, South Africa, and its bearing on their hydrocarbon potential. *Transactions of the Geological Society of South Africa* **79,** 81-145.

RUST, I.C. 1973. The evolution of the Paleozoic Cape Basin, Southern margin of Africa. *In:* NAIRN, A.E.M. & STEHLI, F.G. (eds) *Ocean basins and margins, vol. 1: The South Atlantic.* 247-276.

SANDERSON, D.J. & MARCHINI, W.R.D. 1984. Transpression. *Journal of Structural Geology* **6,** 449-458.

SANDWELL, D.T. & SMITH, W.H.F. 1992. Global marine gravity from ERS-1, Geosat and Seasat reveals new tectonic fabric (abstract). *Eos Transactions of AGU, 73.* Fall Meeting suppliment, **133**.

SANFORD, R.M. & LANGE, F.W. 1960. Basin-study approach to oil evaluation of Parana miogeosyncline, South Brazil. *American Association of Petroleum Geologists Bulletin* **44,** 1316-1370.

SCASSO, R.A. & MENDIA, J.E. 1985. Rasgos estratigraficos y paleoambientales del Paleozoico de las Islas Malvinas. *Asociacion Geologica Argentina* **40,** 26-50.

SCHOPF, J.M. 1969, Ellsworth Mountains: position in West Antarctica due to sea-floor spreading. *Science* **164,** 63-66.

SEILACHER, A. 1970. *Cruziana* stratigraphy of "non-fossiliferous" Palaeozoic sandstones. *In:* CRIMES, T.P. & HARPER, J.C. (eds) *Trace Fossils.* Geological Journal Special Issue **3,** 447-478.

SELLÉS-MARTÍNEZ, J. 1989. The structure of the Sierras Australes (Buenos Aires Province, Argentina) an example of folding in a transpressive environment. *Journal of South American Earth Sciences* **2,** 317-329.

SEWARD, A.C. & WALTON, J. 1923. On fossil plants from the Falkland Islands. *Quarterly Journal of the Geological Society of London* **79,** 313-333.

SHAMIR, G. & EYAL, Y. 1995. Elastic modelling of fault-driven monoclinal fold patterns. *Tectonophysics* **245,** 13-25.

SMITH, R.M.H. 1990. A review of the stratigraphy and sedimentary environments of the Karoo Basin of South Africa. *Journal of African Earth Sciences* **10,** 117-137.

SOUTH AFRICAN COMMITTEE FOR STRATIGRAPHY (SACS), 1980. The stratigraphy of South Africa. Pt1 (compiled by KENT, L.E.) *Lithostratigraphy of the Republic of South Africa, Southwest Africa /Namibia and the Republics of Bophuthaswana, Transkei and Venda.* Handbook of the Geological Survey of South Africa **8,** 690 pp.

SOUTH ATLANTIC GEOLOGICAL RESEARCH GROUP 1997. Mesozoic evolution of SW Gondwana: implications for the hydrocarbon potential of the Falklands /Malvinas Plateau area (abstr.). *Oil and Gas Habitats of the South Atlantic, 24th-26th February 1997,* PESGB/Geological Society of London Petroleum Group Conference, Burlington House, London.

STOREY, B.C., VAUGHAN, A.P.M. & MILLAR, I.L. 1996. Geodynamic evolution of the Antarctic Peninsula during Mesozoic times and its bearing on Weddell Sea history. *In:* STOREY, B.C., KING, E.C. & LIVERMORE, R.A. (eds) *Tectonic evolution of the Weddell Sea and surrounding regions.* Special Publication of the Geological Society of London **108,** 87-104.

SWART, R. 1982. *The stratigraphy and structure of the Kommadagga Subgroup and contiguous rocks*. Masters Thesis, 104 pp. Rhodes University, Grahamstown, South Africa.

TANKARD, A.J. & BARWIS, J.H. 1982. Wave-Dominated Sedimentation in the Devonian Bokkeveld Basin of South Africa. *Journal of Sedimentary Petrology* **52,** 959-974.

TAYLOR, B.J. 1982. Sedimentary dykes, pipes and related structures in the Mesozoic sediments of south-eastern Alexander Island. *British Antarctic Survey Bulletin* **51,** 1-42.

TAYLOR, G.K. & SHAW, J. 1989. The Falkland Islands: New Palaeomagnetic data and their origin as a displaced terrane from Southern Africa. *In:* HILLHOUSE, J.W. (ed) *Deep Structure and Past Kinematics of Accreted Terranes. Geophysical Monograph 50*. International Union of Geodesy and Geophysics **5,** 59-72.

THERON, J.N. 1970. A stratigraphical study of the Bokkeveld Group (series). *2nd Gondwana Symposium (South Africa) Proceedings and Papers.* 197-204

THISTLEWOOD, L., LEAT, P.T., MILLAR, I.R., STOREY, B.C. & VAUGHAN, A.P.W. 1997. Basement geology and Palaeozoic-mesozoic mafic dykes from the Cape Meredith Complex, Falkland Islands: a record of repeated intracontinental extension. *Geological Magazine* **134,** 355-367.

THOMAS, J.-C., CHAUVIN, A., GAPAIS, D., BAZHENOV, M.L., PERROUD, H., COBBBOLD, P.R. & BURTMAN, V.S. 1994. Paleomagnetic evidence for Cenozoic block rotations in the Tadjik depression (Central Asia). *Journal of Geophysical Research* **99,** 15141-15160.

THOMAS, R.J., JACOBS, J. & WEBER, K. 1995. Preliminary results of an examination of the Mesoproterozoic Cape Meredith Complex, West Falkland. *Extended Abstract Geocongress '95, Geological Society of South Africa, Johannesburg*, 414-417.

THOMPSON, R.I. 1981. The nature and significance of large 'blind' thrusts within the northern Rocky Mountains of Canada. *In:* MCCLAY, K.R. & PRICE, N.J. (eds) *Thrust and Nappe Tectonics*. Geological Society of London Special Publication **9,** 449-462.

THOMPSON, R.W. 1976. Mesozoic sedimentation on the Eastern Falkland Plataeu. *In:* BARKER, P.F., DALZIEL, I.W.D. ET AL. (eds) *Initial Reports of the Deep Sea Drilling Project* **36,** 877-891.

TRICKER, P.M. 1991. *Organic maturation in the Lower Palaeozoic Welsh Basin.* PhD Thesis, 311pp. University of Southampton.

TURNER, J.C.M. 1980. Islas Malvinas. *En Geologia Regional Argentina, (2nd Symposio) Academia Nacional Congress, Cordoba II.* 1503-1527.

ULIANA, M.A., BIDDLE, K.T. & CERDAN, J. 1988. Mesozoic Extension and the Formation of Argentine Sedimentary Basins. *In:* TANKARD, A.J. & BALKWILL, H.R.(eds) *Extensional Tectonics and Structure of the North Atlantic Margin.* American Association of Petroleum Geologists Memoir **46,** 599-614.

UNDERHILL, J.R., GAYER, R.A., WOODCOCK, N.A., DONNELLY, R., JOLLEY, E.Y. & STIMPSON, I.G. 1988. The Dent Fault system, northern England- reinterpretation as a major oblique-slip fault zone. *Journal of the Geological Society of London* **145,** 303-316.

VANN, I.R., GRAHAM, R.H. & HAYWARD, A.B. 1986. The structure of mountain fronts. *Journal of Structural Geology* **8,** 215-227.

VEEVERS, J.J. & POWELL, C.MCA. 1987. Late Paleozoic glacial episodes in Gondwanaland reflected in transgressive-regressive depositional sequences in Euramerica. *Geological Society of America Bulletin* **98,** 478-487.

VISSER, J.N.J. 1974. The Table Mountain Group: A study in the deposition of quartz arenites on a stable shelf. *Transactions of the Geological Society of South Africa* **77,** 229-237.

———, 1987. The palaeogeography of part of south western Gondwana during the Permo-Carboniferous glaciation. *Palaeogeography, Palaeoclimatology, Palaeoecology* **61,** 205-219.

———, 1990. The age of the late Palaeozoic glacigene deposits in southern Africa. *South African Journal of Geology* **93,** 366-375.

———, 1991a. The paleoclimatic setting of the late Paleozoic marine ice sheet in the Karoo Basin of southern Africa. *In:* ANDERSON, J.B. & ASHLEY, G.M. (eds) *Glacial marine sedimentation; Paleoclimatic significance: Boulder, Colorado.* Geological Society of America Special Paper **261,** 181-189.

———, 1991b. Geography and climatology of the late Carboniferous to Jurassic Karoo Basin in south-western Gondwana. *Annals of the South African Museum* **99,** 415-431.

———, 1992. Deposition of the Early to Late Permian Whitehill Formation during a sea-level highstand in a juvenile foreland basin. *South African Journal of Geology* **95,** 181-193.

———, 1993. Sea-level changes in a back-arc—foreland transition: late Carboniferous-Permian Karoo Basin of South Africa. *Sedimentary Geology* **83,** 115-131.

———, 1995. Post-glacial Permian stratigraphy and geography of southern and central Africa: boundary conditions for climatic modelling. *Palaeogeography, Palaeoclimatology, Palaeoecology* **118,** 213-243.

VITANAGE, P.W. 1954. Sandstone dykes in the South Platte Area, Colorado. *Journal of Geology* **62,** 493-500.

WATTS, D.R. & BRAMALL, A.M. 1981. Palaeomagnetic evidence for a displaced terrain in Western Antarctica. *Nature* **243,** 638-641.

WATKEYS, M.K. & SOKOUTIS, D.M. 1997. Transtension in southern Africa during Gondwana break-up (abstr). *Continental Transpressional and Transtensional Tectonics, 5-6 March 1997.* Geological Society of London Tectonics Studies Group Conference, Burlington House, London.

WEBERS, G.F., CRADDOCK, C. & SPLETTSTOESSER, J.F. 1992. Geologic history of the Ellsworth Mountains, West Antarctica. *In:* WEBERS, G.F., CRADDOCK, C. & SPLETTSTOESSER, J.F. (eds) *Geology and Paleontology of the Ellsworth Mountains, West Antarctica.* Boulder Colorado, Geological Society of America Memoir **170,** 1-8.

WHITE, R.S. & MCKENZIE, D. 1989. Magmatism at Rift Zones: The Generation of Volcanic Continental Margins and Flood Basalts. *Journal of Geophysical Research* **94,** 7685-7729.

WHITTINGHAM, J.K. 1980. A sedimentary dyke in the Witteberg Group near Kamferspoort, Steytlerville District, C.P.. *Annals of the Geological Survey of South Africa* **14,** 57-59.

WILCOX, R.E., HARDING, T.P. & SEELY, D.R. 1973. Basic Wrench Tectonics. *The American Association of Petroleum Geologists* **57,** 74-96.

YOUNG, G.M. 1972. Downward Intrusive Breccias in the Hurionian Espanola Formation, Ontario, Canada. *Canadian Journal of Earth Sciences* **9,** 756-762.

ZALAN, P.V., WOLFF, S., CONCEICAO, J.C.J., ASTOLFI, A.M., VIERA, I.S., APPI, V.T., ZANOTTO, A. & MARQUES, A. 1991. Tectonics and sedimentationof the Parana Basin. *In:* ULBRICH, H. & ROCHA-CAMPOS, A.C. (eds) *Gondwana Seven Proceedings: Universidadae de Sao Paulo*, 83-117.

Eastern Wickham Heights:
Stanley - Bluff Cove, East Falkland

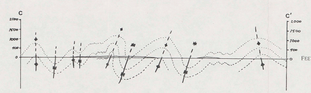

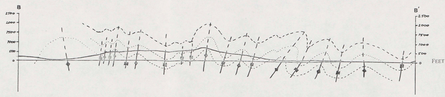

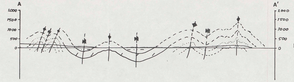

58°05'W 58°00'W 57°55'W 57°50'W 57°45'W

B T

Two Sisters

Tumbledown Mt

Stanley Harbour

Stanley

C T

Sapper Hill

Mt William

Mt Harriet

Wall Mt

C⊥

A T

Port Harriet

Ocean

Rolon Cove

Bluff Cove

Diamictite Dyke

B'⊥

Atlantic

South

A⊥

51°45'S

58°15'W 58°10'W 58°05'W 58°00'W 57°55'W 57°50'W 57°45'W

Key

Stratigraphy

- Port Stanley Formation — Gran Malvina Group
- Bluff Cove Formation — Lower Lafonian Group
- Lafonian Diamictite Formation

Geological features

- Bedding with dip
- Cleavage with dip
- Anticline (with plunge)
- Overturned anticline
- Syncline (with plunge)
- Overturned syncline
- Formation boundary (below / above ground)
- Bedding (below / above ground)

Geographical features

- Spot height
- Named peak
- Road
- Minefield
- Urban area
- Airport
- Bedding with dip in Stanley Common minefield after Ashley (1961)

N W E S

1km

scale 1:25,000

GREENPATCH, EAST FALKLAND

58°10'W

51°33'S

PORT LOUIS HARBOUR

DIAMICTITE DYKE

MONTY DEAN'S CREEK

A

A'

KEY

STRATIGRAPHY

GRAN MALVINA GROUP

- FOX BAY FORMATION (sandstone)
- FOX BAY FORMATION (shale)

GEOLOGICAL FEATURES

- BEDDING WITH DIP
- CLEAVAGE WITH DIP
- ANTICLINE
- SYNCLINE
- LITHOLOGICAL BOUNDARY (BELOW / ABOVE GROUND)

scale 1:25,000

1km

N

W E

S

FEET ABOVE SEA LEVEL

SAN CARLOS, EAST FALKLAND

59°05"W

57°30"S

WRECK POINT

DOCTOR'S HEAD

OLD HOUSE CREEK

LOOKOUT HILL

SAN CARLOS WATER

WHITE RINCON

SAN CARLOS SETTLEMENT

LITTLE RINCON

HEAD OF THE BAY CREEK

MT. CAMPITO

907 FT.

ROUND MT

ROCKY MT.

59°00"W

51°35"S

KEY

STRATIGRAPHY

- LAFONIAN DIAMICTITE FORMATION — LOWER LAFONIAN GROUP
- PORT STANLEY FORMATION — GRAN MALVINA GROUP
- FOX BAY FORMATION (sandstone/shale) — GRAN MALVINA GROUP

GEOGRAPHICAL FEATURES

- 907 FT. — SPOT HEIGHT
- NAMED PEAK
- 500 / 250 — CONTOURS IN FEET ABOVE SEA LEVEL

GEOLOGICAL FEATURES

- BEDDING WITH DIP
- CLEAVAGE WITH DIP
- THRUST WITH DIP
- ANTICLINE (WITH PLUNGE)
- SYNCLINE (WITH PLUNGE)
- ANTICLINE (AFTER CURTIS & HYAM *in press*)
- SYNCLINE (AFTER CURTIS & HYAM *in press*)
- OVERTURNED ANTICLINE
- OVERTURNED SYNCLINE
- LITHOLOGICAL BOUNDARY (BELOW / ABOVE GROUND)

scale 1:25,000
1km

N W E S

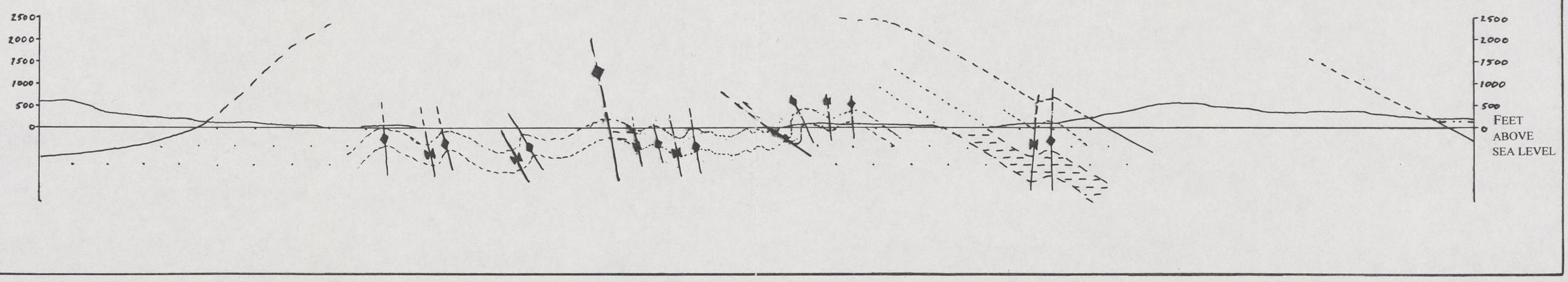

PORT HOWARD, WEST FALKLAND

59°35'W 59°30'W 59°25'W

51°35'S

MT MARIA
2158 FT

PORT HOWARD

BOLD COVE

1068 FT
POKE POINT HILL

FALKLAND SOUND

KEY

STRATIGRAPHY

PORT STEPHENS FORMATION	GRAN	
FOX BAY FORMATION (4 shale horizons)	MALVINA	
PORT STANLEY FORMATION	GROUP	
LAFONIAN DIAMICTITE FORMATION	LOWER LAFONIAN	
BLACK ROCK MEMBER	GROUP	
SHEPHERDS BROOK MEMBER		

GEOLOGICAL FEATURES

- BEDDING WITH DIP
- CLEAVAGE WITH DIP
- ANTICLINE (WITH PLUNGE)
- SYNCLINE (WITH PLUNGE)
- THRUST
- FORMATION BOUNDARY (BELOW / ABOVE GROUND)
- BEDDING (BELOW / ABOVE GROUND)

GEOGRAPHICAL FEATURES

- SPOT HEIGHT
- ROAD
- MINEFIELD

N W E S

1km scale 1:25,000

A B C

4000 3000 2000 1500 1000 500 0 FEET ABOVE SEA LEVEL

CARCASS BAY, WEST FALKLAND

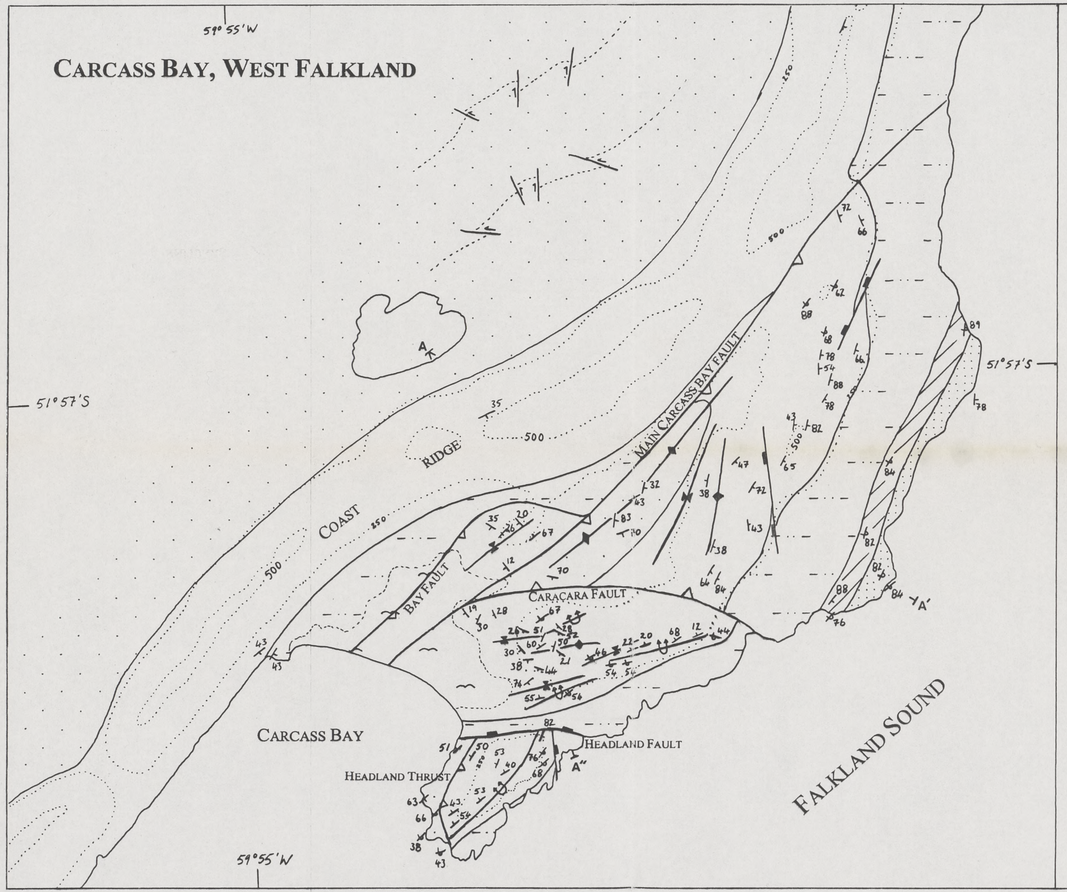

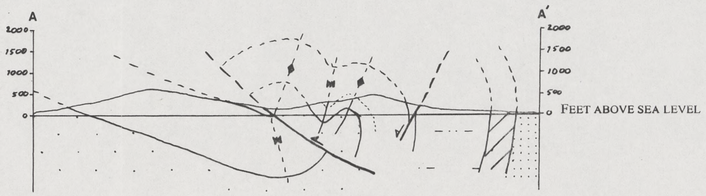

KEY

STRATIGRAPHY

FOX BAY FORMATION	GRAN	MALVINA GROUP
PORT STANLEY FORMATION		
LAFONIAN DIAMICTITE FORMATION	LOWER	LAFONIAN GROUP
BLACK ROCK MEMBER		
SHEPHERDS BROOK MEMBER		
ALLUVIUM		

GEOLOGICAL FEATURES

- BEDDING WITH DIP
- OVERTURNED BEDDING
- ANTICLINE
- OVERTURNED ANTICLINE
- SYNCLINE
- OVERTURNED SYNCLINE
- NORMAL FAULT
- REVERSE FAULT
- FAULT MOVEMENT DIRECTION
- FORMATION BOUNDARY (BELOW / ABOVE GROUND)
- BEDDING (BELOW / ABOVE GROUND)

GEOGRAPHICAL FEATURES

- CONTOURS IN FEET ABOVE SEA LEVEL

N
W E
S

scale 1:25,000

1km

Appendix – removed due to copyright.

Curtis, M. L. and Hyam, D. M., 'Late Palaeozoic to Mesozoic structural evolution of the Falkland Islands: a displaced segment of the Cape Fold Belt', *Journal of the Geological Society,* 155 (1998), pp. 115-129.

DOI: 10.1144/gsjgs.155.1.0115